Oxolipidomic characterization of ischemia-reperfusion injury

By

Zahra Solati

A Thesis Submitted to the Faculty of Graduate Studies of

The University of Manitoba

in partial fulfilment of the requirements for the degree of

Doctor of Philosophy

Department of Physiology and Pathophysiology

University of Manitoba

Winnipeg, Manitoba, Canada

i: Abstract

Hypothesis: Concentrations of bioactive oxidized lipids, such as fragmented oxidized phosphatidylcholines (OxPCs) and oxylipins, will increase significantly following ischemia/reperfusion (I/R) and changes in oxidized lipids concentrations are correlated with markers of tissue injury.

Objective: The goal of this thesis was to determine the changes of bioactive oxidized lipids, including OxPCs and oxylipins during I/R.

Methods: Kidney I/R was induced in male Sprague–Dawley rats by clamping the left renal pedicle for 45 min followed by reperfusion for either 6h or 24h. For myocardial I/R, blood samples were collected from patients presenting with ST-Elevation Myocardial Infarction STEMI before primary percutaneous coronary intervention (PPCI) (Isch) and at 4 time-points post-PPCI, including 2h (R-2h), 24h (R-24h), 48h (R-48h) and 30 days (R-30d). As controls, blood samples were collected from age-matched patients with non-obstructive coronary artery disease. OxPCs and oxylipins were identified and quantitated using high performance liquid chromatography-mass spectrometry (HPLC-MS/MS).

Result: During renal I/R, total tissue concentrations of fragmented aldehyde-containing OxPCs were significantly elevated at 6h and 24h post-reperfusion compared to sham-operated animals ($p<0.05$) and their levels were significantly correlated with plasma creatinine levels ($r=0.888$, $p=0.001$). In patients with STEMI, total plasma levels of fragmented OxPCs increased significantly during ischemia compared with controls ($p<0.05$). Their levels remained elevated for 48h after reperfusion and then decreased significantly at 30-day post-MI compared with R-2h and R-24h groups ($p<0.05$). STEMI patients with an elevated peak of creatine kinase (CK) concentrations had significantly higher ischemic plasma levels of 1-palmitoyl-2-(5'-oxo-valeroyl)-sn-glycero-3-phosphocholine (POVPC) and 1-palmitoyl-2-(9-oxo-nonanoyl)-sn-glycero-3-phosphocholine (PONPC) ($p<0.05$). Plasma concentrations of total docosahexaenoic acid (DHA) derived oxylipins were significantly elevated in the Isch group compared with controls ($p<0.001$). Moreover, their levels during ischemia were significantly correlated with the peak CK and troponin T(TnT) levels ($p<0.05$). Univariate receiver operating characteristic (ROC) curve

analysis showed that the higher ratio of epoxides to diols during the ischemia could be considered as a potential marker of having a smaller infarct size based on CK levels (AUC= 0.77, p=0.03).

Conclusion: We have shown for the first time that bioactive oxidized lipids are produced during I/R and their levels correlate with markers of tissue injury.

ii: Acknowledgements

This thesis would not have been possible without the kind support of many people. Foremost, I would like to express my deepest appreciation to my advisor, Dr. Amir Ravandi for trusting me and giving me the opportunity to join his research team. His passion for science and immense knowledge kept me motivated every day and I could not have imagined myself being here without his generous support, patience, and encouragement during my PhD study. Thank you for helping me to make my dream a reality.

Besides my advisor, I would like to thank my committee members, Dr. Grant Pierce and Dr. Harold Aukema for their guidance and insightful comments. Dr. Pierce, as a director of the research institute, provided the greatest working environment for all students, particularly international students, to feel welcomed and supported. I appreciate Dr. Aukema for letting me use his laboratory facilities and for his intellectual inputs and generous support. I would like to thank Tanja Winter, his lab technician, for training me, providing the most detailed and accurate protocols and answering my never-ending questions.

I would like to thank my fellow lab members: Arun Surendran and Dr. Aleksandra Stamenkovic for being there whenever I was struggling with challenges and difficulties, for all the help, long conversations, laughs and pleasant time we had together. I would like to thank my dear friends: Shiva Shariati, Dr. Nazanin Vafaei, Dr. Ehsan Koohpayeh, and Maryam Samsami. I would not make it without you being on my side.

Last but not least, I would like to thank my parents, Ali and Bahar, my brothers, Mehdi and Mohammad, my sister-in-law, Fereshteh and my lovely niece, Diba for their generous support and love throughout my entire life. Thank you for helping me to follow my dreams. Thank you for all the love, care and sacrifices you made for my happiness.

iii. Contribution of authors

The manuscripts included within this thesis are multi-authored. Therefore, an outline of contribution by manuscript and author are included below in order of appearance in the thesis.

1) Zahra Solati, Amir Ravandi. Lipidomics of bioactive lipids in acute coronary syndromes. International journal of molecular sciences. 2019 Jan;20(5):1051.

- Solati: literature collection and writing of the manuscript
- Ravandi: intellectual input and editing of the manuscript

2) Zahra Solati, Andrea L. Edel, Yue Shang, Karmin O, Amir Ravandi. Oxidized phosphatidylcholines are produced in renal ischemia-reperfusion injury. PloS one. 2018 Apr 23;13(4):e0195172.

- Solati: data generation (lipid extraction and HPLC-MS/MS analysis), statistical data analysis, literature collection/analysis, writing of the manuscript
- Edel: editing of the manuscript
- Shang: conducting the animal experiment
- O: study design, intellectual input on manuscript and editing of the manuscript
- Ravandi: study design, intellectual input on manuscript and editing of the manuscript

3) Zahra Solati, Arun Surendran, Andrea Edel, Marynia Roznik, David Allen, Ashim K Bagchi, Pawan K Singal, and Amir Ravandi. Increase in plasma oxidized phosphatidylcholines (OxPCs) in patients presenting with ST-Elevation Myocardial Infarction (STEMI).

- Solati: blood/clot sample collection, data generation (lipid extraction and HPLC-MS/MS analysis), statistical data analysis, literature collection/analysis, and writing of the manuscript
- Surendran: blood/clot sample collection and editing of the manuscript
- Edel: blood/clot sample collection and editing of the manuscript
- Roznik: clot lipid extraction and writing the part of the manuscript related to clot

- Allen: intellectual input and editing of the manuscript
- Bagchi: cytokine analyses
- Singal: intellectual input on manuscript and editing of the manuscript
- Ravandi: study design, intellectual input on manuscript and editing of the manuscript

4) Zahra Solati, Arun Surendran, Ashim K Bagchi, Pawan K Singal, Harold Aukema and Amir Ravandi. Oxylipin profile alterations in acute ST-segment Elevation Myocardial Infarction (STEMI): role of oxylipins in I/R injury.

- Solati: blood sample collection, data generation (lipid extraction and HPLC-MS/MS analysis), statistical data analysis, literature collection/analysis, and writing of the manuscript
- Surendran: blood sample collection and editing of the manuscript
- Bagchi: cytokine analyses
- Signal: intellectual input on the manuscript and editing of the manuscript
- Aukema: establishment of oxylipin methodology, intellectual input on the manuscript, and editing of the manuscript
- Ravandi: study design, intellectual input on the manuscript, and editing of the manuscript

iii. Table of content

List of tables

List of figures

List of abbreviations

A

AA	Arachidonic acid
ACS	Acute coronary syndrome
ADP	Adenosine di-phosphate
AIF	Apoptosis-inducing factor
AKI	Acute kidney injury
ALR	Absent in melanoma 2-like receptors
Aldo-OxPC	Aldehyde containing oxidized phosphatidylcholine
AMI	Acute myocardial infarction
AMP	Adenosine monophosphate
AMPK	AMP-activated protein kinase
ANG	Angiotensin
ANP	Atrial natriuretic peptide
APAF	Apoptotic protease activating factor-1
Apo (B)	Apo-protein (B)
ATP	Adenosine triphosphate
AUDA-BE	12-(3-adamantan-1-yl-ureido)-dodecanoic acid butyl ester

C

CAD	Coronary artery disease
CAT	Catalase
CHD	Coronary heart disease
CLR	C-type lectin receptors
CMA	Chaperone-mediated autophagy
COX	Cyclooxygenase
CRP	C-reactive protein
Cty c	Cytochrome c
CVD	Cardiovascular disease
CYP450	Cytochrome p450
CYP-e	Cytochrome p450 epoxygenase
CYP-h	Cytochrome p450 hydroxylase
cPLA2	Cytosolic calcium-dependent phospholipase A2

D

DAMP	Damage-associated molecular patterns
DC	Dendrite cell
DC	Direct current
DGLA	Dihomo-γ-linolenic acid
DHA	Docosahexaenoic acid
DiHETrE	Dihydroxyeicosatrienoic acids
DiHDPA	Dihydroxydocosapentanoic acid
DiHOME	Dihydroxyoctadecenoic acid
DNA	Deoxyribonucleic acid
DP	PGD receptor

E

ECM	Extracellular matrix
EpETrE	Epoxyeicosatrienoic acids
EIA	Enzyme immunoassay
ELISA	Enzyme-linked immunosorbent assay
EPA	Eicosapentaenoic acid
EpOME	Epoxyoctadecenoic acid
EPR	Electron spin resonance spectroscopy
ER	Endoplasmic reticulum
ERK	Extracellular signal-regulated protein kinase
ESI	Electrospray ionization
ESR	Electron spin resonance spectroscopy
ETC	Electron transport chain

F

FA	Fatty acid
FADD	Fas-associated protein with death domain
FOX	Ferrous oxidation-xylenol orange
FP	PGF receptor

G

GC	Gas chromatography
GGT	Gamma-glutamyl transferase
GIK	Glucose-insulin-potassium
GLA	Gamma-linolenic acid
GNP	Gold nanoparticles
GPL	Glycerophospholipids
GPX	Glutathione peroxidase
GRP	Glucose-regulated proteins
GSH	Glutathione
GSSG	Glutathione disulfide
GST	Glutathione s-transferase
GTP	Guanosine triphosphate

H

HAEC	Human aortic endothelial cell
HAzPC	1-O-hexadecyl- 2-azelaoyl-sn-glycero-3-phosphocholine
HDdiA-PC	1-acyl-2-(9-hydroxy-10-dodecendioate)-sn-glycero-3-phosphocholine
HDOHE	Hydroxydocosahexanoic acid
HEPE	Hydroxyeicosapentaenoic acids
HEPE	Hydroxyeicosapentanoic acid
HETE	Hydroxyeicosatetraenoic acid
HETrE	Hydroxyeicosatrienoic acid

HF	Heart failure
HHTrE	Hydroxyheptadecatrienoic acid
HNE	Hydroxy-trans-2-nonenal
HODA-PC	Hydroxy-12-oxododec-10-enoic acid ester of 2-lysophosphatidylcholine
HODE	Hydroxyoctadecadienoic acid
HOTrE	Hydroxyoctadecatrienoic acid
HPLC	High-performance liquid chromatography
HSP	Heat shock proteins
hs-CRP	High-sensitive c-reactive protein
HUVEC	Human umbilical vein endothelial cell

I

ICAM	Intercellular adhesion molecule-1
IL	Interleukin
IMM	Inner mitochondrial membrane permeability
IMS	Ion mobility MS
IFN-γ	Interferon-gamma
iPLA2	Calcium-independent phospholipase A2
I/R	Ischemia/reperfusion
isoPG	Isoprostanes

J

JNK	C-Jun N-terminal kinase

K

KODA-PC	1-acyl-2-(9-keto-12-oxo-10-dodecenoate)-sn-glycero-3-phosphocholin
KOdiA-PC	1- acyl -2-(5'-keto-6'-octenedioyl)-sn-glycero-3-phosphocholine
KOHA-PC	1- acyl l-2-(4-oxo-7-oxohept-5-enoyl)-sn-glycero-3-phosphoserine
KOOA-PC	5-Hydroxy-8-oxo-6-octenoic acid ester of 2-lysophosphatidylcholine

L

LAD	Left anterior descending
LC	Lipid chromatography
LCA	Left coronary artery
LCAT	Lecithin-cholesterol acyltransferase
LDH	Lactate dehydrogenase
LDL	Low-density lipoproteins
LOO	Lipid peroxy radical
LOOH	Lipid hydroperoxide
LOX	Lipoxygenase
LP(a)	Lipoprotein (a)
LPC	Lysophosphatidylcholine
LPL	Lysophospholipid
LPS	Bacterial lipopolysaccharide
LT	Leukotrienes
LTA	Leukotrienes A
LTB	Leukotrienes B
LTC	Leukotrienes C
LV	Left ventricular
LVESVI	Left ventricular end-systolic volume index

M

MACE	Major adverse cardiovascular events
MALDI	Matrix-assisted laser desorption/ionization
MAPK	Mitogen-activated protein kinases
MCP	Monocyte chemotactic protein
MCP1	Monocyte chemotactic protein 1
MDA	Malondialdehyde
MI	Myocardial infarction
MIP-1α	Macrophage Inflammatory Proteins-1Alpha
MPTP	Mitochondrial permeability transition pores
MRM	Multiple reaction monitoring
MS	Mass spectrometry
MUFA	Monounsaturated fatty acid
MVO	Microvascular obstruction

N

NADPH	Nicotinamide adenine dinucleotide phosphate
NFAT	Nuclear factor of activated T cells
NF-κB	Nuclear factor kappa-light-chain-enhancer of activated B cells
NK	Natural killer
NLR	Nod-like receptors
NLRP	Nucleotide-binding oligomerization domain
NNCM	Neonatal rat cardiomyocytes
NO	Nitric oxide
NOS	Nitric oxide synthase
Nrf2	Nuclear factor erythroid 2–related factor 2
NSAID	Non-steroid anti-inflammatory drug

O

OH	Hydroxyl
OMM	Outer mitochondrial membrane permeability
OOH	Hydroperoxy
oxoODE	Oxooctadecadienoic acid
oxoOTrE	Oxooctadecatrienoic acid
OxPC	Oxidized phosphatidylcholine
OxPL	Oxidized phospholipid

P

PA	Palmitic acid
PAD	Peripheral artery disease

PAF	Platelet-activating factor
PAMP	Pathogen-associated molecular patterns
PAPC	1-Palmitoyl-2-arachidonoyl-sn-3glycero-3-phosphocholine
PAR	Protease-activated receptors
PARP	(Poly(ADP-Ribose) polymerase)
PAzPC	1-Palmitoyl-2-azelaoyl-sn-glycero-3-phosphocholine
PC	Phosphatidylcholine
PCI	Precarious coronary intervention
PD	Protectin D
PE	Phosphatidylethanolamine
PEIPC	1-Palmitoyl-2-(5,6-epoxyisoprostane e2)-sn-glycero-3-phosphocholine
PG	Prostaglandin
PGD	Prostaglandin D
PGDH	Prostaglandin dehydrogenase
PGE	Prostaglandin E
PGF	Prostaglandin F
PGI	Prostaglandin I
PGJ	Prostaglandin J
PGJ2-SPC	Prostaglandin J2- stearoyl phosphocholine
PGPC	1-Palmitoyl-2-glutaryl-sn-glycero-3-phosphocholine
PI	Phosphatidylinositol
PIP	Phosphatidylinositol bisphosphate
PKA	Protein kinase A
PL	Phospholipid
PLPC	1-Palmitoyl-2-linoleoyl-sn-glycero-3-phosphocholine
PMN	Polymorphonuclear leukocytes
POBN	4-Pyridyl-1-oxide)-N-tert-butyl nitrone
PONPC	1-Palmitoyl-2-(9-oxo-nonanoyl)-sn-glycero-3-phosphocholine
POVPC	1-Palmitoyl-2-(5'-oxo-valeroyl)-sn-glycero-3-phosphocholine
PPAR	Peroxisome proliferator-activated receptor α
PPCI	Primary Percutaneous coronary intervention
PRDX	Peroxiredoxin
PS	Phosphatidylserine
PtG	Phosphatidylglycerol
PUFA	Poly-unsaturated fatty acid

R

RF	Radio-frequency
RIP	Receptor-interacting protein
RLR	Retinoic acid-inducible gene I (RIG-I)-like receptors
ROS	Reactive oxygen species
RT	Retention time
RV	Resolvin

S

SA	Stearic acid
SAPC	1-Stearoyl-2-arachidonoyl-sn-glycero-3-phosphocholine
SAzPC	1-Stearoyl-2-azelaoyl-sn-glycero-3-phosphocholine
sEH	Soluble epoxide hydrolase
SEIPC	1-Stearoyl -2-(5,6-epoxyisoprostane E2)-sn-glycero-3-phosphocholine
SCAD	Spontaneous coronary artery dissection
SGPC	1-Stearoyl-2-glutaroyl-sn-glycero-3-phosphocholine
SLPC	1-Stearoyl-2-linoleoyl-sn-glycero-3- phosphocholine
SM	Sphingomyelin
SOD	Superoxide dismutase
SONPC	1-Stearoyl -2-(9-oxo-nonanoyl)-snglycero-3-phosphocholine
SOVPC	Sn-1-stearoyl-2-oxovaleroyl- phosphocholine
sPLA2	Secreted phospholipaseA2
SPM	Specialized pro-resolving mediators
SREBP	Sterol regulatory element-binding protein
SRM	Selected single reaction monitoring
STEMI	ST-elevation myocardial infarction

T

TG	Triglyceride
TGF-β	Transforming growth factor-beta
TLR	Toll-like receptor
TNF	Tumour necrosis factor
TLC	Thin-layer chromatography
TOF	Time of flight
TP	Thromboxane receptor
TriHOME	Trihydroxyoctadecenoic acid
TX	Thromboxane
TXA	Thromboxane A
TXB	Thromboxane B

U

UPLC	Ultra-performance lipid chromatography

V

VCAM	Vascular cell adhesion protein
VEGF	Vascular endothelial growth factor
VEGFR	Vascular endothelial growth factor receptor
VPS	Vacuolar protein sorting

VSMC	Vascular smooth muscle cells

CHAPTER I-LITRETURE REVIEW

i. Introduction

Ischemia/Reperfusion (I/R) injury is characterized as continued cell injury and death that occurs following revascularization of previously ischemic tissue (1). Although reperfusion is vital to salvage ischemic tissue, it causes further damage, mainly due to an extensive production of reactive oxygen species (ROS) and activation of inflammatory pathways (1). Many organs, including the heart and kidney, are susceptible to I/R injury. Also, I/R injury in one organ can induce systemic damage to distant organs, leading to multi-system organ failure (1). Despite years of comprehensive research, we are still far away from developing therapies to minimize the impact of I/R injury (2). Disorders characterized by I/R, such as acute coronary syndrome (ACS) (3) and ischemic kidney disease (4), continue to be among the most frequent causes of disability and death worldwide (1).

Reperfusion injury is a multi-factorial process. Abrupt oxygen introduction following reperfusion leads to the generation of ROS, as a consequence of antioxidant defense impairment (5). This can cause endothelial dysfunction, oxidation of DNA, protein, and lipid, activation of inflammatory responses and eventually cell death (5). Membrane phospholipids (PL) are more susceptible to oxidation, due to the presence of polyunsaturated fatty acid (PUFA) in their structure (6). Phosphatidylcholines (PC), are the most dominant PLs in mammalian cellular tissues (6). Once PC molecules are oxidized, they generate a pool of heterogeneous oxidized PC (OxPC) molecules, which acquire biological activities not characteristic of their parent molecule (6).

Membrane enzymes, such as phospholipase A2 (PLA2), are also activated during I/R (7). PLA2 releases PUFAs from the sn-2 positions of membrane PL (7). These free fatty acids (FA) can be further oxidized through three main enzymatic pathways, including cyclooxygenase (COX), lipoxygenase (LOX), and cytochrome P450 (CYP450) (7). Various forms of oxidized lipids can be produced through these oxidative pathways, which are generally called oxylipins (7). Oxylipins derived from n-6 PUFA, such as arachidonic acid (AA) and linoleic acid (LA) can initiate inflammation, change ion channel functions, and alter transcriptional programming, which all can contribute to I/R injury (7).

With the advent of powerful and robust mass spectrometric techniques, we now have the capabilities to identify and quantitate oxidized lipid molecules in complex biological mixtures, such as tissue and plasma (8). Genomics and proteomic technologies have allowed us to only determine the changes within the genome and the proteomic expression (8). Lipidomics is a detailed analysis of lipid species with various structural and functional roles that allows for bridging of the phenotype-genotype gap (8). Given the potential roles of oxidized lipids in I/R injury, targeted oxolipidomic analysis will provide new insight into a better understanding of I/R injury.

Therefore, we hypothized that bioactive oxidized lipids concentrations, such as OxPC and oxylipins levels, will alter following I/R and changes in oxidized lipids concentraions are correlated with markers of tissue injury.

Thus, the purpose of the thesis is 3-fold: (1) to determine the changes within the OxPC molecules in an animal model of renal reperfusion injury using high-performance lipid chromatography-tandem mass spectrometry (HPLC-MS/MS), (2): To determine the changes in plasma concentrations of OxPCs during ischemia and reperfusion in patients presenting with ST-segment Elevation Myocardial Infarction (STEMI) using the HPLC-MS/MS technique, (3): to define plasma oxylipin profile alterations in a clinical setting of I/R in patients with STEMI using the HPLC-MS/MS approach.

ii. Ischemia/ reperfusion (I/R) injury

Background

The term ischemia was first used to describe the obstruction of arterial blood flow to a tissue in the early nineteenth century (2). The concept of reperfusion injury, however, was proposed 60 years ago and defined as a phenomenon that induces or aggravates cell death following tissue reperfusion (2). The scale of tissue injury is associated with both the extent and duration of ischemia (9). Every tissue or organ may be able to endure a short period of ischemia, without detectable dysfunction or injury (9). However, if the duration and extent of ischemia exceeds tissue hemostatic safeguards, which is different for various cell types and organs, cell dysfunction and/or

death may occur (9). Therefore, timely re-establishment of blood flow is still the primary approach to limit cell dysfunction/death following ischemia (9).

In the human body, the heart is the second most sensitive organ to ischemia after the brain, as irreversible damage may occur in both human and animal myocardium within only 20 min of ischemia (9). Myocardial cells have a high energy demand due to both contractility and diastolic relaxation. Therefore, the heart requires constant energy supplies as a form of adenosine triphosphate (ATP) (9). The most relevant cause of myocardial ischemia in human is a reduction of blood flow into the coronary microcirculation as a result of atherosclerotic plaque rupture and/or thrombus formation (Type 1 MI) (6). Complete occlusion of coronary arteries usually presents with an elevation of the ST wave in the electrocardiogram (STEMI), which is accompanied by tissue injury and presents with elevated cardiac biomarkers of tissue injury such as troponin (6). In type 2 MI, myocardial ischemia occurs as a result of demand-supply mismatch, due to tachycardia, hypoxia, stress, vasospasm, coronary embolus, and spontaneous coronary artery dissection (SCAD) (10). Myocardial I/R injury is generally characterized by cell swelling, myofibril contractures, and disruption of the sarcolemma in the myocardium and it is thought to be responsible for 50% of final infarct size in MI patients (11). Considering that the myocardium has negligible regenerative capacity, fibrosis occurs when a significant amount of cardiac muscle is lost (12).

The kidney represents the third organ sensitive to I/R (9). Renal I/R injury is the leading cause of acute kidney injury (AKI), affecting 13.3 million patients every year worldwide (13). It is accompanied by rapid kidney dysfunction resulting in an abrupt increase in plasma creatinine as a result of kidney injury (14). The main cause of renal ischemia is a dramatic reduction in renal blood flow as a result of systemic hypotension, renal artery thrombosis, embolism, or atherosclerosis (15). Renal ischemia can also occur during aortic surgery, renal transplantation, or cardiovascular anaesthesia (15). Permanent ischemic damages appear in renal cells when the duration of ischemia exceeds 30 min (16). Tubular epithelial cells are the most abundant cell types in the kidney, which have high metabolic rates and are replete with large number of mitochondria (17).

Cellular mechanism of I/R injury

During ischemia, hypoxia results in defects in the mitochondria electron transport chain (ETC) leading to anaerobic metabolism (5). Anaerobic metabolism is accompanied by lower productions of ATP and antioxidant agents, detachments of ribosomes, and deactivation of ATPases, such as Na^+/K^+ and Ca^{+2} ATPases (5). Failure of Na^+/K^+ ATPase leads to retention of Na^+ ions inside and accumulation of K^+ ions outside of the cells. Na^+ ions are then exchanged with H^+ ions leading to cellular acidocis (5). Elevated levels of cellular Na^+ also activate the Na^+/Ca^{+2} pump, leading to Ca^{+2} ions overload (5). Ca^{+2} accumulation leads to the opening of mitochondrial permeability transition pores (MPTP), which dissipates mitochondrial membrane potential and further impairs ATP production (2). Protein synthesis also decreases as a result of ribosome detachment (5). The extent of these cellular changes and the corresponding injury are impacted by the extent of blood flow obstruction and duration of ischemia (9).

Restoring blood flow (reperfusion) initiates aerobic metabolism, ATP production, and normalizes cellular pH by washing out the accumulated H^+ ions (9). However, reperfusion is accompanied by disturbing events leading to activation of cell death pathways (9). Restoring blood flow to the ischemic tissue supplies the required oxygen via red blood cells, but it also causes oxidative stress due to the increased production of reactive oxygen species (ROS) (9). Besides, depleted cellular levels of antioxidant agents during ischemia exacerbates oxidative stress following reperfusion (9). Oxidative stress can lead to endothelial dysfunction, DNA damage and inflammatory responses (9), which are discussed in the next section.

Role of oxidative stress in I/R injury

ROS are a group of highly reactive compounds, which have an O_2 with an unpaired electron in their chemical structures (18-20). They are produced in the body as a result of cell metabolism and also environmental factors (18-20). Under physiological conditions, they regulate several cellular responses, such as controlling cellular growth, differentiation, and migration (18-20). They can also regulate vascular tone, immune and inflammatory responses, angiogenesis and apoptosis (18-20). However, prolonged and elevated ROS productions cause protein, lipid, and ribonucleic acid oxidation, leading to cell dysfunction or death (21).

In normal conditions, antioxidant enzymes such as superoxide dismutase (SOD), γ-glutamyltransferase (GGT), glutathione (GSH), glutathione reductase (GSSG-Rd), glutathione peroxidase (GPX), glutathione S-transferase (GST), and catalase (CAT) neutralize produced ROS (22). The imbalance between ROS formation and detoxification induces a cellular condition, called oxidative stress (22).

During I/R, ROS can be generated from both non-enzymatic and enzymatic sources (23). Haemoglobin and myoglobin are the non-enzymatic sources of ROS that can be released into extracellular fluid post-reperfusion (23). However, the increased production of ROS following reperfusion is mainly attributed to enzymes reducing oxygen molecules to superoxide (O_2•-) and/or hydrogen peroxide (H_2O_2), with the subsequent release into intra and extracellular spaces (5). Superoxide is considered as the first formed, highly reactive ROS that can also aggravate the production of H_2O_2 (24). H_2O_2 can then be either converted to H_2O by antioxidant enzymes or reacts with ferrous iron (Fe^{2+}) in the Fenton reaction and forms hydroxide (•-OH) (24). Studies have shown that xanthine oxidase (XO), nicotinamide adenine dinucleotide phosphate (NADPH) oxidase, mitochondrial ETC and uncoupled nitric oxide synthase (NOS) are the key enzymes implicating in ROS production following reperfusion (5).

ROS can cause cellular damage by oxidation of lipids, proteins, ribonucleotides (25). For instances, ROS changes membrane permeability and configuration through peroxidation of PL and oxidation of the thiol group of proteins (25). Moreover, they induce functional changes in various cellular proteins such as a depression in Ca^{2+} ATPase and Na^+/K^+ ATPase activities in the cell membranes (25). Excessive ROS can also inhibit endoplasmic or sarcoplasmic reticulum Ca^{2+} ATPases (25). All these pump modifications lead to intracellular accumulation of Ca^{2+} (26). Ca^{2+} overload causes cytotoxicity and results in either apoptotic, necrotic or autophagic cell death, which will be discussed later (27).

ROS can also modulate the expression of several genes involving in inflammation and cell death pathways, such as the nuclear factor kappa-light-chain-enhancer of activated B cells (NF-κB) (26). Following activation of NF-κB through phosphorylation of nuclear factor erythroid 2-related factor 2 (Nrf2), NF-κB binds to the DNA response element and promotes the transcription of several genes involved in inflammation during I/R (26). ROS also upregulate the production of the

transforming growth factor-beta (TGF-β) in endothelial cells, which eventually result in elevated expressions of collagen 1, 3, and 4, fibronectin, and plasminogen activator inhibitor-1 and attenuation of extracellular matrix (ECM) degradation factors activity (28). Activation of these signaling pathways leads to elevated cell proliferation, increased matrix formation, and fibrosis. ROS can also activate aldosterone and angiotensin II (Ang II) signaling, which promotes smooth muscle proliferation, fibronectin and collagen production and therefore, ECM fibrotic expansion (28).

ROS can also promote apoptosis and necrosis (29). ROS-mediated apoptosis occurs through direct activation of caspase 3 and 8 (via cysteine oxidization) (29) and induction of death receptor clustering on the plasma membrane (30). Necrosis, which is described as mitochondrial swelling, dysfunction, and failed ATP production, also occurs as a result of persistent oxidative stress (31).

Activation of the immune system and I/R injury

Activation of innate immunity is an essential component of the acute inflammatory response in the setting of I/R (32). The innate immune system can be activated generally through pathogen-associated molecular patterns (PAMPs) and damage-associated molecular patterns (DAMPs) (32). These patterns can be identified by several components of the innate immune system such as Toll-like receptors (TLRs), RIG-I-like receptors (RLRs), Nod-like receptors (NLRs), AIM2-like receptors (ALRs), C-type lectin receptors (CLRs), and other DNA sensors (32). Activation of these receptors initiates signaling pathways, which induce the pro-inflammatory cytokines and chemokines productions (32).

Prolonged ischemia leads to necrosis, which is accompanied by the release of intracellular content (33). Some of the intracellular proteins, called alarmin, can react with DAMP receptors, act as alarm and send danger signals to nearby cells (34). Interleukin-1(IL-1), high-mobility group box1, S100 family proteins, some heat shock proteins (HSPs), and glucose-regulated proteins (GRPs) are some examples of alarmin proteins (34). A common task of these proteins is to stimulate NF-kB, which is the key regulator of inflammatory responses (34).

Increased intracellular Ca^{2+} during I/R can also give rise to compounds, such as calcium pyrophosphate complexes and uric acid, which can act as DMPSs and activate inflammasomes

(34). Inflammasomes mediate increased production of cytokines, such as IL-1β and tumour necrosis factorα (TNFα), which in turn activate transcription factors, particularly NF-kB, to increase expression of additional cytokines and chemokines, thereby causing a cytokine storm that exacerbates I/R injury (34).

Following reperfusion, infiltration of inflammatory cells occurs very fast and peaks at 24h post-reperfusion (35). Neutrophils are the largest and the first circulating leukocytes that reach the injury site (35) in response to the signals produced by resident macrophages and endothelial cells (36). Upon their transmigration into the endothelium, they release proteases, ROS, and natural killers (NK) (37). They also produce cytokines and chemokines, which attract other leukocytes to the site of injury through the junction of endothelial cells (37). Mononuclear phagocytes, including myeloid-derived monocytes, macrophages and dendritic cells (DC) are also recruited in the injury site through chemotaxis, and then differentiate into tissue macrophages or DCs (38). Macrophages, after exposure to the inflammatory environment of the injury site, take M1 polarization and promote inflammation through cytokine production (39). Following the activation of DCs, they become the dominant TNFα-producing cells, which can activate cell death signaling (40).

Monocytes and neutrophils possess micro-vesicles with tissue factor (39). They release these micro-vesicles and thus, promote coagulation (39). Protease-activated receptors (PARs), which are expressed on all innate immune cells, are activated by released coagulation proteases, such as thrombin, leading to the induction of pro-inflammatory cytokines (39). Platelets also release thrombin, when in contact with DNA released by necrotic cells (39). Moreover, platelets also release serotonin which promotes the recruitment of neutrophils (39). Other than tissue injury, leukocytes can be plugged in the microvasculature and cause a no-reflow phenomenon (39). No-reflow condition is defined as incomplete and uneven reperfusion at the microvascular level despite re-opening of the proximal artery, and it increases the risk of death following revascularization (12).

Taken together, activation of immune cells can lead to I/R injury through the initiation of the inflammatory response, blood coagulation cascade and inducing no-reflow phenomenon.

Activation of cell death pathways during I/R

As mention earlier, tissue injury occurs during both ischemic and reperfusion periods (1). The ischemic condition is accompanied by hypoxia, hyponutrition, and metabolic acidosis (41). Re-establishment of blow flow, however, initiates oxidative stress and local inflammatory responses leading to secondary injury (41). Various forms of cell death pathways are activated during I/R, depending on the severity of I/R (5). Moderate I/R only results in cell dysfunction, due to activation of recovery systems that can modulate ROS generation and activate autophagy. However, severe damage during I/R induces apoptotic or necrotic pathways (5). Four types of cell death mechanisms that occur during I/R will be discussed here.

Apoptosis is a programmed cell death that can be activated under hypoxic conditions during the ischemic period and by ROS production during reperfusion (42, 43). Apoptosis is composed of two main pathways, including extrinsic and intrinsic pathways (5). Both pathways can interact and influence each other (5). The extrinsic or death receptor pathway can be activated by death ligands and receptors namely TNF-α, TNF-like weak inducer of apoptosis (TWEAK), Fas ligand, TNF-related apoptosis-inducing ligand receptor (TRAIL), and TNF-like ligand 1A (TL1A) (5). This complex activates caspase-8, which then cleaves caspase-3. Caspase-3 induces cell death through proteolysis in damaged cells (5). The intrinsic or mitochondrial pathway is defined as changes in membrane integrity of mitochondria which leads to activation of the pro-apoptotic Bcl-2 family (5). The Bcl-2 family are a group of proteins that are either pro-apoptotic or anti-apoptotic and regulate mitochondrial membrane permeability (44). Bcl-2, Bcl-x, Bcl-XL, Bcl-XS, Bcl-w, and BAG are anti-apoptotic proteins and Bcl-10, Bax, Bak, Bid, Bad, Bim, Bik, and Blk are pro-apoptotic proteins in this family (44). Levels of these proteins determine if the cell is undergoing apoptosis or ceasing the process (44). The primary cell death mechanism used by the Bcl-2 protein family is changing mitochondrial membrane permeability, which leads to the release of cytochrome c (cyt c) from mitochondria (44).

In I/R, cytoplasmic Bad is elevated and attached to Bcl-2 and Bcl-XL proteins (45). On the other hand, Bax and Bak are inserted into the membrane of mitochondria, causing the release of pro-apoptotic proteins including cyt c, Smac/Diablo, HTRA2/Omi, apoptosis-inducing factor (AIF), and endonuclease G (Endo G) (45). Cyt c then activates caspase-9 to produce apoptosome by

binding to apoptotic protease activating factor-1 (APAF-1) (45). The apoptosome stimulates the caspase cascade to induce apoptosis (45). Endo G can also induce fragmentation of DNA by interacting with AIF (45). However, apoptosis is not accompanied by local inflammation and not the main cell death pathway during I/R (46).

Necrosis is a form of cell death that occurs due to excessive external stress, such as physical, chemical, or biological damage (47). It is characterized by permeation of the plasma membrane, cell swelling and loss of mitochondrial function (47). It can also activate local inflammatory responses (47). Necrosis extensively occurs in human pathology and is classified as a passive and unregulated form of cell death (47). However, recent studies have shown a form of programmed necrosis named necroptosis in I/R injury (47). Necroptosis is a programmed cell death regulated by death signals but has death characteristics similar to necrosis (47). As mentioned before, proteins such as receptor-interacting protein 1 (RIP1), fas-associated protein with death domain (FADD), cylindromatosis (CYLD), TNF receptor-associated factor 2 (Traf2), TNF-α and caspase-8 are implicated in apoptosis by activating death receptors (48). They can also activate necroptosis in some circumstances (48). When the situation is not optimal for apoptosis or caspase-8 is inhibited, necrosomes are formed, and the necroptosis process is activated (48). Rupture of mitochondrial, lysosomal and cells membranes are the primary characteristic of necroptosis (48).

Autophagy is a biological mechanism used by cells in order to degrade damaged cytoplasmic organelles and macromolecules (49). Under physiological conditions, it happens continuously at low levels in most cells (49). Defects in this process lead to the accumulation of damaged proteins and organelles (49). Therefore, it's considered as a survival mechanism. Nutrient and energy deprivation, oxidative stress, hypoxia, infection, protein aggregation, ER stress and others can trigger autophagy (49) to provide essential amino acids for cell survival. Recently, it is reported that it can selectively remove cytosolic damaged or harmful materials, such as damaged mitochondria (mitophagy) or proteins and act as a cytoprotective system (49). However, persistent autophagy can activate apoptosis (40). Thus, it is recognized as programmed cell death (40).

Previous experimental studies have shown that the autophagy process is activated during I/R, as it is accompanied by nutritional deficiency, acidosis, ER stress and oxidative stress (50). Inhibition of autophagy in I/R has been shown to reduce apoptosis following cold ischemia of the kidney and

improved renal function after transplantation (50). However, in another study, inhibition of autophagy stimulated the apoptosis of renal tubular cells and increased renal I/R injury (51). The results in cardiac I/R are also conflicting. Some studies showed protective effects of autophagy during I/R (52, 53), but others demonstrated that a high level of autophagy might increase cardiac I/R injury (54).

There are three forms of the autophagy process, including macroautophagy (the most abundant forms of autophagy), microautophagy, and chaperone-mediated autophagy (CMA) (55). In macroautophagy, a cell forms a double-layered membrane, derived from ER and Golgi apparatus, called a phagophore (55). The phagophore surrounds the damaged organelles and then fuses with the lysosomal membrane to form an autophagosome (55). In microautophagy, the lysosomal membrane encompasses the damaged component and digests it in the lysosome (55). The CMA pathway has a selectivity for soluble proteins (55). In this process, the chaperone is bound to the damaged protein and transports it to a lysosome (55). Autophagy is regulated and mediated by autophagy-related proteins and hormones (5). TOR complex 1 and Class III PI3K complex have the leading role in the induction of autophagy (40). TOR 1 senses changes in the nutritional status of the cell (40). In starvation, 5' AMP-activated protein kinase (AMPK) is stimulated, the mammalian target of rapamycin (mTOR) is inhibited, and consequently, autophagy is activated (40).

Mitophagy is mitochondrial degradation through macroautophagy, which is a quality control response to remove damaged mitochondria (53). During I/R, mitophagy is suggested to have a protective role against I/R injury through elimination of damaged mitochondria and therefore attenuation of ROS production (53). However, defective mitophagy is associated with mitochondrial damage, oxidative stress, and activation of apoptosis (40). Mitochondrial dynamics are the key factors regulating mitophagy (40). For instance, increased fission, and opening of the mPTP results in defective mitophagy, which occurs during I/R (40). This suggests that I/R interferes with mitophagy and thus mitochondrial damage and I/R injury (40). The detailed mechanism of mitophagy is as follows: stress elevates outer mitochondrial membrane permeability (OMM) through BAX (BCL2 associated X) and BAK (BCL2 antagonist/killer 1), which results in the release of pro-apoptotic proteins and cyt c (53). Moreover, mPTP opening, due to

Ca^{2+} overload in inner mitochondrial membrane (IMM), results in a rapid influx of water, and consequently, mitochondria swelling and rupture (53).

Therapeutic strategies for reducing myocardial I/R injury

Currently, there is no effective treatment for myocardial I/R injury (26). However, several therapeutic options have been tested, which can be classified as mechanical or pharmacological approaches (26). Ischemic preconditioning and post-conditioning are two major mechanical approaches that have been examined in previous works. Murray et al., (56) were the first group that examined the effects of ischemic preconditioning on myocardial I/R in dogs (56). They showed that brief cycles of occlusion before the ischemia reduced infarct size (56). However, this approach can not be applied in a clinical setting of myocardial I/R. Ischemia postconditioning was proposed by Zhao et al. (57). They showed that introducing three cycles of the 30s left anterior descending (LAD) artery occlusion and 30 sec of reperfusion followed by 3h reperfusion reduced infarct size by 44% in canine hearts (57). Staat et al., (58) demonstrated a 36% reduction of infarct size in a clinical setting of myocardial I/R. However, clinical studies with larger sample sizes did not show any significant effects (59, 60). The ongoing DINAMI-3 (Danish Study of Optimal Acute Treatment of Patients with ST-segment Elevation Myocardial Infarction-3) study is examining the effects of post-conditioning in 2000 patients with STEMI (61). The primary outcome of the study will be all-cause mortality or heart failure at 2 years (NCT01435408) (61). The remote conditioning also showed beneficial effects in an experimental model of myocardial I/R, in which several brief ischemic periods are introduced in a distant organ (61). A clinical study showed that using this method (4 cycles of 5 min inflation and 5 min brachial cuff deflations before PCI) decreased infarct size in 333 STEMI patients (62). A larger ongoing clinical trial, CONDI-2 (Effect of Remote Ischemic Conditioning on Clinical Outcomes in STEMI Patients Undergoing PPCI) is examining remote ischemic preconditioning on I/R injury in STEMI patients (NCT02342522) (62). Hypothermia has been reported to generate beneficial effects on myocardial I/R in experimental models (63, 64). However, its application in a clinical setting is limited due to the restricted cooling procedures that reach the targeted temperature (63, 64). Pharmacological interventions, such as cyclosporine A that inhibits the opening of MPTP pore, has shown promising results in experimental studies (65). A pilot study demonstrated that administration of cyclosporine A before PCI reduced infarct size (65). However, in the CIRCUS (Cyclosporine 29

and Prognosis in Acute MI Patients) study with 970 patients with STEMI, cyclosporine administration 12 hr after PCI, did not result in a better primary outcome (recurrent infarction, unstable angina, and stroke) at one year compared with controls. Infarct size was also not significantly different between the two groups (65).

The effects of beta-blockers on infarct size have been investigated in both experimental and clinical studies (66-70). However, the findings of these studies are conflicting (66-70). Metoprolol administration resulted in positive effects on infarct size in experimental studies (66, 67). However, clinical trials found contradictory results (68-69). In METOCARD-CNIC (Effect of early metoprolol on infarct size in ST-segment-elevation myocardial infarction patients undergoing primary PCI: the Effect of Metoprolol in Cardioprotection During an Acute Myocardial Infarction) trial with 270 STEMI patients, infarct size was significantly smaller and left ventricular ejection fraction was significantly higher in the metoprolol group compared with control (68). In the COMMIT trial (Clopidogrel and Metoprolol in Myocardial Infarction Trial) with 45,852 patients, metoprolol elevated the risk of cardiogenic shock, especially during the first few days after admission but reduced rates of ventricular fibrillation and reinfarction (69). Therefore, they concluded that the overall effect on death, reinfarction, arrest, or shock was significantly adverse during days 0-1 and significantly beneficial thereafter (69). A meta-analysis of randomized clinical trials, which included 60 trials with 102,003 patients, suggested that beta-blockers had no beneficial effects on mortality but decreased recurrent MI and angina (short-term) at the cost of increases in heart failure, cardiogenic shock, and drug discontinuation (70).

Experimental studies showed that glucagon-like peptide and its analogues decreased infarct size in animal models of myocardial I/R injury (71, 72). In a clinical study intravenous administration of Exenatide, which is a synthetic glucagon-like peptide analogue led to myocardial salvage (measured by magnetic resonance imaging) compared to placebo (73).

iii. Generation of oxidized lipids during I/R

Lipids are often neglected molecules impacted by I/R (74). As mentioned before, I/R leads to the production of ROS, which can attack cellular lipids, such as membrane PLs, and cause non-enzymatic lipid oxidation (74). Activation of membrane enzymes, for example, PLA2, also increases lipid oxidation by releasing PUFA from membrane phospholipids (74). Librated PUFAs

can enter into enzymatic oxidation pathways and thus another group of oxidized lipids, namely oxylipins, are generated (74).

Glycerophospholipids (GPL): general characteristics

Glycerophospholipids (GPL) are a group of lipids containing a phosphate head ester-bound to a glycerol backbone and two FAs (in sn-1 and sn-2 positions) linked through acyl chains to glycerol (75). The phosphate head group is further esterified with molecules, such as choline, ethanolamine, serine, glycerol and inositol (75). This makes several groups of GPL that named based on the structure of the phosphate head group (75). There are five groups of GPLs, including phosphatidylcholine (PC), phosphatidylethanolamine (PE), phosphatidylserine (PS), phosphatidylglycerol (PtG) and phosphatidylinositol (PI) (75). PC and PE are zwitterionic lipids whereas PS, PG and PI are anionic molecules (75). PC is the dominant PL in mammalian cells, which accounts for 40–50% of total cellular PLs (76). PE is the next most abundant PLs which comprises 40% of total PLs in mitochondrial inner membranes (76). In other organelles, however, it constitutes around 15–25% of total membrane PLs (76).

FAs in PL structure are varied in terms of carbon chain length and saturation degree (77). Palmitic acid (PA) (16:0) and stearic acids (SA)(18:0) are the two most abundant FAs in the *sn-1* position of PLs. AA (20:4) and LA (18:2) are the two most abundant FAs in the *sn-2* position of membrane PLs, which contain unsaturated covalent double bonds in their structures (77). Besides n-6 PUFA, n-3 PUFA, such as eicosapentaenoic acid (EPA) (20:5), and docosahexaenoic acid (DHA) (22:6) can be found in the *sn-2* position of membrane PLs (77).

PUFAs in the *sn-2* position of the PL membrane are generally the target of non-enzymatic or enzymatic oxidation, as the energy needed for the dissociation of bisallylic carbon-hydrogen bonds is low and therefore, the hydrogen atom can quickly react with molecular oxygen (78). Non-enzymatic oxidation initiates with non-radical ROS (singlet oxygen) or free radicals from endogenous (oxidative enzymes)/exogenous sources (air pollution, UV radiation, smoking) (79, 80). Superoxide radicals are the main radical that interacts with membrane PLs, thus, membranes close to the site of superoxide generation, such as mitochondria, are more likely to become oxidized (79, 80).

Non-enzymatic oxidation of PLs: mechanism and products

The overall process of FA peroxidation consists of three steps: initiation, propagation, and termination (81). In the initiation step, prooxidants like the hydroxyl radical abstract the allylic hydrogen forming the carbon-centred lipid radical (L•) (81). In the propagation phase, a lipid radical (L•) rapidly reacts with oxygen to form a lipid peroxy radical (LOO•) which is accompanied by the abstraction of hydrogen from another lipid molecule, generating a new L• (that continues the chain reaction) and a lipid hydroperoxide (LOOH) (81). In the termination reaction, antioxidants like vitamin E donate a hydrogen atom to the LOO• species and form a corresponding antioxidant radical that reacts with another LOO• forming nonradical products (81).

Peroxyl radical of FA esterified to PL can also undergo cyclization, rearrangements or further oxidation to produce new forms of products (6). These oxidized forms of PLs, which remained esterified to PLs, are called non-fragmented OxPLs (6). Isoprostanes, isolevuglandins, isothromboxanes, and isofuran are examples of non-fragmented oxidized PLs (OxPLs) (82).

On the other hand, lipid hydroperoxide (LOOH) can be transformed into cleaved oxidized molecules (83). For instance, fragmentation/cleavage of hydroperoxides through b-scission, Hock rearrangement, or cyclization of alkoxy/radicals give rise to hydroxyl or keto PLs with saturated /unsaturated FAs and an aldehyde terminal group (83). Aldehydes can be further oxidized to carboxylic unsaturated PLs (81). In addition to a direct generation from hydroperoxides, further oxidation of fragmented PUFA-PLs can produce saturated fragmented compounds with the carbonyl group, which are more stable and resistant to further oxidation (81). The most common species are oxononanoate and azelaoate produced from LA and oxovaleroate, and glutaroate generated from AA (81).

There are several mechanisms for the termination of PL oxidation and elimination of OxPLs (81). Reactive peroxide groups of OxPLs can react with antioxidants, or reduced by GPX4, peroxiredoxin VI (PRDX6) and GST (81). Reactive carbonyl groups in OxPLs can be also reduced by aldo-keto-reductases (81). Lipoprotein-associated PLA2 (Lp-PLA2) and lecithin-cholesterol acyltransferase (LCAT) can also cleave oxidized residues of PLs producing lyso-PLs and oxidized free fatty acids (81). Moreover, carbonyl-containing OxPLs can form covalent complexes with amines through Schiff's base (reacting with lysine residues) and Michael reactions (reacting

with histidine, cysteine and lysine) and make protein adducts (81). The formation of a protein adduct inactivates OxPLs but can cause protein damage (81).

As an example, simplified steps of non-enzymatic oxidation of 1-palmitoyl-2-arachidonoyl-sn-phosphatidylcholine (PAPC), which is a membrane PL, and production of fragmented and non-fragmented OxPCs are presented in Figure 1.

Figure 1: Non-enzymatic oxidation of membrane phospholipids

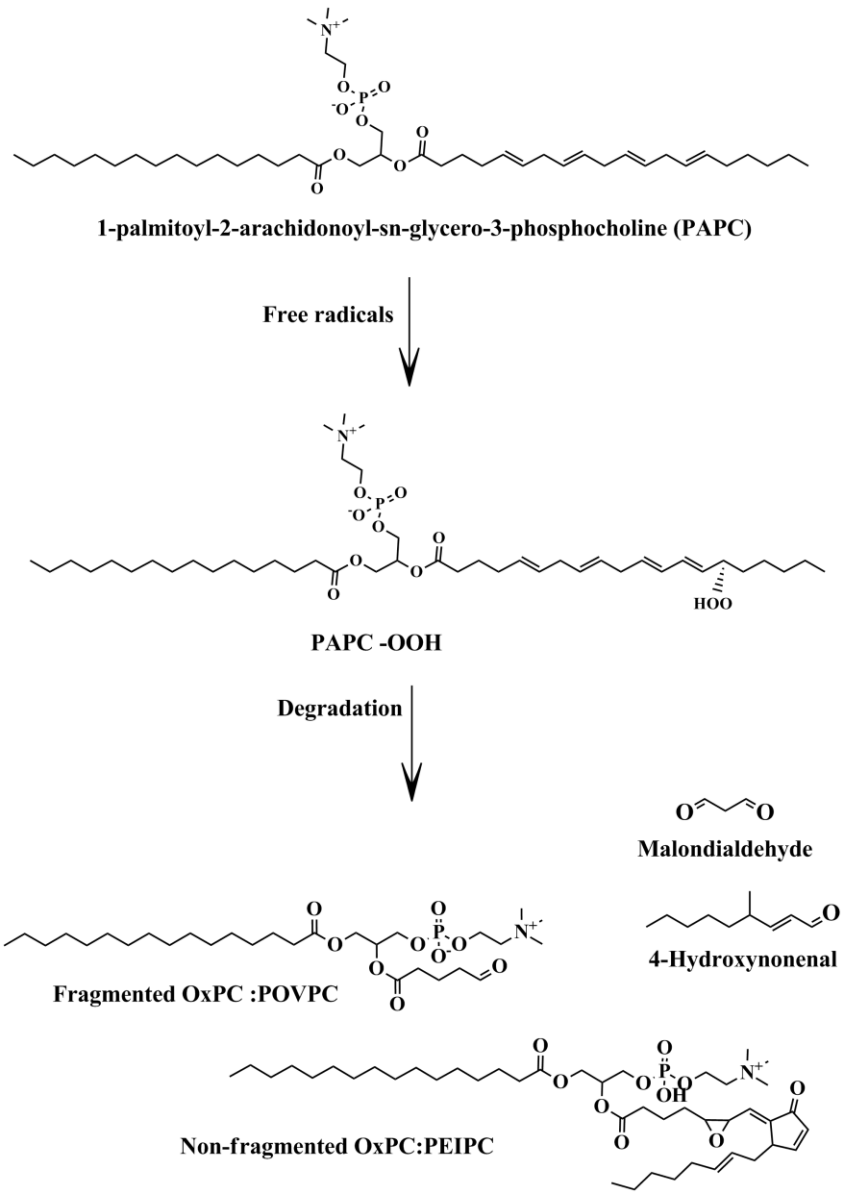

Free radicals can attack membrane phospholipids, such as PAPC, leading to the production of bioactive lipid molecules. Abbreviations: PAPC: 1-palmitoyl-2-arachidonoyl-sn-phosphatidylcholine, PAPC-OOH: PAPC hydroperoxide. OxPC: oxidized phosphatidylcholine. PEIPC: 1-palmitoyl-2-(5,6-epoxyisoprostane E2)-sn-glycero-3-phosphocholine. Solati Z, Ravandi A. Lipidomics of bioactive lipids in acute coronary syndromes. International journal of molecular sciences. 2019 Jan;20(5):1051.

Impact of PL oxidation on the structure of the cell membrane and immune responses

One of the first consequences of PLs oxidation is significant increases in membrane permeability, resulting in disruption of ionic gradients and accumulation of Ca^{2+} in the cells (84). Increased intracellular Ca^{2+} concentrations are accompanied by the activation of Ca^{2+} dependent phospholipases leading to the generation of PL hydrolysis products, such as free FAs and lyso-PLs, and thus membrane disruption (84). Increased production and accumulation of lipid peroxidation products can change nucleophilic sites of membrane proteins and cause more oxidative damage (84). These dramatic consequences of non-specific lipid peroxidation are associated with pathogenic oxidative injury and chronic inflammation in diseases, such as arteriosclerosis, neurodegenerative diseases, and renal disorders (84). Furthermore, PL oxidized products are immunogenic and can activate immune responses in the cells. For example, various antibodies have been identified that have specific reactivity toward oxidized products of PC (OxPCs) (85, 86).

E0 antibodies are natural antibodies (N-Abs), which are germ-line encoded recognizing DAMPS that are produced from sub-set of B-lymphocytes (87). The E0 antibodies produced against OxPLs were derived from mice lacking apolipoprotein E (88). Among 17 different E0 antibodies identified, the E06 antibody has the least reactivity to native PC but is highly sensitive to oxidized 1-palmitoyl-2-arachidonyl-sn-glycero-3-phosphocholine (Ox-PAPC), and 1-palmitoyl-2-oxovaleroyl-sn-glycero-3-phosphorylcholine (POVPC) in comparison with other E0 antibodies (88). Over 85% of plasma E06 is bound to Lp (a); from these, about 50% are bound to apoB and apoA covalently, and the rest non-covalently (89). By using the E06 antibody, the presence of OxPCs was confirmed on OxLDL, macrophages and apoptotic cells (89).

Biological properties of OxPLs on the cardiovascular system

As discussed above, PL oxidation leads to the formation of several oxidized metabolites, including different species of fragmented and non-fragmented species (81). Oxidation of each PUFA gives rise to at least 50 metabolites with different biological activities (90). It has been shown that only

4 hours of treatment of human aortic endothelial cells (HAEC) with 40 µg/ml of Ox-PAPC, modulates more than 1000 genes implicated in inflammation, angiogenesis, cell division, thrombosis, vasoconstriction, etc. These effects, however, were not seen after non-oxidized PL exposure (91).

Atherosclerosis

OxPLs have been implicated in various stages of atherosclerosis. Hörkkö et al. were the first group that revealed that OxPLs have roles in Ox-LDL recognition by macrophages, which results in foam cell formation (92). Subsequently, they showed that monoclonal antibody E06, prevented Ox-LDL recognition by macrophages, which demonstrates the importance of OxPLs in the initiation of atherosclerosis (88). Besides lipoproteins, OxPLs have been identified in atherosclerotic lesions, and in membrane vesicles released from activated and apoptotic cells, which play an essential role in the development of atherosclerosis (93-95). OxPLs can interact with CD36 receptors on macrophages (96). In CD36-null mice, there is a lack of uptake of macrophages, resulting in an increase in apoptotic cells and their debris, and thus plaque progression (96). OxPLs can also induce apoptosis in macrophages, which can lead to the formation of a necrotic core and advanced atheroma, provided that it occurs after foam cell formation (97).

Another mechanism that links OxPLs to atherosclerosis is through activation of inflammatory responses in the endothelium (98). Pro-inflammatory effects of the OxPLs were suggested when it was shown that minimally modified-LDL (MM-LDL) triggered inflammatory reactions in endothelial cells (98). Later studies revealed that the inflammatory properties of MM-LDL are mediated by OxPLs in cultured endothelial cells and animal models (99-101).

Endothelial cells

The mechanisms of OxPL-mediated endothelial cell activation are complex and distinct from those induced by other inflammatory stimuli, such as bacterial lipopolysaccharide (LPS) or TNF-α (81). For instance, treatment of endothelial cells with bacterial LPS leads to the recruitment of both monocytes and neutrophils whereas Ox-PAPC stimulates only monocyte recruitment (not neutrophils) (102). Furthermore, unlike bacterial LPS or TNFα that upregulate the expression of cell adhesion molecules (such as E-selectin or VCAM-1), Ox-PAPC did not affect the expression of these cytokines in an *in vitro* model (103) or a mouse air pouch model of inflammation (102).

One of the proposed mechanisms is that Ox-PAPC activates the cAMP-dependent R-Ras/PI3-kinase pathway (104). OxPCs elevate connecting segment-1 (CS-1) fibronectin by increasing cAMP activated R-Ras proteins, which are small GTPases located at the inner surface of the plasma membrane (104). Fibronectin acts as a cross-link between α5β1 integrin on endothelial cells and α4β1 integrin (VLA-4) on leukocytes (306). This mechanism is likely related to the atherogenicity of OxPCs as activated β1 integrin and CS-1 fibronectin was reported in atherosclerotic plaques at the sites of mononuclear cell infiltration (306). Moreover, administration of peptide mimicking the VLA-4-binding site of CS-1 fibronectin inhibited the formation of lesions in LDL receptor knockout mice (305). Non-fragmented isoprostane containing OxPC (PEIPC) was identified as a potent component of Ox-PAPC activating this pathway via prostaglandin E2 receptor (105).

OxPLs can interact with peroxisome proliferator-activated receptor α (PPARα) in endothelial cells, and therefore, stimulating the secretion of monocyte chemotactic protein-1 (MCP-1) and interleukin-8 (IL-8) (106). MCP-1 is a member of the CC family of chemokines and have a critical part in monocyte transmigration, whereas IL-8 mediates monocyte arrest to vascular endothelium (107). Once monocytes are present in an atherosclerotic lesion, they continue to induce inflammation via stimulation of the Toll-like receptor 2, inducing inflammatory cytokine production and further macrophage recruitment (108).

Inflammation

Besides the endothelium, OxPLs can also induce pro-inflammatory reactions in mononuclear leukocytes, such as monocytes, macrophages, and DCs, through activation of the inflammasome (109). Recent evidence demonstrated that POVPC stimulated activation of procaspase-1 and generation of mature IL-1β and IL-18 in primary mouse bone marrow-derived macrophage (109). The proposed mechanism was that POVPC activated the NLRP3 inflammasome by inducing the generation of mitochondrial ROS (109). The authors confirmed their hypothesis by showing that suppression of ROS production, using NADPH oxidase inhibitors, resulted in the blockade of mitochondrial ROS production and the NLRP3 inflammasome (109). Another study showed that Ox-PAPC in DCs could directly bind to caspase-11 and induced the release of IL-1β (110). Caspase-11 is an LPS receptor that promotes IL-1β release by noncanonical inflammasomes (110). Neutrophils are another group of immune cells that can serve as OxPCs targets (111-113). POVPC

and PAzPC can interact with the PAF receptor, which is highly expressed on neutrophils and stimulates adhesion, lysosomal enzyme release, and an oxidative burst by neutrophils (111-113).

Coagulation cascade

Besides the inflammatory and atherogenic properties of OxPLs, they also affect the coagulation cascade (114). It has been shown that treatment of HUVECs with Ox-PAPC upregulates the expression of tissue factor (TF), a known procoagulant protein, in endothelial cells by increasing the levels of free cytosolic Ca^{+2} and nuclear factor of activated T cells (NFAT) (114). OxPLs also modulate TF expression through activation of sterol regulatory element-binding protein (SREBP) and extracellular signal-regulated protein kinase (Erk1/2) via activation of vascular endothelial growth factor receptor 2 (VEGFR2) in endothelial cells (115). Moreover, fragmented OxPLs generated from sn-2 arachidonoyl-, docosahexaenoyl-, or linoleoyl-phospholipids containing sn-1 alkyl or acyl bonds have structural similarities with platelet-activating factor (PAF) and can cause platelet aggregation by elevating the expression of P-selectin and thus conformational changes in platelet (116, 117). Moreover, fragmented OxPLs characterized by sn-2 residues containing terminal γ-hydroxy(or oxo)-α,β-unsaturated carbonyl, such as KODA-PC (1-acyl-2-(9-keto-12-oxo-10-dodecenoate)-sn-glycero-3-phosphocholine), can bind to bind platelets via CD36 receptor and stimulated activation of fibrinogen receptor on platelets and induced binding of fibrinogen (118).

Cell death

OxPLs have been reported to be involved in cell death pathways (119). They can be generated during apoptosis and can also induce apoptosis in different cell types (119). As a result of apoptosis, lipid asymmetry in the membrane is lost, causing the exposure of PS on the outer leaflet of the plasma membrane (119). PS can be oxidized in apoptotic cells by cyt c, which is released into the cytosol during apoptosis, at the inner side of the plasma membrane (119). Both exposed PS and oxidized PS (OxPS) can be served as a signal for macrophages to phagocytose the apoptotic cell (120, 121). Oxidation increases the probability of phagocytosis (120, 121). OxPCs also have been identified on apoptotic cells using the monoclonal antibody E06 (92). E06 antibody can interfere with phagocytosis of the apoptotic cells, demonstrating that in addition to OxPS, the

presence of OxPCs on the surface of the apoptotic cell is a crucial factor for macrophage phagocytosis (122).

OxPCs can induce apoptosis in different cell types (123). Treatment of rat vascular smooth muscle cells (rVSMCs) with low concentrations of POVPC and PGPC led to DNA laddering, PS exposure on the cell surface, and reduction of the nuclear volume, which all are apoptotic events (123). In another study conducted by Ramprecht et al., POPVC and PGPC induced apoptosis in human melanoma cells isolated from different stages of tumour progression (124). The mechanism that has been proposed for cell toxicity of POVPC and PGPC in these studies was through the "sphingomyelinase-MAPK" pathway (124). These fragmented OxPCs can activate sphingomyelinase, which leads to the formation of ceramide from sphingomyelin (SM) (124). Ceramide is a lipid messenger that mediates numerous cellular phenomena including apoptosis, proliferation, cytokine release, and differentiation (125, 126). Ceramide activates mitogen-activated protein kinases (MAPK) c-Jun N-terminal kinase (JNK) and p38 MAPK, which leads to caspase activation, PS exposure, and apoptosis (127). The sphingomyelinase-MAPK pathway is usually activated in conditions associated with oxidative stress (127).

Some studies reported that OxPC species induce apoptosis through mitochondrial damage and the intrinsic pathway (94). Treatment of promyelocytic HL60 cells and HUVEC with 1-O-hexadecyl-2-azelaoyl-sn-glycero-3-phosphocholine (HAzPC) induced apoptosis through interacting with Bcl-2 family proteins, released of mitochondrial cyt c, apoptosis-inducing factor (AIF) and activated caspase 9 in these cells (94). They also showed that HAzPC induced mitochondria swelling, cyt c and AIF release, suggesting that exogenous OxPCs target intracellular mitochondria, in order to activate the intrinsic apoptotic cascade (94).

New evidence shows that OxPLs also have a role in ferroptosis (128). Ferroptosis is an iron-mediated form of regulated cell death that occurs as a result of depletion of glutathione, inhibition of GPX4, and thus the accumulation of lipid hydroperoxide (128). It has been reported that ferroptosis is implicated in the pathology of tumorigenesis, renal failure, I/R injury, nervous system diseases, and haematological system disease (128). GPX4 enzyme converts the toxic lipid peroxide to a lipid alcohol by oxidizing GSH to GSSG (129, 130). Inhibition or absence of GPX4 leads to the accumulation of lipid peroxides, which are lethal signals of ferroptosis (131).

Oxolipidomic analysis of kidneys in Gpx4−/− mice revealed that accumulation of several classes of phospholipid hydroperoxides such as PC, PE and cardiolipin peroxide in the kidney led to ferroptosis (132). This data suggests the involvement of mitochondria in the deregulated lipid peroxidation caused by GPX4 deficiency. However, the exact mechanism is yet to be known (132).

The role of OxPLs in cardiovascular disease (CVD): evidence from experimental studies

Que et al., (133) evaluated the proatherogenic and proinflammatory effects of OxPLs in an i*n vivo* model. They generated transgenic *Ldlr−/−* mice that expressed a single-chain variable fragment of E06 (E06-scFv) (133). E06-scFv can be secreted into the plasma from liver and macrophages and deactivate endogenously produced OxPLs (133). The E06-scFv antibody can only bind to OxPLs and does not have the functional effects of an intact antibody (133). In this study, *Ldlr*$^{-/-}$E06-scFv mice, fed with a hyper-cholesterol diet, had significantly lower atherosclerosis (calculated by per cent of aortic surface involved by en face analysis) compared to *Ldlr*$^{-/-}$ mice fed the same diet (133). Moreover, necrotic core areas of plaques were significantly smaller and contained more collagen in *Ldlr*$^{-/-}$E06-scFv mice compared with size-matched lesion controls (133). Furthermore, *in vivo* macrophage uptake and cholesterol content of macrophages of *Ldlr*$^{-/-}$E06-scFv mice were significantly lower compared with *Ldlr−/−* mice (133). Serum amyloid A was also significantly lower in *Ldlr−/−E06-scFv* mice (133). This study suggested that antibodies against OxPLs can attenuate atherosclerosis and reduce systemic inflammation (133).

Recently, Cherepanova et al., (134) generated a novel IgM autoantibody against POVPC and PGPC, named10C12, from the spleens of Apoe–/– mice fed a long-term Western diet (134). They found that treatment with the 10C12 antibody prevented the early inflammatory response and macrophage accumulation within arteries of Apoe–/– mice fed a short-term Western diet (134). 10C12 antibody administration also reduced atherosclerosis in aged IgM–/–Apoe–/– mice fed a standard low-fat diet with modest hyperlipidemia (134). However, it did not change pre-existing atherosclerotic plaque pathogenesis in hyperlipidemic Apoe–/– mice fed a long-term Western diet (134). These results suggested that treatment with an anti-OxPL IgM antibody have atheroprotective effects (134).

Recent data from our lab showed that OxPCs are involved in I/R injury and deactivating them can prevent cell death during I/R. In the *in vitro* part of the study, it is shown that OxPCs, namely,

PONPC, POVPC, PGPC and KOdiAPC were produced following I/R in cultured neonatal rat cardiomyocytes (NNCM) (135). Furthermore, incubating cultured NNCM with OxPCs species induced cardiomyocytes cell death in a concentration-dependant pattern (135). Cell death was attenuated when OxPCs species were co-administered with E06 (135). Next, the changes in OxPCs were investigated in the rat myocardium during coronary I/R (135). After 1 h of ischemia (induced by the ligation of the coronary artery) and subsequent 24 h of reperfusion, levels of OxPCs, namely POVPC, PGPC, PONPC, KOdiAPC, and PAzPC, were elevated in rat myocardium compared with control (135). Levels of POVPC and PONPC, but not other identified OxPCs, were elevated in the mitochondrial fraction of cardiomyocytes and mitochondria membrane (135). Transgenic Ldlr−/− mice that overexpress a single-chain variable fragment of E06 (Ldlr−/−-E06-scFv-Tg) were used to show how inactivating endogenously formed OxPL *in vivo* can affect myocardial infarct size (135). It was shown that Ldlr−/−-E06-scFv-Tg mice had significantly smaller myocardial infarct size compared with controls (135).

In a recent study by Pluijmert et al., (136) the effects of PC-mAb, which is anti-phosphorylcholine IgG was assessed in an *in vivo* model of myocardial I/R injury in hypercholesterolemic mice (136). MI was induced in 12- to 14-week-old female APOE∗3-Leiden mice by ligation of the left anterior descending coronary artery (136). Subsequently, 10 mg/kg PC-mAb or NaCl 0.9% w/v (vehicle) was administered intraperitoneally (every third day until 3 weeks) in the intervention and control group, respectively (136). Infarct size and LV fibrosis were significantly lower in the PC-mAb group compared with the control (136). PC-mAb treatment also decreased the post-ischemic inflammatory response following I/R by reducing inflammatory cytokine CCL2 levels and circulating Ly-6Chi monocytes, which resulted in reduced myocardial leukocyte infiltration and preservation of LV wall thickness (136).

The role of OxPLs in ACS: evidence from clinical studies

As mentioned before, Tsimikas et al. developed a method to measure OxPL per apoB-100 (OxPL/poB) in plasma using E06 antibody (137). They showed that OxPL levels increase significantly in MI patients after PCI, suggesting that these compounds are released and/or generated in plasma as a result of plaque rupture (137, 138). Later, prospective studies have shown that OxPLs levels can be considered as a biomarker to predict the progression of atherosclerosis, cardiovascular death, MI and stroke (139-143). In a study of 504 patients who underwent

angiography, levels of oxLDL-E06 (OxPL/apoB) were significantly correlated with lipoprotein (a) (LP(a)) levels (139). Moreover, both OxPL/apoB and Lp(a) were strongly associated with the extent of coronary artery disease (CAD) defined as the number of vessels with stenosis of more than 50% of the luminal diameter (139). In the Bruneck study, 765 Caucasian patients were followed for 15 years (140). After 10 years of follow-up, it is found that patients with the highest tertile of OxPL/apoB had significantly elevated cardiovascular events compared with those in the lowest tertile, after adjustment for traditional risk factors, high-sensitivity c-reactive protein (hs-CRP) and lipoprotein-associated PLA2 activity (140). At 15-year of follow-up, the highest quartile of OxPL/apoB was associated with having an ischemic stroke, acute CAD and death compared with the lowest tertile (141). The results of the EPIC-Norfolk study were also in line with the Bruneck study (142). EPIC-Norfolk study was a prospective, case-controlled study of 763 cases and 1397 healthy controls followed for 6 years (142). They found that subjects with the highest tertile of OxPL/apoB had a significantly higher risk of CAD events (142). This association was independent of the Framingham Risk Score (142). These findings were supported by a study by Dijk et al., (143). They showed that levels of epitopes of OxPLs recognized by E06 on the atherosclerotic plaque were elevated in progressive rather than early lesions, demonstrating that OxPLs were specifically associated with unstable and ruptured plaques (143). Two clinical studies showed that plasminogen, which has a structural similarity with LP(a), is the second pool of OxPL in plasma (144-145). In a study by Leibundgut et al., levels of OxPL-Plasminogen increased acutely over the first month after MI (144). However, in a recent study by DeFilippis et al., levels of OxPL-Plasminogen did not change following MI but it was lower in patients with atherothrombotic MI (Type 1) compared with patients with non-atherothrombotic MI (Type 2) (145). They suggested that OxPL-Plasminogen plays a clinically relevant role in clot lysis (145).

Oxylipins: general characteristics

Oxylipins are a group of oxidized lipids that are produced in response to inflammatory conditions, mainly by the activation of PLA2 (7). Once PLA2 is activated, FAs are released from membrane PLs into the cytoplasm, resulting in the generation of substrates for downstream enzymes (7). Released FAs can enter into several oxidation pathways and produce bioactive oxidized lipids named eicosanoids or oxylipins (Figure 2) (7). Over 100 oxylipins have been identified in human plasma and many with potent biological activities (7). However, changes in oxylipin levels in

human myocardial I/R injury is poorly understood. In this section, we describe the important roles that oxylipins play in inflammatory pathologies and their potential impacts on I/R injury.

Figure 2: Enzymatic oxidation of PAPC, a membrane PL

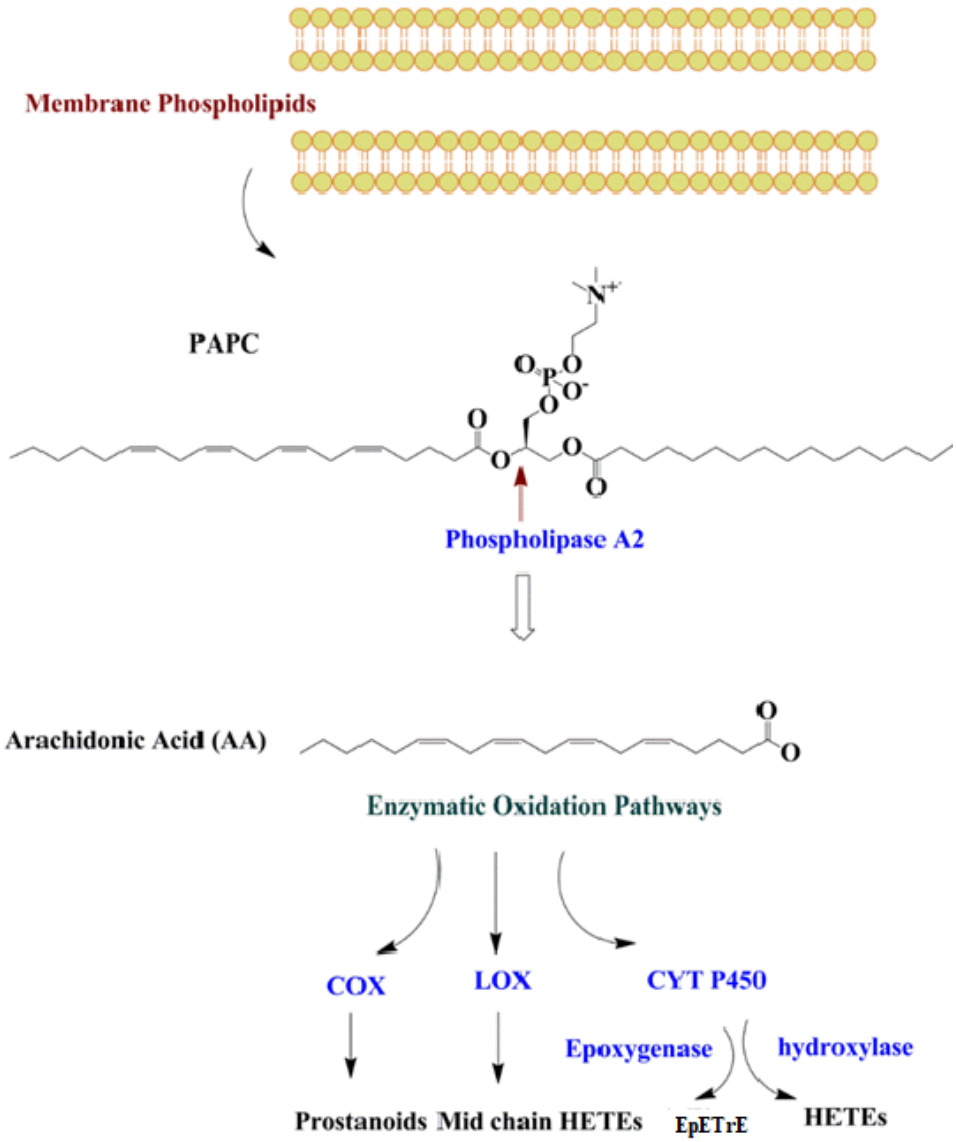

Fatty acids, such as arachidonic acid, can be released from membrane phospholipids (here PAPC) by a phospholipase A2 enzyme. Released FA can undergo oxidation through three oxidative pathways including COX, LOX and CYT P450. **Abbreviations**: AA: Arachidonic acid, COX: Cyclooxygenase, CTY P450: Cytochrome P450. HETE: Hydroxyeicosatetraenoic acids, EpETrE: Epoxyeicosatrienoic acids, PAPC:1-Palmitoyl-2-arachidonyl-sn-glycero-3-phosphatidylcholine, LOX: Lipoxygenase. Solati Z, Ravandi A. Lipidomics of bioactive lipids in acute coronary syndromes. International journal of molecular sciences. 2019 Jan;20(5):1051(Article is licensed under an open access Creative Commons CC BY 4.0 license).

Oxylipins biosynthetic pathways

There are several groups of PLA2 enzymes in eukaryotic cells, based on their structure, function, and co-factor requirement (146). Secreted PLA2s (sPLA2), cytosolic calcium-dependent PLA2s (cPLA2) and calcium-independent PLA2s (iPLA2) are three main groups of PLA2 enzymes (146). sPLA2s are low molecular weight enzymes (13–15 kDa), which contain histidine in the catalytic site and Ca^{2+} bound in the active site (146). The sPLA2s demonstrate similar preferences to PLs with different FAs in the *sn-2* position (146). It has been shown that they have potent antimicrobial properties since they can be mobilized to the sites of inflammation and hydrolyze membrane PLs of gram-positive bacteria (147). Its been also suggested that sPLA2s have pro-inflammatory activity, not only by releasing AA from PLs but also through binding to integrins αvβ3, which is expressed by both endothelial cells and macrophages during inflammation (148). cPLA2s are another group of PLA2s that require Ca^{2+} for their activity (149). They contain serine in the active site and are the only PLA2s that have preferences for AA in the *sn-2* position of PLs, thus they play a significant role in inflammatory diseases (149). The second messengers, including ceramide-1-phosphate and phosphatidylinositol bisphosphate (PIP2), have been reported to activate the cPLA2 enzymes (150). iPLA2 enzymes do not require Ca^{+2} for their catalytic activities (150). They also contain a serine in the active site but do not exhibit specificity for an AA in the sn-2 position (150). Their activities are regulated by ATP binding, caspase cleavage, calmodulin, and possible ankyrin repeat mediated protein aggregation (150).

Released FAs by PLA2s can be further oxidized through three main enzymatic pathways including COX, LOX, and CYP450 (151). COX enzymes are present in nearly every cell of the human body and convert PUFA into prostanoids (i.e. prostaglandins (PGs) and thromboxanes (TXs) (151). There are two forms of COX enzymes in the human body: COX-1 and COX-2. COX-1 is expressed in most tissues and demonstrate housekeeping functions under normal conditions (151). COX-2, however, is not normally expressed or present only in a very low concentration in cells (151). Pro-inflammatory cytokines (such as IL-1β and TNFα), hormones, growth factors and lipid peroxide (i.e. 4-hydroxy-trans-2-nonenal (HNE)) increase COX-2 expression (151). Prostaglandin H2 (GH2) is the first AA-derived product produced by COX enzymes, which can be subsequently converted to other series 2 prostanoids including PGE2, PGI2, PGD2, PGF2α, and TXA2a (151).

γ-linolenic acid (GLA), and EPA are also substate of COX enzymes and precursors of series 1 and 3 of prostanoids, respectively (152).

Prostanoids mediate their biological effects through both cell surface and intracellular receptors, such as G protein-coupled receptors and PPARγ, respectively (152). Prostanoid receptors are divided into three groups, based on the way of signals transformation: IP (PGI receptor), DP (PGD receptor), EP2 (PGE receptor), and EP4 mediate signals by increasing the intracellular level of cAMP and are considered as "relaxant" receptors (152). TP (TX receptor), FP (PGF receptor), and EP1 elevate intracellular Ca^{2+} and are denoted as "contractile" receptors (152). EP3 induces a reduction in the intracellular concentration of cAMP and is termed an "inhibitory" receptor (152).

LOX enzymes are the second oxidative pathway oxidizing free FAs (153). There are 8 types of LOX enzymes in the body, but 3 of them (5/12/15-LOX) are the most studied enzymes (153). 4-series leukotrienes (LTs) and hydroxyeicosatetraenoic acids (HETE) are derived from the AA from LOX pathways (153). EPA metabolism is similar to AA, but it is the precursor of 5-series leukotrienes and hydroxyeicosapentaenoic acids (HEPE) (153). DHA can also be oxidized by LOX enzymes (153). Similar to COX derived oxylipins, LOX derived oxylipins interact with G protein-coupled receptors and intracellular effectors to mediate their effects (153).

CYP450 enzymes, the third enzymatic pathways in oxylipin metabolism, are a diverse group of membrane-bound enzymes present within all cells and initially known for their roles in xenobiotic metabolism (7). These enzymes have epoxygenase (CYP2C or CYP2J enzymes) or ω-hydroxylase (CYP4A or CYP4F enzymes) activities (7). CYP450 epoxygenases oxidize AA to epoxyeicosatrienoic acids (EpETrE), which can be converted into the corresponding diols (dihydroxyeicosatrienoic acids (DiHETrE)) by soluble epoxide hydrolase (sEH) enzyme (7). 11,12- and 14,15- EpETrE constitutes 67–80% of all produced EpETrEs (154). CYP450 epoxygenases oxidize LA to epoxyoctadecenoic acids (EpOME), and EPA/DHA to epoxyeicosatetraenoic acids (EpETE) /epoxydocosapentaenoic acids (EpDPE), respectively (154). 9,10-EpOME is the main LA-derived epoxide, which is subsequently hydrolyzed by the sEH enzyme to 9,10-dihydroxyoctadecaenoic acid (9,10-DiHODE) (155). Plasma concentrations of 9,10-DiHODE are much higher than other PUFA-derived diols in healthy American adults showing that the western diet is rich in LA (156).

CYP450 hydroxylases are other groups of enzymes in this pathway that produce HETEs from AA, HEPEs, and HDoHEs from EPA and DHA, respectively (157). Oxylipins derived from this pathway mediate their effects via specific receptors or by cross-reacting with other oxylipin receptors (7). Moreover, they can also enter the cells and modulate transcription factors and ion channels (7).

Biological properties of oxylipins

Since the identification of oxylipins nearly 80 years ago, numerous physiological and pathological properties have been attributed to them (158). PGs were the first group of oxylipins discovered in the early 1930s (158). Since then, many studies have investigated their roles in different conditions, such as blood pressure, thrombosis, atherosclerosis, etc (158). Prostanoids have pleiotropic cardiovascular effects (152). For example, PGI2, which is mainly produced by vascular endothelial cells, has potent vasodilatory effects (152). However, TXA2, which is primarily produced by platelets, demonstrates vasoconstricting actions. Moreover, PGI2 and TXA2 demonstrate opposite effects in thrombosis through their opposing actions on platelet aggregation (152), expression of tissue factor (159), and plasminogen activator inhibitor-1 (PAI-1) (160). Inhibition of COX enzymes using pharmacological drugs also demonstrated contrary results on the cardiovascular system (161-163). For instance, aspirin, which is a non-steroid anti-inflammatory drug (NSAIDs) and a COX-1 inhibitor, suppresses TXA2 generation and demonstrates cardiovascular protection (163). However, the results of two epidemiological studies, including SCOT (161) with 7297 participants and PRECISION (162) with 24,081 patients, confirmed that other NSAIDs increase the risk of cardiovascular and thrombotic events. It is proposed that all NSAIDs, except aspirin, increase the risk of a cardiovascular event by as much as 30% (163). The proposed mechanism for the beneficial effects of aspirin is that it only targets TXA2 production by permanent inhibition of platelet COX-1, but not the other prostanoids (163). COX-2 inhibition is associated with decreased levels of PGI2 and increased sensitivity to TXA2 and therefore, thrombosis (164). Endothelial cells can also produce COX-1 dependent PGI2, but platelet COX-1 dependent TXA2 production plays a dominant role in thrombogenesis (164).

Prostanoids are also implicated in atherosclerosis and their roles in atherosclerosis have been extensively investigated (164). Both inflammatory cytokines secreted by macrophages (namely IL-6 and TNF-α) and oxidized lipids produced within the macrophages (such as HNE), induce

COX-2 production at the site of atherosclerotic plaque (165). The role of COX-2 in atherogenesis is complex, as generated prostanoids have both pro and anti-atherogenic effects (166). Among all COX-derived oxylipins, PGD2, PGE2, TXA2 and PGI2 are most involved with atherosclerosis (166). PGD2 is mainly produced in leukocytes by PGD synthase, in response to inflammation (167) and PAF (168), and causes platelet activation (166). However, it is also the precursor of 15-deoxy-12,14-prostaglandin J2 (15-dPGJ2), which is a ligand for PPARγ (166). Activation of PPARγ impacts atherosclerosis through a variety of mechanisms, such as inhibition of VSMC cell growth and migration, stimulation of VSMC apoptosis, and modulation of macrophage recruitment (166).

PGE2 is generated within myeloid-lineage derived cells (169). It's reported that PGE synthase-1 colocalizes with COX-2 in a setting of inflammation and its deletion reduces atherogenesis in fat-fed hyperlipidemic mice (169). Nevertheless, PGE2 has complex biological activities as it can interact with different receptors (166). For instance, EP-1 and EP-3 receptors mediate PGE2-induced vasoconstriction, whereas the EP-4 receptor is the primary mediator of the anti-inflammatory effects of PGE2 (166).

As mentioned before, TX synthase presents mainly in platelets, but it can be expressed in monocytes and vascular smooth muscle cells as well (170). Previously, it has been shown that blocking platelet TXA2-dependent formation is associated with primary and secondary prevention of the vascular complication of atherosclerosis (170). Furthermore, inhibition of TXA2 biosynthesis or blocking its receptors, led to the suppression of atherosclerosis progress in mice (171, 172). PGI2, on the other hand, is generated mainly by vascular endothelial cells via the prostacyclin synthase enzymatic pathway (173). PGI2 also demonstrates anti-atherogenic activities by decreasing vascular proliferation, remodelling, and hypertension (173). As mentioned above, the cardiovascular adverse effects of selective inhibition of COX-2 is mechanistically attributed to the suppression of cardioprotective COX-2-derived prostanoids, especially PGI2 (173).

As mentioned earlier, 5/12/15-LOX are the most studied enzymes in terms of their roles in inflammation and atherosclerosis (174). LTA4 is the first product produced from AA by 5-LOX. Subsequently, it can be hydrolyzed or conjugated to generate other forms of LTs (174). LTA4

hydrolysis leads to the generation of LTB4, whereas conjugation with glutathione (by the action of LTC4 synthase) results in the production of LTC4, D4, and E4 (174). 5-LOX is expressed mainly in immune system cells, namely, polymorphonuclear leukocytes (PMNs), monocytes/macrophages, dendritic cells, mast cells, and B lymphocytes (175). The role of 5-LOX in asthma and hay fever is well documented (175). Some studies also suggested that it associates with low-grade inflammatory diseases, such as cardiovascular, neurodegenerative, metabolic diseases, and cancer (175). Previous studies also demonstrated 4-series LTs participate in various stages of atherosclerosis, such as foam cell formation, intimal thickening, advanced atherosclerotic lesions, and degradation of extracellular matrix and therefore, plaque rupture (174). Antileukotrienes medications have been proposed for the prevention of atherosclerosis and treatment of MI (175). EPA is another substrate for 5-LOX. The EPA-derived 5-LOX products are less biologically active than AA-derived LTs (176). Since they compete with series-4 LTs to interact with the receptors, they can be anticipated to act as inhibitors of inflammation (176).

12/15-LOX are the other groups of lipoxygenases that convert AA to 12-hydroperoxy-eicosatetraenoic acid (12-HpETE) and 15-HpETE, respectively (177). Subsequently, cellular glutathione peroxidases change them to hydroxy compounds namely12-HETE and 15-HETE, respectively (177). It has been reported that 12/15-LOX can oxidize LDL, modulate the expression of Th1 cytokine and IL-12, increase the monocytes adhesion to the endothelial cells by inducing ICAM-1 (177). HETEs have been implicated in oxidative stress and vasoconstriction. For instance, Ang II and endothelin-1 can stimulate 20-HETE production in vascular smooth muscle cells (58). Furthermore, a cross-sectional study on patients with peripheral artery disease (PAD) showed that levels 16- HETE was significantly associated with cerebrovascular events (178). LA is another substrate for 12/15-LOX to produce 13-HODE (177). Regarding their roles in atherosclerosis, HODEs are the most abundant oxidized lipids in atheroma and present in all advanced lesions (179, 180). 13-HODE is generated by 15-LOX in the early stage in macrophages as a protective mechanism (181). 13-HODE by interacting with PPAR-g receptor enhances the clearance of lipid and lipid-laden cells from the arterial wall (181). In later stages of atherosclerosis, however, 9-HODE and 13-HODE are generated nonenzymatically and enhance vascular cell apoptosis, which leads to plaque formation (181). Therefore, increased concentrations of HODE is associated with

atherosclerosis progression and the risk of clinical events such as myocardial infarction or stroke (181).

DHA can be converted into 14-hydroxy-DHA and 17-hydroxy-DHA by 12/15-LOX, which are further metabolized to RvDs and protectin Ds (PDs) (182). Similar to DHA, EPA oxidation by 12/15-LOX generates 12-hydroxy-EPA and 15-hydroxy-EPA, which is further metabolized to resolving E3 (182). Resolvins produced from both DHA and EPA possess anti-inflammatory activities (183). They can enhance the generation of NO and prostacyclin, and can also reduce the production of adhesion molecules and ROS in endothelial cells (183). Taken together, 12/15-LOX enzymes reveal opposite effects on atherosclerosis (153). Proatherogenic effects are usually attributed to the role of 12/15-LOX in LDL oxidation. on the contrary, protective effects can be related to the synthesis of pro-resolving mediators (153).

EpETrEs, which are generated by CYP450 epoxygenases, exert diverse biological properties, such as vascular vasorelaxation, apoptosis inhibition, and enhancement of proliferation (153). Vasodilatory effects are mediated through the cAMP/protein kinase A (PKA) signaling pathway, activated by a receptor coupled to Gαs-protein (184, 185) whereas other EpETrE-dependent effects occur through PI3K/Akt, MAP kinase, or Src kinase pathways (186). EpETEs and EpDPEs affect many of these processes, and thus, it is likely that they act through a similar receptor-dependent mechanism (155). EpETrEs and ω-3 PUFA epoxides also express anti-inflammatory properties in the cardiovascular system, which are mediated through attenuation of NF-κB-dependent inflammatory responses (187). Moreover, inhibition of the sEH enzyme, which is accompanied by increased levels of EpETrEs, has been associated with decreases in the development of atherosclerosis and aneurysm (153). On the contrary, the biological effects of EPOME and DiHOME on the cardiovascular system are more complex (188-194). Some studies suggested that high concentrations of 12,13-EpOMEs and 12,13-DiHOMEs are toxic to cardiac cells (188, 189). However, evidence shows that most of the cytotoxic effects attributed to EpOMEs are mediated by their diol metabolites, DiHOMEs (190-194). For example, some studies suggested that EpOMEs have cardioprotective effects through maintaining mitochondrial function (190, 191), whereas high levels of DiHOMEs in the heart are correlated with impaired cardiac function (192, 193). Furthermore, inhibition of sEH, which significantly reduces DiHOME and increases the

levels of EpOME, prevented cytotoxic effects suggesting the DiHOME metabolite was causing the adverse response (194).

As mentioned before, CYP450 hydroxylases produce HETEs from AA (7). 19 and 20-HETEs are the most studied CYP450 hydroxylases derived from AA (7). 20-HETE and 19-HETE usually exert opposite effects (7). 20-HETE is mainly generated in VSMCs (but not endothelial cells in the vasculature) (195, 196). Myeloid cells (197), neutrophils, and platelets can also produce 20-HETE (198). Release of 20-HETE by these calls can lead to smooth muscle cell migration, proliferation, angiogenesis, inflammation, and therefore endothelial dysfunction (199-201). However, 20-HETE is most well-known for its vasoconstrictive effects through PKC, MAPK, and c-src-type tyrosine kinase pathways (202). Endothelin-1, Ang II, atrial natriuretic peptide (ANP), serotonin, and NO mediate 20-HETE release and its vasoconstrictive effects in the vasculature of the heart, brain, and kidney (203). 20-HETE can also stimulate the production of proinflammatory mediators such as PGE2, TNFα, and IL-8, IL-12, and IL-14 (201). It can also mediate cardiac hypertrophy and fibrosis by increasing inflammatory cytokines and chemokine productions (204). Interestingly, 19-HETE has the opposite effects on blood pressure. For example, it causes vascular vasodilation (205), inhibit 20-HETE-mediated endothelial dysfunction (199), and Ang II-mediated hypertrophy and heart failure (HF) (206, 207). However, in a retrospective case-control study, patients with ACS had higher levels of 19-HETE compared to patient controls without coronary heart disease (CHD) (208). But among ACS patients, higher levels of 19-HETE were correlated with a lower risk of major adverse cardiovascular events (MACE) following treatment with coronary artery bypass and stenting (208). Therefore, further research needs to be done on the effects of HETEs in cardiac disease (204). CYP-hydroxylases convert EPA to 19- and 20-HEPE and DHA to 22-HDoHE, which are the counterparts of 20-HETE (209). However, since no data are available regarding the biological role of 20-HEPE and 22-HDoHE in humans, it is not known if these oxylipins share or antagonize the vasoconstrictor action of 20-HETE (210).

Oxylipin changes during I/R: evidence from experimental studies

Pioneering research has shown oxylipin changes during I/R in various experimental models (211-215). For example, Kuzuya et al., measured the levels of (12, 15, 5) HETEs, LTB4, and TXB2

after 90 min of ischemia and 5 hrs of reperfusion in canine myocardial I/R (n=10) (211). HETEs were measured using HPLC/MS whereas LTB, and TXB2 were quantified by radioimmunoassay (211). They found increased levels of HETEs and TXB2 in the infarcted area compared with normal myocardium (211). There were also significant correlations between infarct size (which was estimated by percentage risk area infarcted) and levels of 12-HETE and TXB2 (211). In another canine model of I/R, elevated levels of 12-HETE were reported in myocardial tissue after 1 day of reperfusion measured by reverse-phase HPLC (212). However, in this study, 12-HETE levels reduced during 7 days post-reperfusion (212). Engles et al., examined the effects of various periods of global ischemia (30, 45, and 60 min of ischemia) and reperfusion (5, 10, 15, 20, 25, 30 mins) on PGs, TXs, and (5, 12, 15) HETE concentrations in isolated, perfused rat hearts (n=5) (213). Radioimmunoassays (for PGs and TXs) and HPLC (for HETE) were used for oxylipins analyses (213). They found that levels of 6-keto-PGF1α were elevated by increasing the time of ischemia in isolated hearts (213). Following reperfusion, its concentrations increased further and reached the highest levels at 5 mins of reperfusion but decreased gradually over 30 min post-reperfusion in myocardial tissue (213). TXB2, conversely, produced only after 60 mins of ischemia, but similar to 6-keto-PGF1α, its levels reduced during 30 min of reperfusion (213). In another study, Hughes et al., assessed the oxylipin changes in rabbit myocardium after 45 min ischemia and 3 hrs of reperfusion using gas chromatography-mass spectrometry (GC-MS) (n=6) (214). Significantly elevated levels of LTB4, 5-HETE and 12-HETE were detected in the ischemic myocardium of rabbit compared with non-ischemic controls (214). Nithipatikom et al. assessed the levels of CYP450 metabolites of AA following I/R in canines (n=8) (215). Levels of 5,6-, 8,9-, 11,12-, and 14,15- EpETrEs, their corresponding DiHETrEs, and 20-HETE were measured using GC-MS in coronary venous plasma samples (215). Total levels of EpETrEs, 14,15- DiHETrE, and 20-HETE elevated significantly at 60 mins of reperfusion in coronary venous plasma compared with controls (215). Their levels remained elevated until 60 min of reperfusion but decreased at 120 min of reperfusion (215). Recently, Horii et al. showed increased levels of 5-HETE, 11-HETE, 12-HETE, and 15-HETE in the infarct area of mouse heart at day-3 after MI compared to the non-infarct area and sham group using HPLC-MS/MS (216).

Role of oxylipins in ACS: evidence from clinical studies

Plasma concentrations of AA-derived oxylipins, including TXB2, 6-keto-PGF1α, LTB4, LTC4, LTD4, and LTE4 were measured in 19 patients with MI using radioimmunoassay (217). Plasma levels of TXB2 and LTB4 increased significantly at 24 hrs following reperfusion compared with healthy control but decreased to baseline levels at 30 days of reperfusion (217). In another study changes in LTC4 levels in arterial and pulmonary artery blood were measured in patients with chronic stable angina (n=14) and MI (n=14) using radioimmunoassay (218). They found that LTC4 concentrations were significantly elevated in patients with AMI in both arterial and pulmonary artery blood in the acute phase compared with patients with chronic stable angina (218). Previously, 8-iso-prostaglandin F2α was measured in 3 groups of patients, including patients with no or minimal CAD (n =15), stable CAD (n =31) and AMI (n =13) using the enzyme immunoassay (219). The blood samples in patients with MI and stable CAD were collected at a median time of 40 hrs and 72 hrs after the start of chest pain, respectively (219). They found significantly elevated plasma levels of 8-iso-prostaglandin F2α in patients with MI compared with patients with or without CAD, even after correcting for coronary atherosclerosis risk factors, age, the extent of atherosclerosis, and CRP levels (219). Strassburg et al. developed an analytical method to measure oxylipins in patients who underwent cardiac surgery (220). Blood samples were collected at baseline and 24 h post-reperfusion in 5 patients (220). They found that elevated levels of 12-HETE and 5-HETE after surgery compared with baseline values (220). Metabolites of COX and CYP450 were not significantly different in their study participants before and after surgery (220).

A retrospective nested case-control study, comprised of 470 patients with ACS and 39 subjects without CHD (as a control group), was conducted in the Chinese population (208). In this study, LTB4, 8-HETE, 11-HETE, 12-HETE, and 15-HETE were significantly elevated in ACS patients compared with controls (208). In addition, levels of 5-HETE and 9-HETE were significantly higher in the ACS group with events compared with controls suggesting the potential diagnostic value of these oxylipins in ACS (208). The level of the 20-HETE level was also significantly elevated in the STEMI group comparing with the non-STEMI group (208). In a prospective study by Sun et al., (221) the association between oxylipins and incidence of MI was investigated in 744 AMI cases and 744 matched controls aged 47–83 years within the Singapore Chinese Health Study (221). They found inverse correlations between pro-thrombotic TXB2 and AMI risk. They

suggested that this unexpected association would be more related to sample collection, processing, and storage conditions rather than biological differences (221). Moreover, in this study, only 19 oxylipins that had potential roles in inflammation, blood pressure, and platelet degranulation were measured not the full spectrum (221). In a study by Caligiuri et al., the role of oxylipins in odds of cardiovascular/cerebrovascular events was assessed in patients with peripheral artery disease (PAD) (178). Among 98 patients with PAD, there were 24 patients with ACS defined as STEMI, non-STEMI and unstable angina (178). They found that elevated levels of 16-HETE, TXB2, and 11,12-DiHETrE are significantly associated with increased odds of cardiovascular/cerebrovascular events in patients with PAD (178). In this study, the odds of ACS increased by 92-fold in patients who had higher levels of plasma 8,9-DiHETrE (178). A large prospective study investigated the prognostic impacts of oxylipins on clinical outcomes in CAD in 2,239 patients with stable CAD (222). After 2 years of follow-up, 25 patients presented with a new onset of acute MI (222). Gender and age-matched patients with CAD (n=50) without clinical cardiovascular events were also recruited as a control group (222). They found that the baseline concentrations of AA-derived metabolites were significantly elevated in patients with subsequent AMI compared with controls (222). The incident of future MI was associated with elevated baseline levels of 8-HETE, 9-HETE, 11-HETE, 12-HETE, 15-HETE, 19-HETE, 20-HETE, 5,6-EpETrE, 8,9- EpETrE, 11,12- EpETrE, or 14-15- EpETrE (222). These data suggested that HETE and EPETREs levels can be potential targets for secondary prevention in clinically stable CAD patients (222). In a recent prospective observational study, specialized pro-resolving mediators (SPM) were quantified in patients with STEMI (n=15), stable CAD (n=10), and healthy controls (n=10) (223). They found that levels of DHA-derived oxylipins generated through the LOX pathway, namely, protectins, increased significantly after the onset of STEMI compared with both CAD and control groups (223).

IV. Oxidized lipids analyses in biological samples

A part of this chapter is published in**:**

Lipidomics of bioactive lipids in acute coronary syndromes. International journal of molecular sciences. 2019 Jan;20(5):1051. Zahra Solati, Amir Ravandi

Oxidative lipidomics

As discussed in the previous section, it's well documented that products of both enzymatic and non-enzymatic lipid oxidation are bioactive which can interact with several cell-surface receptors and immune cells (224). Lipid oxidation usually generates a massive variety of oxidized products (224). Hence, analytical techniques that can provide molecular-level detail, such as MS, are required to distinguish heterogeneous mixtures of oxidized lipids in different biological samples (224).

One of the challenges in oxidized lipid analysis is the diversity of products of lipid oxidation (81). For example, during PL oxidation, unsaturated FA in the *sn-2* position and headgroup can be oxidized by oxidants (81). PUFA, such as AA or PA, are more vulnerable to free radical attack whereas monounsaturated FA (MUFA) and reactive headgroups in PLs, such as PE or PS, are more susceptible to reactive nitrogen species and hypohalous acids (derived from myeloperoxidase and eosinophil peroxidase) (81). The possible products include the full-length and short-chain oxidized PLs that are esterified to the glycerol backbone of PL and called non-fragmented and fragmented OxPL (81). The non-fragmented oxidized products can differ from products with simple oxidative alteration, such as hydroperoxide, hydroxide, etc, to more complex forms such as isoprostane-like structures or isolevuglandins (81). Fragmented OxPLs contain an aldehyde or carboxyl groups in their structures (81). PL oxidation also produce fragments of the oxidized fatty acyl chains, which are not esterified to the glycerol backbone, such as malondialdehyde (MDA) and 4-HNE (81).

Similar to PLs, oxidation of free FAs released from PLs give rise to diverse groups of products, which is the consequence of a large number of existed FAs and oxidative pathways (7). N-6 (such as AA and LA) and n-3 FAs (such as EPA and DHA) can enter into three main oxidative pathways including COX, LOX, and CYP450 (7). Prostanoids (namely prostaglandin and thromboxanes) are generated through the COX pathway (7). LOX enzymes catalyze the generation of short-chain hydroxy FAs (7). CYP450 enzymes have epoxygenase or ω-hydroxylase activities, which produce epoxides and long-chain hydroxy FAs, respectively (7). Smaller portions of oxylipins can be produced from non-enzymatic oxidation (7).

Oxidized lipid: method of detection of

Given that the first product of lipid oxidation by radicals contains carbon-centred or oxygen-centred radicals, lipid peroxidation products can be detected by spin traps (224). Electron spin resonance spectroscopy (ESR or EPR) is one of the analytical methods to analyze oxidized lipids generated by free radical oxidation (224). For instance, -(4-pyridyl-1-oxide)-N-tert-butyl nitrone (POBN) was used to interact with radical produced from DHA by ESR (226). However, this method is not suitable for measuring non-radical compounds (225). Colourimetric or fluorimetric assays have been applied for non-radical forms of oxidized lipids (227-233). To perform these analyses, oxidized lipids are required to react with compounds to generate chromophores or fluorophores. For instance, iodometric titration (227), ferrous oxidation-xylenol orange (FOX) assays (228), and isoluminol-dependent assays (229, 230) have been used for the detection of hydroperoxide groups. Other examples include using 2,4-dinitrophenyl hydrazine (231, 232), cyclohexanedione, or pentafluorobenzyl hydroxylamine (231, 233) for detecting lipid aldehyde or ketones in biological samples. The main drawback of these assays is that they can detect a class of oxidized lipid rather than an individual compound. However, applying a separation technique before detection can minimize this problem (224).

Thin-layer chromatography (TLC) is one of the basic separation methods that has been applied for lipid analysis (225, 234, 235). It is a technique that separates metabolites based on their polarity differences (236). It is composed of a stationary phase, which is usually a silica gel and a mobile phase (236). In normal-phase TLC, a non-polar mobile phase, such as hexane or chloroform, is used while in reverse phase TLC, The mobile phase is polar (such as methanol) (236). TLC is a convenient, simple inexpensive method compared with other methods of separation. However, lipid oxidation can occur (236). GC has been used for the separation of epoxy FAs from hydroxy and non-oxidized FAs (237). In this method, metabolites are separated based on their boiling point/vapour pressure and polarity using a gaseous mobile phase and a solid or liquid stationary phase (237). For GC analysis, the metabolite is required to be volatile and thermally stable. Therefore, derivatization is required for oxylipins to elevate their metabolites volatility (237). For example, N, O-bis(trimethylsilyl)-trifluoroacetamide (BSTFA) have been used for oxylipin derivatization (238). GC can be coupled to MS which increases the sensitivity and specificity of analysis (233). The ionization technique used in GS-MS is high energy electron ionization (hard

ionization) or chemical ionization. GC-MS usually use for the quantification of isoprostanes (239, 240) hydroperoxides and hydroxides forms of FAs (233). However, this method is not suitable for OxPL analysis (224). HPLC is the main separation method that has been used for OxPL analysis which can be also readily coupled with soft ionization MS (224). The most common used HPLC columns are normal-phase and reverse-phase columns, although other column types have also been used (224). The normal-phase column separates lipids based on their class or headgroup, while the reverse-phase column separates lipids based on chain polarity and thus can be used for separating oxidized forms from unoxidized lipids (224).

Immunoassays including enzyme immunoassay (EIA) and radioimmunoassays (RIA) are very sensitive approaches for oxidized lipid analysis but rely on the availability of antibodies (224). For example for OxPL analysis, E06, which is a natural antibody of IgM class can recognize PC in OxPC and OxPC adducts to proteins, such as lipoprotein (a) and oxidized LDL (224). This method has been extensively used to study PL oxidation in cardiovascular diseases (242). The advantage of this method is a high speed, sensitivity and cost-effectiveness (224). However, this method is not able to identify specific OxPC species, which is necessary to understand the biological properties of individual OxPC species (224). EIA and RIA have been widely used for oxylipin analysis as well (224). For instance, RIA has been developed to measure IsoPs (8-iso-PGF2) (243),15-keto-dihydro-PGF2 (244), Prostaglandin E2 (PGE2) and LTB4 (240), PGE2 (245, 246), PGE2, PGF2, PGI2, 6-oxo-PGF2, TXA2, TXB2 (247) in biological samples. EIA, however, is not a suitable method for oxylipin analysis due to the structural similarity of oxylipins that makes it unlikely for an antibody to differentiate between them (248). Moreover, plasma proteins can be also attached to oxylipins (249). To overcome this challenge, separation techniques can be applied to separate oxylipins from plasma protein (249). Thus, due to these challenges of immunoassay, HPLC-MS/MS has been extensively applied for oxylipin analysis.

Oxidized lipids analysis by HPLC-MS/MS

Sample preparation

The first step in preparing samples for lipidomic analysis is extracting the lipids from the biological samples (cell/tissue/plasma) (250). Conventional liquid-liquid extraction has been widely used for the extraction of OxPLs (250). Folch extraction, which uses chloroform/methanol, is one of the

most common extraction approaches for OxPLs extraction (251). Adding antioxidants, such as BHT, is recommended to minimize further oxidation during extraction (251). Recently, it has been suggested that enrichment strategies such as using gold nanoparticles (GNP) and/or antibodies on a crude sample or lipid extract increases the efficacy of OxPL analysis (252-253). Hinterwirth et al. (252) used GNPS with four different Ox-LDL antibodies, namely E06 antibody, Cu Ox-LDL antibody, MDA-LDL antibody, and carboxymethyl lysine-LDL antibody, to increase the sensitivity of OxPL detection in plasma. Stübiger et al., (253) also shown that adding 2-aminobenzoic acid (2-AA) as the reagent with GNP, elevated the carbonyl-containing OxPC identification at sub-nanomolar concentrations, with up to 90% recoveries.

Oxylipins can be extracted using liquid-liquid extraction and/or solid-phase extraction procedures (6). The use of chloroform/methanol mixtures, according to Bligh and Dyer, is the most common liquid-liquid extraction protocol for oxylipins (254). In this method, oxylipins are suspended in organic solvents, but hydrophilic materials, such as proteins, are eliminated following phase separation (254). However, the main drawback of the Bligh and Dyer protocol is that most lipid groups including non-oxidized lipids (cholesterol, triacylglycerols and phospholipids), which usually present in very high concentrations, are also extracted and can interfere with oxylipin analysis (255). Solid-phase extraction can be conducted using commercial columns pre-packed with various sorbents (256). SPE separates different metabolites between the liquid and the solid phase (255). Thus, it removes the unwanted compounds that can cause matrix effects during the analysis and increases the concentrations of target analytes. This leads to higher sensitivity and improves the limits of detection (255).

Separation of oxidized compounds using liquid chromatography (LC)

To separate the OxPLs species, reverse-phase HPLC with C8 or C18 columns with either isocratic or gradient elution has been widely used (238). OxPLs are separated on the HPLC column based on their polarity and molecular weights before interfacing with the MS, which increases the sensitivity of the assessment (238). Reverse-phase mobile phases are usually a mixture of water, methanol, or acetonitrile (257). Hexane or isopropanol can also be applied as co-solvents (257). Ammonium acetate, ammonium formate, or acetic or formic acid can also be added to the solvents to facilitate ionization in MS. There are no deuterated internal standards for OxPLs analysis (257). Non-oxidized PLs and lyso-PL, such as PI (31:1) for OxPI analysis and PC (9:0)/LPC(17:0) for

OxPC analysis, have been used as internal standards (257). These PLs have the same structures and fragmentation patterns and are not produced in the body. Therefore, they can be used as internal standards to assess the extraction efficacy and instrument response (257). Reverse-phase HPLC or ultra-performance LC (UPLC) with a C18 column or has been used widely to separate oxylipins (208, 256, 258). The UPLC column has better resolution, lower detection limits, and a shorter chromatographic run in comparison with HPLC (257). Besides, UPLC can also decrease ion suppression caused by co-eluting lipids, and isobaric and isomeric metabolites interferences (256). Gradient elution is usually applied for oxylipins LC separation (256). Solvent A is composed of 0.1% acetic acid or 0.1% formic acid in water (v/v) (256). Solvent B can consist of different solvents, namely, acetonitrile, isopropanol, methanol, individually or mixed in different proportions (256). For instance, acetonitrile/isopropanol (90/10 or 70/30, or 50/50) (256). Deuterated oxylipins are commercially available, which are used as internal standards (257). These standards are matched with groups of endogenous oxylipin species in terms of chemistry, retention time, and ionization efficiencies (257). As mentioned previously, internal standards are needed to assess the extraction efficacy and instrument response (257).

MS and oxidative lipidomics

Considering all the above-mentioned challenges of conventional analytical methods, MS has been extensively applied for OxPLs and oxylipin analysis (224). Electrospray ionization (ESI) and matrix-assisted laser desorption/ionization (MALDI) are two forms of low energy (soft) ionization approaches that have been used for labile compounds, such as PLs (259, 260). The main advantage of soft ionization is that unlike GC-MS, it does not require chemical manipulation (to release FA) and derivatization (to make volatile compounds) (224). Therefore, it's a simpler method, handling is minimized and PL structure remains untouched (224). ESI and MALDI are able to ionize several species in the sample simultaneously (224). Thus, samples can be introduced into the mass spectrometer without prior separation, which is called shotgun lipidomics (224). This method is not a desirable technique for oxidized lipids analysis, as the concentrations of oxidized compounds in a sample are considerably lower compared with non-oxidized metabolites (224). Using separation techniques, such as HPLC, prior to MS prevents the ion-suppression caused by highly abundant molecular ions (224). MS has advanced vastly from 15 years ago, in respect to sensitivity, resolution, scanning speed and identifying fragmentation patterns (261). This has made MS the

desirable approach for OxPC and oxylipin analyses (261). ESI has been used more extensively in the lipidomics area compared with MALDI, as MALDI needs co-crystallization of a matrix with the sample, which affects the signal and thus absolute quantification (261). However, some studies have applied MALDI for oxidized or chlorinated PLs and cardiolipin (243, 262-265). The advantages of MALDI over ESI is that, unlike ESI, it does not need cleanup samples and tolerates salts or detergents in the samples (224). Moreover, it can be used for MS imaging which provides information on spatial distributions of molecular species across tissues, while ESI needs tissue extraction (224). The schematic steps of soft ionization by ESI versus MALDI are summarized in Figure 3.

Figure 3: Soft ionization mass-spectrometry: ESI versus MALDI

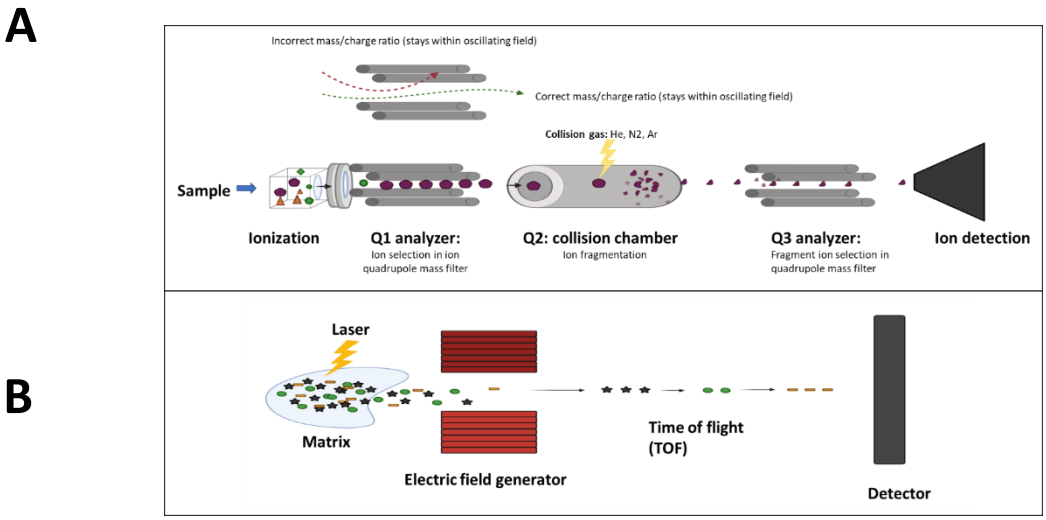

In triple quadrupole mass spectrometers, metabolites are ionized in the ion source. Subsequently, the ion with the specific mass/charge ratio crosses a first mass analyzer (Q1). Then the selected ion (precursor or parent ion) enters into the collision chamber and is fragmented by gas (He, N2, or Ar) to the product/daughter ion. A particular product ion is then selected in the Q3 analyzer. The metabolite is identified in the detector. B: Matrix-assisted laser desorption/ionization (MALDI): Samples are coated with a solution of an organic, energy-absorbent compound, called matrix. The sample inside the matrix is ionized with a laser ray. Electric field increases the detection of ions within the matrix. Ions identified based on the time to reach the detector (TOF). Small ions reach the detector faster than large ones.

Soft-ionization technique in MS

Mass spectrometers are comprised of mass analyzers, which differentiate ions based on their mass-to-charge (m/z) ratio (224). A tandem mass spectrometer (MS/MS) has two analyzers and a

collision cell connecting two analyzers. The first analyzer selects a precursor (parent) ion molecule (224). In collision cells, the precursor ion breaks down to fragment (daughter) ions by an inert gas (He, N2, Ar, etc) (224). Fragment (daughter) ions are then identified in the second analyzer (224). Quadrupole mass analyzer is the most common analyzer in tandem mass spectrometers, which contains four parallel rods of a circular or hyperbolic cross-section, which are supplied with radio-frequency (RF) and direct-current (DC) voltages (224). Ions are scanned by varying the DC/Rf quadrupole voltages, thus only ions with the selected mass to charge ratio will have the correct oscillatory pathway in the Rf field (224). Finally, each ion that reaches the detector, makes a unique signal in the spectrum. To differentiate ions with similar mass (isobaric compounds), high-resolution mass instruments are needed with a mass resolution of 40–100 k and mass accuracies of 0.5–5 ppm (224). On the other hand, to identify compounds that have the same elemental composition but different structures (isomeric compounds), fragmentation or separated chromatographically can help to differentiate them in a mass spectrometer (224). Ion mobility MS (IMS) can also separate isomeric compounds as it separates ions based on their shape (collisional cross-section) (224). IMS also remove chemical background from the mass spectra which makes the assignment and detection more sensitive. IMS has been also used in mass spectrometric imaging (224).

Modes of scanning in MS

There are three main methods for targeted analysis with different levels of selectivity, which are presented in Figure 4.

Figure 4: Mass-spectrometry fragmentation routines

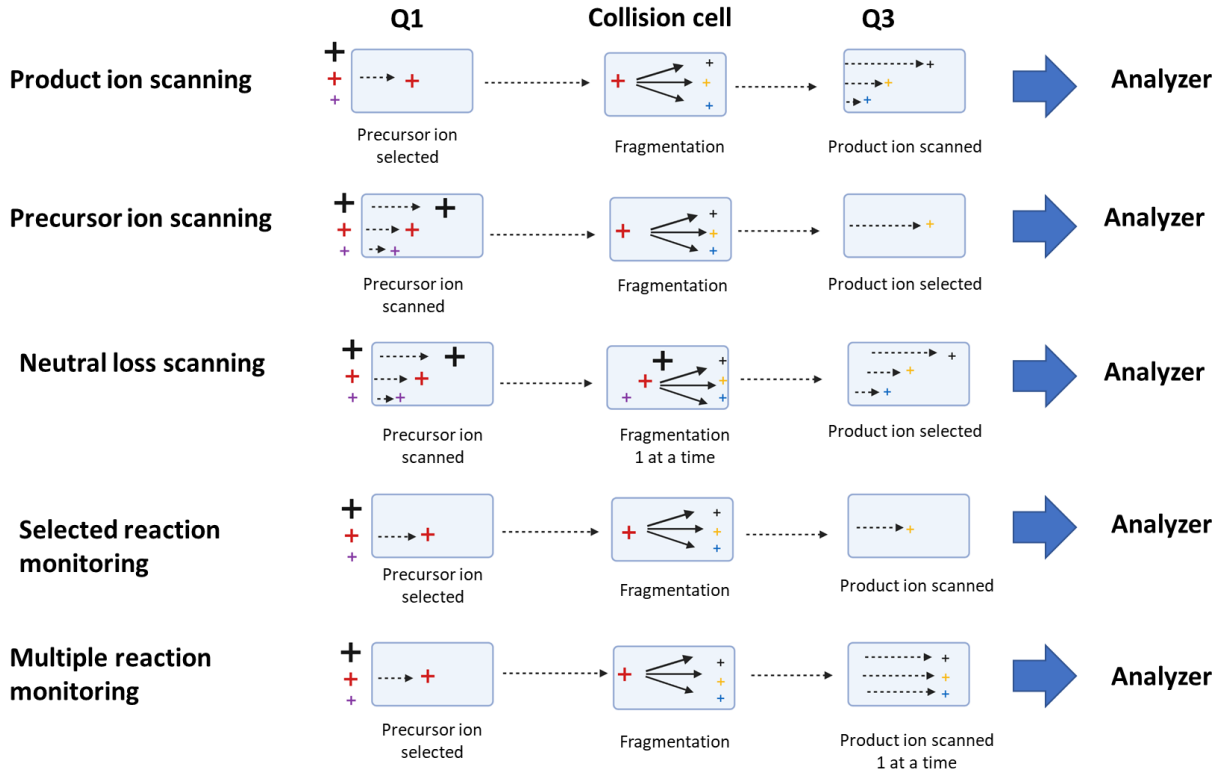

This figure was remade from "Spickett CM, Pitt AR. Oxidative lipidomics coming of age: advances in the analysis of oxidized phospholipids in physiology and pathology. Antioxidants & redox signaling. 2015 Jun 20;22(18):1646-66". (Free accsess article).

Precursor ion scanning recognizes parent ions that give rise to desired fragment ion (daughter ion) by scanning through the masses in the first analyzer (266). The second analyzer is set to identify the m/z of the daughter ion (266). Neutral loss scanning recognizes precursors that fragment by loss of a specific uncharged fragment, regardless of the mass of the parent ion (266). In this approach, scanning occurs in the first and second mass analyzers with a fixed mass offset between them corresponding to the mass of the neutral fragment lost (266). These two methods can be applied when the identification of a group of compounds containing a specific group is desired (266). For instance, precursor ion scanning for m/z 184 recognizes phosphocholine-containing lipids such as sphingomyelin (SM) or PC (266) or the neutral loss of 18 atomic mass unit (amu) corresponds to water, showing the presence of a hydroxyl group (267). Combining neutral loss

and precursor ion scanning has been used for MS-based shotgun lipidomics, in which different classes of lipids can be identified without prior separation (267). However, the main limitation is ion-suppression and a difficulty in differentiating isomeric and isobaric lipid molecular species (268). On the contrary, when a single metabolite is to be identified, selected single reaction monitoring (SRM) is applied (224). Thus, the m/z of the parent ion in the first analyzer and m/z of the daughter in the second analyzer is set (224). The specificity of this method can increase by repeating multiple "transitions'' from precursor to fragment ions, which is called multiple reaction monitoring (MRM) (224). The sensitivity of SRM and MRM is higher compared with scanning approaches which makes the desired approach for the targeted quantification of compounds (224).

Identification and quantification of oxidized lipids by MS

Although MS has been used for several years for lipid analysis, the application of MS to measure oxidized lipids, particularly OxPL and oxylipins, has been initiated recently after the emerge of soft ionisation techniques (224). In the field of PL analysis, most of the studies have focused on PC, as it is the most abundant PLs. Mass to charge ratio of 184.1, which corresponds to PC headgroup, can be used to identify PC and SM (as it has PC in its structure) in either precursor ion scan or SRM/MRM (224). Gruber et al. (269) provided an extensive list of OxPC transitions that applied to quantify OxPCs in human dermal fibroblasts subjected to UVA irradiation using reversed-phase HPLC-MS/MS analysis (269). PL standards including PAPC, PLPC, SAPC, and SLPC were exposed to dry air (for 48 hrs) to be oxidized and then were injected into HPLC-MS/MS system to estimate retention time of non-oxidized PCs and OxPCs (269). As OxPCs elute from the column earlier than non-oxidized forms, they can be separated well from the unoxidized PCs (269). Using this method, they were able to identify 97 OxPC compounds in human dermal fibroblasts subjected to UVA irradiation (269). In another study by Stübiger et al. (270) also developed a method using PL autooxidation to identify OxPCs in the plasma and lipoproteins of patients with familial hypercholesterolemia and normolipidemic individuals using reverse-phase HPLC-MS/MS (270). They were able to quantify 10 OxPCs derived from PAPC, PLPC, SAPC and SLPC in the plasma of their participants (270). They also confirmed their results by using MALDI-QTOF-MS/MS (270).

Our lab has previously identified OxPC species in patients that have undergone percutaneous coronary and peripheral procedures using normal phase HPLC/MS (271). In this study, six of the most abundant OxPCs, including POVPC, PONPC, PGPC, PAzPC, KOdiAPC and KDdiAPC were quantified in embolized material captured by distal protection filter devices (271). Commercially available OxPC standards were used for OxPC species identification in MS by MRM (271). We also previously measured the levels of OxPI in Ox-LDL and human atherosclerotic plaque by using reversed-phase HPLC-MS/MS (272). To generate OxPI species, bovine liver PIs were subjected to non-enzymatic and lipoxygenase-catalyzed oxidation (272). After finding the retention times for OxPI species and using the MRM method, we were able to quantify 23 OxPI species in human Ox-LDL and atherosclerotic plaque (272). Recently, Ademowo et al., (273) have measured 10 OxPC species in the plasma of patients with chronic kidney disease and periodontitis and healthy controls. They oxidized PL standards, including PAPC, PLPC, SAPC and SLPC, using Fenton reaction between H2O2 and FeCl2, to generate OxPC species (273). Similar to previous studies, HPLC-MS/MS was applied for OxPC identification and quantification. As there is no deuterated standard for OxPL analysis, non-oxidized PLs and lyso PL (LPL, such as PI (31:1), PC (9:0), and LPC (17:0), have been used for OxPL quantification in MS (273).

MS has been also widely used for targeted oxylipin analysis (257). One of the factors that makes oxylipin analysis more accurate using MS is that deuterated oxylipins are commercially available which can be used as internal standards (257). These standards are matched with groups of endogenous oxylipins species in terms of chemistry, retention time, and ionization efficiencies (257). A recent review by Liakh et al, (238) mentioned that more than 30 studies were cited that used HPLC-MS/MS for oxylipin analysis in cells, tissue and human serum/plasma. For instances, some recent studies investigated the role of oxylipins in the diagnosis and prognosis of ACS using HPLC-MS/MS (238). In a prospective study by Sun et al., (221), the association between oxylipins and incidence of MI was investigated in patients with myocardial infarction (MI) and controls within the Singapore Chinese Health Study. In this study, only 19 oxylipins which had potential roles in inflammation, blood pressure, and platelet degranulation were measured not the full spectrum (221). In a study by Caligiuri et al., (178) the effects of oxylipins on odds of cardiovascular/cerebrovascular events were assessed in patients with peripheral artery disease (PAD) (178). Seventy-eight oxylipin metabolites were quantified in the plasma of their participants

using LC/MS/MS (178). A large prospective study investigated the prognostic impacts of oxylipins on clinical outcomes in patients with stable cardiovascular disease (CAD) and 45 oxylipin metabolites were quantified in the plasma of study participants using HPLC-MS/MS (222). In a recent prospective observational study, specialized pro-resolving mediators (SPM) were quantified in patients with STEMI, stable CAD, and healthy controls. In this study, 24 oxylipin species derived from DHA and EPA were measured in the plasma of their participants using HPLC-MS/MS (223).

In summary, among the available analytical methods for oxidized lipid analysis, tandem MS/MS instruments have recently become the most common approach (6). MS is a powerful tool that provides another layer of the detailed molecular levels of oxidized lipid assessments (6). Using this approach, several groups of compounds can be assessed at the same time in a targeted and non-targeted fashion (6). Coupling LC to MS increases the selectivity and sensitivity of the oxidized lipid analysis (6). The steps of oxidized lipid analysis are summarized in Figure 5.

Figure 5: Steps of oxidized lipid analysis by HPLC-MS/MS

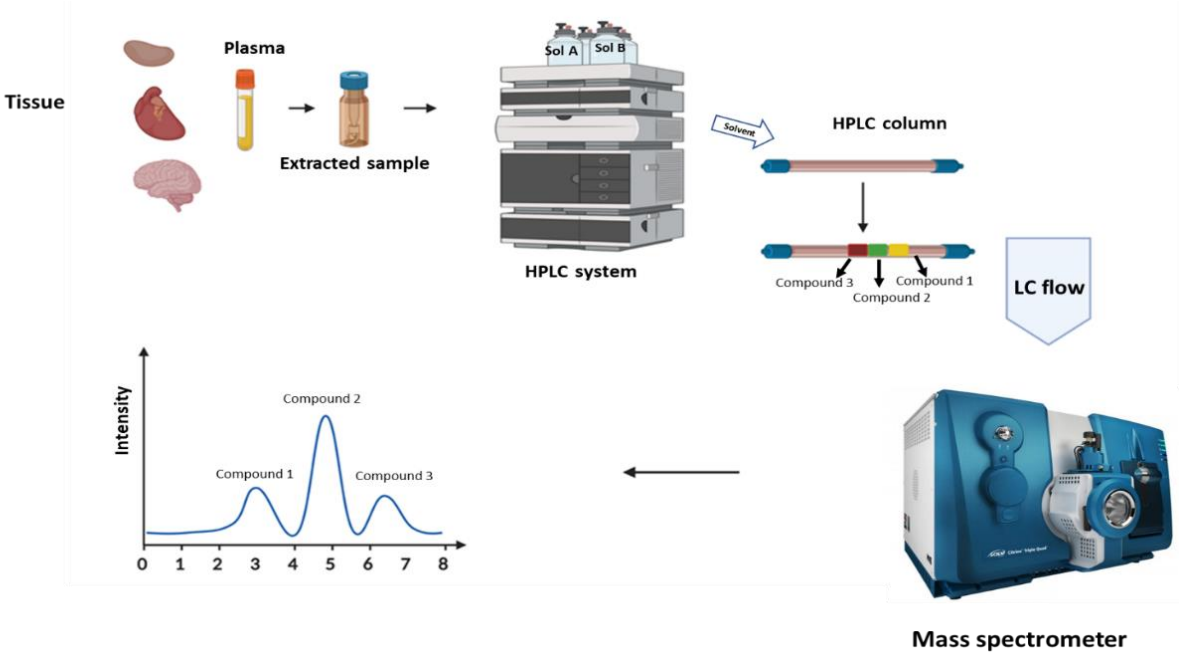

Conclusion

It is well documented that I/R results in the generation of ROS which leads to the activation of both non-enzymatic and enzymatic lipid oxidations. Products of lipid oxidations, such as OxPLs and oxylipins are biologically active and can initiate inflammatory responses and cell death pathways. In order to identify and quantify oxidized lipids in biological samples, sophisticated analytical systems are needed, considering that they are a heterogeneous group of compounds in low abundance. Given that their roles in I/R injury are still poorly understood, we aimed to describe the first detailed oxolipidomic analysis during IR injury.

Chapter I References

1. Cowled P, Fitridge R. Pathophysiology of reperfusion injury. Mechanisms of Vascular Disease: A Reference Book for Vascular Specialists [Internet]. 2011.
2. Kalogeris T, Baines CP, Krenz M, Korthuis RJ. Cell biology of ischemia/reperfusion injury. International review of cell and molecular biology. 298: Elsevier; 2012. p. 229-317.
3. Vedanthan R, Seligman B, Fuster V. Global perspective on acute coronary syndrome: a burden on the young and poor. Circulation research. 2014;114(12):1959-75.
4. Nielsen PM, Qi H, Bertelsen LB, Laustsen C. Metabolic reprogramming associated with progression of renal ischemia reperfusion injury assessed with hyperpolarized [1-13C]pyruvate. Scientific Reports. 2020;10(1):8915.
5. Wu M-y, Yiang G-t, Liao W-T, Tsai AP-Y, Cheng Y-L, Cheng P-W, et al. Current mechanistic concepts in ischemia and reperfusion injury. Cellular Physiology and Biochemistry. 2018;46(4):1650-67.
6. Solati Z, Ravandi A. Lipidomics of bioactive lipids in acute coronary syndromes. International journal of molecular sciences. 2019;20(5):1051.
7. Gabbs M, Leng S, Devassy JG, Monirujjaman M, Aukema HM. Advances in our understanding of oxylipins derived from dietary PUFAs. Advances in nutrition. 2015;6(5):513-40.
8. Ekroos K, Jänis M, Tarasov K, Hurme R, Laaksonen R. Lipidomics: a tool for studies of atherosclerosis. Current atherosclerosis reports. 2010;12(4):273-81.
9. Kalogeris T, Baines CP, Krenz M, Korthuis RJ. Ischemia/reperfusion. Comprehensive Physiology. 2011;7(1):113-70.
10. Akbar H, Foth C, Kahloon RA, Mountfort S. Acute ST Elevation Myocardial Infarction. StatPearls [Internet]: StatPearls Publishing; 2020.
11. Prabhu SD, Frangogiannis NG. The biological basis for cardiac repair after myocardial infarction: from inflammation to fibrosis. Circulation research. 2016;119(1):91-112.
12. Yang C-F. Clinical manifestations and basic mechanisms of myocardial ischemia/reperfusion injury. Tzu-Chi Medical Journal. 2018;30(4):209.
13. Devarajan P. Update on mechanisms of ischemic acute kidney injury. Journal of the American Society of Nephrology. 2006;17(6):1503-20.
14. Solati Z, Edel AL, Shang Y, O K, Ravandi A. Oxidized phosphatidylcholines are produced in renal ischemia reperfusion injury. PloS one. 2018;13(4):e0195172.
15. Koza Y. Acute kidney injury: current concepts and new insights. Journal of Injury and Violence Research. 2016;8(1):58.
16. McDougal WS. Renal perfusion/reperfusion injuries. The Journal of urology. 1988;140(6):1325-30.
17. Tammaro A, Kers J, Scantlebery AM, Florquin S. Metabolic Flexibility and Innate Immunity in Renal Ischemia Reperfusion Injury: The Fine Balance Between Adaptive Repair and Tissue Degeneration. Frontiers in Immunology. 2020;11:1346.
18. Martinon F. Signaling by ROS drives inflammasome activation. European journal of immunology. 2010;40(3):616-9.
19. Ray PD, Huang B-W, Tsuji Y. Reactive oxygen species (ROS) homeostasis and redox regulation in cellular signaling. Cellular signalling. 2012;24(5):981-90.
20. Valko M, Leibfritz D, Moncol J, Cronin MT, Mazur M, Telser J. Free radicals and antioxidants in normal physiological functions and human disease. The international journal of biochemistry & cell biology. 2007;39(1):44-84.
21. Phaniendra A, Jestadi DB, Periyasamy L. Free radicals: properties, sources, targets, and their implication in various diseases. Indian journal of clinical biochemistry : IJCB. 2015;30(1):11-26.
22. Limón-Pacheco J, Gonsebatt ME. The role of antioxidants and antioxidant-related enzymes in protective responses to environmentally induced oxidative stress. Mutation Research/Genetic Toxicology and Environmental Mutagenesis. 2009;674(1-2):137-47.

23. Granger DN, Kvietys PR. Reperfusion injury and reactive oxygen species: the evolution of a concept. Redox biology. 2015;6:524-51.
24. Bugger H, Pfeil K. Mitochondrial ROS in myocardial ischemia reperfusion and remodeling. Biochimica et Biophysica Acta (BBA)-Molecular Basis of Disease. 2020;1866(7):165768.
25. Hool LC. The L-type Ca2+ channel as a potential mediator of pathology during alterations in cellular redox state. Heart, Lung and Circulation. 2009;18(1):3-10.
26. González-Montero J, Brito R, Gajardo AI, Rodrigo R. Myocardial reperfusion injury and oxidative stress: Therapeutic opportunities. World Journal of Cardiology. 2018;10(9):74.
27. Zhivotovsky B, Orrenius S. Calcium and cell death mechanisms: a perspective from the cell death community. Cell calcium. 2011;50(3):211-21.
28. Ratliff BB, Abdulmahdi W, Pawar R, Wolin MS. Oxidant mechanisms in renal injury and disease. Antioxidants & redox signaling. 2016;25(3):119-46.
29. Borutaite V, Brown GC. Caspases are reversibly inactivated by hydrogen peroxide. FEBS letters. 2001;500(3):114-8.
30. Ryter SW, Kim HP, Hoetzel A, Park JW, Nakahira K, Wang X, et al. Mechanisms of cell death in oxidative stress. Antioxidants & redox signaling. 2007;9(1):49-89.
31. Choi K, Kim J, Kim GW, Choi C. Oxidative stress-induced necrotic cell death via mitochondira-dependent burst of reactive oxygen species. Current neurovascular research. 2009;6(4):213-22.
32. Minutoli L, Puzzolo D, Rinaldi M, Irrera N, Marini H, Arcoraci V, et al. ROS-mediated NLRP3 inflammasome activation in brain, heart, kidney, and testis ischemia/reperfusion injury. Oxidative medicine and cellular longevity. 2016;2016.
33. Chen GY, Nuñez G. Sterile inflammation: sensing and reacting to damage. Nature Reviews Immunology. 2010;10(12):826-37.
34. Toldo S, Mauro AG, Cutter Z, Abbate A. Inflammasome, pyroptosis, and cytokines in myocardial ischemia-reperfusion injury. American Journal of Physiology-Heart and Circulatory Physiology. 2018;315(6):H1553-H68.
35. Nathan C. Neutrophils and immunity: challenges and opportunities. Nature reviews immunology. 2006;6(3):173-82.
36. Phillipson M, Kubes P. The neutrophil in vascular inflammation. Nature medicine. 2011;17(11):1381-90.
37. Brinkmann V, Reichard U, Goosmann C, Fauler B, Uhlemann Y, Weiss DS, et al. Neutrophil extracellular traps kill bacteria. science. 2004;303(5663):1532-5.
38. Geissmann F, Manz MG, Jung S, Sieweke MH, Merad M, Ley K. Development of monocytes, macrophages, and dendritic cells. Science. 2010;327(5966):656-61.
39. Slegtenhorst BR, Dor FJ, Rodriguez H, Voskuil FJ, Tullius SG. Ischemia/reperfusion injury and its consequences on immunity and inflammation. Current transplantation reports. 2014;1(3):147-54.
40. Dai S, Xu Q, Liu S, Yu B, Liu J, Tang J. Role of autophagy and its signaling pathways in ischemia/reperfusion injury. American journal of translational research. 2017;9(10):4470.
41. Gottlieb RA. Cell death pathways in acute ischemia/reperfusion injury. Journal of cardiovascular pharmacology and therapeutics. 2011;16(3-4):233-8.
42. Kalogeris T, Bao Y, Korthuis RJ. Mitochondrial reactive oxygen species: a double edged sword in ischemia/reperfusion vs preconditioning. Redox biology. 2014;2:702-14.
43. Liu H, Jing X, Dong A, Bai B, Wang H. Overexpression of TIMP3 protects against cardiac ischemia/reperfusion injury by inhibiting myocardial apoptosis through ROS/Mapks pathway. Cellular Physiology and Biochemistry. 2017;44(3):1011-23.
44. Elmore S. Apoptosis: a review of programmed cell death. Toxicologic pathology. 2007;35(4):495-516.
45. Chen X, Zhang X, Xue L, Hao C, Liao W, Wan Q. Treatment with enriched environment reduces neuronal apoptosis in the periinfarct cortex after cerebral ischemia/reperfusion injury. Cellular Physiology and Biochemistry. 2017;41(4):1445-56.

46. Yu H, Zhang H, Zhao W, Guo L, Li X, Li Y, et al. Gypenoside protects against myocardial ischemia-reperfusion injury by inhibiting cardiomyocytes apoptosis via inhibition of CHOP pathway and activation of PI3K/Akt pathway in vivo and in vitro. Cellular Physiology and Biochemistry. 2016;39(1):123-36.
47. Linkermann A, Hackl M, Kunzendorf U, Walczak H, Krautwald S, Jevnikar A. Necroptosis in immunity and ischemia-reperfusion injury. American journal of transplantation. 2013;13(11):2797-804.
48. Zhe-Wei S, Li-Sha G, Yue-Chun L. The Role of Necroptosis in Cardiovascular Disease. Frontiers in Pharmacology. 2018;9(721).
49. Dikic I, Elazar Z. Mechanism and medical implications of mammalian autophagy. Nature reviews Molecular cell biology. 2018;19(6):349-64.
50. Turkmen K, Martin J, Akcay A, Nguyen Q, Ravichandran K, Faubel S, et al. Apoptosis and autophagy in cold preservation ischemia. Transplantation. 2011;91(11):1192-7.
51. Suzuki C, Isaka Y, Takabatake Y, Tanaka H, Koike M, Shibata M, et al. Participation of autophagy in renal ischemia/reperfusion injury. Biochemical and biophysical research communications. 2008;368(1):100-6.
52. Hamacher-Brady A, Brady NR, Gottlieb RA. Enhancing macroautophagy protects against ischemia/reperfusion injury in cardiac myocytes. Journal of Biological Chemistry. 2006;281(40):29776-87.
53. Yan L, Sadoshima J, Vatner DE, Vatner SF. Autophagy in ischemic preconditioning and hibernating myocardium. Autophagy. 2009;5(5):709-12.
54. Valentim L, Laurence KM, Townsend PA, Carroll CJ, Soond S, Scarabelli TM, et al. Urocortin inhibits Beclin1-mediated autophagic cell death in cardiac myocytes exposed to ischaemia/reperfusion injury. Journal of molecular and cellular cardiology. 2006;40(6):846-52.
55. Li C-J, Liao W-T, Wu M-Y, Chu P-Y. New insights into the role of autophagy in tumor immune microenvironment. International journal of molecular sciences. 2017;18(7):1566.
56. Murry CE, Jennings RB, Reimer KA. Preconditioning with ischemia: a delay of lethal cell injury in ischemic myocardium. Circulation. 1986;74(5):1124-36.
57. Zhao Z-Q, Corvera JS, Halkos ME, Kerendi F, Wang N-P, Guyton RA, et al. Inhibition of myocardial injury by ischemic postconditioning during reperfusion: comparison with ischemic preconditioning. American Journal of Physiology-Heart and Circulatory Physiology. 2003;285(2):H579-H88.
58. Staat P, Rioufol G, Piot C, Cottin Y, Cung TT, L'Huillier I, et al. Postconditioning the human heart. Circulation. 2005;112(14):2143-8.
59. Sörensson P, Saleh N, Bouvier F, Böhm F, Settergren M, Caidahl K, et al. Effect of postconditioning on infarct size in patients with ST elevation myocardial infarction. Heart. 2010;96(21):1710-5.
60. Tarantini G, Favaretto E, Marra MP, Frigo AC, Napodano M, Cacciavillani L, et al. Postconditioning during coronary angioplasty in acute myocardial infarction: the POST-AMI trial. International journal of cardiology. 2012;162(1):33-8.
61. Przyklenk K, Bauer B, Ovize M, Kloner RA, Whittaker P. Regional ischemic'preconditioning'protects remote virgin myocardium from subsequent sustained coronary occlusion. Circulation. 1993;87(3):893-9.
62. Bøtker HE, Kharbanda R, Schmidt MR, Bøttcher M, Kaltoft AK, Terkelsen CJ, et al. Remote ischaemic conditioning before hospital admission, as a complement to angioplasty, and effect on myocardial salvage in patients with acute myocardial infarction: a randomised trial. The Lancet. 2010;375(9716):727-34.
63. Dash R, Mitsutake Y, Pyun WB, Dawoud F, Lyons J, Tachibana A, et al. Dose-Dependent Cardioprotection of Moderate (32°C) Versus Mild (35°C) Therapeutic Hypothermia in Porcine Acute Myocardial Infarction. JACC Cardiovasc Interv. 2018;11(2):195-205.
64. Kern KB, Hanna JM, Young HN, Ellingson CJ, White JJ, Heller B, et al. Importance of both early reperfusion and therapeutic hypothermia in limiting myocardial infarct size post–cardiac arrest in a porcine model. JACC: Cardiovascular Interventions. 2016;9(23):2403-12.

65. Piot C, Croisille P, Staat P, Thibault H, Rioufol G, Mewton N, et al. Effect of cyclosporine on reperfusion injury in acute myocardial infarction. New England Journal of Medicine. 2008;359(5):473-81.
66. Ibanez B, Cimmino G, Prat-González S, Vilahur G, Hutter R, García MJ, et al. The cardioprotection granted by metoprolol is restricted to its administration prior to coronary reperfusion. International journal of cardiology. 2011;147(3):428-32.
67. Gersh B. Early Metoprolol Administration Before Coronary Reperfusion Results in Increased Myocardial Salvage: Analysis of Ischemic Myocardium at Risk Using Cardiac Magnetic Resonance Ibanez B, Prat-González S, Speidl WS, et al (Mount Sinai School of Medicine, NY) Circulation 115: 2909-2916, 2007. Year Book of Cardiology. 2008;2008:203-5.
68. Ibanez B, Macaya C, Sánchez-Brunete V, Pizarro G, Fernández-Friera L, Mateos A, et al. Effect of early metoprolol on infarct size in ST-segment–elevation myocardial infarction patients undergoing primary percutaneous coronary intervention: The effect of metoprolol in cardioprotection during an acute myocardial infarction (METOCARD-CNIC) trial. Circulation. 2013;128(14):1495-503.
69. group Cc. Early intravenous then oral metoprolol in 45 852 patients with acute myocardial infarction: randomised placebo-controlled trial. The Lancet. 2005;366(9497):1622-32.
70. Bangalore S, Makani H, Radford M, Thakur K, Toklu B, Katz SD, et al. Clinical outcomes with β-blockers for myocardial infarction: a meta-analysis of randomized trials. The American journal of medicine. 2014;127(10):939-53.
71. Bose AK, Mocanu MM, Carr RD, Brand CL, Yellon DM. Glucagon-like peptide 1 can directly protect the heart against ischemia/reperfusion injury. Diabetes. 2005;54(1):146-51.
72. Ossum A, van Deurs U, Engstrøm T, Jensen JS, Treiman M. The cardioprotective and inotropic components of the postconditioning effects of GLP-1 and GLP-1 (9–36) a in an isolated rat heart. Pharmacological Research. 2009;60(5):411-7.
73. Lønborg J, Vejlstrup N, Kelbæk H, Bøtker HE, Kim WY, Mathiasen AB, et al. Exenatide reduces reperfusion injury in patients with ST-segment elevation myocardial infarction. European heart journal. 2012;33(12):1491-9.
74. Wu L, Xiong X, Wu X, Ye Y, Jian Z, Zhi Z, et al. Targeting oxidative stress and inflammation to prevent ischemia-reperfusion injury. Frontiers in molecular neuroscience. 2020;13:28.
75. Casares D, Escribá PV, Rosselló CA. Membrane Lipid Composition: Effect on Membrane and Organelle Structure, Function and Compartmentalization and Therapeutic Avenues. International journal of molecular sciences. 2019;20(9):2167.
76. van der Veen JN, Kennelly JP, Wan S, Vance JE, Vance DE, Jacobs RL. The critical role of phosphatidylcholine and phosphatidylethanolamine metabolism in health and disease. Biochimica et Biophysica Acta (BBA) - Biomembranes. 2017;1859(9, Part B):1558-72.
77. Fruhwirth GO, Loidl A, Hermetter A. Oxidized phospholipids: from molecular properties to disease. Biochimica et Biophysica Acta (BBA)-Molecular Basis of Disease. 2007;1772(7):718-36.
78. McIntyre TM, Zimmerman GA, Prescott SM. Biologically active oxidized phospholipids. Journal of Biological Chemistry. 1999;274(36):25189-92.
79. Oskolkova OV, Afonyushkin T, Preinerstorfer B, Bicker W, von Schlieffen E, Hainzl E, et al. Oxidized phospholipids are more potent antagonists of lipopolysaccharide than inducers of inflammation. The Journal of Immunology. 2010;185(12):7706-12.
80. Lambeth JD. Nox/Duox family of nicotinamide adenine dinucleotide (phosphate) oxidases. Current opinion in hematology. 2002;9(1):11-7.
81. Bochkov VN, Oskolkova OV, Birukov KG, Levonen A-L, Binder CJ, Stöckl J. Generation and biological activities of oxidized phospholipids. Antioxidants & redox signaling. 2010;12(8):1009-59.
82. Yin H, Xu L, Porter NA. Free radical lipid peroxidation: mechanisms and analysis. Chemical reviews. 2011;111(10):5944-72.
83. Gugiu BG, Mesaros CA, Sun M, Gu X, Crabb JW, Salomon RG. Identification of oxidatively truncated ethanolamine phospholipids in retina and their generation from polyunsaturated phosphatidylethanolamines. Chemical research in toxicology. 2006;19(2):262-71.

84. Tyurina YY, St. Croix CM, Watkins SC, Watson AM, Epperly MW, Anthonymuthu TS, et al. Redox (phospho) lipidomics of signaling in inflammation and programmed cell death. Journal of leukocyte biology. 2019;106(1):57-81.
85. Tsimikas S, Lau HK, Han K-R, Shortal B, Miller ER, Segev A, et al. Percutaneous coronary intervention results in acute increases in oxidized phospholipids and lipoprotein (a) short-term and long-term immunologic responses to oxidized low-density lipoprotein. Circulation. 2004;109(25):3164-70.
86. Tsimikas S, Brilakis ES, Miller ER, McConnell JP, Lennon RJ, Kornman KS, et al. Oxidized phospholipids, Lp (a) lipoprotein, and coronary artery disease. New England Journal of Medicine. 2005;353(1):46-57.
87. Chou M-Y, Fogelstrand L, Hartvigsen K, Hansen LF, Woelkers D, Shaw PX, et al. Oxidation-specific epitopes are dominant targets of innate natural antibodies in mice and humans. The Journal of clinical investigation. 2009;119(5):1335-49.
88. Hörkkö S, Bird DA, Miller E, Itabe H, Leitinger N, Subbanagounder G, et al. Monoclonal autoantibodies specific for oxidized phospholipids or oxidized phospholipid–protein adducts inhibit macrophage uptake of oxidized low-density lipoproteins. The Journal of clinical investigation. 1999;103(1):117-28.
89. Philippova M, Oskolkova OV, Bochkov VN. OxPLs-Masking/Degradation Immune Assay: An "All-Included" Analysis of Mechanisms Detoxifying Oxidized Phospholipids. European Journal of Lipid Science and Technology. 2019;121(9):1800511.
90. Berliner JA, Leitinger N, Tsimikas S. The role of oxidized phospholipids in atherosclerosis. Journal of Lipid Research. 2009;50(Supplement):S207-S12.
91. Gargalovic PS, Imura M, Zhang B, Gharavi NM, Clark MJ, Pagnon J, et al. Identification of inflammatory gene modules based on variations of human endothelial cell responses to oxidized lipids. Proceedings of the National Academy of Sciences. 2006;103(34):12741-6.
92. Chang M-K, Bergmark C, Laurila A, Hörkkö S, Han K-H, Friedman P, et al. Monoclonal antibodies against oxidized low-density lipoprotein bind to apoptotic cells and inhibit their phagocytosis by elicited macrophages: evidence that oxidation-specific epitopes mediate macrophage recognition. Proceedings of the National Academy of Sciences. 1999;96(11):6353-8.
93. Yang JX, Szeto WL, Honda H, Berliner JA. Ox-PAPC activation of plasma membrane electron transport (PMET) system increases expression of heme oxygenase 1 (HO-1) in human aortic endothelial cell (HAEC). 2009.
94. Chen R, Yang L, McIntyre TM. Cytotoxic phospholipid oxidation products cell death from mitochondrial damage and the intrinsic caspase cascade. Journal of Biological Chemistry. 2007;282(34):24842-50.
95. Blüml S, Kirchberger S, Bochkov VN, Krönke G, Stuhlmeier K, Majdic O, et al. Oxidized phospholipids negatively regulate dendritic cell maturation induced by TLRs and CD40. The Journal of Immunology. 2005;175(1):501-8.
96. Greenberg ME, Li XM, Gugiu BG, Gu X, Qin J, Salomon RG, et al. The lipid whisker model of the structure of oxidized cell membranes. J Biol Chem. 2008;283(4):2385-96.
97. Seimon TA, Nadolski MJ, Liao X, Magallon J, Nguyen M, Feric NT, et al. Atherogenic lipids and lipoproteins trigger CD36-TLR2-dependent apoptosis in macrophages undergoing endoplasmic reticulum stress. Cell metabolism. 2010;12(5):467-82.
98. Watson AD, Subbanagounder G, Welsbie DS, Faull KF, Navab M, Jung ME, et al. Structural identification of a novel pro-inflammatory epoxyisoprostane phospholipid in mildly oxidized low density lipoprotein. Journal of Biological Chemistry. 1999;274(35):24787-98.
99. Dever GJ, Benson R, Wainwright CL, Kennedy S, Spickett CM. Phospholipid chlorohydrin induces leukocyte adhesion to ApoE−/− mouse arteries via upregulation of P-selectin. Free Radical Biology and Medicine. 2008;44(3):452-63.
100. Furnkranz A, Schober A, Bochkov VN, Bashtrykov P, Kronke G, Kadl A, et al. Oxidized phospholipids trigger atherogenic inflammation in murine arteries. Arteriosclerosis, thrombosis, and vascular biology. 2005;25(3):633-8.

101. Watson AD, Leitinger N, Navab M, Faull KF, Hörkkö S, Witztum JL, et al. Structural identification by mass spectrometry of oxidized phospholipids in minimally oxidized low density lipoprotein that induce monocyte/endothelial interactions and evidence for their presence in vivo. Journal of Biological Chemistry. 1997;272(21):13597-607.
102. Kadl A, Galkina E, Leitinger N. Induction of CCR2-dependent macrophage accumulation by oxidized phospholipids in the air-pouch model of inflammation. Arthritis & Rheumatism. 2009;60(5):1362-71.
103. Bochkov VN, Kadl A, Huber J, Gruber F, Binder BR, Leitinger N. Protective role of phospholipid oxidation products in endotoxin-induced tissue damage. Nature. 2002;419(6902):77-81.
104. Cole AL, Subbanagounder G, Mukhopadhyay S, Berliner JA, Vora DK. Oxidized phospholipid-induced endothelial cell/monocyte interaction is mediated by a cAMP-dependent R-Ras/PI3-kinase pathway. Arteriosclerosis, thrombosis, and vascular biology. 2003;23(8):1384-90.
105. Li R, Mouillesseaux KP, Montoya D, Cruz D, Gharavi N, Dun M, et al. Identification of prostaglandin E2 receptor subtype 2 as a receptor activated by OxPAPC. Circulation research. 2006;98(5):642-50.
106. Lee H, Shi W, Tontonoz P, Wang S, Subbanagounder G, Hedrick CC, et al. Role for peroxisome proliferator-activated receptor α in oxidized phospholipid–induced synthesis of monocyte chemotactic protein-1 and interleukin-8 by endothelial cells. Circulation research. 2000;87(6):516-21.
107. Gargalovic PS, Gharavi NM, Clark MJ, Pagnon J, Yang W-P, He A, et al. The unfolded protein response is an important regulator of inflammatory genes in endothelial cells. Arteriosclerosis, thrombosis, and vascular biology. 2006;26(11):2490-6.
108. Kadl A, Sharma PR, Chen W, Agrawal R, Meher AK, Rudraiah S, et al. Oxidized phospholipid-induced inflammation is mediated by Toll-like receptor 2. Free Radical Biology and Medicine. 2011;51(10):1903-9.
109. Yeon SH, Yang G, Lee HE, Lee JY. Oxidized phosphatidylcholine induces the activation of NLRP3 inflammasome in macrophages. Journal of leukocyte biology. 2017;101(1):205-15.
110. Zanoni I, Tan Y, Di Gioia M, Broggi A, Ruan J, Shi J, et al. An endogenous caspase-11 ligand elicits interleukin-1 release from living dendritic cells. Science. 2016;352(6290):1232-6.
111. Pégorier S, Stengel D, Durand H, Croset M, Ninio E. Oxidized phospholipid: POVPC binds to platelet-activating-factor receptor on human macrophages: implications in atherosclerosis. Atherosclerosis. 2006;188(2):433-43.
112. Latchoumycandane C, Nagy LE, McIntyre TM. Myeloperoxidase formation of PAF receptor ligands induces PAF receptor-dependent kidney injury during ethanol consumption. Free Radical Biology and Medicine. 2015;86:179-90.
113. Smiley P, Stremler K, Prescott S, Zimmerman G, McIntyre T. Oxidatively fragmented phosphatidylcholines activate human neutrophils through the receptor for platelet-activating factor. Journal of Biological Chemistry. 1991;266(17):11104-10.
114. Bochkov VN, Mechtcheriakova D, Lucerna M, Huber J, Malli R, Graier WF, et al. Oxidized phospholipids stimulate tissue factor expression in human endothelial cells via activation of ERK/EGR-1 and Ca++/NFAT. Blood. 2002;99(1):199-206.
115. Zimman A, Mouillesseaux KP, Le T, Gharavi NM, Ryvkin A, Graeber TG, et al. Vascular endothelial growth factor receptor 2 plays a role in the activation of aortic endothelial cells by oxidized phospholipids. Arterioscler Thromb Vasc Biol. 2007;27(2):332-8.
116. Marathe GK, Zimmerman GA, Prescott SM, McIntyre TM. Activation of vascular cells by PAF-like lipids in oxidized LDL. Vascular pharmacology. 2002;38(4):193-200.
117. Haserück N, Erl W, Pandey D, Tigyi G, Ohlmann P, Ravanat C, et al. The plaque lipid lysophosphatidic acid stimulates platelet activation and platelet-monocyte aggregate formation in whole blood: involvement of P2Y1 and P2Y12 receptors. Blood. 2004;103(7):2585-92.
118. Podrez EA, Byzova TV, Febbraio M, Salomon RG, Ma Y, ValiyavEpETrEtil M, et al. Platelet CD36 links hyperlipidemia, oxidant stress and a prothrombotic phenotype. Nature Medicine. 2007;13(9):1086-95.

119. Tyurina YY, Kawai K, Tyurin VA, Liu S-X, Kagan VE, Fabisiak JP. The plasma membrane is the site of selective phosphatidylserine oxidation during apoptosis: role of cytochrome C. Antioxidants and Redox Signaling. 2004;6(2):209-25.
120. Borisenko GG, Matsura T, Liu S-X, Tyurin VA, Jianfei J, Serinkan FB, et al. Macrophage recognition of externalized phosphatidylserine and phagocytosis of apoptotic Jurkat cells—existence of a threshold. Archives of biochemistry and biophysics. 2003;413(1):41-52.
121. Kagan V, Borisenko G, Serinkan B, Tyurina Y, Tyurin V, Jiang J, et al. Appetizing rancidity of apoptotic cells for macrophages: oxidation, externalization, and recognition of phosphatidylserine. American Journal of Physiology-Lung Cellular and Molecular Physiology. 2003;285(1):L1-L17.
122. Kagan VE, Fabisiak JP, Shvedova AA, Tyurina YY, Tyurin VA, Schor NF, et al. Oxidative signaling pathway for externalization of plasma membrane phosphatidylserine during apoptosis. FEBS letters. 2000;477(1-2):1-7.
123. Fruhwirth GO, Moumtzi A, Loidl A, Ingolic E, Hermetter A. The oxidized phospholipids POVPC and PGPC inhibit growth and induce apoptosis in vascular smooth muscle cells. Biochimica et Biophysica Acta (BBA)-Molecular and Cell Biology of Lipids. 2006;1761(9):1060-9.
124. Ramprecht C, Jaritz H, Streith I, Zenzmaier E, Köfeler H, Hofmann-Wellenhof R, et al. Toxicity of oxidized phosphatidylcholines in cultured human melanoma cells. Chemistry and physics of lipids. 2015;189:39-47.
125. Gómez-Muñoz A. Ceramide 1-phosphate/ceramide, a switch between life and death. Biochimica et Biophysica Acta (BBA)-Biomembranes. 2006;1758(12):2049-56.
126. Taha TA, Mullen TD, Obeid LM. A house divided: ceramide, sphingosine, and sphingosine-1-phosphate in programmed cell death. Biochimica et Biophysica Acta (BBA)-Biomembranes. 2006;1758(12):2027-36.
127. Fruhwirth GO, Hermetter A. Mediation of apoptosis by oxidized phospholipids. Lipids in Health and Disease: Springer; 2008. p. 351-67.
128. Lei P, Bai T, Sun Y. Mechanisms of ferroptosis and relations with regulated cell death: a review. Frontiers in physiology. 2019;10:139.
129. Brigelius-Flohé R, Maiorino M. Glutathione peroxidases. Biochimica et Biophysica Acta (BBA)-General Subjects. 2013;1830(5):3289-303.
130. Yang WS, SriRamaratnam R, Welsch ME, Shimada K, Skouta R, Viswanathan VS, et al. Regulation of ferroptotic cancer cell death by GPX4. Cell. 2014;156(1-2):317-31.
131. Yang WS, Kim KJ, Gaschler MM, Patel M, Shchepinov MS, Stockwell BR. Peroxidation of polyunsaturated fatty acids by lipoxygenases drives ferroptosis. Proceedings of the National Academy of Sciences. 2016;113(34):E4966-E75.
132. Friedmann Angeli JP, Schneider M, Proneth B, Tyurina YY, Tyurin VA, Hammond VJ, et al. Inactivation of the ferroptosis regulator Gpx4 triggers acute renal failure in mice. Nature cell biology. 2014;16(12):1180-91.
133. Que X, Hung M-Y, Yeang C, Gonen A, Prohaska TA, Sun X, et al. Oxidized phospholipids are proinflammatory and proatherogenic in hypercholesterolaemic mice. Nature. 2018;558(7709):301-6.
134. Cherepanova OA, Srikakulapu P, Greene ES, Chaklader M, Haskins RM, McCanna ME, et al. Novel Autoimmune IgM Antibody Attenuates Atherosclerosis in IgM Deficient Low-Fat Diet–Fed, but Not Western Diet–Fed Apoe^{–/–} Mice. Arteriosclerosis, Thrombosis, and Vascular Biology. 2020;40(1):206-19.
135. Yeang C, Hasanally D, Que X, Hung M-Y, Stamenkovic A, Chan D, et al. Reduction of myocardial ischaemia-reperfusion injury by inactivating oxidized phospholipids. Cardiovascular research. 2019;115(1):179-89.
136. Pluijmert NJ, de Jong RCM, de Vries MR, Pettersson K, Atsma DE, Jukema JW, et al. Phosphorylcholine Antibodies Preserve Cardiac Function and Reduce Infarct Size by Attenuating the Post-Ischemic Inflammatory Response. JACC: Basic to Translational Science. 2020;5(12):1228-39.

137. Tsimikas S, Bergmark C, Beyer RW, Patel R, Pattison J, Miller E, et al. Temporal increases in plasma markers of oxidized low-density lipoprotein strongly reflect the presence of acute coronary syndromes. Journal of the American College of Cardiology. 2003;41(3):360-70.
138. Tsimikas S, Lau HK, Han K-R, Shortal B, Miller ER, Segev A, et al. Percutaneous coronary intervention results in acute increases in oxidized phospholipids and lipoprotein (a): short-term and long-term immunologic responses to oxidized low-density lipoprotein. Circulation. 2004;109(25):3164-70.
139. Tsimikas S, Brilakis ES, Miller ER, McConnell JP, Lennon RJ, Kornman KS, et al. Oxidized Phospholipids, Lp(a) Lipoprotein, and Coronary Artery Disease. New England Journal of Medicine. 2005;353(1):46-57.
140. Kiechl S, Willeit J, Mayr M, Viehweider B, Oberhollenzer M, Kronenberg F, et al. Oxidized phospholipids, lipoprotein (a), lipoprotein-associated phospholipase A2 activity, and 10-year cardiovascular outcomes: prospective results from the Bruneck study. Arteriosclerosis, thrombosis, and vascular biology. 2007;27(8):1788-95.
141. Tsimikas S, Willeit P, Willeit J, Santer P, Mayr M, Xu Q, et al. Oxidation-specific biomarkers, prospective 15-year cardiovascular and stroke outcomes, and net reclassification of cardiovascular events. Journal of the American College of Cardiology. 2012;60(21):2218-29.
142. Ravandi A, Boekholdt SM, Mallat Z, Talmud PJ, Kastelein JJ, Wareham NJ, et al. Relationship of IgG and IgM autoantibodies and immune complexes to oxidized LDL with markers of oxidation and inflammation and cardiovascular events: results from the EPIC-Norfolk Study. Journal of lipid research. 2011;52(10):1829-36.
143. Van Dijk RA, Kolodgie F, Ravandi A, Leibundgut G, Hu PP, Prasad A, et al. Differential expression of oxidation-specific epitopes and apolipoprotein (a) in progressing and ruptured human coronary and carotid atherosclerotic lesions. Journal of lipid research. 2012;53(12):2773-90.
144. Leibundgut G, Arai K, Orsoni A, Yin H, Scipione C, Miller ER, et al. Oxidized phospholipids are present on plasminogen, affect fibrinolysis, and increase following acute myocardial infarction. Journal of the American College of Cardiology. 2012;59(16):1426-37.
145. DeFilippis AP, Chernyavskiy I, Amraotkar AR, Trainor PJ, Kothari S, Ismail I, et al. Circulating levels of plasminogen and oxidized phospholipids bound to plasminogen distinguish between atherothrombotic and non-atherothrombotic myocardial infarction. Journal of thrombosis and thrombolysis. 2016;42(1):61-76.
146. Singer AG, Ghomashchi F, Le Calvez C, Bollinger J, Bezzine S, Rouault M, et al. Interfacial kinetic and binding properties of the complete set of human and mouse groups I, II, V, X, and XII secreted phospholipases A2. Journal of Biological Chemistry. 2002;277(50):48535-49.
147. Weiss JP. Molecular determinants of bacterial sensitivity and resistance to mammalian Group IIA phospholipase A2. Biochimica et biophysica acta. 2015;1848(11 Pt B):3072-7.
148. Saegusa J, Akakura N, Wu C-Y, Hoogland C, Ma Z, Lam KS, et al. Pro-inflammatory secretory phospholipase A2 type IIA binds to integrins αvβ3 and α4β1 and induces proliferation of monocytic cells in an integrin-dependent manner. Journal of Biological Chemistry. 2008;283(38):26107-15.
149. Clark JD, Lin L-L, Kriz RW, Ramesha CS, Sultzman LA, Lin AY, et al. A novel arachidonic acid-selective cytosolic PLA2 contains a Ca2+-dependent translocation domain with homology to PKC and GAP. Cell. 1991;65(6):1043-51.
150. Burke JE, Dennis EA. Phospholipase A2 structure/function, mechanism, and signaling. Journal of lipid research. 2009;50(Supplement):S237-S42.
151. Ricciotti E, FitzGerald GA. Prostaglandins and inflammation. Arteriosclerosis, thrombosis, and vascular biology. 2011;31(5):986-1000.
152. Narumiya S. Physiology and pathophysiology of prostanoid receptors. Proceedings of the Japan Academy, Series B. 2007;83(9+ 10):296-319.
153. Araújo AC, Wheelock CE, Haeggström JZ. The eicosanoids, redox-regulated lipid mediators in immunometabolic disorders. Antioxidants & redox signaling. 2018;29(3):275-96.
154. Oliw EH. Oxygenation of polyunsaturated fatty acids by cytochrome P450 monooxygenates. Progress in lipid research. 1994;33(3):329-54.

155. Spector AA, Kim H-Y. Cytochrome P450 epoxygenase pathway of polyunsaturated fatty acid metabolism. Biochimica et Biophysica Acta (BBA)-Molecular and Cell Biology of Lipids. 2015;1851(4):356-65.
156. Shearer GC, Harris WS, Pedersen TL, Newman JW. Detection of omega-3 oxylipins in human plasma and response to treatment with omega-3 acid ethyl esters. Journal of lipid research. 2010;51(8):2074-81.
157. Johnson AL, Edson KZ, Totah RA, Rettie AE. Cytochrome P450 ω-hydroxylases in inflammation and cancer. Advances in Pharmacology. 74: Elsevier; 2015. p. 223-62.
158. Nayeem MA. Role of oxylipins in cardiovascular diseases. Acta Pharmacologica Sinica. 2018;39(7):1142-54.
159. Bode M, Mackman N. Regulation of tissue factor gene expression in monocytes and endothelial cells: Thromboxane A2 as a new player. Vascular pharmacology. 2014;62(2):57-62.
160. Riehl T, He L, Zheng L, Greco S, Tollefsen D, Stenson W. COX-1+/− COX-2−/− genotype in mice is associated with shortened time to carotid artery occlusion through increased PAI-1. Journal of Thrombosis and Haemostasis. 2011;9(2):350-60.
161. MacDonald TM, Hawkey CJ, Ford I, McMurray JJ, Scheiman JM, Hallas J, et al. Randomized trial of switching from prescribed non-selective non-steroidal anti-inflammatory drugs to prescribed celecoxib: the Standard care vs. Celecoxib Outcome Trial (SCOT). European heart journal. 2017;38(23):1843-50.
162. Nissen SE, Yeomans ND, Solomon DH, Lüscher TF, Libby P, Husni ME, et al. Cardiovascular safety of celecoxib, naproxen, or ibuprofen for arthritis. New England Journal of Medicine. 2016;375:2519-29.
163. Mitchell JA, Kirkby NS. Eicosanoids, prostacyclin and cyclooxygenase in the cardiovascular system. British journal of pharmacology. 2019;176(8):1038-50.
164. Zhu L, Zhang Y, Guo Z, Wang M. Cardiovascular Biology of Prostanoids and Drug Discovery. Arteriosclerosis, Thrombosis, and Vascular Biology. 2020:ATVBAHA. 119.313234.
165. Uchida K. A lipid-derived endogenous inducer of COX-2: a bridge between inflammation and oxidative stress. Molecules & Cells (Springer Science & Business Media BV). 2008;25(3).
166. Linton MF, Fazio S. Cyclooxygenase products and atherosclerosis. Drug Discovery Today: Therapeutic Strategies. 2008;5(1):25-36.
167. Piper K, Garelnabi M. Eicosanoids: Atherosclerosis and cardiometabolic health. Journal of clinical & translational endocrinology. 2020;19:100216.
168. Schaloske RH, Provins JW, Kessen UA, Dennis EA. Molecular characterization of the lipopolysaccharide/platelet activating factor-and zymosan-induced pathways leading to prostaglandin production in P388D1 macrophages. Biochimica et Biophysica Acta (BBA)-Molecular and Cell Biology of Lipids. 2005;1687(1-3):64-75.
169. Wang M, Zukas AM, Hui Y, Ricciotti E, Puré E, FitzGerald GA. Deletion of microsomal prostaglandin E synthase-1 augments prostacyclin and retards atherogenesis. Proceedings of the National Academy of Sciences. 2006;103(39):14507-12.
170. Smyth EM. Thromboxane and the thromboxane receptor in cardiovascular disease. Clinical lipidology. 2010;5(2):209-19.
171. Egan KM, Wang M, Lucitt MB, Zukas AM, Puré E, Lawson JA, et al. Cyclooxygenases, thromboxane, and atherosclerosis: plaque destabilization by cyclooxygenase-2 inhibition combined with thromboxane receptor antagonism. Circulation. 2005;111(3):334-42.
172. Kobayashi T, Tahara Y, Matsumoto M, Iguchi M, Sano H, Murayama T, et al. Roles of thromboxane A 2 and prostacyclin in the development of atherosclerosis in apoE-deficient mice. The Journal of clinical investigation. 2004;114(6):784-94.
173. Smyth EM, Grosser T, Wang M, Yu Y, FitzGerald GA. Prostanoids in health and disease. Journal of lipid research. 2009;50(Supplement):S423-S8.
174. Bäck M. Leukotriene signaling in atherosclerosis and ischemia. Cardiovascular drugs and therapy. 2009;23(1):41-8.

175. Haeggström JZ. Leukotriene biosynthetic enzymes as therapeutic targets. The Journal of clinical investigation. 2018;128(7):2680-90.
176. Bäck M. Omega-3 fatty acids in atherosclerosis and coronary artery disease. Future Science OA. 2017;3(4):FSO236.
177. Funk CD. Lipoxygenase pathways as mediators of early inflammatory events in atherosclerosis. Am Heart Assoc; 2006.
178. Caligiuri SP, Aukema HM, Ravandi A, Lavallée R, Guzman R, Pierce GN. Specific plasma oxylipins increase the odds of cardiovascular and cerebrovascular events in patients with peripheral artery disease. Canadian Journal of Physiology and Pharmacology. 2017;95(8):961-8.
179. Waddington EI, Croft KD, Sienuarine K, Latham B, Puddey IB. Fatty acid oxidation products in human atherosclerotic plaque: an analysis of clinical and histopathological correlates. Atherosclerosis. 2003;167(1):111-20.
180. Waddington E, Sienuarine K, Puddey I, Croft K. Identification and quantitation of unique fatty acid oxidation products in human atherosclerotic plaque using high-performance liquid chromatography. Analytical biochemistry. 2001;292(2):234-44.
181. Vangaveti V, Baune BT, Kennedy RL. Hydroxyoctadecadienoic acids: novel regulators of macrophage differentiation and atherogenesis. Therapeutic advances in endocrinology and metabolism. 2010;1(2):51-60.
182. Singh NK, Rao GN. Emerging role of 12/15-Lipoxygenase (ALOX15) in human pathologies. Progress in lipid research. 2019;73:28-45.
183. Spite M, Serhan CN. Novel lipid mediators promote resolution of acute inflammation: impact of aspirin and statins. Circulation research. 2010;107(10):1170-84.
184. Li P-L, Chen C-L, Bortell R, Campbell WB. 11, 12-Epoxyeicosatrienoic acid stimulates endogenous mono-ADP-ribosylation in bovine coronary arterial smooth muscle. Circulation research. 1999;85(4):349-56.
185. Carroll MA, Doumad AB, Li J, Cheng MK, Falck J, McGiff JC. Adenosine2A receptor vasodilation of rat preglomerular microvessels is mediated by EPETREs that activate the cAMP/PKA pathway. American Journal of Physiology-Renal Physiology. 2006;291(1):F155-F61.
186. Spector AA, Norris AW. Action of epoxyeicosatrienoic acids on cellular function. American journal of physiology-cell physiology. 2007;292(3):C996-C1012.
187. Deng Y, Edin ML, Theken KN, Schuck RN, Flake GP, Kannon MA, et al. Endothelial CYP epoxygenase overexpression and soluble epoxide hydrolase disruption attenuate acute vascular inflammatory responses in mice. The FASEB Journal. 2011;25(2):703-13.
188. Moran JH, Mitchell LA, Bradbury JA, Qu W, Zeldin DC, Schnellmann RG, et al. Analysis of the cytotoxic properties of linoleic acid metabolites produced by renal and hepatic P450s. Toxicology and applied pharmacology. 2000;168(3):268-79.
189. Konkel A, Schunck W-H. Role of cytochrome P450 enzymes in the bioactivation of polyunsaturated fatty acids. Biochimica et Biophysica Acta (BBA)-Proteins and Proteomics. 2011;1814(1):210-22.
190. Hou H-H, Hammock BD, Su K-H, Morisseau C, Kou YR, Imaoka S, et al. N-terminal domain of soluble epoxide hydrolase negatively regulates the VEGF-mediated activation of endothelial nitric oxide synthase. Cardiovascular research. 2012;93(1):120-9.
191. Moran JH, Nowak G, Grant DF. Analysis of the toxic effects of linoleic acid, 12, 13-cis-epoxyoctadecenoic acid, and 12, 13-dihydroxyoctadecenoic acid in rabbit renal cortical mitochondria. Toxicology and applied pharmacology. 2001;172(2):150-61.
192. Chaudhary KR, Zordoky BN, Edin ML, Alsaleh N, El-Kadi AO, Zeldin DC, et al. Differential effects of soluble epoxide hydrolase inhibition and CYP2J2 overexpression on postischemic cardiac function in aged mice. Prostaglandins & other lipid mediators. 2013;104:8-17.
193. Edin ML, Wang Z, Bradbury JA, Graves JP, Lih FB, DeGraff LM, et al. Endothelial expression of human cytochrome P450 epoxygenase CYP2C8 increases susceptibility to ischemia-reperfusion injury in isolated mouse heart. The FASEB Journal. 2011;25(10):3436-47.

194. Samokhvalov V, Jamieson KL, Darwesh AM, Keshavarz-Bahaghighat H, Lee TY, Edin M, et al. Deficiency of Soluble Epoxide Hydrolase Protects Cardiac Function Impaired by LPS-Induced Acute Inflammation. Frontiers in pharmacology. 2019;9:1572.
195. Garcia V, Schwartzman ML. Recent developments on the vascular effects of 20-hydroxyeicosatetraenoic acid. Current opinion in nephrology and hypertension. 2017;26(2):74-82.
196. Sarkis A, Roman R. Role of cytochrome P450 metabolites of arachidonic acid in hypertension. Current drug metabolism. 2004;5(3):245-56.
197. Hill E, Murphy RC. Quantitation of 20-hydroxy-5, 8, 11, 14-eicosatetraenoic acid (20-HETE) produced by human polymorphonuclear leukocytes using electron capture ionization gas chromatography/mass spectrometry. Biological mass spectrometry. 1992;21(5):249-53.
198. Tsai I-J, Croft K, Puddey IB, Beilin LJ, Barden A. 20-Hydroxyeicosatetraenoic acid synthesis is increased in human neutrophils and platelets by angiotensin II and endothelin-1. American Journal of Physiology-Heart and Circulatory Physiology. 2011;300(4):H1194-H200.
199. Cheng J, Ou J-S, Singh H, Falck JR, Narsimhaswamy D, Pritchard Jr KA, et al. 20-hydroxyeicosatetraenoic acid causes endothelial dysfunction via eNOS uncoupling. American Journal of Physiology-Heart and Circulatory Physiology. 2008;294(2):H1018-H26.
200. Cheng J, Wu C-C, Gotlinger KH, Zhang F, Falck JR, Narsimhaswamy D, et al. 20-Hydroxy-5, 8, 11, 14-eicosatetraenoic acid mediates endothelial dysfunction via IκB kinase-dependent endothelial nitric-oxide synthase uncoupling. Journal of Pharmacology and Experimental Therapeutics. 2010;332(1):57-65.
201. Ishizuka T, Cheng J, Singh H, Vitto MD, Manthati VL, Falck JR, et al. 20-Hydroxyeicosatetraenoic acid stimulates nuclear factor-κB activation and the production of inflammatory cytokines in human endothelial cells. Journal of Pharmacology and Experimental Therapeutics. 2008;324(1):103-10.
202. Ito O, Nakamura Y, Tan L, Ishizuka T, Sasaki Y, Minami N, et al. Expression of cytochrome P-450 4 enzymes in the kidney and liver: regulation by PPAR and species-difference between rat and human. Molecular and cellular biochemistry. 2006;284(1-2):141-8.
203. McGiff JC, Quilley J. 20-Hydroxyeicosatetraenoic acid and epoxyeicosatrienoic acids and blood pressure. Current opinion in nephrology and hypertension. 2001;10(2):231-7.
204. Jamieson KL, Endo T, Darwesh AM, Samokhvalov V, Seubert JM. Cytochrome P450-derived eicosanoids and heart function. Pharmacology & therapeutics. 2017;179:47-83.
205. Alonso-Galicia M, Falck JR, Reddy KM, Roman RJ. 20-HETE agonists and antagonists in the renal circulation. American Journal of Physiology-Renal Physiology. 1999;277(5):F790-F6.
206. El-Sherbeni AA, El-Kadi AO. Alterations in cytochrome P450-derived arachidonic acid metabolism during pressure overload-induced cardiac hypertrophy. Biochemical pharmacology. 2014;87(3):456-66.
207. Elkhatali S, El-Sherbeni AA, Elshenawy OH, Abdelhamid G, El-Kadi AO. 19-Hydroxyeicosatetraenoic acid and isoniazid protect against angiotensin II-induced cardiac hypertrophy. Toxicology and applied pharmacology. 2015;289(3):550-9.
208. Zu L, Guo G, Zhou B, Gao W. Relationship between metabolites of arachidonic acid and prognosis in patients with acute coronary syndrome. Thrombosis research. 2016;144:192-201.
209. Miller PE, Van Elswyk M, Alexander DD. Long-chain omega-3 fatty acids eicosapentaenoic acid and docosahexaenoic acid and blood pressure: a meta-analysis of randomized controlled trials. American journal of hypertension. 2014;27(7):885-96.
210. Bonafini S, Fava C. Omega-3 fatty acids and cytochrome P450-derived eicosanoids in cardiovascular diseases: Which actions and interactions modulate hemodynamics? Prostaglandins & Other Lipid Mediators. 2017;128-129:34-42.
211. KUZUYA T, HOSHIDA S, NISHIDA M, KIM Y, KAMADA T, TADA M. Increased production or arachidonate metabolites in an occlusion-reperfusion model of canine myocardial infarction. Cardiovascular research. 1987;21(8):551-8.
212. McCluskey E, Murphree S, Saffitz J, Morrison A, Needleman P. Temporal changes in 12-HETE formation in two models of canine myocardial infarction. Prostaglandins. 1985;29(3):387-403.

213. Engels W, Van Bilsen M, De Groot M, Lemmens P, Willemsen P, Reneman RS, et al. Ischemia and reperfusion induced formation of eicosanoids in isolated rat hearts. American Journal of Physiology-Heart and Circulatory Physiology. 1990;258(6):H1865-H71.
214. Hughes H, Gentry D, McGuire G, Taylor A. Gas chromatographic-mass spectrometric analysis of lipoxygenase products in post-ischemic rabbit myocardium. Prostaglandins, leukotrienes and essential fatty acids. 1991;42(4):225-31.
215. Nithipatikom K, DiCamelli RF, Kohler S, Gumina RJ, Falck JR, Campbell WB, et al. Determination of cytochrome P450 metabolites of arachidonic acid in coronary venous plasma during ischemia and reperfusion in dogs. Analytical biochemistry. 2001;292(1):115-24.
216. Horii Y, Nakaya M, Ohara H, Nishihara H, Watari K, Nagasaka A, et al. Leukotriene B4 receptor 1 exacerbates inflammation following myocardial infarction. The FASEB Journal. 2020;34(6):8749-63.
217. Takase B, Maruyama T, Kurita A, Uehata A, Nishioka T, Mizuno K, et al. Arachidonic acid metabolites in acute myocardial infarction. Angiology. 1996;47(7):649-61.
218. Takase B, Kurita A, Maruyama T, Uehata A, Nishioka T, Mizuno K, et al. Change of plasma leukotriene C4 during myocardial ischemia in humans. Clinical cardiology. 1996;19(3):198-204.
219. Elesber AA, Elesber AA, Best PJ, Elesber AA, Best PJ, Lennon RJ, et al. Plasma 8-iso-prostaglandin F2α, a marker of oxidative stress, is increased in patients with acute myocardial infarction. Free radical research. 2006;40(4):385-91.
220. Strassburg K, Huijbrechts AM, Kortekaas KA, Lindeman JH, Pedersen TL, Dane A, et al. Quantitative profiling of oxylipins through comprehensive LC-MS/MS analysis: application in cardiac surgery. Analytical and bioanalytical chemistry. 2012;404(5):1413-26.
221. Sun Y, Koh HW, Choi H, Koh W-P, Yuan J-M, Newman JW, et al. Plasma fatty acids, oxylipins, and risk of myocardial infarction: the Singapore Chinese Health Study. Journal of lipid research. 2016:jlr. P066423.
222. Huang C-C, Chang M-T, Leu H-B, Yin W-H, Tseng W-K, Wu Y-W, et al. Association of Arachidonic Acid-derived Lipid Mediators with Subsequent onset of Acute Myocardial infarction in patients with coronary Artery Disease. Scientific reports. 2020;10(1):1-15.
223. Fosshaug LE, Colas RA, Anstensrud AK, Gregersen I, Nymo S, Sagen EL, et al. Early increase of specialized pro-resolving lipid mediators in patients with ST-elevation myocardial infarction. EBioMedicine. 2019;46:264-73.
224. Spickett CM, Pitt AR. Oxidative lipidomics coming of age: advances in analysis of oxidized phospholipids in physiology and pathology. Antioxidants & redox signaling. 2015;22(18):1646-66.
225. Maciel E, Da Silva RN, Simões C, Domingues P, Domingues MRM. Structural characterization of oxidized glycerophosphatidylserine: evidence of polar head oxidation. Journal of the American Society for Mass Spectrometry. 2011;22(10).
226. Purwaha P, Gu Y, Kelavkar U, Kang JX, Law B, Wu E, et al. LC/ESR/MS study of pH-dependent radical generation from 15-LOX-catalyzed DPA peroxidation. Free Radical Biology and Medicine. 2011;51(7):1461-70.
227. Jessup W, Dean RT, Gebicki JM. [29] Iodometric determination of hydroperoxides in lipids and proteins. Methods in Enzymology. 233: Elsevier; 1994. p. 289-303.
228. Wolff SP. [18] Ferrous ion oxidation in presence of ferric ion indicator xylenol orange for measurement of hydroperoxides. Methods in enzymology. 1994;233:182-9.
229. Miyazawa T, Fujimoto K, Suzuki T, Yasuda K. [34] Determination of phospholipid hydroperoxides using luminol chemiluminescence—high-performance liquid chromatography. Methods in enzymology. 233: Elsevier; 1994. p. 324-32.
230. Yamamoto Y. [33] Chemiluminescence-based high-performance liquid chromatography assay of lipid hydroperoxides. Methods in enzymology. 233: Elsevier; 1994. p. 319-24.
231. Moore K, Roberts LJ. Measurement of lipid peroxidation. Free radical research. 1998;28(6):659-71.
232. Ungvari Z, Bailey-Downs L, Gautam T, Sosnowska D, Wang M, Monticone RE, et al. Age-associated vascular oxidative stress, Nrf2 dysfunction, and NF-κB activation in the nonhuman primate

Macaca mulatta. Journals of Gerontology Series A: Biomedical Sciences and Medical Sciences. 2011;66(8):866-75.
233. Spickett CM, Wiswedel I, Siems W, Zarkovic K, Zarkovic N. Advances in methods for the determination of biologically relevant lipid peroxidation products. Free radical research. 2010;44(10):1172-202.
234. Shvedova AA, Kommineni C, Jeffries BA, Castranova V, Tyurina YY, Tyurin VA, et al. Redox cycling of phenol induces oxidative stress in human epidermal keratinocytes. Journal of investigative dermatology. 2000;114(2):354-64.
235. Tyurina YY, Tyurin VA, Kaynar AM, Kapralova VI, Wasserloos K, Li J, et al. Oxidative lipidomics of hyperoxic acute lung injury: mass spectrometric characterization of cardiolipin and phosphatidylserine peroxidation. American Journal of Physiology-Lung Cellular and Molecular Physiology. 2010;299(1):L73-L85.
236. Fuchs B, Süß R, Teuber K, Eibisch M, Schiller J. Lipid analysis by thin-layer chromatography—a review of the current state. Journal of chromatography A. 2011;1218(19):2754-74.
237. Mubiru E, Shrestha K, Papastergiadis A, De Meulenaer B. Improved gas chromatography-flame ionization detector analytical method for the analysis of epoxy fatty acids. Journal of Chromatography A. 2013;1318:217-25.
238. Liakh I, Pakiet A, Sledzinski T, Mika A. Methods of the analysis of oxylipins in biological samples. Molecules. 2020;25(2):349.
239. Cracowski J-L, Baguet J-P, Ormezzano O, Bessard J, Stanke-Labesque F, Bessard G, et al. Lipid peroxidation is not increased in patients with untreated mild-to-moderate hypertension. Hypertension. 2003;41(2):286-8.
240. Milne GL, Gao B, Terry ES, Zackert WE, Sanchez SC. Measurement of F2-isoprostanes and isofurans using gas chromatography–mass spectrometry. Free Radical Biology and Medicine. 2013 Jun 1;59:36-44.
241. Yoshida Y, Kodai S, Takemura S, Minamiyama Y, Niki E. Simultaneous measurement of F2-isoprostane, hydroxyoctadecadienoic acid, hydroxyeicosatetraenoic acid, and hydroxycholesterols from physiological samples. Analytical biochemistry. 2008;379(1):105-15.
242. Taleb A, Witztum JL, Tsimikas S. Oxidized phospholipids on apoB-100-containing lipoproteins: a biomarker predicting cardiovascular disease and cardiovascular events. Biomarkers in medicine. 2011;5(5):673-94.
243. Flemmig J, Arnhold J. Interaction of hypochlorous acid and myeloperoxidase with phosphatidylserine in the presence of ammonium ions. Journal of inorganic Biochemistry. 2010;104(7):759-64.
244. Lesnefsky EJ, Minkler P, Hoppel CL. Enhanced modification of cardiolipin during ischemia in the aged heart. Journal of molecular and cellular cardiology. 2009;46(6):1008-15.
245. Lim S, Byeon SK, Lee JY, Moon MH. Computational approach to structural identification of phospholipids using raw mass spectra from nanoflow liquid chromatography–electrospray ionization–tandem mass spectrometry. Journal of mass spectrometry. 2012;47(8):1004-14.
246. Lima ÉS, Di Mascio P, Rubbo H, Abdalla DS. Characterization of linoleic acid nitration in human blood plasma by mass spectrometry. Biochemistry. 2002;41(34):10717-22.
247. Lintonen TP, Baker PR, Suoniemi M, Ubhi BK, Koistinen KM, Duchoslav E, et al. Differential mobility spectrometry-driven shotgun lipidomics. Analytical chemistry. 2014;86(19):9662-9.
248. Liu W, Porter NA, Schneider C, Brash AR, Yin H. Formation of 4-hydroxynonenal from cardiolipin oxidation: intramolecular peroxyl radical addition and decomposition. Free Radical Biology and Medicine. 2011;50(1):166-78.
249. Maciel E, da Silva RN, Simões C, Melo T, Ferreira R, Domingues P, et al. Liquid chromatography–tandem mass spectrometry of phosphatidylserine advanced glycated end products. Chemistry and physics of lipids. 2013;174:1-7.
250. Reis, A. Oxidative Phospholipidomics in health and disease: Achievements, challenges and hopes. Free Radical Biology and Medicine 2017, 111, 25-37.

251. Folch J, Lees M, Stanley GS. A simple method for the isolation and purification of total lipides from animal tissues. Journal of biological chemistry. 1957;226(1):497-509.
252. Hinterwirth H, Stübiger G, Lindner W, Lämmerhofer M. Gold nanoparticle-conjugated anti-oxidized low-density lipoprotein antibodies for targeted lipidomics of oxidative stress biomarkers. Analytical chemistry. 2013;85(17):8376-84.
253. Stübiger G, Wuczkowski M, Bicker W, Belgacem O. Nanoparticle-based detection of oxidized phospholipids by MALDI mass spectrometry: Nano-MALDI approach. Analytical chemistry. 2014;86(13):6401-9.
254. Bligh EG, Dyer WJ. A rapid method of total lipid extraction and purification. Canadian journal of biochemistry and physiology. 1959;37(8):911-7.
255. Liakh I, Pakiet A, Sledzinski T, Mika A. Modern methods of sample preparation for the analysis of oxylipins in biological samples. Molecules. 2019;24(8):1639.
256. Liakh I, Pakiet A, Sledzinski T, Mika A. Modern Methods of Sample Preparation for the Analysis of Oxylipins in Biological Samples. Molecules. 2019;24(8):1639.
257. Astarita G, Kendall AC, Dennis EA, Nicolaou A. Targeted lipidomic strategies for oxygenated metabolites of polyunsaturated fatty acids. Biochimica et Biophysica Acta (BBA)-Molecular and Cell Biology of Lipids. 2015;1851(4):456-68.
258. Chen G-y, Zhang Q. Comprehensive analysis of oxylipins in human plasma using reversed-phase liquid chromatography-triple quadrupole mass spectrometry with heatmap-assisted selection of transitions. Analytical and bioanalytical chemistry. 2019;411(2):367-85.
259. Fuchs B, Süß R, Schiller J. An update of MALDI-TOF mass spectrometry in lipid research. Progress in lipid research. 2010;49(4):450-75.
260. Pulfer M, Murphy RC. Electrospray mass spectrometry of phospholipids. Mass spectrometry reviews. 2003;22(5):332-64.
261. Donovan EL, Pettine SM, Hickey MS, Hamilton KL, Miller BF. Lipidomic analysis of human plasma reveals ether-linked lipids that are elevated in morbidly obese humans compared to lean. Diabetology & metabolic syndrome. 2013;5(1):24.
262. Fuchs B, Bresler K, Schiller J. Oxidative changes of lipids monitored by MALDI MS. Chemistry and Physics of Lipids. 2011;164(8):782-95.
263. Spalteholz H, Wenske K, Arnhold J. Interaction of hypohalous acids and heme peroxidases with unsaturated phosphatidylcholines. Biofactors. 2005;24(1-4):67-76.
264. Stübiger G, Belgacem O, Rehulka P, Bicker W, Binder BR, Bochkov V. Analysis of oxidized phospholipids by MALDI mass spectrometry using 6-aza-2-thiothymine together with matrix additives and disposable target surfaces. Analytical chemistry. 2010;82(13):5502-10.
265. Flemmig J, Spalteholz H, Schubert K, Meier S, Arnhold J. Modification of phosphatidylserine by hypochlorous acid. Chemistry and physics of lipids. 2009;161(1):44-50.
266. Taguchi R, Houjou T, Nakanishi H, Yamazaki T, Ishida M, Imagawa M, et al. Focused lipidomics by tandem mass spectrometry. Journal of Chromatography B. 2005;823(1):26-36.
267. Spickett CM, Reis A, Pitt AR. Identification of oxidized phospholipids by electrospray ionization mass spectrometry and LC–MS using a QQLIT instrument. Free Radical Biology and Medicine. 2011;51(12):2133-49.
268. Au A. Metabolomics and lipidomics of ischemic stroke. Advances in clinical chemistry. 2018;85:31-69.
269. Gruber F, Bicker W, Oskolkova OV, Tschachler E, Bochkov VN. A simplified procedure for semi-targeted lipidomic analysis of oxidized phosphatidylcholines induced by UVA irradiation. Journal of lipid research. 2012;53(6):1232-42.
270. Stübiger G, Aldover-Macasaet E, Bicker W, Sobal G, Willfort-Ehringer A, Pock K, et al. Targeted profiling of atherogenic phospholipids in human plasma and lipoproteins of hyperlipidemic patients using MALDI-QIT-TOF-MS/MS. Atherosclerosis. 2012;224(1):177-86.
271. Ravandi A, Leibundgut G, Hung M-Y, Patel M, Hutchins PM, Murphy RC, et al. Release and capture of bioactive oxidized phospholipids and oxidized cholesteryl esters during percutaneous coronary

and peripheral arterial interventions in humans. Journal of the American College of Cardiology. 2014;63(19):1961-71.
272. Hasanally D, Edel A, Chaudhary R, Ravandi A. Identification of oxidized phosphatidylinositols present in OxLDL and human atherosclerotic plaque. Lipids. 2017;52(1):11-26.
273. Ademowo OS, Sharma P, Cockwell P, Reis A, Chapple IL, Griffiths HR, et al. Distribution of plasma oxidised phosphatidylcholines in chronic kidney disease and periodontitis as a co-morbidity. Free Radical Biology and Medicine. 2020;146:130-8.

CHAPTER II – METHODS AND RESULTS

i: Role of oxidized phosphatidylcholines (OxPCs) in renal ischemia/reperfusions (I/R) injury

Previous data from our laboratory revealed that oxidised phosphatidylcholines (OxPCs) are produced in cultured neonatal rat cardiomyocytes (NNCM) following I/R. However, it's unknown if OxPC species are also produced at the tissue levels during I/R. It has been reported that 50% of kidney lipid mass is composed of phospholipids (PLs) and PCs account for 35% of the total PL content of kidneys. Given that fragmented OxPCs are potent apoptotic molecules, changes in OxPCs concentrations can contribute to renal I/R injury. Therefore, the current objectives of the following study include:

To examine if OxPC molecules are generated following renal I/R at the tissue level.

To identify groups/individual OxPCs species that experience significant alteration during I/R.

To investigate if increasing the time of reperfusion affects the OxPCs levels.

To understand if changes in tissue levels of OxPCs are correlated with the marker of tissue injury.

The hypotheses of the current study are: both fragmented and non-fragmented OxPCs are produced during renal I/R. Fragmented OxPCs become dominant molecules by increasing the time of reperfusion. Changes in OxPCs concentrations are correlated with the creatinine levels, which is a marker of kidney injury.

Oxidized phosphatidylcholines are produced in renal ischemia-reperfusion injury

Zahra Solati[1,2], Andrea L. Edel[1], Yue Shang [2,3], Karmin O [2,3], Amir Ravandi [1,2]

[1]Institute of Cardiovascular Sciences, St. Boniface Hospital Research Centre, University of Manitoba, Winnipeg, Manitoba, Canada,

[2] Department of Physiology and Pathophysiology, University of Manitoba, Winnipeg, Manitoba, Canada,

[3] Department of Animal Science, University of Manitoba, Winnipeg, Manitoba, Canada

Published in: PloS one. 2018 Apr 23;13(4):e0195172

Abstract

Background: The aim of this study was to determine the individual oxidized phosphatidylcholine (OxPC) molecules generated during renal ischemia/reperfusion (I/R) injury.

Methods: Kidney ischemia was induced in male Sprague–Dawley rats by clamping the left renal pedicle for 45 min followed by reperfusion for either 6h or 24h. Kidney tissue was subjected to lipid extraction. Phospholipids and OxPC species were identified and quantitated using liquid chromatography coupled to electrospray ionization tandem mass spectrometry using internal standards.

Result: We identified fifty-five distinct OxPC in rat kidney following I/R injury. These included a variety of fragmented (aldehyde and carboxylic acid-containing species) and non-fragmented products. 1-stearoyl-2-linoleoyl-phosphatidylcholine (SLPC-OH), which is a non-fragmented OxPC and 1-palmitoyl-2-azelaoyl-sn-glycero-3-phosphocholine (PAzPC), which is a fragmented OxPC, were the most abundant OxPC species after 6h and 24 h I/R respectively. Total fragmented aldehyde OxPC were significantly higher in 6h and 24h I/R groups compared to sham-operated groups (p=0.03, 0.001, respectively). Moreover, levels of aldehyde OxPC at 24h I/R were significantly greater than those in 6h I/R (p=0.007). Fragmented carboxylic acid increased significantly in the 24h I/R group compared with sham and 6h I/R groups (p=0.001, 0.001). Moreover, levels of fragmented OxPC were significantly correlated with plasma creatinine levels (r=0.885, p=0.001). Among non-fragmented OxPC, only isoprostanes were elevated significantly in the 6h I/R group compared with the sham group but not in the 24h I/R group (p=0.01). No significant changes were observed in other non-fragmented OxPC including long-chain products and terminal furans.

Conclusion: We have shown for the first time that bioactive OxPC species are produced in renal I/R and their levels increased with increasing time of reperfusion in a kidney model of I/R and correlated with the severity of I/R injury. Given the pathological activity of fragmented OxPCs, therapies focused on their reduction can be a mechanism to attenuate renal I/R injury.

Keyword: Kidney, ischemia/reperfusion, phospholipids, oxidized phosphatidylcholine, mass-spectrometry

Introduction

Renal ischemia/reperfusion (I/R) injury is the leading cause of acute kidney injury (AKI) affecting 13.3 million patients every year (1). AKI is considered to be the main risk factor for acute renal failure in conditions such as kidney transplantation, renal surgery, contrast media-induced nephropathy, sepsis, aortic bypass surgery and cardiopulmonary surgery (2). It is accompanied by rapid kidney dysfunction resulting in an abrupt increase in plasma creatinine as a result of kidney injury. The exact mechanisms underlying renal injury are complex and yet to be fully understood. Reduced supply of blood during renal ischemia leads to decreased oxygen in peripheral tissue, depletion of ATP and activation of enzymes such as phospholipases and protease (3). However, during reperfusion, there is a rapid influx of blood and oxygen to the injury site that is accompanied by robust inflammatory and oxidative stress responses resulting in abrupt kidney dysfunction (1). Previous evidence has shown that renal I/R injury is a final consequence of various pathological events including inflammation, oxidative stress, apoptosis and fibrosis (4).

One of the most abundant membrane phospholipids in renal tissue is phosphatidylcholine (PC). Aside from being a part of the membrane bilayer, membrane phospholipids (PL) have roles in energy storage and cell signaling (5). Previous evidence also demonstrated that phospholipids (PL) such as phosphatidylethanolamine (PE), PC, and phosphatidylinositol (PI) are potential markers of kidney disease (6).

Oxidative stress is the key meditator of I/R injury due to the inability of the innate antioxidant defense system to buffer the large burst of free radicals, which ultimately results in membrane lipid peroxidation (4). Polyunsaturated fatty acids in the Sn-2 position of membrane PLs can be oxidized by reactive oxygen species (ROS), forming heterogeneous pools of end products, particularly fragmented and non-fragmented oxidized phospholipids (OxPLs) (7). Fragmented OxPCs are biologically active compounds that can be recognized by the innate immune system through interaction with Toll-like receptors (8, 9), scavenger receptors (10-12), and natural antibodies (13, 14). They have also been implicated in many disease states such as atherosclerosis and calcific aortic valve stenosis (15, 16). OxPLs participate in the pathophysiology of atherosclerosis (17) via induction of vascular inflammation (18) and apoptosis in foam cells (19). In addition, patients with peripheral artery disease (20), and acute coronary syndromes (21) have elevated OxPL plasma levels. Epidemiological studies also reveal that OxPC can predict the occurrence of cardiac death,

myocardial infarction (MI) and stroke (22-24). We have recently shown that during cardiomyocyte I/R injury, there is a significant increase in fragmented oxidized phosphatidylcholine (OxPC) leading to cell death and pretreatment of cardiomyocytes with alpha-linolenic acid (ALA) can reduce OxPC levels and improve cell survival during I/R (25).

Considering that PLs constitute 50% of total kidney lipid mass (26), their changes during I/R can contribute to I/R injury. Given that fragmented OxPCs are potent apoptotic molecules, the aim of this study was to identify and measure these compounds during renal I/R injury.

Material and methods

Chemicals

HPLC grade solvents were obtained from VWR International (Mississauga, Ontario, Canada). The standard phospholipids; 1,2-dinonanoyl-sn-glycero-3-phosphocholine (09:0 PC), 1-heptadecanoyl-2-hydroxy-sn-glycero-3-phosphocholine (17:0 LPC), 1-palmitoyl-2-linoleoyl-sn-glycero-3-phosphocholine (PLPC), 1-palmitoyl-2-arachidonoyl-sn-glycero-3-phosphocholine (PAPC), 1-stearoyl-2-linoleoyl-sn-glycero-3-phosphocholine (SLPC), 1-stearoyl-2-arachidonoyl-sn-glycero-3-phosphocholine (SAPC), 1-palmitoyl-2-docosahexaenoyl-sn-glycero-3-phosphocholine (PDHPC), 1-palmitoyl-2-(5'-oxo-valeroyl)-sn-glycero-3-phosphocholine (POVPC), 1-palmitoyl-2-azelaoyl-sn-glycero-3-phosphocholine (PAzPC) and 1-palmitoyl-2-(9'-oxo-nonanoyl)-sn-glycero-3-phosphocholine (PONPC) were obtained from Avanti Polar Lipids (Alabaster, AL, USA). 1-palmitoyl-2-glutaryl-sn-glycero-3-phosphocholine (PGPC), 1-palmitoyl-2-(5’-keto-6’-octenedioyl)-sn-glycero-3-phosphocholine (KOdiA-PC) and 1-palmitoyl-2(4’-keto-dodec-3’-ene-dioyl)-sn-glycero-3-phosphocholine (KDdiA-PC) were purchased from Cayman Chemicals (Ann Arbor, Michigan, USA). All other chemicals were purchased from Sigma Aldrich (St. Louis, Missouri, USA).

Renal ischemia-reperfusion (I/R)

Kidney ischemia was induced in 8 male Sprague–Dawley rats (250–300 g) by clamping the left renal pedicle for 45 min followed by reperfusion for 24h (n=4 in each group). In brief, rats were anaesthetized by 3% isoflurane/oxygen gas prior to surgery. Surgery was performed when rats reached stage 3 anaesthesia. During surgery, 1–2% isoflurane/oxygen gas was maintained via

inhalation. Rats were kept on a heating pad and the rectal temperature was maintained at 37°C throughout the experimental procedure. To prevent decreases in body temperature, rats were placed in a warm incubator for 12h after surgery. As a control, a sham-operated group of rats were subjected to the same surgical procedure, but without inducing I/R, and were euthanized at corresponding time points. A blood sample was collected and plasma was separated by centrifugation at 3,000 g for 20 min at 4°C. A portion of kidney tissue was used for lipid extraction and the other portions were used for staining. Kidney sections were stained with hematoxylin and eosin (HE) staining kit (Baibo Biotechnology Co., Ltd., Shandong, China).

All procedures were performed in accordance with the Guide to the Care and Use of Experimental Animals published by the Canadian Council on Animal Care and approved by the University of Manitoba Protocol Management and Review Committee (permit number: B2015-039). Plasma creatinine concentrations were measured using a commercial assay kit (Genzyme Diagnostics, Canada). Harvested kidneys were rinsed in ice-cold potassium phosphate buffer and then were snap-frozen in liquid nitrogen and kept in a -80 freezer to be used for analysis. Then, at the time of lipid extraction, they were pulverized in liquid nitrogen. Creatinine levels in plasma were measured using the Cobas C111 Analyzer (Roche, Laval, QC, Canada).

Phospholipid extraction from renal tissue

Frozen renal tissue was thawed on ice. Rat kidney was pulverized in liquid nitrogen until a fine powder was obtained. A portion of each sample (30-50 mg) was weighed and subjected to lipid extraction with 2:1 (vol/vol) chloroform: methanol using the method described by Folch *et al* (27). An internal standard mixture of 09:0 PC (0.1 µg/ml), 20:0 PC (1 µg/ml), 17:0 PC (LPC) (0.1 µg/ml), 17:0 PE (1 µg/ml), 16:0 PS (1 µg/ml), 14:0 CL (2 µg/ml), 14:0 PtG (1 µg/ml), and 17:0-14:1 PI (1 µg/ml) was added to each sample prior to lipid extraction. A portion of lipid extract was reconstituted in the mobile phase prior to injection on the HPLC-MS/MS system.

Reverse-phase HPLC

Separation of OxPC species was done as described previously (25). Briefly, 30 µL of sample extracts, reconstituted in reverse phase solvent, were injected onto an Ascentis Express C18 HPLC column (15 cm × 2.1 mm, 2.7 µm; Supelco Analytical, Bellefonte, Pennsylvania, USA) using a Prominence HPLC system (Shimadzu Corporation, Canby, Oregon, USA). Elution was performed

by a linear gradient of solvent A (acetonitrile/water, 60:40 vol/vol) and solvent B (isopropanol/acetonitrile, 90:10, vol/vol) both solvents containing 10 mM ammonium formate and 0.1% formic acid. The time program used was as follows: initial solvent B at 32%, increased to 45% B until 4.00 min; 5.00 min 52% B; 8.00 min 58% B; 11.00 min 66% B; 14.00 min 70% B; 18.00 min 75% B; 21.00 min 97% B; 25.00 min 97% B; 25.10 min 32% B until the elution was stopped at 30.10 min. A flow rate of 0.26 ml/min was used for analysis. The temperature of the column oven and sample tray was maintained at 45 and 4˚C, respectively.

Normal-phase HPLC

For the separation of non-oxidized phospholipids, 10µL of sample extract reconstituted in normal phase solvent was injected onto an Ascentis Si HPLC column (15 cm × 1mm, 3 µm; Supelco Analytical, Bellefonte, Pennsylvania, USA) (28). Elution was performed by linear gradient of solvent A (chloroform/methanol/ammonium hydroxide, 80:19.5:0.5 vol/vol/vol) and solvent B (chloroform/methanol/water/ammonium hydroxide, 60:34:5.5:0.5 vol/vol/vol/vol). The normal phase time program used was initial solvent B at 0%; ramped to 100% B at 14.00 min; held until 24.00 min at 100% B; then dropped at 24.10 min to 0% B until the elution was stopped at 30.10 min. A flow rate of 0.070 ml/min was used for analysis. The temperature of the column oven and sample tray was maintained at 25 and 4˚C, respectively.

Mass spectrometry

The HPLC system was coupled to a 4000 QTRAP® triple quadrupole linear ion trap hybrid mass spectrometer system equipped with a Turbo V electrospray ion source (AB Sciex, Framingham, Massachusetts, USA)(16). OxPC, PC, LPC (lysophosphatidylcholine), and SM (sphingomyelin) species were detected in positive ion mode via Multiple Reaction Monitoring (MRM) using the product ion 184.3 *m/z*, Da corresponding to the fragmented phosphatidylcholine head group. PI (Phosphatidylinositol), PtG (phosphatidylglycerol), and PE (phosphatidylethanolamine) were detected in negative ion mode via MRM using the product ions 241, 170, and 139.8 *m/z*, Da, respectively. The mass spectrometer settings for positive ion mode analyses were as follows: electrospray ionization (ESI), 5500 V; declustering potential (DP), 125 V; entrance potential (EP), 10 V; collision energy (CE), 53 V; collision cell exit potential (CXP), 9V; curtain plate (CP), 26 psi; ion source gas 1 (GS1), 40 psi; ion source gas 2 (GS2), 30 psi, a retention time window of 50

msec was used and the temperature of the ion source was 500^0C. The mass spectrometer settings for negative ion mode analyses were: ESI, -4500 V; DP, -80 V; EP, -10 V; CE, -60 V; CXP, -20V; CP, 20 psi; GS1, 30 psi; GS2, 30 psi, a retention time window of 100 msec and the temperature of the ion source was 500^0C. Data were collected utilizing Analyst® Software 1.6 (AB Sciex). MultiQuant® Software 2.1 (AB Sciex) was used to compare peak areas of specific phospholipid compounds with their respective internal standard. Relative amounts of each phospholipid or oxidized phospholipid were then calculated based upon the amount of internal standard added. Final results are presented as the amount of phospholipid detected per mg of renal tissue extracted.

Statistical analysis

One-way analysis of variance (ANOVA) with a Tukey post-hoc test for multiple comparisons was used to determine statistically significant differences between the three groups using a *P*-value < 0.05 (SPSS Software version 24, IBM Corporation, Armonk, NY, USA). Pearson's correlation analysis was used to determine significant associations between study variables. All data are presented as mean ± SEM.

Results

Creatinine concentrations, histological analysis, and I/R injury

Plasma creatinine concentration, a marker of acute kidney injury, was assessed in each of the three experimental groups. Levels in plasma significantly increased both 6 and 24h after reperfusion (p<0.05) relative to the sham group (Figure 6A). Creatinine concentrations were statistically greater at 24h I/R compared to 6h I/R (p=0.001). Hematoxylin and eosin (H&E) staining revealed that kidneys in the I/R groups showed interstitial congestion compared with the sham group (Figure 6B).

Figure 6: Markers of acute kidney injury measured in (A) plasma and (B) renal slices from sham, 6 and 24h I/R groups

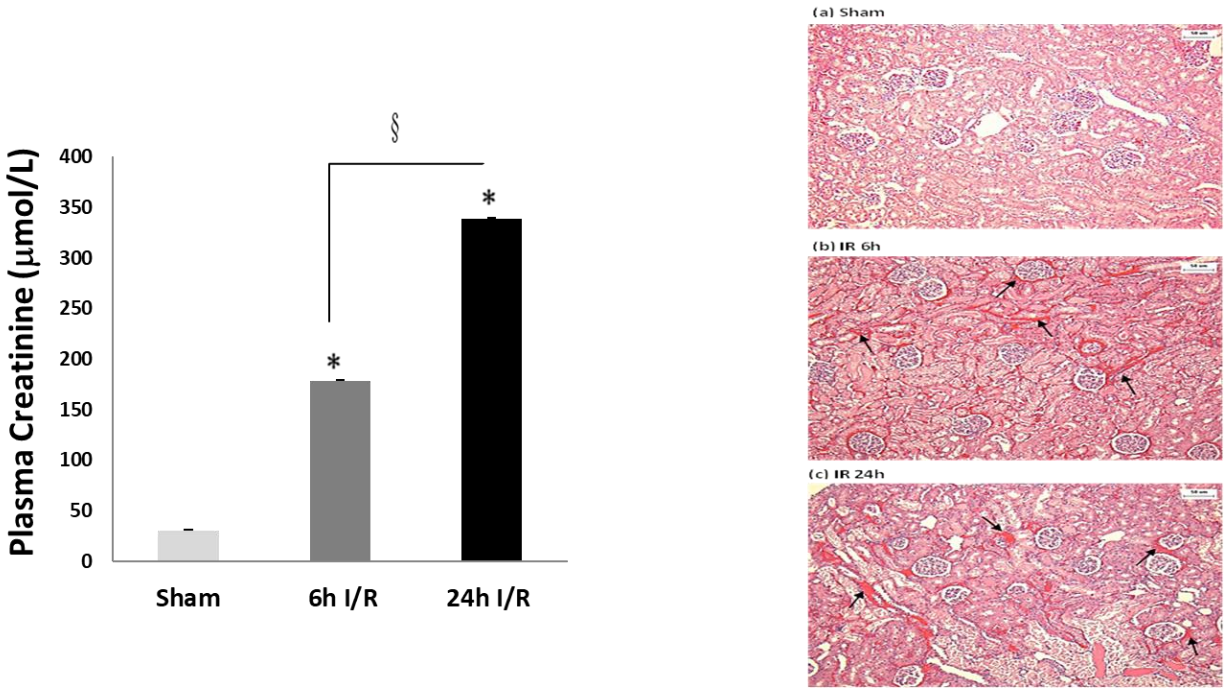

A Plasma creatinine concentrations from sham, 6 and 24h I/R groups.

Values are means ± SEM (n=4 in each group). * Significant difference compared to sham, $p<0.05$. § Significant difference between I/R groups, $p<0.05$. **B** Hematoxylin and eosin (H&E) staining of renal tissue in sham, 6 and 24h I/R groups. The left kidney of rats was subjected to 45 min ischemia followed by 6h or 24h of reperfusion (I/R). As a control, rats were subjected to a sham-operation without inducing ischemia (Sham). The gross appearance of a mid-transverse plane of the kidney was examined by H&E staining and analyzed at ×100 magnification. Kidneys in the I/R group followed by 6h or 24h of reperfusion (b and c) showed interstitial congestion (arrow) compared with the Sham group (a).

OxPCs levels in rat renal tissue following I/R injury

Mass spectral analysis of kidney lipid extracts identified fifty-five distinct OxPC in rat kidney following I/R injury. These included a variety of fragmented (aldehyde and carboxylic acid-containing species) and non-fragmented (terminal furans, isoprostanes, and long-chain products) OxPC derivatives. Representative chromatograms of four prominent OxPC species detected in renal tissue from sham (dashed line) and 24h I/R (solid line) are presented in Figure 7. These include the fragmented species POVPC (A), PAzPC (B), and PONPC (C) as well as the non-fragmented OxPC, SLPC-OH. For each OxPC identified, there was a significant increase in relative intensities in the I/R group relative to sham.

Figure 7: Fragmented and non-fragmented OxPC identified in rat renal tissue in sham-operated and 24h I/R groups by HPLC-MS/MS

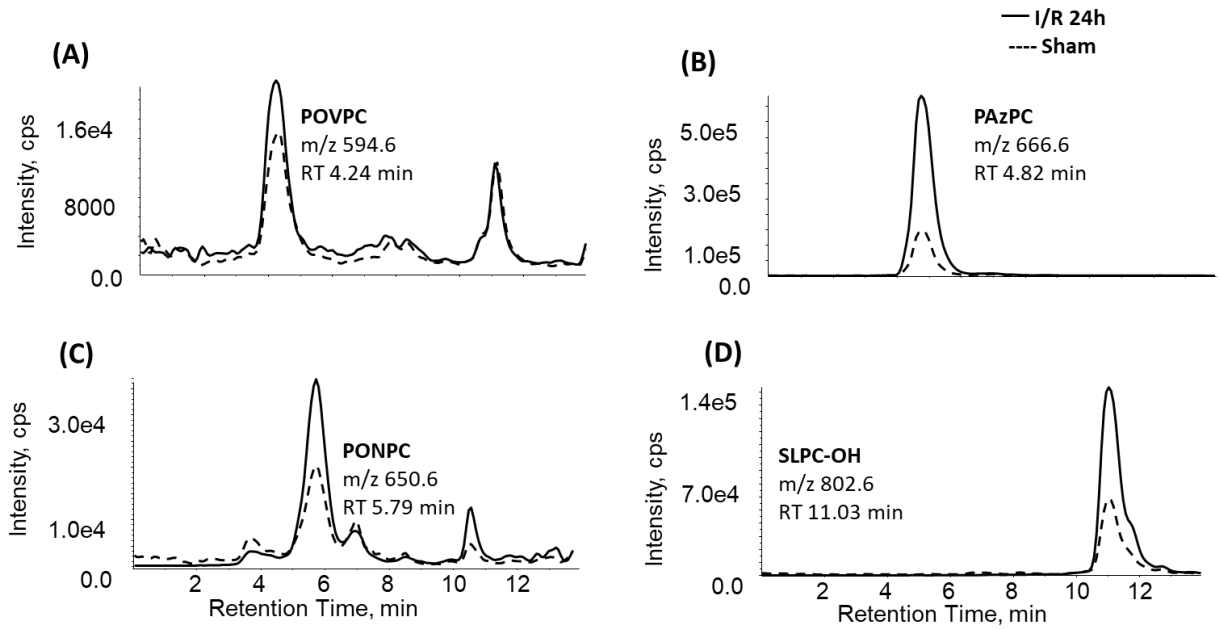

MRM chromatogram of (A) POVPC, (B) PAzPC, (C) PONPC and (D) SLPC-OH in renal tissue in I/R 24h (black line) and sham (dotted line) groups as measured by reverse-phase HPLC-MS/MS. **Abbreviations**: POVPC:1-palmitoyl-2-(5'-oxo-valeroyl)-sn-glycero-3-phosphocholine, PAzPC: 1-palmityl-2-azelayl-sn-glycero-3-phosphocholine, PONPC: 1-palmitoyl-2-(9'-oxo-nonanoyl)-sn-glycero-3-phosphocholine, SLPC-OH: 1-stearoyl-2-linoleoyl-phosphatidylcholine.

Total OxPC levels significantly increased following both 6h (p=0.01) and 24h (p=0.001) reperfusion when compared to the sham group. There was a trend towards an increase in total OxPC levels at 24h I/R compared to 6h I/R, but it did not reach statistical significance (p=0.06) (Figure 8).

Figure 8: Total OxPC levels during renal I/R injury including fragmented and non-fragmented OxPC species measured in renal tissue in sham (light grey bar), 6h I/R (dark grey bar), and 24h I/R (black bar) groups

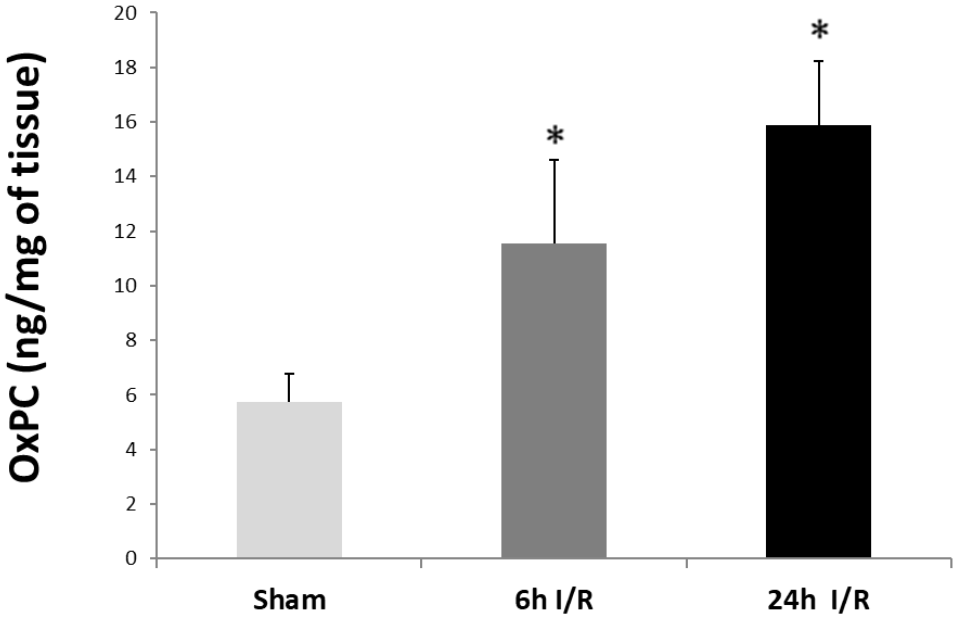

Abbreviation: Values are means ± SEM (n=4 in each group), * Significant difference compared to sham, $p<0.05$. OxPC: Oxidized phosphatidylcholine.

A significant positive correlation was observed between total OxPC levels and severity of AKI as measured by creatinine levels ($r=0.863$, $p=0.001$) (Figure 9A). Similar associations were observed for the OxPC subspecies, total fragmented (9B), aldehydes (9C) and carboxylic acids (9D), with the exception of total non-fragmented OxPCs (9E).

Figure 9: Correlations between tissue OxPC species and plasma creatinine levels

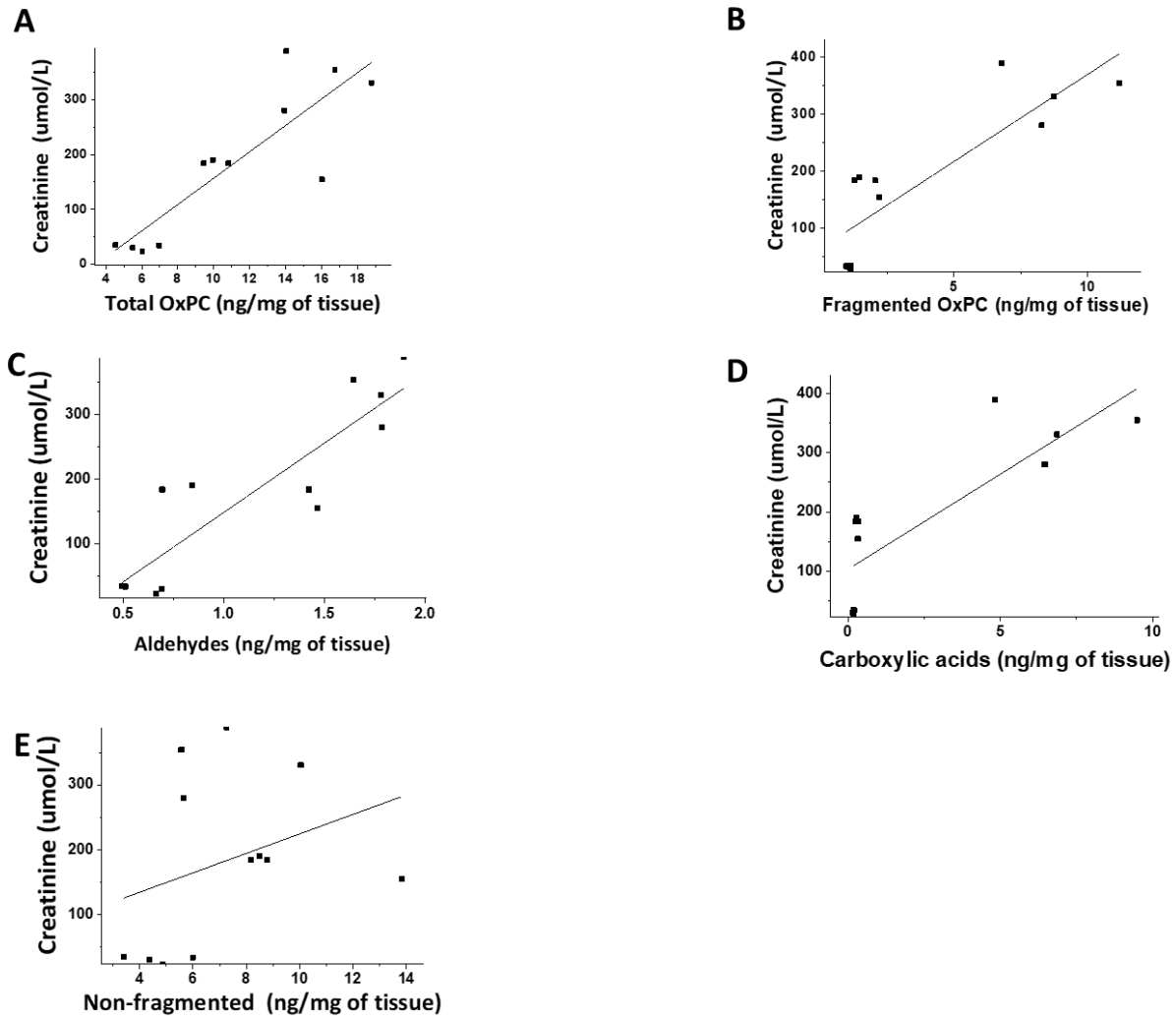

4

Correlations between (A) total OxPC (r=0.863, p=0.001), (B) fragmented OxPC (r=0.885, p=0.001), (C) aldehyde (r=0.888, p=0.001) and (D) carboxylic acid containing OxPCs (r=0.821, p=0.001), non-fragmented OxPC (r=0.324, p=0.305) and creatinine levels. n=4 in each group. **Abbreviation**: OxPC: Oxidized phosphatidylcholine.

To investigate which groups of OxPCs contributed most to the overall change in OxPC levels in each of the sham, 6h and 24h study groups, compounds were subdivided into fragmented and non-fragmented species. Percentages of total fragmented and non-fragmented OxPC in all groups are shown in Figure 10.

Figure 10: Percent of total OxPC in rat kidney in sham and I/R groups

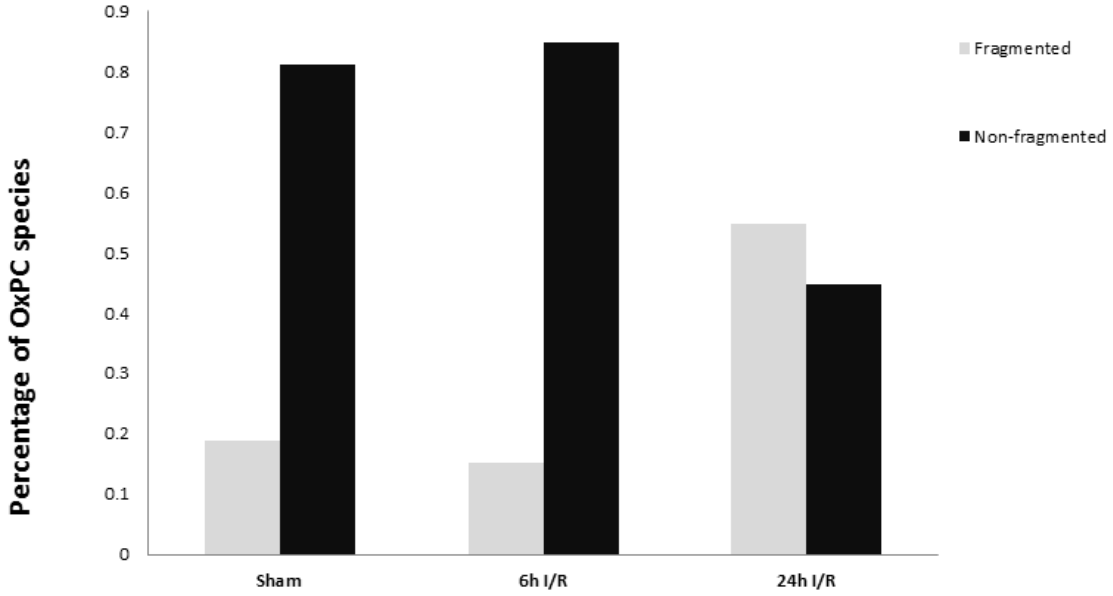

Values represent the average relative percentage of a particular OxPC species compared to the total OxPC. n=4 in each group. **Abbreviation**: OxPC: Oxidized phosphatidylcholine.

Total fragmented OxPC increased significantly in the 24h I/R experimental group when compared to both sham-operated and 6h I/R groups (8.74±1.83 versus 1.08±0.07 and1.75±0.44 ng/mg of renal tissue, p=0.001) (Figure 11A). However, no significant differences were observed between sham and 6h I/R groups. When correlated with creatinine levels to assess AKI severity, a strong positive correlation was observed between total fragmented OxPC levels and creatinine levels (r=0.885, p=0.001) (Figure 9B).

Figure 11: OxPC subgroups classified by fragmentation pattern and species in sham, 6h, and 24h I/R groups

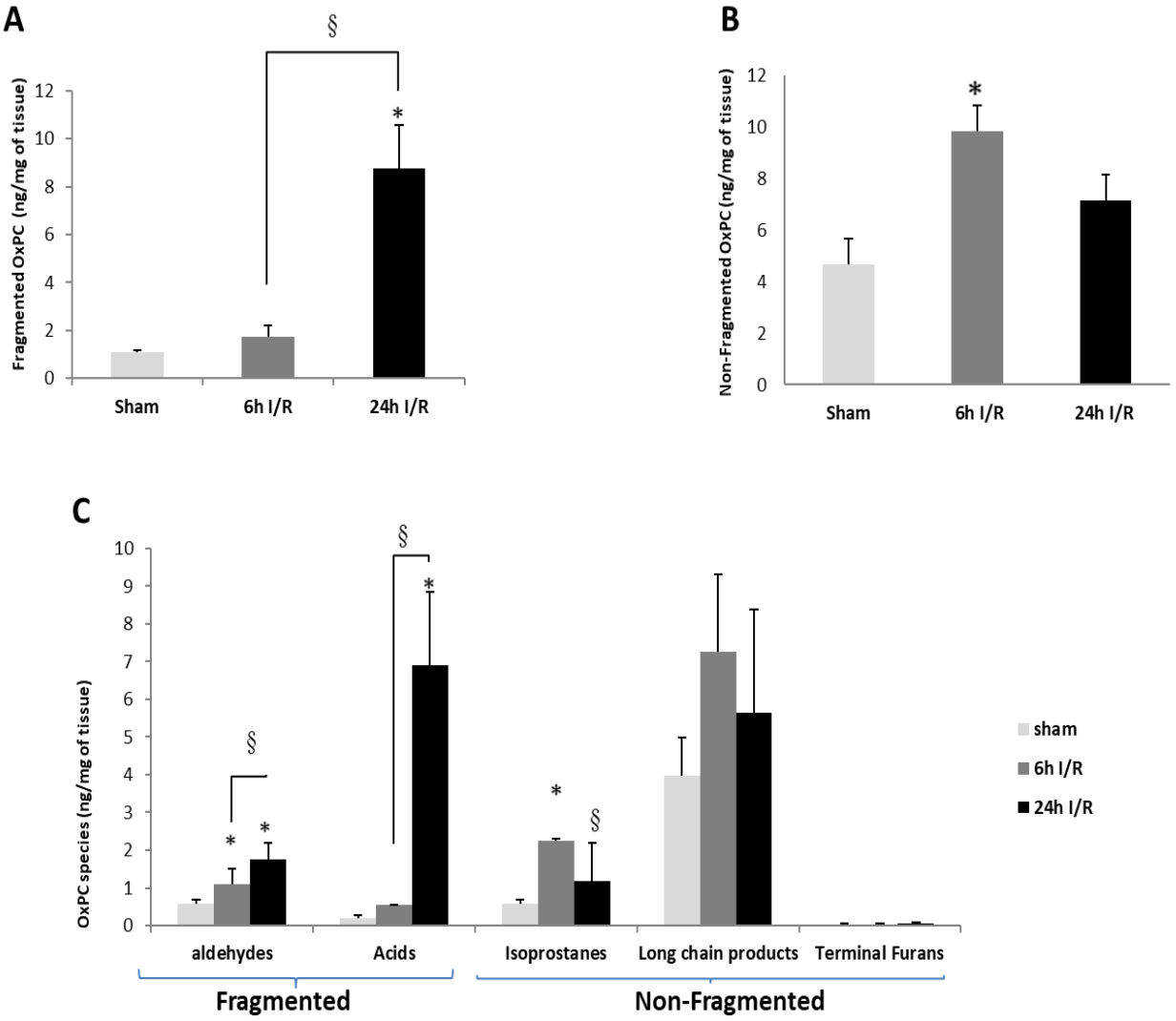

Total fragmented OxPC (A), non-fragmented OxPC (B) and OxPC by species (C) in sham (light gray bar), 6h I/R (dark gray bar) and 24h I/R (black bar) groups. Values are means ± SEM. * Significant difference compared to sham, $p<0.05$. § Significant difference between I/R groups, $p<0.05$.
Abbreviation: OxPC: Oxidized phosphatidylcholine.

The most abundant fragmented OxPC measured in renal tissue after 6 and 24h I/R were PONPC and PAzPC. Average amounts consisted of 0.25±0.09 and 0.24±0.03 ng/mg after 6h and 0.57±0.02 and 6.37±1.99 ng/mg of renal tissue after 24h, respectively (Table 1). All fragmented OxPC species identified in rat kidney tissue are presented in Table 1.

Table 1: Identified fragmented OxPC species in kidney tissue in sham and I/R groups

Fragmented OxPC	Sham (ng/mg of tissue)	6h I/R (ng/mg of tissue)	24h I/R (ng/mg of tissue)
4-oxo-butyryl-PC	0.04±0.00	0.06±0.02	0.09±0.00*§
POVPC	0.1±0.02	0.18±0.07	0.27±0.01*
Succinoyl-PC	0.03±0.00	0.07±0.01*	0.08±0*
PGPC	0.02±0.01	0.03±0.01	0.07±0.01*
SOVPC	0.17±0.04	0.31±0.11	0.36±0.06*
Furylbutanoyl-PC	0.01±0.00	0.01±0.00	0.02±0.00
KOHA-PC	0.01±0.00	0.01±0.00	ND
8-oxo-octanoyl-PC	0.04±0.00	0.07±0.03	0.11±0.01*
SGPC	0.06±0.00	0.06±0.04	0.07±0.02
KOOA-PC	ND	0.01±0.01	0.04±0.01*
PONPC	0.13±0.02	0.25±0.09*	0.57±0.02*
Furylbutanoyl-SPC	0.01±0.00	0.02±0.01	0.03±0.02
KOdiA-PC	0.04±0.01	0.07±0.03	0.10±0.02*
PAzPC	0.21±0.08	0.24±0.03	6.37±1.99*§
KOOA-SPC	ND	ND	0.01±0.00*
SONPC	0.06±0.01	0.16±0.06*	0.28±0.02*
Furyloctanoyl-PC	0.01±0.00	0.00±0.00	0.01±0.00
SAzPC	0.08±0.02	0.10±0.01	0.29±0.13*
HODA-PC	0.002±0.00	0.003±0.00	0.007±0.00*§
HDdiA-PC	ND	ND	0.01±0.00*

Values are means ± SEM. * Significant differences compared with the sham group. §Significant differences compared with 6h I/R group, $p<0.05$. **Abbreviations**: HDdiA-PC: 1-palmitoyl-2-(9-hydroxy-11-carboxyundec-6-enoyl)-sn-glycero3-phosphocholine, HODA-PC: 9-hydroxy-12-oxododec-10-enoic acid ester of 2-lysophosphatidylcholine, KOdiA-PC: 1-palmitoyl-2-(5'-keto-6'-octenedioyl)-sn-glycero-3-phosphocholine, PAzPC: 1-palmityl-2-azelayl-sn-glycero-3-phosphocholine, KOHA-PC: 1-palmityl-2-(4-oxo-7-oxohept-5-enoyl)-sn-glycero-3-phosphoserine, KOOA-PC: 1- stearoyl-(5-keto-8-oxo-6-octenoyl)-sn-glycero-3-phosphocholine, KOOA-SPC: 1-palmitoyl-(5-keto-8-oxo-6-octenoyl)-sn-glycero-3-phosphocholine, PGPC: 1-palmitoyl-2-glutaryl-sn-glycero-3-phosphocholine, PONPC: 1-palmitoyl-2-(9'-oxo-nonanoyl)-sn-glycero-3-phosphocholine, POVPC: 1-palmitoyl-2-(5'-oxo-valeroyl)-sn-glycero-3-phosphocholine, SAzPC: 1-stearoyl-2-azelaoyl-sn-glycero-3-phosphocholine, SGPC : 1-stearoyl-2-glutaroyl-sn-glycero-3-phosphocholine, SONPC: 1-stearoyl -2-(9-oxo-nonanoyl)-snglycero-3-phosphocholine, SOVPC: sn-1-stearoyl-2-oxovaleroyl-PC.

Fragmented OxPC were then classified into two groups: aldehyde and carboxylic acid-containing OxPC. Total aldehydes were significantly higher in the 6h and 24h I/R groups in comparison to the sham group. Moreover, levels of aldehyde OxPC at 24h I/R were significantly greater than those in 6h I/R (p=0.007) (Figure 11C). Significant correlations were also observed between levels of aldehyde containing OxPC and plasma creatinine levels (r=0.888, p=0.001) (Figure 9C). For total fragmented carboxylic acids, significant increases were observed in the 24h I/R group compared with both sham and 6h I/R group (6.91±1.92 versus 0.18±0.09 and 0.53±0.01 ng/mg of renal tissue, p=0.001) (Figure 11C). No significant changes were identified between the sham-operated and 6h I/R group. Similar to aldehyde containing OxPC, levels of a carboxylic acid-containing OxPC were positively correlated with the severity of I/R injury as measured by creatinine levels (r=0.821, p=0.001) (Figure 9D).

Non-fragmented species also had significant changes as a result of I/R injury (Figure 11B). The most abundant non-fragmented OxPC after 6h and 24h I/R was SLPC-OH (2.49±1.62 and 1.87±0.41 ng/mg of tissue) (Table 2). Total non-fragmented OxPC concentrations in the 6h I/R group were significantly greater than the sham group, but not at 24h I/R (Figure 11B). This is likely attributed to the high prevalence of isoprostanes after 6h I/R (Figure 11C). IsoPG (E2, I2, D2)-SPC, the most prevalent isoprostane identified in renal tissue after 6h I/R, was detected at concentrations of 0.46±0.19 ng/mg tissue with 0.071±0.02 ng/mg tissue in sham tissue. Although non-fragmented isoprostanes increased significantly in the 6h I/R group compared with the sham group, their levels dropped significantly at 24h I/R when compared to the 6h group (p=0.02) and were unchanged compared to control (P =0.488) (sham: 0.57±0.10, 6h I/R: 2.24±0.04 and 24h I/R: 1.16±1.03 ng/mg of renal tissue). Non-fragmented OxPC derivatives including long-chain products and terminal furans were unchanged in any of the I/R groups (Figure 11C). Interestingly, no significant correlations were observed between any of the non-fragmented OxPC (including total non-fragmented OxPC, terminal furans, isoprostanes, and long-chain products) with creatinine levels (r=0.324, p=0.305). All non-fragmented OxPC species identified are presented in Table 2.

Table 2: Identified non-fragmented OxPC species in kidney tissue in sham and I/R groups

Non-Fragmented OxPC	Sham (ng/mg of tissue)	6h I/R (ng/mg of tissue)	24h I/R (ng/mg of tissue)
PLPC-keto	0.19±0.04	0.4±0.14	0.53±0.246*
PLPC-OH	0.19±0.05	0.32±0.10	0.27±0.158
PLPC-epoxy	0.12±0.04	0.31±0.15	0.2±0.053
PLPC-OOH	0.09±0.03	0.18±0.07	0.14±0.101
PAPC-keto	0.16±0.05	0.42±0.20	0.36±0.185
PAPC-OH	0.09±0.02	0.28±0.22	0.17±0.093
SLPC-keto	0.18±0.06	0.51±0.21*	0.35±0.134
SLPC-OH	1.73±0.56	2.49±1.62	1.87±0.417
PLPC-OOH	0.01±0.00	0.01±0.01	0.01±0.011
PLPC-OOH	0.11±0.08	0.12±0.05	0.14±0.07
PLPC-diOH	0.06±0.10	0.05±0.06	0.02±0.00
isoPG(A2,J2)-PC	0.05±0.02	0.17±0.05*	0.08±0.05
PAPC-OOH	0.04±0.03	0.06±0.06	0.02±0.01
SLPC-epoxy	0.10±0.03	0.25±0.07*	0.24±0.08
SLPC-OOH	0.05±0.03	0.09±0.03	0.06±0.04
PGJ2-SPC	0.06±0.01	0.17±0.05	0.29±0.10*
SAPC-keto	0.10±0.03	0.30±0.06*	0.35±0.13
SAPC-OH	0.53±0.24	0.73±0.46	0.43±0.11
PEIPC	0.03±0.02	0.10±0.06	0.06±0.02
isoPG(E2,I2,D2)-PC	0.09±0.05	0.16±0.10	0.08±0.05
isoPGF2α-PC	0.04±0.02	0.18±0.03*	0.09±0.04
SAPC-OH	0.53±0.24	0.73±0.46	0.43±0.11
SLPC-OOH	0.05±0.03	0.09±0.03	0.06±0.04
SLPC-triOH	0.04±0.01	0.08±0.02*	0.05±0.01
SECPC	0.05±0.00	0.23±0.05*	0.12±0.04
isoPG(A2,J2)-SPC	0.03±0.00	0.17±0.05*	0.10±0.06
SAPC-OOH	0.05±0.01	0.38±0.15*	0.26±0.13
SEIPC	0.07±0.01	0.27±0.02*	0.11±0.04
isoPG(E2,I2,D2)-SPC	0.07±0.02	0.46±0.19*	0.18±0.12
isoPGF2α-SPC	0.02±0.00	0.15±0.07*	0.05±0.02
SLPC-OOH,OH	0.01±0.00	0.05±0.03	0.04±0.03
SLPC-triOH	0.05±0.00	0.23±0.05	0.12±0.04
SECPC	0.03±0.00	0.17±0.05	0.12±0.06
isoPG(A2,J2)-SPC	0.05±0.01	0.38±0.15	0.26±0.13
SAPC-OOH	0.07±0.01	0.27±0.02	0.11±0.04
SEIPC	0.07±0.02	0.46±0.19	0.18±0.12

isoPG(E2,I2,D2)-SPC	0.02±0.00	0.15±0.07	0.05±0.02
isoPGF2α-SPC	0.05±0.00	0.23±0.05	0.12±0.04
SAPC-OOH,diketo	0.02±0.00	0.04±0.00*	0.02±0.01
SAPC-OOH,OH,keto	0.04±0.01	0.08±0.02*	0.05±0.02
SAPC-diOOH	0.05±0.00	0.17±0.01*	0.08±0.04
Isofuran-SPC	0.01±0.00	0.12±0.08*	0.05±0.03
SAPC-OOH,OH,epoxy	0.00±0.00	0.00±0.00*	0.01±0.00
SAPC-diOOH,OH	0.02±0.00	0.07±0.03	0.04±0.02
SAPC-triOOH	0.02±0.00	0.03±0.00	0.03±0.01

Values are means ± SEM. *Significant differences compared with sham group. § Significant differences compared with 6h I/R group, $p<0.05$. **Abbreviations**: isoPG: isoprostanes, OH: hydroxyl, OOH: hydroperoxyl, PAPC: 1-palmitoyl-2-arachidonoyl-snglycero-3-phosphocholine, PEIPC: 1-palmitoyl-2-(5,6-epoxyisoprostane E2)-sn-glycero-3-phosphocholine, PGJ2-SPC : prostaglandin J2- stearoyl phosphocholine, PLPC: 1-palmitoyl-2-linoleoyl-sn-glycero-3-phosphocholine, SAPC: 1-stearoyl-2-arachidonoyl-sn-glycero-3-phosphocholine, SEIPC: 1- stearoyl -2-(5,6-epoxyisoprostane E2)-sn-glycero-3-phosphocholine, SLPC: 1-stearoyl-2-linoleoyl-sn-glycero-3- phosphocholine.

Non-oxidized phospholipids in rat renal tissue following I/R injury

PC and sphingomyelin (SM) were the most abundant PLs in the sham group (25.78±1.94 and 7.27±0.69 µg/mg of tissue, respectively), followed by PI (0.55±0.12 µg/mg of tissue) and PE (0.87±0.20 µg/mg of tissue), then PS (0.43±0.08 µg/ mg of tissue) and PtG (0.025±0.003 µg/mg of tissue). Average concentrations of total PC content in renal tissue for each of the experimental groups are represented in Figure 12A. Although there were no changes in total PC levels after 6h I/R compared to sham, PC levels significantly increased after 24h I/R when compared to both sham and 6h I/R groups (3.36±4.80 versus 2.57±1.94 and 2.37±2.41 µg/mg of renal tissue respectively p=0.015, 0.004) (Figure 12A).

Figure 12: Representative amounts of non-oxidized lipids in renal tissue from sham, 6h, and 24h I/R groups

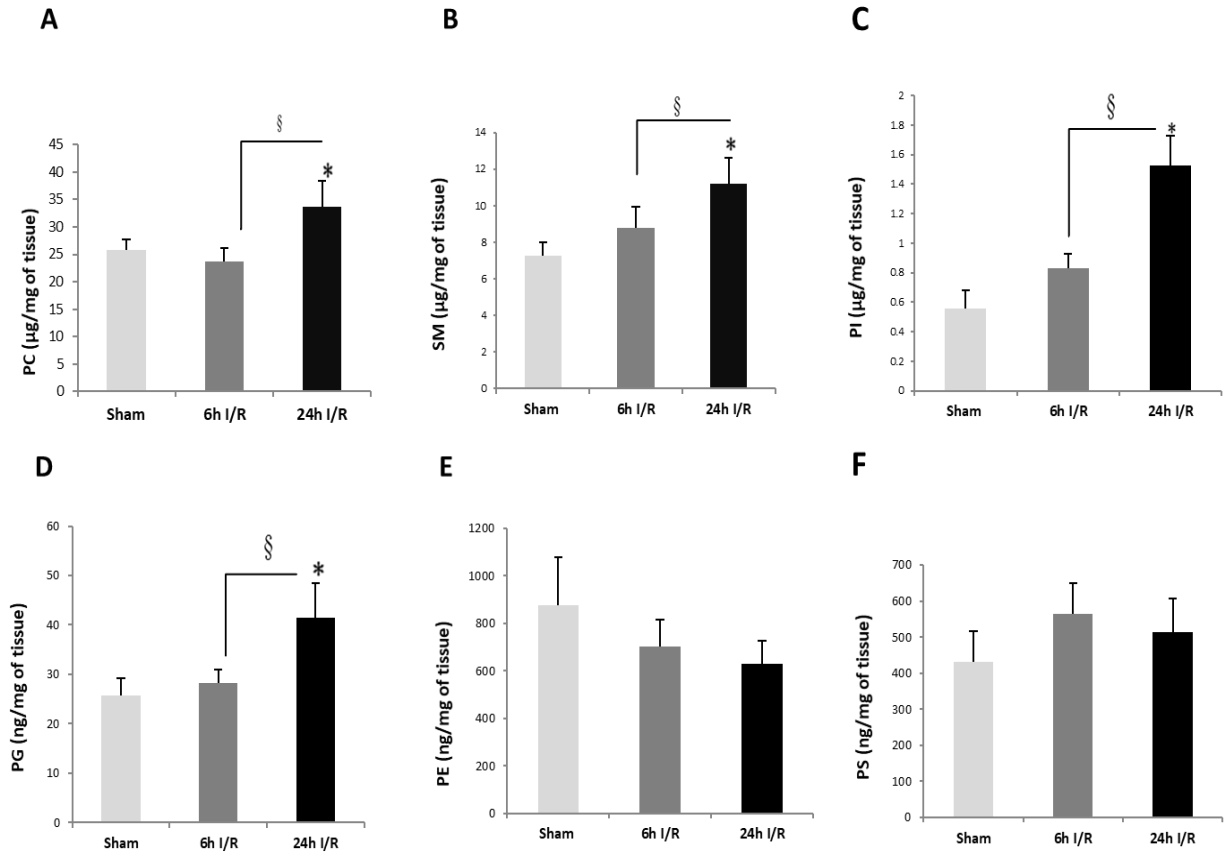

Average (A) PC, (B) SM, (C) PI, (D) PtG, (E) PE and (F) PS concentrations in rat renal tissue in sham and 6 and 24h I/R groups (n=4 in each group). Values are means ± SEM. * Significant difference compared to sham, $p< 0.05$. § Significant difference between I/R groups, $p<0.05$.
Abbreviations: PC: Phosphatidylcholine, SM: Sphingomyelin, PI: Phosphatidylinositol, PtG: Phosphatidylglycerol, PE: Phosphatidylethanolamine, PS: Phosphatidylserine.

Thirty-six PC species were identified in renal tissue in all three experimental groups. Of these, PC (36:4) was the most abundant (Table 3). There were no significant increases in any PC after only 6h I/R; however, after 24h I/R, of the 36 individual PC compounds identified, 29 and 27 were significantly greater than those in the sham and 6h I/R groups, respectively. Of these, the top 10 PC compounds after 24h I/R, beginning with the most abundant, were PC (34:1)> PC (34:2)> PC (38:4)> PC (36:2)> PC (38:5)> PC (36:1)> PC (34:0)> PC (38:3)> PC (32:1)> PC (40:6) (Table 3). Of interest, three PC compounds were significantly reduced after 6h I/R compared to the sham

group, including PC (34:2), PC (34:3), and PC (36:5). All identified PC species in kidney tissue are presented in Table 3.

Table 3: Identified PC species in kidney tissue in sham and I/R groups

	Sham (µg/mg of tissue)	6h I/R (µg/mg of tissue)	24h I/R (µg/mg of tissue)
PC(28:0)	0.006±0.00	0.007±0.00	0.01±0.00
PC(30:0)	0.24±0.05	0.25±0.06	0.42±0.11*§
PC(32:0)	3.23±0.24	2.98±0.32	3.51±0.33
PC(34:0)	0.47±0.06	0.56±0.04	0.93±0.14*§
PC(36:0)	0.08±0.00	0.12±0.01	0.18±0.05*§
PC(30:1)	0.01±0.00	0.01±0	0.02±0.00*§
PC(32:1)	0.40±0.05	0.34±0.04	0.66±0.03*§
PC(32:2)	0.04±0.00	0.05±0	0.09±0.01*§
PC(34:1)	2.92±0.23	2.79±0.43	4.42±0.71*§
PC(34:1 p)	0.14±0.01	0.14±0.02	0.22±0.02*§
PC(34:2)	3.68±0.32	2.88±0.37*	4.31±0.39*
PC(34:2p)	0.1±0.01	0.09±0.01	0.14±0.01*§
PC(34:3)	0.15±0.02	0.12±0.00*	0.25±0.01*§
PC(36:1)	0.48±0.05	0.56±0.09	0.95±0.24*§
PC(36:1p)	0.05±0.00	0.05±0.00	0.08±0.01*§
PC(36:2)	1.63±0.16	1.56±0.23	2.35±0.36*§
PC(36:2p)	0.06±0.00	0.05±0.01	0.09±0.01*§
PC(36:3)	1.20±0.15	0.99±0.10	1.47±0.16
PC(36:4)	4.52±0.33	3.79±0.45	4.72±0.80
PC(36:4p)	0.33±0.04	0.37±0.04	0.47±0.14
PC(36:5)	0.31±0.04	0.21±0.02*	0.24±0.03*
PC(36:6)	0.01±0.00	0.01±0.00	0.02±0.00
PC(38:2)	0.06±0.00	0.07±0.01	0.11±0.02*§
PC(38:3p)	0.005±0.00	0.005±0.00	0.009±0.00*§
PC(38:3)	0.44±0.04	0.5±0.03	0.65±0.125*
PC(38:4)	2.35±0.17	2.59±0.22	3.47±0.67*§
PC(38:5p)	0.01±0.00	0.02±0.00	0.03±0.01*§
PC(38:5)	0.89±0.08	0.75±0.08	1.16±0.11*§
PC(38:6)	1.23±0.15	0.99±0.12	1.32±0.19§
PC(40:2)	0.00±0.00	0.00±0.00	0.01±0.00*§
PC(40:3)	0.00±0.00	0.01±0.00	0.02±0.00*§
PC(40:4)	0.03±0.00	0.05±0.01	0.1±0.02*§
PC(40:5)	0.09±0.00	0.13±0.02	0.25±0.05*§
PC(40:6)	0.22±0.00	0.3±0.03	0.5±0.12*§
PC(40:7)	0.09±0.00	0.09±0.01	0.14±0.01*§
PC(40:8)	0.14±0.01	0.13±0.02	0.14±0.02

Values are means ± SEM. * Significant differences compared with the sham group. §Significant differences compared with 6h I/R group, $p<0.05$. **Abbreviation**: PC: Phosphatidylcholine.

Thirteen LPC compounds were detected in all groups. LPC (18:0) was the most abundant LPC species in all groups with average values representing 116.07±15.69, 118.35 ±5.30 and 108.56±16.26 ng/mg of tissue for sham-operated, 6h and 24h I/R groups, respectively (Table 4). No significant changes were detected in total LPC levels amongst any of the study groups (data not shown). However, LPC (16:0p) dropped significantly in 24h I/R group compared with 6h I/R group. LPC (20:3) decreased significantly in 24h I/R group in compared with sham and 6h I/R groups (p= 0.014, 0.005 respectively). There were also significant reductions in LPC (22:6) levels in 24h I/R group when compared to 6h I/R group (p=0.019). On the contrary, LPC (22:5) levels were elevated significantly in 6h I/R group compared to operated group (p=0.012), but no change was observed following 24h I/R. All identified LPC species in kidney tissue are presented in Table 4.

Table 4: Identified LPC species in kidney tissue in sham and I/R groups

	Sham (ng/mg of tissue)	6h I/R (ng/mg of tissue)	24h I/R (ng/mg of tissue)
LPC (14:0)	0.06±0.00	0.08±0.02	0.06±0.02
LPC(16:0)	94.73±8.7	92.64±7	78.29±14.6
LPC(16:0 Alkenyl)	0.32±0.10	0.42±0.17	0.24±0.07
LPC(16:0p)	1.19±0.12	1.23±0.19	0.91±0.15§
LPC(16:1)	1.01±0.12	0.94±0.20	0.85±0.08
LPC(18:0)	116.07±15.69	118.35±5.30	108.56±16.26
LPC(18:1)	11.26±0.83	12.26±2.54	9.75±1.43
LPC(18:2)	11.09±0.70	11.24±2.71	9.41±1.64
LPC(18:3)	0.22±0.05	0.18±0.01	0.15±0.02
LPC(20:3)	1.27±0.00	1.38±0.30	0.75±0.15*§
LPC(22:5)	0.45±0.00	0.73±0.12*	0.55±0.11
LPC(22:6)	1.92±0.18	2.53±0.43	1.60±0.46§

Values are means ± SEM. * Significant differences compared with the sham group. § Significant differences compared with 6h I/R group, p<0.05. **Abbreviation**: LPC: Lysophosphatidylcholine.

SM was the next most prevalent PL species identified in renal tissue of sham and I/R groups. Mean total concentrations of SM increased with increasing I/R time; however, levels in the 24h I/R group (11.18±0.14 µg/mg tissue) were significantly greater than those in the sham-operated (7.27± 0.69 µg/mg of tissue; p=0.002) and 6h I/R groups (8.79± 1.15 µg/mg of tissue, p=0.029) (Figure 12B). No significant differences were detected between sham and 6h I/R groups. Of the 40 SM compounds identified, SM (34:1), SM (42:1) and SM (42:2) (Table 5) were the three most

abundant SM compounds in all groups. All identified SM species in kidney are presented in Table 5.

Table 5: SM species identified in rat kidney following I/R

	Sham (µg/mg of tissue)	6h I/R (µg/mg of tissue)	24h I/R (µg/mg of tissue)
SM 31:0	ND	ND	0.001±0.00§*
SM 33:0	0.002±0.00	0.002±0.00	0.002±0.00
SM 34:0	0.30±0.01	0.39±0.05	0.43±0.06*
SM 35:0	0.009±0.00	0.01±0.00*	0.005±0.00
SM 36:0	0.02±0.00	0.02±0.00	0.031±0.00
SM 38:0	0.03±0.02	0.01±0.00	0.014±0.00
SM 40:0	0.02±0.00	0.03±0.00	0.091±0.02*
SM 44:0	0.003±0.00	0.005±0.00	0.011±0.00*
SM 32:2	0±0.00	0±0.00	0.001±0.00
SM 32:1	0.01±0.00	0.01±0.00	0.01±0.00
SM 32:2i	0.001±0.00	0.001±0.00	0.001±0.00
SM 31:2	0.001±0.00	0.002±0.00	0.002±0.00
SM 31:1	0.02±0.00	0.03±0.00	0.03±0.00
SM 34:2	0.14±0.01	0.19±0.03	0.23±0.02*
SM 34:1	2.99±0.22	3.36±0.58	3.53±0.53
SM 35:1	0.04±0.00	0.05±0.00	0.06±0.01
SM 36:3	0±0.00	0±0.00	0.001±0.00
SM 36:2	0.02±0.00	0.03±0.00	0.04±0.01
SM 36:1	0.18±0.02	0.25±0.03	0.33±0.06*
SM 37:1	0.006±0.00	0.007±0.00	0.01±0.00*
SM 38:3	0±0.00	0±0.00	0.001±0.00
SM 38:1	0.14±0.05	0.15±0.01	0.22±0.04*
SM 39:2	0.001±0.00	0.001±0.00	0.001±0.00
SM 39:1	0.009±0.00	0.01±0.00	0.01±0.00§*
SM 40:3	0.02±0.03	0.01±0.00	0.01±0.003
SM 40:2	0.05±0.01	0.07±0.00	0.1±0.00*
SM 40:1	0.29±0.06	0.36±0.05	0.55±0.10*
SM 41:3	0.006±0.00	0.007±0.00	0.01±0.00*
SM 41:2	0.02±0.00	0.03±0.00	0.04±0.00*
SM 41:1	0.07±0.01	0.09±0.01	0.15±0.02*
SM 42:4	0.02±0.00	0.03±0.00	0.05±0.00*
SM 42:3	0.31±0.08	0.35±0.04	0.57±0.09§*
SM 42:2	1.10±0.23	1.42±0.11	1.95±0.21§*
SM 42:1	1.24±0.24	1.64±0.217	2.35±0.25§*
SM 43:3	0.002±0.00	0.00±0.00	0.004±0.00§*
SM 43:2	0.01±0.00	0.01±0.00	0.02±0.00§*

SM 43:1	0.02±0.00	0.03±0.00*	0.05±0.00§*
SM 44:3	0.006±0.00	0.00±0.00	0.01±0.00§*
SM 44:2	0.02±0.00	0.03±0.00*	0.05±0.00§*
SM 44:1	0.03±0.00	0.04±0.00*	0.08±0.01§*

Values are means ± SEM. * Significant differences compared with the sham group. §Significant differences compared with 6h I/R group, $p<0.05$. **Abbreviation**: SM: Sphingomyelin, ND: not detected.

Total concentrations of PI followed a similar pattern as that observed for SM with concentrations significantly elevated in the 24h I/R group (1.52±0.20 µg/mg of tissue) compared to sham (0.55±0.12 µg/mg of tissue $p=0.001$) and 6h I/R groups (0.82±0.10 µg/mg of tissue, $p=0.001$) (Figure 12C). Twenty PI compounds were also identified in renal tissue in all groups. Of these, only 9 species increased significantly following 6h I/R, but all 20 PI species increased significantly following 24h I/R compared with the sham-operated group (Table 6). The most abundant PI compound was PI (38:4) with average values representing 0.31±0.07, 0.38±0.95 and 0.68±0.12 µg/mg of tissue in sham, 6h and 24h IR groups, respectively (Table 6).

Table 6: PI species identified in rat kidney following I/R

	Sham (µg/mg of tissue)	**6h I/R (µng/mg of tissue)**	**24h I/R (µng/mg of tissue)**
PI 30:0	ND	ND	0.003±0.00§*
PI 32:0	ND	ND	0.05±0.00§*
PI 32:1	0.00±0.00	0.00±0.00	0.006±0.00*
PI 34:0	ND	ND	0.05±0.00§*
PI 34:1	0.02±0.00	0.05±0.00*	0.06±0.01*
PI 34:2	0.02±0.00	0.04±0.00*	0.05±0.00*
PI 36:0	ND	ND	0.004±0.00
PI 36:1	0±0.00	0.01±0.00*	0.03±0.00*
PI 36:2	0.02±0.00	0.05±0.00*	0.12±0.01§*
PI 36:3	0.02±0.00	0.03±0.00	0.05±0.00§*
PI 36:4	0.07±0.01	0.1±0.01	0.18±0.02§*
PI 36:5	0.00±0.00	0.0005±0.00*	0.005±0.00*
PI 36:6	0.00±0.00	0.00±0.00	0.004±0.00*
PI 38:4	0.31±0.07	0.38±0.09	0.68±0.12*
PI 38:5	0.02±0.00	0.03±0.00	0.06±0.00§*
PI 38:6	0.01±0.00	0.01±0.00*	0.02±0.00§*
PI 40:3	0.00±0.00	0.00±0.00	0.01±0.00§*
PI 40:5	0.00±0.00	0.01±0.00*	0.02±0.00*
PI 40:6	0.01±0.00	0.03±0.00*	0.04±0.00*

PI 40:7	0.00±0.00	0.006±0.00*	0.008±0.00*

* Significant differences compared with the sham group. §Significant differences compared with 6h I/R groups, $P < 0.05$. **Abbreviation**: PI: Phosphatidylinositol.

Of the less abundant PL species, namely PE, PS and PtG, only total PtG concentrations increased significantly following 24h I/R when compared to sham-operated and 6h I/R groups (41.39±6.96 versus 25.78±3.47 and 28.23±2.78 ng/mg of tissue, respectively) (Figure 12D). Of the 16 identified PtG species in renal tissue, 9 and 15 PtG species increased significantly in 6h and 24h I/R groups respectively compared with sham-operated group. PtG (34:1) was the most abundant PtG, which constituted almost 50% of total PtG amounts, with average values representing 15.87±2.20, 14.62±2.82 and 20.64±3.97 ng/mg of tissue in sham-operated, 6h and 24h IR groups, respectively (Table 7).

Table 7: PtG species identified in rat kidney following I/R

	Sham (ng/mg of tissue)	**6h I/R (ng/mg of tissue)**	**24h I/R (ng/mg of tissue)**
PtG (34:1)	15.87±2.20	14.62±2.82	20.64±3.97
PtG (34:2)	2.45±0.40	2.51±0.27	3.23±0.77
PtG (36:1)	0.86±0.10	0.88±0.04	1.93±0.33§*
PtG (36:2)	2.2±0.30	2.20±0.15	4.2±0.81§*
PtG (36:3)	0.84±0.10	1.54±0.44*	2.05±0.30*
PtG (36:4)	1.86±0.30	3.46±0.58*	5.41±0.64§*
PtG (36:5)	0.06±0.01	0.08±0.00	0.11±0.01§*
PtG (38:4)	0.45±0.03	0.75±0.08*	1.11±0.18§*
PtG (38:5)	0.28±0.04	0.46±0.07*	0.8±0.04§*
PtG (38:6)	0.4±0.07	0.78±0.17*	0.95±0.03*
PtG (40:4)	0.01±0.00	0.02±0.00	0.04±0.00§*
PtG (40:5)	0.05±0.01	0.09±0.00*	0.1±0.01*
PtG (40:6)	0.15±0.02	0.28±0.04*	0.24±0.02*
PtG (40:7)	0.1±0.00	0.22±0.03*	0.22±0.00*
PtG (40:8)	0.12±0.00	0.28±0.10*	0.29±0.03*
PtG (40:9)	ND	ND	0.01±0.00§*

Values are means ± SEM. * Significant differences compared with the sham group. §Significant differences compared with the 6h I/R group, $P < 0.05$. **Abbreviation**: PtG: Phosphatidylglycerol, ND: not detected.

Despite the appearance of attenuating levels of PE with increasing time of I/R, overall levels remained unchanged (Figure 12E). This apparent attenuation is attributed to the significant reductions in levels of PE (32:0), PE (32:1), PE (34:2) and PE (36:3) that were observed in both 6h and 24h I/R groups compared to sham-operated group (Table 8). An additional six PE compounds decreased significantly after 24h I/R, but not 6h. These include PE (36:2), PE (36:4), PE (38:3), PE (38:5), PE (38:6) and PE (38:6e) (Table 8).

Table 8: PE species identified in rat kidney following I/R

	Sham (ng/mg of tissue)	**6h I/R (ng/mg of tissue)**	**24h I/R (ng/mg of tissue)**
PE(32:0)	6.04±0.98	4.12±0.23*	3.17±0.46*
PE(36:0)	26.46±6.1	23.32±4.38	20.98±4.48
PE(32:1)	2.99±0.32	1.64±0.44*	1.55±0.11*
PE(34:1)	17.16±2.45	15.03±2.48	13.39±1.57
PE(34:1p)	0.48±0.08	0.45±0.06	0.39±0.14
PE(34:2)	32.32±3.00	23.89±2.45*	21.29±3.92*
PE(34:2p)	1.96±0.23	1.91±0.35	1.5±0.30
PE(36:1)	11.31±1.99	11.36±0.96	10.9±2.29
PE(36:2)	49.16±6.24	42.95±3.23	38.64±4.33*
PE(36:2e)(36:1p)	3.93±0.72	3.4±0.60	3.36±0.88
PE(36:3)	29.57±5.54	20.55±1.48*	19.78±2.98*
PE(36:3e)(36:2p)	4.26±0.93	3.89±0.79	3.86±1.11
PE(36:4)	81.17±23.77	61.14±9.85	47.34±6.48*
PE(36:4e)(36:3p)	10.82±2.21	9.51±2.12	8.25±2.33
PE(36:5)	9.78±2.79	7.66±1.30	6.71±1.06
PE(36:5e)(36:4p)	67.48±14.56	54.86±14.37	48.94±13.46
PE(38:1)	7.26±1.11	7.74±1.04	7.82±1.89
PE(38:2)	2.77±0.39	2.36±0.25	2.47±0.50
PE(38:3)	26.85±6.82	19.57±2.85	17.81±1.66
PE(38:4)	221.93±61.75	168.53±33.39	155.31±19.3
PE(38:5)	66.51±21.43	48.33±7.14	40.02±3.88*
PE(38:5e)(38:4p)	58±15.92	51.07±11.41	47.48±10.16
PE(38:6)	27.68±8.79	17.27±2.55	16.17±2.07*
PE(38:6e)(38:5p)	58.12±9.52	51.2±12.57	36.72±7.45*
PE(40:1)	0.58±0.21	0.29±0.00	0.46±0.15
PE(40:4)	4.5±1.54	4.12±0.78	6.01±1.93
PE(40:5)	5.01±1.31	4.7±0.48	6.37±1.87
PE(40:5e)	4.79±1.00	4.74±1.27	5.15±1.41
PE(40:6)	8.05±2.61	8.51±1.02	10.46±2.77
PE(40:6e)	5.78±1.40	6.24±1.72	6.08±1.41
PE(40:7)	7.08±1.66	6.2±0.56	7.53±1.29
PE(40:7e)	13.77±3.60	13.12±1.98	12.69±2.85

PE(42:1)	ND	ND	0.17±0.11
PE(42:5)	ND	ND	0.21±0.2
PE(42:5p)	0.41±0.12	0.44±0.13	0.57±0.3
PE(42:6)	ND	ND	0.24±0.15
PE(42:6p)	0.65±0.12	0.79±0.05	0.55±0.3
PE(42:7)	0.66±0.41	0.42±0.06	0.64±0.3

Values are means ± SEM. * Significant differences compared with the sham group, $P < 0.05$.
Abbreviation: PE: Phosphatidylethanolamine, ND: not detected

No significant changes in overall PS concentrations were observed between any of the study groups (Figure 12F); however, some individual PS compounds increased with increased I/R time which is presented in Table 9.

Table 9: PS species identified in rat kidney following I/R

	Sham (ng/mg of tissue)	**6h I/R (ng/mg of tissue)**	**24h I/R (ng/mg of tissue)**
PS(32:1)	0.49±0.06	0.59±0.12	0.83±0.15*§
PS(34:0)	ND	ND	4.96±1.08*§
PS(34:1)	14.92±1.30	23.15±4.51*	22.4±4.98
PS(34:2)	5.11±0.17	5.34±0.96	10.27±4.02*§
PS(36:0)	ND	ND	10.44±1.55*§
PS(36:1)	53.47±5.16	87.88±11.53*	82.17±10.12*
PS(36:2)	35.47±3.03	46.32±6.03	62.84±13.93*
PS(38:1)	5.86±1.14	6.84±1.23	6.27±1.61*
PS(38:6)	36.4±8.48	41.85±7.78	28.23±8.30*§
PS(40:3)	2.30±0.46	3.37±0.80	3.66±0.52
PS(40:4)	3.70±0.83	4.78±0.63	4.72±0.62*
PS(40:5)	45.26±10.87	57.27±9.01	44.28±8.01*
PS(40:6)	180.04±46.35	219.12±39.28	157.71±32.75*§

Values are means ± SEM. * Significant differences compared with the sham group. § Significant differences compared with 6h I/R group, $P < 0.05$. **Abbreviation**: PS: Phosphatidylserine, ND: not detected.

Discussion

Our study identified bioactive fragmented OxPCs during renal I/R in an *in vivo* model of renal I/R injury. We found significant increments in fragmented OxPC molecules after 6 and 24h of reperfusion. OxPC levels were also significantly positively correlated with creatinine levels during the reperfusion period. In this study, we identified fifty-five OxPC species involving fragmented aldehyde and carboxylic acid-containing OxPC derivatives, and also non-fragmented OxPC compounds with terminal furans, isoprostanes, and long-chain products in renal I/R. Interestingly, we found that fragmented OxPC, including fragmented aldehyde and carboxylic acid-containing OxPC, were produced at greater levels following 24h reperfusion compared to sham-operated and 6h I/R groups. Fragmented aldehyde containing OxPC increased significantly as early as 6h reperfusion. Their levels increased by increasing the time of reperfusion, as there were significant differences between 24h I/R groups compared to 6h I/R and sham-operated groups. Fragmented carboxylic acid-containing OxPC were produced later in renal I/R, as significant elevations in their levels were observed only after 24h I/R, but not 6h. In the current study, both fragmented aldehyde and carboxylic acid-containing OxPC levels were significantly correlated with the severity of I/R injury as measured by creatinine levels. The three most abundant fragmented OxPCs in the rat kidney were PazPC, SONPC, and PONPC. Similar to our results, Lloberas et al., (2002) showed that OxPLs with platelet-activating factor (PAF) activity (PAF-like lipids) are produced following 15 min of reperfusion in rat kidney. Phospholipid oxidation has also been implicated in other renal disease models. In patients with lecithin: cholesterol acyltransferase (LCAT) deficiency, renal tissue displayed increased OxLDL antibody binding to the glomeruli, indicating OxLDL epitopes increased in these patients (29). Also, fragmented OxPC species are potent inducers of cell death in smooth muscle cells, macrophages, oligodendrocytes, and endothelial cells (30-32). Previous data from our laboratory demonstrate that exogenous administration of POVPC, PONPC, PGPC, and PAzPC to postnatal cardiac cells triggers cell death in a dose-dependent manner (33). Additionally, fragmented OxPC species, namely POVPC and PGPC, increased significantly following ischemia and I/R in adult rat cardiomyocytes. Ganguly et al.,(2017) further demonstrated that in cardiomyocytes exposed to fragmented OxPC, specifically PGPC and PONPC, apoptotic pathways are activated, resulting in cell death (25).

In the current study, despite a significant increase in non-fragmented isoprostane levels after 6h I/R, a significant decrease was observed after 24h reperfusion. Isoprostanes are formed via non-enzymatic oxidation from arachidonic acid and exert prostaglandin-like properties. Unlike enzymatic oxidation, non-enzymatic oxidation, which occurs during I/R, is not site-specific. Therefore, oxidative stress can also result in the production of OxPL with anti-inflammatory properties; however, most OxPLs have potent inflammatory effects (34). Cyclopentenone containing OxPLs like 1-palmitoyl-2-epoxyisoprostane-sn-glycero-3-PC (PEIPC) and 15-deoxy-D12,14-prostaglandin J2 share similar structures. Both 15-deoxy-D12,14-prostaglandin J2 and cyclopentenone containing OxPLs can block NFκB- dependent inflammatory responses and activate NF-E2-related factor 2 (Nrf2), which is a transcriptional regulator of the antioxidant response (35). In a study by Bretscher et al., (2015), administration of cyclopentenone OxPCs to myeloid cells inhibited expression of proinflammatory cytokines and chemokines via activation of Nrf2 (35). Moreover, they also showed the protective effects of cyclopentenone OxPC against sepsis-associated lung injury (35). As previously mentioned, isoprostanes increased following 6h, but not 24h, I/R. AKI severity does not appear to be dependent upon the presence of isoprostanes or other non-fragmented OxPC molecules as suggested by the poor correlation of these compounds in renal tissue with plasma creatinine levels. It should be considered that the potential increase in renal OxPCs could be underestimated given that isoflurane was used as an anaesthetic agent. It has been previously shown that volatile anaesthetics can result in renal protection during I/R (36).

Membrane phospholipid concentrations in renal tissue following I/R injury were also assessed in our three study groups. Significant increases in PC, SM, PI, and PtG were observed after 24 I/R. PC represented the most abundant PL in kidney tissue for all study groups and is the precursor of OxPC compounds. Surprisingly, total PC concentrations were unchanged after 6h I/R, despite increases in OxPC levels at the same time point. In addition, 24h I/R resulted in significant increases in both PC and OxPC molecules. Rao et al., (2016), has demonstrated elevations in PC levels in a mouse model of renal I/R involving 12 mice after 30 min renal ischemia followed by 6h and 24h reperfusion. In this non-targeted lipidomic analysis, 52 PC species increased significantly after 24h reperfusion (37). Similar to our results, they observed significant elevations in PC (34:1), PC (36:1), PC (36:2), PC (38:2), PC (38:4), PC (38:5), PC (40:2) and PC (40:4) following 24h reperfusion. Moreover, choline incorporation into PL is accelerated during renal

ischemia and I/R particularly in the proximal tubule, which result in more PC biosynthesis in renal I/R.

Phospholipase A2 is activated in renal I/R. Phospholipase A2 hydrolyses the fatty acid at the Sn-2 position of PLs resulting in elevations of free fatty acid and lysophospholipids (38). In the current study, LPC (22:5) was the only lysoPC species that increased significantly after 6h I/R but was normalized after 24h. Rao et al., (2016) reported significant elevations in lysoPC (18:0) and (20:4) levels after 24h reperfusion (37). Similarly, Liu et al., (2012) observed significant increases in three LPC species in a rat model of kidney I/R, namely 1-stearoylglycerophosphocholine (18:0), oleoyl-glycerophosphocholine (18:1), and palmitoyl-glycerophosphocholine (16:0) after 24h I/R (3). Wie et al., (2014) also evaluated metabolomic changes in renal I/R and determined that levels of 2-palmitoyl-glycerophosphocholine (16:0), decreased significantly in plasma after 2h I/R and normalized after 7 days (39). Given that LPC is the breakdown product of membrane phospholipids, it was suggested that membrane breakdown and remodeling activity might be transiently inhibited early after renal I/R.

SM is a membrane PL composed of a choline head group and ceramide. In the current study, total SM concentrations increased only after 24h I/R compared to both the sham and 6h I/R groups. No changes were observed after 6h I/R relative to sham. Rao et al., (2016) reported elevations in SM concentrations in 34 of 40 identified SM species after 24h I/R (37). Wie et al., (2014) (39) observed elevations in palmitoyl sphingomyelin and stearoyl sphingomyelin, which are the hydrolyzed form of SM, post 48h I/R. In addition, the present study measured significant increases in total concentrations of PI and PtG after 24h I/R. Rao et al., (2016) (37) and Liu et al., (2012) (3) did not report PI and PtG levels. No other literature to our knowledge has identified specific PI and PtG molecules in renal tissue from rats undergoing 6 and 24h I/R. Despite a non-significant decreasing trend in overall PE compounds with increased I/R time, 10 PE molecules significantly decreased in both I/R groups compared to sham. These results agree with Rao et al., (2016) who observed significant reductions in PE compounds after 24h reperfusion (37). There are two distinct forms of cytosolic PLA2 in rat kidneys that are activated following reperfusion. Unlike the large molecular weight form, which is active against both PE and PC, the small molecular weight form of PLA2 has activity only against PE (40). This could be a potential mechanism towards a decreased trend in PE levels in our study.

Previous studies report the accumulation of lipids in various renal diseases. In diabetic nephropathy, lipid accumulation occurs due to increases in glomerular filtration of protein-bound lipids, which results in proteinuria (41). Evidence from *in vitro* and *in vivo* renal I/R injury studies has also revealed that accumulation of triglycerides and cholesterol can occur (42-44).

It has also been suggested that renal cells, contrary to cardiac or brain cells, can recover from injury even after prolonged ischemia through various intrinsic, extrinsic mechanisms and also paracrine influences (37). Increased levels of growth factors IGF-1(38, 39), fibroblast growth factors (40-42), and hepatocyte growth factor (43, 44) have been reported in the post-ischemic kidney which all can lead to repair processes. A few hours after I/R injury, the proliferation of surviving tubular epithelial cells (TECs), which contain phospholipids in their structure (45), begins which eventually results in kidney damage recovery. Wan et al., 2015 showed that proliferation and differentiation of surviving TECs begin at 24h after kidney IR injury (46). In addition, an abnormal repair can occur which results in renal fibrosis and then chronic kidney disease. Due to abnormalities in glomerular filtration, lipoproteins contain phospholipids accumulate in the kidney (46).

Membrane polarity can also change following changes in membrane phospholipids and their oxidized form. The lipid polarity of apical and basolateral membranes of renal epithelial cells are vastly different. The apical membrane of the rat kidney is rich in sphingomyelin, phosphatidylserine, and a high ratio of cholesterol-to-phospholipid. However, phosphatidylcholine and phosphatidylinositol are prevalent in the basolateral membrane (47). It has been shown that following ischemia, ratios of sphingomyelin-to-phosphatidylcholine, and the cholesterol-to-phospholipid decrease significantly which results in partial loss of surface membrane polarity (48). Bruce et al., (1988) also assessed surface membrane polarity following 15 min of ischemia and 2 hr of reperfusion. They isolated apical membrane fractions and found that both apical Na/K-ATPase specific activity and enrichment increased following 15 min of ischemia. They also observed a partial loss of apical lipid polarity, which was accompanied by significant reductions in ratios of sphingomyelin to phosphatidylcholine and cholesterol to phospholipid. They suggested that apical and basolateral membrane lipids move to the alternate surface membrane domain during ischemic injury which is the reason for a marked reduction in the SM/PC ratio in apical membrane

fractions (48). On the other hand, OxPL can also alter the properties of biological membranes, since they have different polarity and shape compared with their non-oxidized molecules (49).

Conclusions

To conclude, we have shown for the first time that bioactive OxPC species are produced during renal I/R, with levels increasing with increased reperfusion time. Fragmented OxPCs, including both aldehyde and carboxylic acid molecules, had the strongest positive correlation related to AKI. These compounds can serve as potential therapeutic targets for mitigating the progression of oxidative injury in studies involving renal I/R. We can utilize the potential attenuation of OxPCs activity to reduce renal I/R injury. One potential agent is E06 which is a monoclonal IgM antibody that specifically binds to fragmented OxPCs. E06 has been used in LDL -/- animals to inhibit OxPC activity resulting in a 46% reduction in atherosclerotic lesion formation (50, 51).

References

1. Devarajan P. Update on mechanisms of ischemic acute kidney injury. Journal of the American Society of Nephrology. 2006;17(6):1503-20.
2. Lv J, Wang X, Liu SY, Liang PF, Feng M, Zhang LL, et al. Protective effect of Fenofibrate in renal ischemia reperfusion injury: Involved in suppressing kinase 2 (JAK2)/transcription 3 (STAT3)/p53 signaling activation. Pathologie-biologie. 2015.
3. Liu Y, Yan S, Ji C, Dai W, Hu W, Zhang W, et al. Metabolomic changes and protective effect of L-carnitine in rat kidney ischemia/reperfusion injury. Kidney and Blood Pressure Research. 2012;35(5):373-81.
4. Rovcanin B, Medic B, Kocic G, Cebovic T, Ristic M, Prostran M. Molecular dissection of renal ischemia-reperfusion: oxidative stress and cellular events. Current medicinal chemistry. 2016;23(19):1965-80.
5. Zhao Y-Y, Vaziri ND, Lin R-C. Chapter Six - Lipidomics: New Insight Into Kidney Disease. In: Gregory SM, editor. Advances in Clinical Chemistry. Volume 68: Elsevier; 2015. p. 153-75.
6. Zhao Y-Y. Metabolomics in chronic kidney disease. Clinica Chimica Acta. 2013;422:59-69.
7. Hasanally D, Chaudhary R, Ravandi A. Role of phospholipases and oxidized phospholipids in inflammation. Phospholipases in Health and Disease: Springer; 2014. p. 55-72.
8. Kadl A, Sharma PR, Chen W, Agrawal R, Meher AK, Rudraiah S, et al. Oxidized phospholipid-induced inflammation is mediated by Toll-like receptor 2. Free Radical Biology and Medicine. 2011;51(10):1903-9.
9. Weismann D, Binder CJ. The innate immune response to products of phospholipid peroxidation. Biochimica et Biophysica Acta (BBA)-Biomembranes. 2012;1818(10):2465-75.
10. Greenberg ME, Sun M, Zhang R, Febbraio M, Silverstein R, Hazen SL. Oxidized phosphatidylserine–CD36 interactions play an essential role in macrophage-dependent phagocytosis of apoptotic cells. Journal of Experimental Medicine. 2006;203(12):2613-25.
11. Uderhardt S, Herrmann M, Oskolkova O, Voll R, Nimmerjahn F, Bochkov V, et al. 12/15-lipoxygenase orchestrates the clearance of apoptotic cells and maintains immunologic tolerance. Journal of translational medicine. 2011;9(2):P5.
12. Leitinger N, Tyner TR, Oslund L, Rizza C, Subbanagounder G, Lee H, et al. Structurally similar oxidized phospholipids differentially regulate endothelial binding of monocytes and neutrophils. Proceedings of the National Academy of Sciences. 1999;96(21):12010-5.
13. Ma Z, Li J, Yang L, Mu Y, Xie W, Pitt B, et al. Inhibition of LPS-and CpG DNA-induced TNF-α response by oxidized phospholipids. American Journal of Physiology-Lung Cellular and Molecular Physiology. 2004;286(4):L808-L16.
14. Erridge C, Kennedy S, Spickett CM, Webb DJ. Oxidized phospholipid inhibition of toll-like receptor (TLR) signaling is restricted to TLR2 and TLR4 roles for cd14, lps-binding protein, and md2 as targets for specificity of inhibition. Journal of Biological Chemistry. 2008;283(36):24748-59.
15. Hasanally D, Edel A, Chaudhary R, Ravandi A. Identification of Oxidized Phosphatidylinositols Present in OxLDL and Human Atherosclerotic Plaque. Lipids. 2017;52(1):11-26.
16. Torzewski M, Ravandi A, Yeang C, Edel A, Bhindi R, Kath S, et al. Lipoprotein (a)-Associated Molecules Are Prominent Components in Plasma and Valve Leaflets in Calcific Aortic Valve Stenosis. JACC: Basic to Translational Science. 2017;2(3):229-40.
17. Tsimikas S, Kiechl S, Willeit J, .r M, Miller ER, Kronenberg F, et al. Oxidized phospholipids predict the presence and progression of carotid and femoral atherosclerosis and symptomatic cardiovascular disease: five-year prospective results from the Bruneck study. Journal of the American College of Cardiology. 2006;47(11):2219-28.
18. Binder CJ, Hörkkö S, Dewan A, Chang M-K, Kieu EP, Goodyear CS, et al. Pneumococcal vaccination decreases atherosclerotic lesion formation: molecular mimicry between Streptococcus pneumoniae and oxidized LDL. Nature medicine. 2003;9(6):736-43.

19. Hartvigsen K, Chou M-Y, Hansen LF, Shaw PX, Tsimikas S, Binder CJ, et al. The role of innate immunity in atherogenesis. Journal of lipid research. 2009;50(Supplement):S388-S93.
20. Bertoia ML, Pai JK, Lee J-H, Taleb A, Joosten MM, Mittleman MA, et al. Oxidation-specific biomarkers and risk of peripheral artery disease. Journal of the American College of Cardiology. 2013;61(21):2169-79.
21. Tsimikas S, Lau HK, Han K-R, Shortal B, Miller ER, Segev A, et al. Percutaneous Coronary Intervention Results in Acute Increases in Oxidized Phospholipids and Lipoprotein(a). Short-Term and Long-Term Immunologic Responses to Oxidized Low-Density Lipoprotein. 2004;109(25):3164-70.
22. Kiechl S, Willeit J, .r M, Viehweider B, Oberhollenzer M, Kronenberg F, et al. Oxidized Phospholipids, Lipoprotein(a), Lipoprotein-Associated Phospholipase A2 Activity, and 10-Year Cardiovascular Outcomes. Prospective Results From the Bruneck Study. 2007;27(8):1788-95.
23. Tsimikas S, Willeit P, Willeit J, Santer P, .r M, Xu Q, et al. Oxidation-Specific Biomarkers, Prospective 15-Year Cardiovascular and Stroke Outcomes, and Net Reclassification of Cardiovascular Events. Journal of the American College of Cardiology. 2012;60(21):2218-29.
24. Tsimikas S, Mallat Z, Talmud PJ, Kastelein JJP, Wareham NJ, Sandhu MS, et al. Oxidation-Specific Biomarkers, Lipoprotein(a), and Risk of Fatal and Nonfatal Coronary Events. Journal of the American College of Cardiology. 2010;56(12):946-55.
25. Ganguly R, Hasanally D, Stamenkovic A, Maddaford TG, Chaudhary R, Pierce GN, et al. Alpha linolenic acid decreases apoptosis and oxidized phospholipids in cardiomyocytes during ischemia/reperfusion. Molecular and Cellular Biochemistry. 2017.
26. Bobulescu IA. Renal lipid metabolism and lipotoxicity. Current opinion in nephrology and hypertension. 2010;19(4):393.
27. Folch J. A simple method for the isolation and purification of total lipids from animal tissues.
28. Ravandi A, Leibundgut G, Hung M-Y, Patel M, Hutchins PM, Murphy RC, et al. Release and capture of bioactive oxidized phospholipids and oxidized cholesteryl esters during percutaneous coronary and peripheral arterial interventions in humans. Journal of the American College of Cardiology. 2014;63(19):1961-71.
29. Jimi S, Uesugi N, Saku K, Itabe H, Zhang B, Arakawa K, et al. Possible induction of renal dysfunction in patients with lecithin: cholesterol acyltransferase deficiency by oxidized phosphatidylcholine in glomeruli. Arteriosclerosis, thrombosis, and vascular biology. 1999;19(3):794-801.
30. Stemmer U, Dunai ZA, Koller D, Pürstinger G, Zenzmaier E, Deigner HP, et al. Toxicity of oxidized phospholipids in cultured macrophages. Lipids in health and disease. 2012;11(1):110.
31. Loidl A, Sevcsik E, Riesenhuber G, Deigner H-P, Hermetter A. Oxidized phospholipids in minimally modified low density lipoprotein induce apoptotic signaling via activation of acid sphingomyelinase in arterial smooth muscle cells. Journal of Biological Chemistry. 2003;278(35):32921-8.
32. Gargalovic PS, Imura M, Zhang B, Gharavi NM, Clark MJ, Pagnon J, et al. Identification of inflammatory gene modules based on variations of human endothelial cell responses to oxidized lipids. Proceedings of the National Academy of Sciences. 2006;103(34):12741-6.
33. Hasanally D, Chan D, Chaudhary R, Margulets V, Premecz S, Kirshenbaum L, et al., editors. Novel bioactive oxidized phospholipids are produced in myocardium during ischemia reperfusion and act as mediators of cell death within cardiac myocytes. European Heart Journal; 2014: OXFORD UNIV PRESS GREAT CLARENDON ST, OXFORD OX2 6DP, ENGLAND.
34. Friedli O, Freigang S. Cyclopentenone-containing oxidized phospholipids and their isoprostanes as pro-resolving mediators of inflammation. Biochimica et Biophysica Acta (BBA)-Molecular and Cell Biology of Lipids. 2017;1862(4):382-92.
35. Bretscher P, Egger J, Shamshiev A, Trötzmüller M, Köfeler H, Carreira EM, et al. Phospholipid oxidation generates potent anti-inflammatory lipid mediators that mimic structurally related pro-resolving eicosanoids by activating Nrf2. EMBO molecular medicine. 2015;7(5):593-607.

36. Hashiguchi H, Morooka H, Miyoshi H, Matsumoto M, Koji T, Sumikawa K. Isoflurane protects renal function against ischemia and reperfusion through inhibition of protein kinases, JNK and ERK. Anesthesia & Analgesia. 2005;101(6):1584-9.
37. Rao S, Walters KB, Wilson L, Chen B, Bolisetty S, Graves D, et al. Early lipid changes in acute kidney injury using SWATH lipidomics coupled with MALDI tissue imaging. American Journal of Physiology - Renal Physiology. 2016.
38. Nakamura H, Nemenoff RA, Gronich JH, Bonventre JV. Subcellular characteristics of phospholipase A2 activity in the rat kidney. Enhanced cytosolic, mitochondrial, and microsomal phospholipase A2 enzymatic activity after renal ischemia and reperfusion. Journal of Clinical Investigation. 1991;87(5):1810.
39. Wei Q, Xiao X, Fogle P, Dong Z. Changes in metabolic profiles during acute kidney injury and recovery following ischemia/reperfusion. PLoS One. 2014;9(9):e106647.
40. Nakamura H, Nemenoff RA, Gronich JH, Bonventre JV. Subcellular characteristics of phospholipase A2 activity in the rat kidney. Enhanced cytosolic, mitochondrial, and microsomal phospholipase A2 enzymatic activity after renal ischemia and reperfusion. The Journal of Clinical Investigation. 1991;87(5):1810-8.
41. Sun L, Halaihel N, Zhang W, Rogers T, Levi M. Role of sterol regulatory element-binding protein 1 in regulation of renal lipid metabolism and glomerulosclerosis in diabetes mellitus. Journal of Biological Chemistry. 2002;277(21):18919-27.
42. Johnson A, Stahl A, Zager RA. Triglyceride accumulation in injured renal tubular cells: alterations in both synthetic and catabolic pathways. Kidney international. 2005;67(6):2196-209.
43. Naito M, Bomsztyk K, Zager RA. Renal ischemia-induced cholesterol loading: transcription factor recruitment and chromatin remodeling along the HMG CoA reductase gene. The American journal of pathology. 2009;174(1):54-62.
44. Zager RA, Andoh T, Bennett WM. Renal cholesterol accumulation: a durable response after acute and subacute renal insults. The American journal of pathology. 2001;159(2):743-52.
45. Sampaio JL, Gerl MJ, Klose C, Ejsing CS, Beug H, Simons K, et al. Membrane lipidome of an epithelial cell line. Proceedings of the National Academy of Sciences. 2011;108(5):1903-7.
46. Bonventre JV, Yang L. Cellular pathophysiology of ischemic acute kidney injury. The Journal of clinical investigation. 2011;121(11):4210.
47. Caplan MJ, Anderson HC, Palade GE, Jamieson JD. Intracellular sorting and polarized cell surface delivery of (Na+, K+) ATPase, an endogenous component of MDCK cell basolateral plasma membranes. Cell. 1986;46(4):623-31.
48. Molitoris BA, Wilson PD, Schrier R, Simon F. Ischemia induces partial loss of surface membrane polarity and accumulation of putative calcium ionophores. The Journal of clinical investigation. 1985;76(6):2097-105.
49. Fruhwirth GO, Loidl A, Hermetter A. Oxidized phospholipids: from molecular properties to disease. Biochimica et Biophysica Acta (BBA)-Molecular Basis of Disease. 2007;1772(7):718-36.
50. Hörkkö S, Bird DA, Miller E, Itabe H, Leitinger N, Subbanagounder G, et al. Monoclonal autoantibodies specific for oxidized phospholipids or oxidized phospholipid–protein adducts inhibit macrophage uptake of oxidized low-density lipoproteins. The Journal of clinical investigation. 1999;103(1):117-28.
51. Tsimikas S, Miyanohara A, Hartvigsen K, Merki E, Shaw PX, Chou M-Y, et al. Human oxidation-specific antibodies reduce foam cell formation and atherosclerosis progression. Journal of the American College of Cardiology. 2011;58(16):1715-27.

ii: Role of OxPCs in a clinical setting of myocardial I/R

Based on our previous study, we found that OxPC species are elevated in renal tissue during I/R. In this study, we investigated how plasma OxPCs concentrations are affected in patients presenting with STEMI undergoing primary PCI for coronary reperfusion. Thus, the objectives of this study were as follows:

To determine if OxPC species increase in the plasma during the first 30 days following myocardial I/R.

To investigate if the concentrations of any OxPCs species/group are correlated with the levels of markers of myocardial injury, including creatine kinase (CK) and troponin T (TnT) after myocardial infarction (MI).

We hypothesized that fragmented OxPCs increase following reperfusion and are correlated with CK/TnT levels.

Increase in plasma oxidized phosphatidylcholines (OxPCs) in patients presenting with ST-Elevation Myocardial Infarction (STEMI)

Zahra Solati[1,2], Arun Surendran[1,2], Andrea Edel[1,2], Marynia Roznik[3], David Allen[4], Ashim K Bagchi[2], Pawan K Singal[2], and Amir Ravandi[1,2,3,4]

[1]Cardiovascular Lipidomics Laboratory, St. Boniface Hospital, Albrechtsen Research Centre, [2]Department of Physiology and Pathophysiology, Rady Faculty of Health Sciences, University of Manitoba

[3]Department of Medicine, Rady Faculty of Health Sciences, University of Manitoba

[4] Section of Cardiology, Department of Medicine, Rady Faculty of Health Sciences, University of Manitoba

Abstract

Objective: ST-segment Elevation Myocardial Infarction (STEMI) occurs as a result of acute occlusion of the coronary artery. Despite successful reperfusion using primary percutaneous coronary intervention (PPCI), a large percentage of myocardial cells die after reperfusion which is recognized as ischemia/reperfusion injury (I/R). Oxidized phosphatidylcholines (OxPCs) are a group of oxidized lipids generated through non-enzymatic oxidation and have pro-inflammatory properties. This study aimed to examine the roles of OxPCs in a clinical setting of myocardial I/R.

Methods: Blood samples were collected from STEMI patients at presentation prior to primary PCI (PPCI) (Isch) and at 4 time-points post-PPCI, including 2h (R-2h), 24h (R-24h), 48h (R-48h) and 30 days (R-30d) post-PPCI. As controls, blood samples were collected from patients with non-obstructive coronary artery disease after diagnostic coronary angiography. Aspiration thrombectomy was also done in selected STEMI patients. High-performance lipid chromatography mass spectrometry (HPLC-MS/MS) was used for OxPCs analysis.

Results: Twenty-two and 38 distinct OxPC species were identified and quantified in plasma and thrombus samples, respectively. These compounds were categorized as fragmented and non-fragmented species. Plasma levels of OxPC compounds were first compared between Isch and control groups. Using one-way analysis of variance (ANOVA), total levels of OxPCs did not significantly differ between Isch and control groups. However, total levels of fragmented OxPCs increased significantly during the ischemic period compared with controls (Isch: 4.79±0.94, Control: 1.69±0.19 ng/µl of plasma, $p<0.05$). Simultaneously, total concentrations of non-fragmented OxPCs experienced significant reductions during ischemia compared to the control group (Isch: 4.84±0.30, Control: 6.6±0.51 ng/µl of plasma, $p<0.05$). Next, we compared OxPC concentrations during I/R. Total concentrations of OxPCs in STEMI patients were not significantly different during I/R. However, fragmented OxPCs levels remained elevated for 48h post-reperfusion but decreased at 30 days following MI, which was statistically significant in comparison with the levels of R-2h and R-24h groups (Isch: 4.79±0.94, R-2h: 5.33±1.17, R-24h: 5.20±1.1, R-48h: 4.18±1.07, R-30d: 1.87±0.31 ng/µl of plasma, $p<0.05$). Conversely, levels of non-fragmented OxPCs did not change over 30 days following MI (Isch: 4.84±0.30, R-2h: 5.15±0.40, R-24h: 5.03±0.37, R-48h: 5.01±0.47, R-30d: 6.19±0.80 ng/µl of plasma). Moreover,

plasma levels of POVPC and PONPC during ischemia were significantly elevated in STEMI patients with an elevated peak of creatine kinase (CK) concentrations ($p<0.05$). Levels of POVPC and PONPC were also significantly correlated with the levels of inflammatory cytokines, namely interferon-gamma (INF-γ) and interleukin-1β (IL-1β) during I/R (POVPC and INF-γ correlation: $r=0.20$, $p=0.01$, POVPC and IL-1β correlation: $r=0.16$, $p=0.045$) (PONPC and INF-γ correlation: $r=0.41$, $p=0.001$, PONPC and IL-1β correlations: $r=0.25$, $p=0.001$). In thrombus, fragmented OxPCs were dominant metabolites, which constituted 77% of total OxPCs concentrations.

Conclusion: This study is the first comprehensive OxPC analysis in plasma and thrombus of STEMI patients undergoing PPCI. OxPC profiles demonstrated a higher concentration of fragmented OxPC in STEMI patients during ischemia when compared to controls. However, its levels decreased during the 30 days post-reperfusion. Levels of POVPC and PONPC during the ischemic episode were significantly elevated in patients with elevated peak CK levels. Their concentrations were also significantly correlated with inflammatory cytokines levels, namely IL-1 β and INF- γ, during I/R.

Keywords: Ischemia/reperfusion injury, STEMI, oxidized phosphatidylcholine, lipidomics, mass-spectrometry

Introduction

Acute myocardial infarction (MI) is one of the leading causes of morbidity and mortality worldwide (1). The occurrence of total coronary artery occlusion, as a consequence of atherosclerotic plaque rupture and thrombosis, results in acute MI (2). Thrombosis occurs when the lipid-rich core is exposed to the arterial lumen after atherosclerotic plaque rupture. Exposure to plaque contents initiates platelet aggregation and fibrin formation, which leads to reduced blood flow and can cause distal embolization (3, 4). Therefore, restoration of blood flow by the use of thrombolytic agents or percutaneous coronary intervention (PCI) is an effective approach to re-perfuse myocardium, limit infarct size, preserve systolic cardiac function, prevent heart failure and improve mortality (5).

Despite significant reductions in rates of post-MI-mortality and heart failure (HF) over the last 20 years, their incidences are still high (10% and 25%, respectively), which are attributed to ischemia-reperfusion (I/R) injury (6). I/R injury is defined as myocardial cell death following reperfusion, which is thought to be responsible for 50% of the final infarct size (6). A large component of this ongoing myocardial injury is the result of an extensive production of reactive oxygen species (ROS) and inflammation post-reperfusion. One group of compounds susceptible to oxidation are cellular lipids. Myocardial phosphatidylcholines (PC) are specifically susceptible to oxidation, due to having a high proportion of polyunsaturated fatty acids (PUFA) in their structures. Oxidation of PC molecules at the site(s) of unsaturation can lead to the formation of a variety of OxPC molecules; however, despite similar structures, the acquired biological activities are uncharacteristic of the parent molecule (7). It has been shown that only 4-hour treatment of human aortic endothelial cells (HAEC) with 40 µg/ml of oxidized 1-palmitoyl-2-arachidonyl-sn-glycerol-3-phosphocholine (Ox-PAPC) modulates more than 1000 genes which are implicated in inflammation, angiogenesis, cell division, thrombosis, and vasoconstriction (8).

The role of OxPC in coronary artery disease (CAD) has been explored extensively utilizing the monoclonal antibody E06 (9, 10). E06 is an IgM antibody that binds to OxPCs, but not naive PC (11). OxPCs not only serve as a damage-associated molecular pattern (DAMPs), which are recognized by pattern-recognition receptors (such as TLR2 and/or CD36) but also induce the production of inflammatory cytokines (12). Studies have shown that levels of OxPCs bound to

apoB100 increase acutely following ACS (13) and PCI (14). We have recently shown that there are large increases in levels of OxPC molecules in both *in vitro* and *in vivo* model of myocardial I/R. Among the OxPC species, fragmented OxPCs are potent inducers of cell death through a mitochondrial-mediated pathway. We went on to show that inactivating OxPCs resulted in a significant increase in myocardial recovery (15).

Our goal in this study is to identify the plasma OxPC molecules in patients presenting with ST-Elevation Myocardial Infarction (STEMI) undergoing reperfusion. Identifying specific OxPC species is necessary as each compound has unique biologic activities, specific downstream targets, and half-lives. This will allow us to see the temporal changes in these compounds and to see the impact of reperfusion. We also investigated the correlation of these molecules with inflammatory cytokines.

Material and methods

Materials:

Phospholipid and oxidized phospholipids including 1,2-dinonanoyl-sn-glycero-3-phosphocholine (09:0 PC), 1-palmitoyl-2-linoleoyl-sn-glycero-3-phosphocholine (PLPC), 1-palmitoyl-2-arachidonoyl-sn-glycero-3-phosphocholine (PAPC), 1-stearoyl-2-linoleoyl-sn-glycero-3-phosphocholine (SLPC), 1-stearoyl-2-arachidonoyl-sn-glycero-3-phosphocholine (SAPC), 1-palmitoyl-2-docosahexaenoyl-sn-glycero-3-phosphocholine (PDHPC), 1-palmitoyl-2-(5'-oxo-valeroyl)-sn-glycero-3-phosphocholine (POVPC), 1-palmitoyl-2-azelaoyl-sn-glycero-3-phosphocholine (PAzPC) and 1-palmitoyl-2-(9'-oxo-nonanoyl)-sn-glycero-3-phosphocholine (PONPC), and 1-palmitoyl-2-glutaryl-sn-glycero-3-phosphocholine (PGPC) were obtained from Avanti Polar Lipids (Alabaster, AL, USA). 1-palmitoyl-2-(5’-keto-6’-octenedioyl)-sn-glycero-3-phosphocholine (KOdiA-PC) and 1-palmitoyl-2(4’-keto-dodec-3’-ene-dioyl)-sn-glycero-3-phosphocholine (KDdiA-PC) were purchased from Cayman Chemicals (Ann Arbor, Michigan, USA). Analytical grade chloroform, methanol, and formic acid were purchased from Fisher-Scientific (Hampton, NH). Mobile phase solvents including acetonitrile, isopropanol, and water (LC/MS grade) were purchased from Fisher-Scientific.

Sample collection:

All samples were collected at St. Boniface Hospital with the study approval by the University of Manitoba and the St. Boniface Hospital Research ethics boards. Blood samples from 52 patients presenting with STEMI to St. Boniface cardiac catheterization laboratory for PPCI. Written informed consent was collected from all patients. Samples were collected by venipuncture at presentation (Isch), post-procedure after successful PPCI and revascularization (R-2h), 24h (R-24h), 48h (R-48h) and 30-day post-PPCI (R-30d). All samples were collected in EDTA venipuncture tubes and immediately centrifuged at 3000 rpm for 10 minutes in a refrigerated centrifuge. Plasma was aliquoted in cryovials and frozen at -80℃ until analysis. During PPCI, selected groups of patients underwent aspiration thrombectomy (n=15). The recovered material collected in the filter supplied by the manufacturer was kept in 1 ml of PBS with EDTA and kept at -80 until analysis. The overall study design is shown in Figure 13.

Figure 13: Overall study design

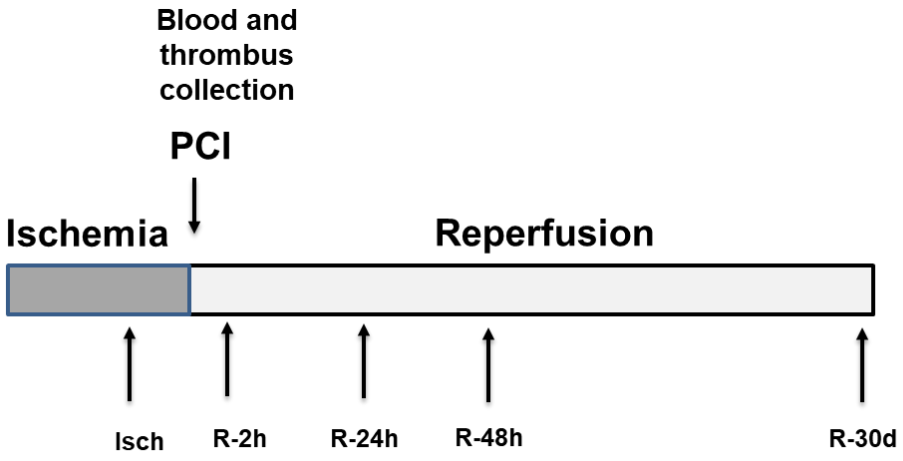

Plasma samples were collected at five different time points including the time of arrival at the cardiac catheterization laboratory for primary PCI (Isch), 2h post angioplasty (R-2h), 24h post angioplasty (R-24h), 48h post angioplasty (R-48h) and 30 days following PPCI (R-30d).

Inclusion criteria included patients greater than 18 years of age, confirmation of STEMI on 12 lead ECG, the presentation with chest pain, no contraindication for collection of 10 ml of blood at the time of the procedure, and documentation of occluded coronary artery with coronary angiography. Control samples were collected from age-matched controls, who were referred for coronary angiography without any evidence of coronary artery disease, as documented by coronary angiography. Blood samples used as controls were collected from 59 patients before and after coronary angiography.

Plasma oxidized phospholipids extraction:

Plasma lipid extraction was performed with 2:1 (vol/vol) chloroform: methanol using the method described by Folch et al. (16). The ratio of sample to solvent was 1:10 to achieve optimal extraction (17). Di 9:0 PC (10 ng/µl) was purchased and used as an internal standard. A lipid extract was then reconstituted in solvent A (acetonitrile and water 60:40 with 10mM ammonium formate and 0.1% formic acid) and analyzed by HPLC-MS/MS (18).

Thrombus lipid extraction:

Frozen thrombus samples in PBS-EDTA were thawed on ice and homogenized with the Polytron PT 1600 E homogenizer until a delicate particulate matter was suspended in PBS-EDTA solution. To prevent heating of the solution, cycles of 20 seconds of homogenization and 60 seconds on the ice were performed until complete homogenization. The sample was aliquoted and frozen at -80°C until the time of lipid extraction. Homogenized samples were thawed on ice and lipid extraction was performed using the 2:1 (vol/vol) chloroform: methanol. The protocol was adjusted for STEMI thrombus samples to allow 1 ml of sample to be extracted in comparison to 100 µl of a sample as initially described by Folch et al. (16). An internal standard mixture of 9:0 PC (10 ng/µl) was added to each sample before lipid extraction. Similar to plasma samples, a portion of lipid extract was reconstituted in solvent A and analyzed by HPLC-MS/MS.

The total protein concentration of the homogenate sample was quantified with the Pierce Microplate BCA Protein Assay Kit by Thermo Scientific. Optical Density was read at 570 nm with the Dynex MRX Revelation Microplate Reader. Protein was quantified in micrograms per millilitre of homogenate.

OxPCs identification and quantification:

Plasma and thrombus lipid extracts were injected to ZORBAX RRHD Eclipse Plus C18, HPLC column (2.1 x 50 mm, 1.8 µm; Agilent Technology, CA, USA). Gradient elution was performed to separate OxPC species. Solvent A and solvent B were a mixture of Acetonitrile/Water (60:40 vol/vol) and Isopropanol/Acetonitrile (90:10 vol/vol), respectively. Both solvents contained 10 mM ammonium formate and 0.1% formic acid. The time program used was as follows: initial solvent B at 32% until 4.00 min; switched to 45% B; 5.00 min 52% B; 8.00 min 58% B; 11.00 min 66% B; 14.00 min 70% B; 18.00 min 75% B; 21.00 min 97% B; 25.00 min 97% B; 25.10 min 32% B until the elution was stopped at 30.10 min. A flow rate of 0.4 ml/min was used for analysis. The temperature of the column oven and sample tray was 45 and 4˚C, respectively.

The HPLC system was coupled to a 4000 QTRAP® triple quadrupole linear ion trap hybrid mass spectrometer system equipped with a Turbo V electrospray ion source (AB Sciex, Framingham, Massachusetts, USA). Identification of OxPCs was carried out using scheduled Multiple Reaction Monitoring (MRM) using product-ion (184.3 m/z, Da), which corresponds to the PC head group. The electrospray ionization voltage and temperature of the ion source were set to 5500 V and 5000C, respectively. High purity nitrogen was used as curtain gas with 26 psi and high purity air was used as nebulizer and heater gas with pressure set at 40 and 30, respectively. The MRM settings were as follows: declustering potential=125, entrance potential=10, collision energy=53, collision cell exit potential=9 and dwell time= 50 msec. The retention time (RT) window in MRM was set to detect peaks of significance within 60 seconds of confirmed retention time and data was collected utilizing Analyst® Software 1.6 (AB Sciex). Multi-quant® Software 2.1 (AB Sciex) was used to compare peak areas of internal standards and unknown analytes to quantitate the results.

OxPC standards including POVPC, PAzPC, PONPC, PGPC, KOdiA-PC and KDdiA-PC were purchased (as mentioned in the material section) and verified by injecting them to HPLC-MS/MS first to find retention find (RT) for these standards (Figure 14). To find RTs for other OxPC species with no available commercial standards, phospholipids standards including PAPC, SAPC, PLPC, SLPC, PDHPC and SDHPC were undergone air oxidation to produce a pool of fragmented and non-fragmented OxPC species derived from these phospholipids as previously described (18-19). Thin evaporated layers of standard phospholipids in separate test tubes were exposed to air for

2,6,12 and 24 hrs. Non-fragmented OxPCs are produced after a short period of air oxidation (2-6 hrs) versus fragmented species obtained following a longer period of oxidation (12-24hrs). A mixture of air oxidized lipids (constituted of fragmented, non-fragmented and non-oxidized lipids) was then reconstituted in Sol A and injected into HPLC-MS/MS (18-19). Even though close to 84 OxPC species can be identified in plasma, we selected compounds with levels 5 x above baseline and reproducibility in all plasma samples. By using this method, we were able to identify 22 OxPC species in human plasma (Table 10).

Figure 14: MRM chromatogram of OxPC standards

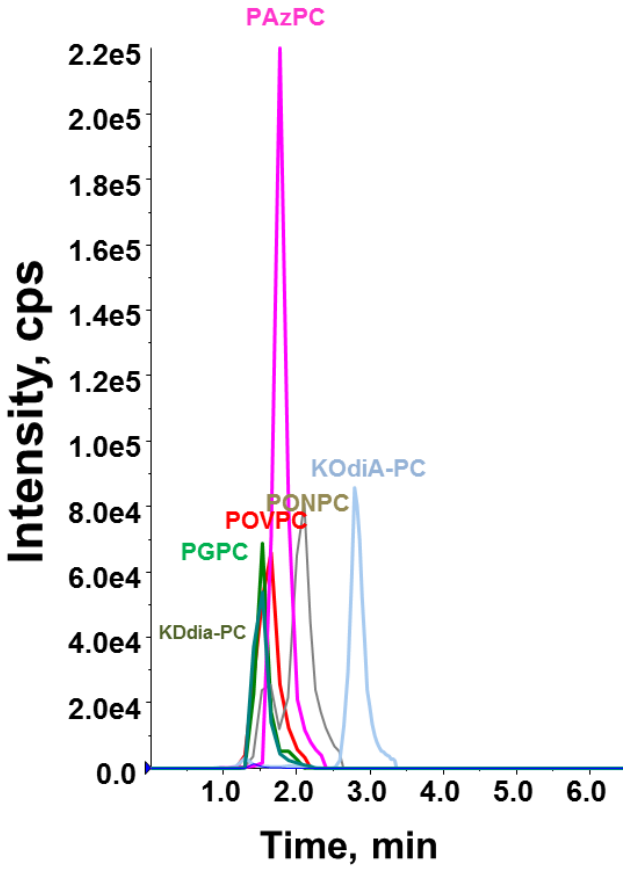

Identification of commercial OxPC standards by reversed-phase HPLC-MS/MS. **Abbreviations**: POVPC: 1-palmitoyl-2-(5'-oxo-valeroyl)-sn-glycero-3-phosphocholine; PAzPC: 1-palmityl-2-azelayl-sn-glycero-3-phosphocholine, PONPC: 1-palmitoyl-2-(9'-oxo-nonanoyl)-sn-glycero-3-phosphocholine, PGPC: 1-palmitoyl-2-glutaryl-sn-glycero-3-phosphocholine, KOdiA-PC: 1-palmitoyl-2-(5'-keto-6'-octenedioyl)-sn-glycero-3-phosphocholine, KDdia-PC: 1-palmitoyl-2(4'-keto-dodec-3'-ene-dioyl)-sn-glycero-3-phosphocholine.

Table 10: List of OxPC compounds identified by reversed-phase HPLC-MS/MS:

Identification of OxPC species in human plasma using HPLC-MS/MS.

OxPC Compound	Q1 Mass (Da)	Q3 Mass (Da)	Retention time
di-9:0-PC (internal standard)	538.6	184.3	1.29
4-oxo-butyryl-PC	580.6	184.3	1.45
POVPC	594.6	184.3	1.48
Succinoyl-PC	596.6	184.3	1.39
PGPC	610.6	184.3	1.4
SOVPC	622.6	184.3	2.16
KOHA-PC	634.6	184.3	1.39
8-oxo-octanoyl-PPC	636.6	184.3	1.75
SGPC	638.6	184.3	1.98
Acetal-POVPC	640.6	184.3	1.37
KOOA-PC	648.6	184.3	1.44
PONPC	650.6	184.3	1.98
KOdiA-PC	664.6	184.3	2.72
PAzPC	666.6	184.3	1.7
KOOA-SPC	676.6	184.3	2.1
SONPC	678.6	184.3	3.15
Furyloctanoyl-PC	688.6	184.3	1.46
SAzPC	694.6	184.3	2.56
Acetal-PONPC	696.6	184.3	1.54
KODA-PPC	704.6	184.3	1.74
HODA-PPC	706.6	184.3	1.62
Furyloctanoyl-PC	716.6	184.3	2.08
KDdiA-PC	720.6	184.3	1.51
HDdiA-PPC	722.6	184.3	1.51
Acetal-SONPC	724.6	184.3	2.18
HODA-SPC	734.6	184.3	2.44
KDiA-SPC	748.6	184.3	2.11
HDiA-PC	750.6	184.3	2.1
PLPC-keto	772.6	184.3	5.57
PLPC-OH	774.6	184.3	5.48
PLPC-epoxy,	788.6	184.3	4.53
PLPC-OOH	790.6	184.3	4.28
PAPC-keto	796.6	184.3	5.88
PAPC-OH	798.6	184.3	7.09
SLPC-keto	800.6	184.3	6.51
SLPC-OH	802.6	184.3	6.7
PLPC-OOH	806.6	184.3	6.74
PLPC-diOH	808.6	184.3	6.71
PAPC-OOH	814.6	184.3	6.73
SLPC-epoxy	816.6	184.3	6
SLPC-OOH	818.6	184.3	5.7
SAPC-keto	824.6	184.3	6.83
SAPC-OH	826.6	184.3	8.19
isoPGF2alpha-PC	832.6	184.3	7.6
SLPC-OOH,OH	834.6	184.3	5.58
SLPC-triOH	836.6	184.3	7.31
SAPC-OOH	842.6	184.3	6.98
SEIPC	856.6	184.3	4.83
isoPGF2alpha-PC	860.6	184.3	8.13
SAPC-OOH	872.6	184.3	4.32
SLPC-triOOH	882.6	184.3	6.93

Abbreviations: HDdiA-PC: 1-palmitoyl-2-(9-hydroxy-11-carboxyundec-6-enoyl)-sn-glycero3-phosphocholine, HODA-PC: 1-palmitoyl-2- (9-hydroxy-12-oxododec-10- enoyl)-sn- glycero3-phosphocholine, isoPG: isoprostanes, KOdiA-PC: 1-palmitoyl-2-(5'-keto-6'-octenedioyl)-sn-glycero-3-phosphocholine, KOHA-PC: 1-palmityl-2-(4-oxo-7-oxohept-5-enoyl)-sn-glycero-3-phosphoserine, KOOA-PC: 1- stearoyl-(5-keto-8-oxo-6-octenoyl)-sn-glycero-3-phosphocholine, KOOA-SPC: 1-palmitoyl-(5-keto-8-oxo-6-octenoyl)-sn-glycero-3-phosphocholine, OH: hydroxyl, OOH: hydroperoxy. PAPC: 1-palmitoyl-2-arachidonoyl-snglycero-3-phosphocholine, PAzPC: 1-palmityl-2-azelayl-sn-glycero-3-phosphocholine, PEIPC: 1-palmitoyl-2-(5,6-epoxyisoprostane E2)-sn-glycero-3-phosphocholine, PGPC: 1-palmitoyl-2-glutaryl-sn-glycero-3-phosphocholine, PLPC: 1-palmitoyl-2-linoleoyl-sn-glycero-3-phosphocholine, PONPC: 1-palmitoyl-2-(9'-oxo-nonanoyl)-sn-glycero-3-phosphocholine, POVPC: 1-palmitoyl-2-(5'-oxo-valeroyl)-sn-glycero-3-phosphocholine , SAPC: 1-stearoyl-2-arachidonoyl-sn-glycero-3-phosphocholine, SAzPC: 1-stearoyl-2-azelaoyl-sn-glycero-3-phosphocholine, SEIPC: 1- stearoyl -2-(5,6-epoxyisoprostane E2)-sn-glycero-3-phosphocholine, SGPC : 1-stearoyl-2-glutaroyl-sn-glycero-3-phosphocholine, SLPC: 1-stearoyl-2-linoleoyl-sn-glycero-3-phosphocholine, SONPC: 1-stearoyl -2-(9-oxo-nonanoyl)-snglycero-3-phosphocholine, SOVPC: sn-1-stearoyl-2-oxovaleroyl-PC.

Plasma cytokine analysis in STEMI patients

Levels of 10 cytokines/chemokines measured in STEMI patients using Mesoscale Discovery (MSD) ELISA protocol and read on MSD sector imager (20). Any sample below the detection limit of < 0.01 pg/ml for a given cytokine was excluded from the study.

Statistical analysis

One-way analysis of variance (ANOVA) with a Fisher post-hoc test for multiple comparisons was used to determine statistical significance between study groups. Associations between specific OxPCs compounds and cytokine levels were assessed by applying Pearson Correlations. All data are presented as mean ± SEM. $p<0.05$ was considered statistically significant.

Results

In this study, 66.6% of the STEMI population and 56.3% of the controls were male ($p=0.08$). The mean age was 65.2±2.08 in the STEMI population and 60.2±1.49 in controls ($p=0.06$). The average body mass index (BMI) was significantly different between STEMI and controls populations (25.8±1.14 and 30.2±1.05, respectively) ($p=0.005$). Based on the laboratory data, the STEMI patients had normal triglycerides (TG), cholesterol (TC), low and high-density lipoprotein (LDL and HDL). There were no significant differences regarding angiotensin-converting enzyme inhibitors/ angiotensin-receptor blockers (ACEI/ARB), beta-blockers and statins use between STEMI and control groups (Table 11).

Table 11: Characteristics of study participants

Characteristics	STEMI patients (n=52)	Controls (n=59)	*P*-Value
Male %	66.6	56.3	0.08
Age , yr (mean±SEM)	65.2±2.08	60.2±1.49	0.06
Body mass index (BMI) (mean±SEM)	25.8±1.14	30.2±1.05	0.005*
Left ventricular ejection fraction (LVEF) %	62%	-	
Time (min), onset of chest pain to reperfusion (Median (min-max))	150 (52-738)	NA	
Left anterior descending coronary artery (LAD) Infarct (%)	41.6	NA	
Right coronary artery (RCA) Infarct (%)	50	NA	
Circumflex Infarct (%)	8	NA	
Peak CK (Median (min-max)) (units/L)	1105 (141-10655)	NA	
Peak TnT (Median (min-max)) (ng/L)	1093 (1-10000)	NA	
Co-morbidity			
Type 2 diabetes mellitus (%)	20.8	14.5	0.4
Smoker (%)	12.7	18.7	0.3
Hypertension (%)	41.6	48.1	0.5
Dyslipidemia (%)	41.6	25.9	0.08
Lipids			
Triglyceride (TG) (mean±SEM) (mmol/l)	1.7±1.4	-	
High-density lipoprotein (HDL) (mean±SEM) (mmol/l)	1.2±0.4	-	
Low-density lipoprotein (LDL) (mean±SEM) (mmol/l)	2.8±0.9	-	
Total cholesterol (mean±SEM) (mmol/l)	4.2±1.2	-	
Medications at baseline			
Angiotensin-Converting Enzyme Inhibitors (ACEI)/Angiotensin II Receptor Blockers (ARB) (%)	20.8	21.8	0.9
Betablocker (%)	6.2	16.3	0.1
Statin (%)	16.6	14.5	0.7

*significantly different compared with controls ($p<0.05$).

The median ischemic period (from the onset of chest pain to reperfusion) was 150 min. Fifty per cent of participants had a right coronary artery (RCA) infarct, whereas 41.6% and 8% had left anterior descending coronary artery (LAD) and circumflex coronary artery occlusions,

respectively. The prevalence of type 2 diabetes (20.8%), hypertension (41.6%) and dyslipidemia (41.6%) at presentation to the hospital were not significantly different in compared with controls (Table 11). The prevalence of these chronic diseases was similar to the previous study of STEMI populations (13).

OxPC species that were identified in STEMI patients and controls

Twenty-two distinct OxPCs were quantified in the plasma of STEMI patients, which include 8 aldehyde-containing OxPC (aldo-OxPC), 6 carboxylic acid-containing OxPC (acid-OxPC) and 8 non-fragmented OxPCs with hydroxyl and hydroperoxyl groups as well as isoprostanes (Table 12). The single ion chromatograms of POVPC, PONPC and PAPC-OH, which are among the highest OxPC species in human plasma, are presented in both Isch and control groups as examples (Figure 15). MRM transitions of other identified OxPC compounds are presented in Table 10.

Table 12: Average plasma concentrations of identified OxPCs in study groups

OxPC species [M-H]+/PC[[M-H]+)	OxPC categories	Control (n=59) (ng/µl)	Isch (n=52) (ng/µl)	R-2h (n=52) (ng/µl)	R-24h (n=52) (ng/µl)	R-48h (n=51) (ng/µl)	R-30d (n=30) (ng/µl)
4-oxo-butyryl-PC (580.6 / 184.3)	Aldo-OxPC	0.07±0.00	0.11±0.01	0.11±0.01	0.13±0.02	0.11±0.02	0.08±0.02
POVPC (524.6 / 184.3)		0.29±0.02	0.44±0.06	0.46±0.08	0.53±0.09	0.42±0.09	0.29±0.04
SOVPC (622.6 / 184.3)*		0.05±0.00	0.24±0.05	0.25±0.05	0.29±0.07	0.24±0.07	0.12±0.02
8-oxo-octanoyl-PPC (636.6/ 184.3)		0.02±0.00	0.18±0.04	0.2±0.05	0.22±0.05	0.19±0.06	0.07±0.02
PONPC (650.6 / 184.3)*		0.48±0.08	1.88±0.39	2.33±0.50	2.36±0.50	1.98±0.50	0.52±0.13
KOOA-SPC (676.6 / 184.3)		0.07±0.01	0.06±0.01	0.05±0.02	0.04±0.01	0.06±0.02	0.07±0.02
SONPC (678.6 / 184.3)*		0.16±0.03	0.57±0.13	0.69±0.17	0.68±0.17	0.60±19	0.13±0.03
HODA-PPC (706.6 / 184.3)		0.00±0.00	0.01±0.00	0.01±0.00	0.02±0.00	0.01±0.00	0.00±0.00
Succinoyl-PPC (526.6 / 184.3)	Acid-OxPC	0.17±0.00	0.40±0.07	0.33±0.05	0.18±0.02	0.15±0.01	0.27±0.03
PGPC (610.6 / 184.3)		0.21±0.02	0.15±0.02	0.14±0.02	0.13±0.02	0.10±0.01	0.12±0.01
SGPC (638.6 / 184.3)		0.00±0.00	0.02±0.00	0.02±0.00	0.02±0.00	0.03±0.00	0.03±0.01
KOdiA-PC (664.6 / 184.3)		0.07±0.01	0.05±0.01	0.05±0.01	0.04±0.01	0.04±0.00	0.05±0.01

PAzPC (666.6 / 184.3)		0.06±0.01	0.66±0.40	0.60±0.30	0.49±0.20	0.21±0.08	0.09±0.01
HDdiA-PPC (722.6 / 184.3)		0.00±0.00	0.01±0.00	0.02±0.00	0.02±0.00	0.02±0.00	0.00±0.00
PLPC-keto (772.6 / 184.3)	Non-fragmented OxPC	0.39±0.11	0.25±0.04	0.35±0.08	0.24±0.04	0.28±0.08	0.18±0.02
PLPC-OH (774.6 / 184.3)		0.47±0.09	0.60±0.09	0.64±0.12	0.50±0.13	0.44±0.12	0.36±0.06
PAPC-OH (798.6 / 184.3)*		2.00±0.2	1.13±0.10	1.16±0.15	1.54±0.19	1.88±0.20	2.66±0.30
PLPC-OOH,OH (806.6 / 184.3)		0.39±0.04	0.66±0.11	0.61±0.08	0.52±0.07	0.36±0.05	0.36±0.06
SLPC-epoxy,keto (816.6 / 184.3)		0.10±0.03	0.15±0.03	0.17±0.04	0.16±0.03	0.14±0.03	0.09±0.02
SAPC-OH (826.6 / 184.3)*		0.50±0.07	0.34±0.03	0.40±0.04	0.61±0.09	0.63±0.1	0.69±0.1
IsoPGF2alpha-PPC (832.6 / 184.3)*		2.36±0.20	1.50±0.10	1.61±0.20	1.27±0.10	1.10±0.10	1.54±0.30
IsoPGF2alpha-SPC (860.6 / 184.3)*		0.40±0.02	0.22±0.02	0.22±0.02	0.20±0.02	0.19±0.02	0.31±0.03

Data are presented as Mean±SEM. *significantly different among study groups (p<0.05). **Abbreviations:** HDdiA-PC: 1-palmitoyl-2-(9-hydroxy-11-carboxyundec-6-enoyl)-sn-glycero3-phosphocholine, HODA-PC: 1-palmitoyl-2- (9-hydroxy-12-oxododec-10- enoyl)-sn- glycero3-phosphocholine,, isoPG: isoprostanes, KOdiA-PC: 1-palmitoyl-2-(5'-keto-6'-octenedioyl)-sn-glycero-3-phosphocholine, KOHA-PC: 1-palmityl-2-(4-oxo-7-oxohept-5-enoyl)-sn-glycero-3-phosphoserine, KOOA-PC: 1- stearoyl-(5-keto-8-oxo-6-octenoyl)-sn-glycero-3-phosphocholine, KOOA-SPC: 1-palmitoyl-(5-keto-8-oxo-6-octenoyl)-sn-glycero-3-phosphocholine, OH: hydroxyl, OOH: hydroperoxy. PAPC: 1-palmitoyl-2-arachidonoyl-snglycero-3-phosphocholine, PAzPC: 1-palmityl-2-azelayl-sn-glycero-3-phosphocholine, PEIPC: 1-palmitoyl-2-(5,6-epoxyisoprostane E2)-sn-glycero-3-phosphocholine, PGPC: 1-palmitoyl-2-glutaryl-sn-glycero-3-phosphocholine, PLPC: 1-palmitoyl-2-linoleoyl-sn-glycero-3-phosphocholine, PONPC: 1-palmitoyl-2-(9'-oxo-nonanoyl)-sn-glycero-3-phosphocholine, POVPC: 1-palmitoyl-2-(5'-oxo-valeroyl)-sn-glycero-3-phosphocholine , SAPC: 1-stearoyl-2-arachidonoyl-sn-glycero-3-phosphocholine, SAzPC: 1-stearoyl-2-azelaoyl-sn-glycero-3-phosphocholine, SEIPC: 1- stearoyl -2-(5,6-epoxyisoprostane E2)-sn-glycero-3-phosphocholine, SGPC : 1-stearoyl-2-glutaroyl-sn-glycero-3-phosphocholine, SLPC: 1-stearoyl-2-linoleoyl-sn-glycero-3- phosphocholine, SONPC: 1-stearoyl -2-(9-oxo-nonanoyl)-snglycero-3-phosphocholine, SOVPC: sn-1-stearoyl-2-oxovaleroyl-PC.

Figure 15: MRM chromatogram of OxPC species

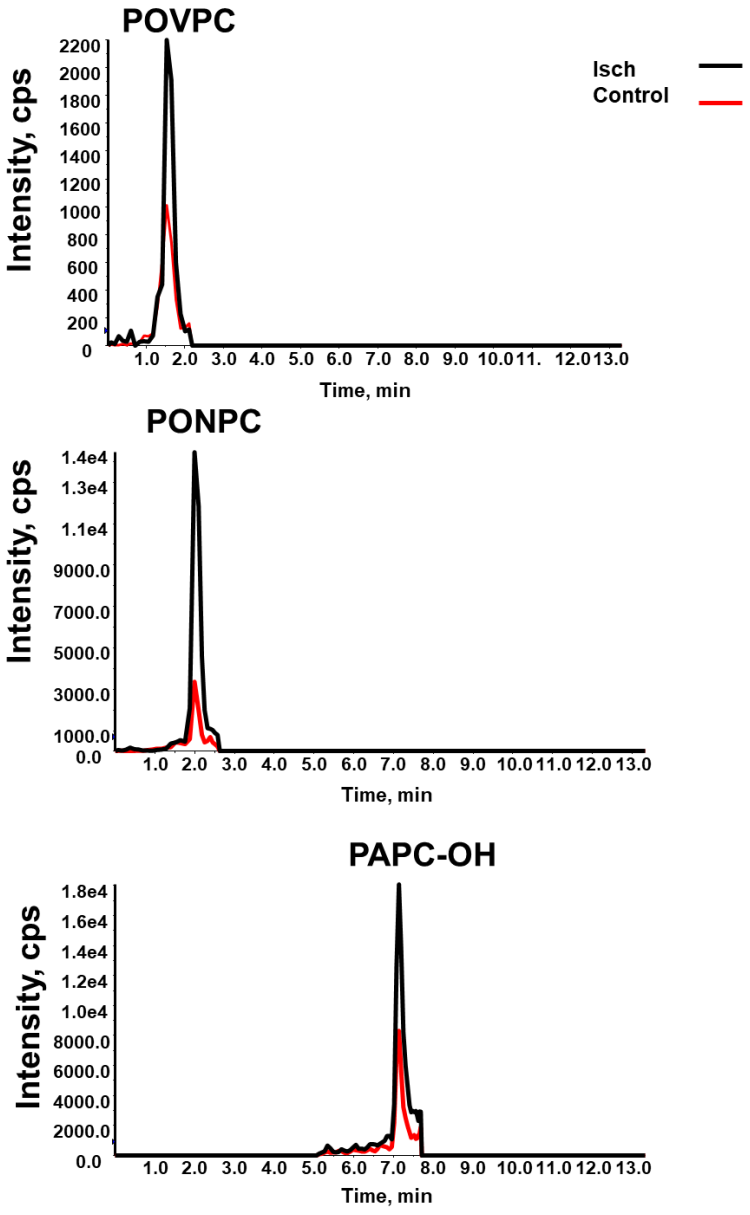

MRM chromatograms of POVPC, PONPC and PAPC-OH in STEMI patients (Isch group) (black line) and controls (red line) measured by reverse-phase HPLC-MS/MS. **Abbreviations:** POVPC: 1-palmitoyl-2-(5'-oxo-valeroyl)-sn-glycero-3-phosphocholine, PONPC: 1-palmitoyl-2-(9'-oxo-nonanoyl)-sn-glycero-3-phosphocholine, PAPC-OH: 1-palmitoyl-2-arachidonoyl-snglycero-3-phosphocholine.

Plasma OxPCs levels in STEMI patients during ischemia compared with controls

As it is presented in Table 13 and Figure 16A, total OxPCs levels did not significantly differ between Isch and control groups (Isch: 9.63±1.08, control: 8.31±0.54 ng/µl of plasma). However, total levels of fragmented OxPCs were significantly elevated during ischemia in STEMI patients compared with control (Isch: 4.79±0.94, control: 1.69±0.19 ng/µl of plasma, $p<0.05$) (Figure 16B). On the other hand, total levels of non-fragmented OxPCs were reduced significantly in STEMI patients during the ischemic episode compared with controls (Isch: 4.84±0.30, control: 6.6±0.51 ng/µl of plasma, $p<0.05$) (Figure 16C).

Table 13: Average plasma levels of total OxPCs, fragmented, non-fragmented OxPCs in study groups

OxPC categories (ng/µl)	Control (n=59)	Isch (n=52)	R-2h (n=52)	R-24h (n=52)	R-48h (n=51)	R-30d (n=30)
Total OxPC	8.31±0.54	9.63±1.08	10.48±1.37	10.24±1.27	9.20±1.29	8.07±1.09
Total fragmented OxPC	1.69±0.19	4.79±0.94*	5.33±1.17 Ł	5.20±1.11 Ł	4.18±1.07	1.87±0.31
Total non-fragmented OxPC	6.6±0.51	4.84±0.30*	5.15±0.40	5.03±0.37	5.01±0.47	6.19±0.80

Values are means ± SEM. *significantly different compared with controls ($p<0.05$). Ł significantly different compared with R-30d, ($p<0.05$). **Abbreviation:** OxPC: Oxidized phosphatidylcholine.

Figure 16: Average plasma levels of total OxPCs, fragmented, non-fragmented OxPCs in STEMI patients during ischemia compared with controls

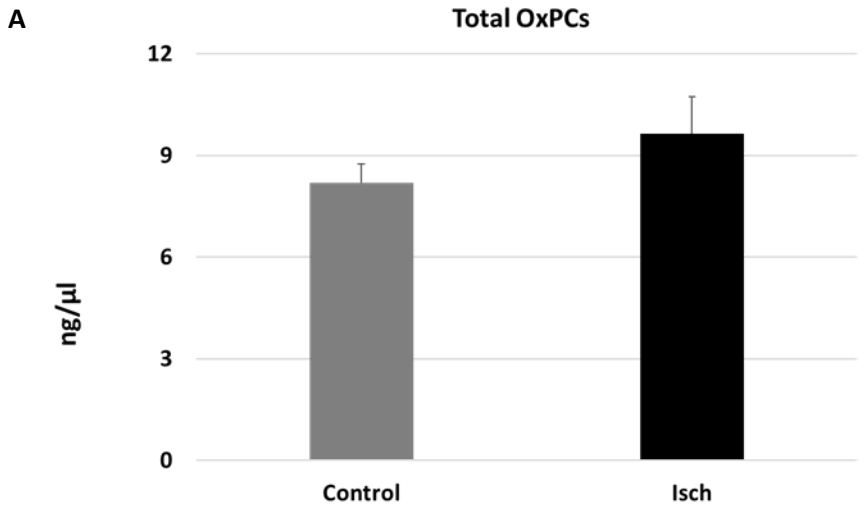

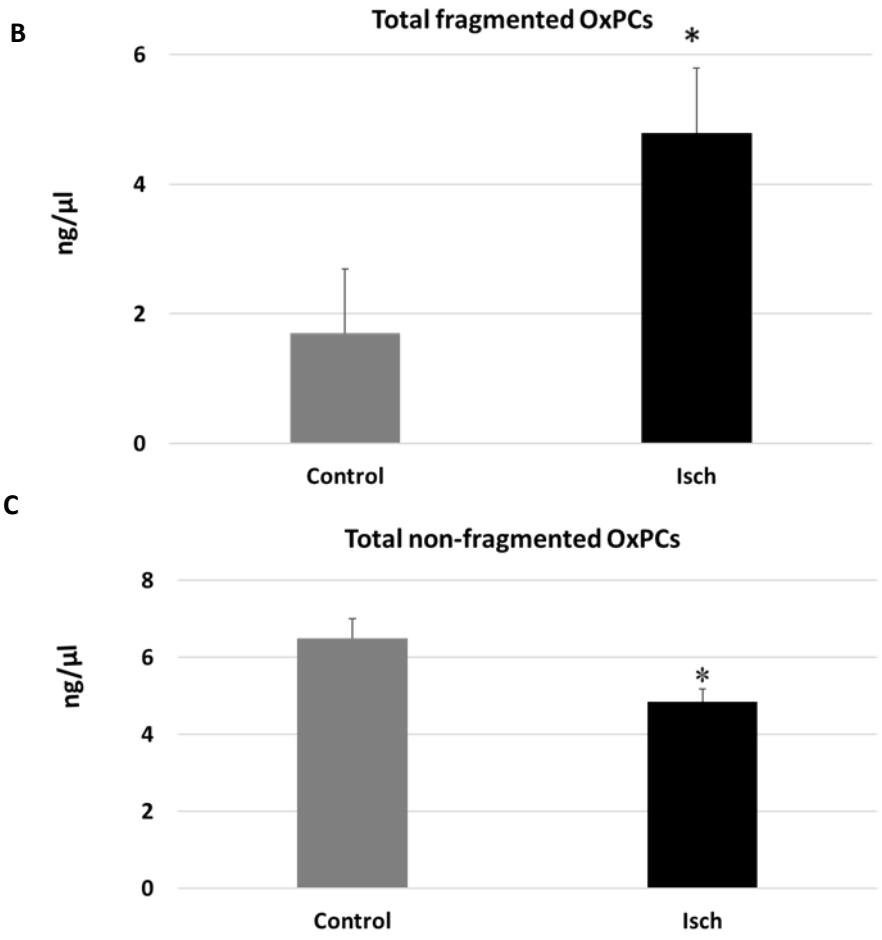

Values are means ± SEM. *Significantly different compared with controls (p<0.05). **Abbreviation:** OxPC: Oxidized phosphatidylcholine.

Looking at individual OxPC species, it is revealed that 4 out of 8 identified aldo-OxPC species, namely POVPC, SOVPC, PONPC, and SONPC, were significantly different between Isch and control groups. POVPC concentrations increased 1.5 times in the Isch group compared with the control (Isch: 0.44±0.06, control: 0.29±0.02 ng/µl of plasma, p<0.05) (Figure 17A). Similarly, there were significant differences between the Isch and control groups in terms of SOVPC levels. As it is shown in Figure 17B, the average levels of SOVPC increased 4.6-fold during ischemia compared with controls (from 0.05±0.0 in controls to 0.2±0.05 ng/µl of plasma in Isch), which was statistically significant (p=0.01). PONPC levels, which were the most abundant OxPCs in STEMI patients, were significantly different among STEMI patients and control as well. The average levels of PONPC were 0.48±0.08 ng/µl of plasma in controls, which rose to 1.87±0.39 ng/µl in the

ischemic period in STEMI patients (p=0.02) (Figure 17C). Similar alterations were observed in the plasma levels of SONPC. The average levels of SONPC were significantly higher during ischemia compared with controls (Isch: 0.57±0.13 versus controls: 0.15±0.03 ng/µl of plasma, p=0.03) (Figure 17D).

Regarding non-fragmented OxPCs, 3 out of 8 non-fragmented OxPCs differed significantly in STEMI patients before-PCI compared with controls. The average levels of PAPC-OH reduced significantly in ischemia compared with controls (Isch: 1.13±0.14, control: 2.00±0.2 ng/µl of plasma, p<0.05) (Figure 17E). Plasma levels of SAPC-OH were also lower in the Isch group compared with controls, although it did not reach statistical significance (Isch: 0.33±0.03 and control: 0.49±0.07 ng/µl of plasma, p=0.08) (Figure 17F). Levels of IsoPGF2alpha-PPC and IsoPGF2alpha-SPC were also significantly elevated in controls compared with Isch group (IsoPGF2alpha-PPC: Isch: 1.49±0.1, control: 2.35±0.2, ng/µl of plasma, p<0.05) (Figure 17G) (IsoPGF2alpha-SPC: Isch:0.2±0.02, control: 0.4±0.02 ng/µl of plasma, p<0.05) (Figure 17H).

Figure 17: OxPC species that were significantly different in the Isch group compared with controls

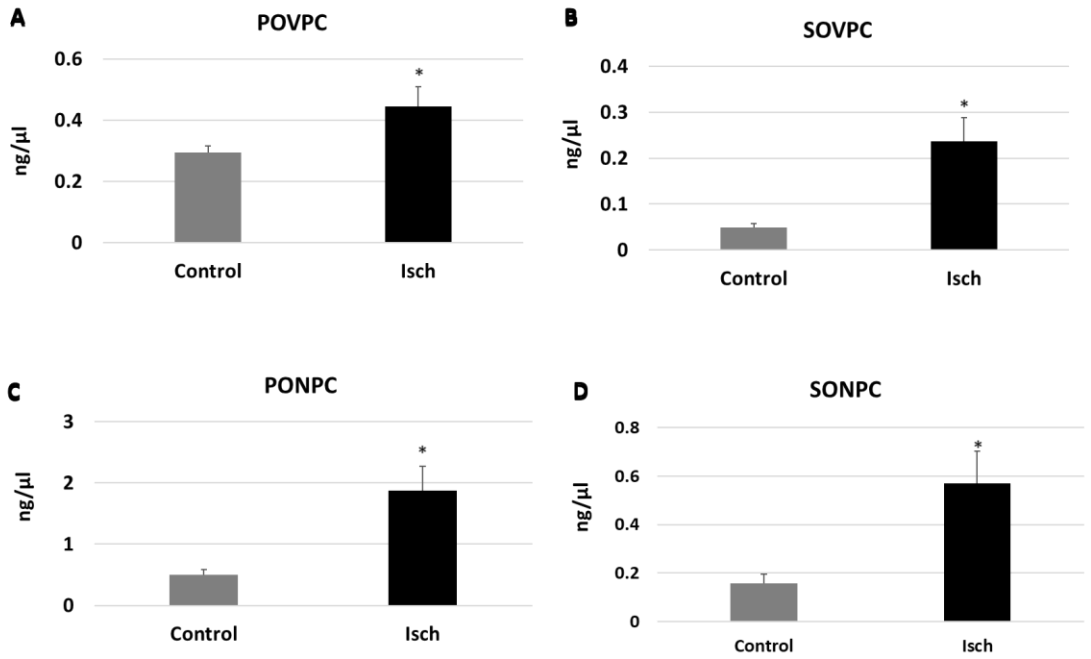

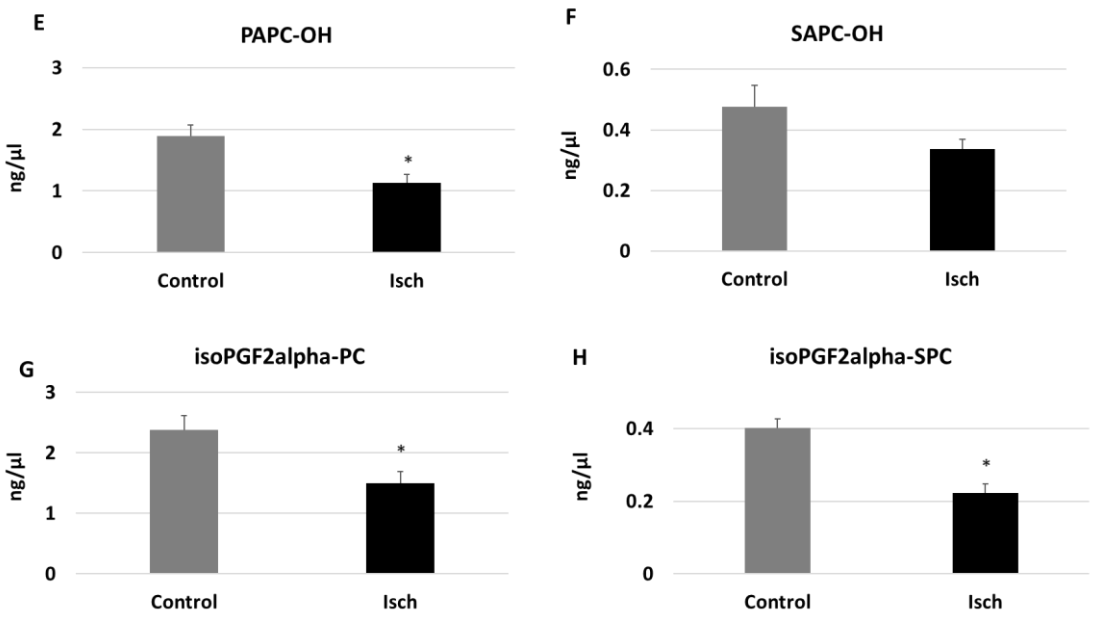

Values are means ± SEM. *Significantly different compared with controls (p<0.05). **Abbreviations:** isoPG: isoprostanes, PAPC: 1-palmitoyl-2-arachidonoyl-snglycero-3-phosphocholine, PONPC: 1-palmitoyl-2-(9'-oxo-nonanoyl)-sn-glycero-3-phosphocholine, POVPC: 1-palmitoyl-2-(5'-oxo-valeroyl)-sn-glycero-3-phosphocholine, SAPC: 1-stearoyl-2-arachidonoyl-sn-glycero-3-phosphocholine, SONPC: 1-stearoyl -2-(9-oxo-nonanoyl)-snglycero-3-phosphocholine, SOVPC: sn-1-stearoyl-2-oxovaleroyl-PC.

Changes in plasma OxPCs levels in STEMI patients during I/R

Subsequently, levels of OxPCs were compared in STEMI patients during I/R. Total levels of OxPCs were not significantly different in STEMI patients during I/R (Isch: 9.63±1.08, R-2h: 10.48±1.37, R-24h: 10.24±1.27, R-48h: 9.20±1.29, and R-30d: 8.07±1.09 ng/µl of plasma) (Table 13 and Fig 18A). However, levels of fragmented OxPCs remained elevated during 48h post-PCI and then decreased during 30 days of reperfusion, which was statistically significant compared with Isch and R-2h groups (Isch: 4.79±0.94, R-2h: 5.33±1.17, R-24h: 5.20±1.11, R-48h: 4.18±1.07, R-30d: 1.87±0.31 ng/µl of plasma, p<0.05) (Table 13) (Figure 18B). In contrast, total levels of non-fragmented OxPCs increased during 30 days after reperfusion, although changes were not statistically significant (Isch: 4.84±0.30, R-2h: 5.15±0.40, R-24h: 5.03±0.37, R-48h: 5.01±0.47, R-30d: 6.19±0.80 ng/µl of plasma) (Table 13 and Figure 18C).

Figure 18: Plasma levels of total OxPCs, fragmented, and non-fragmented OxPCs in STEMI patients during I/R

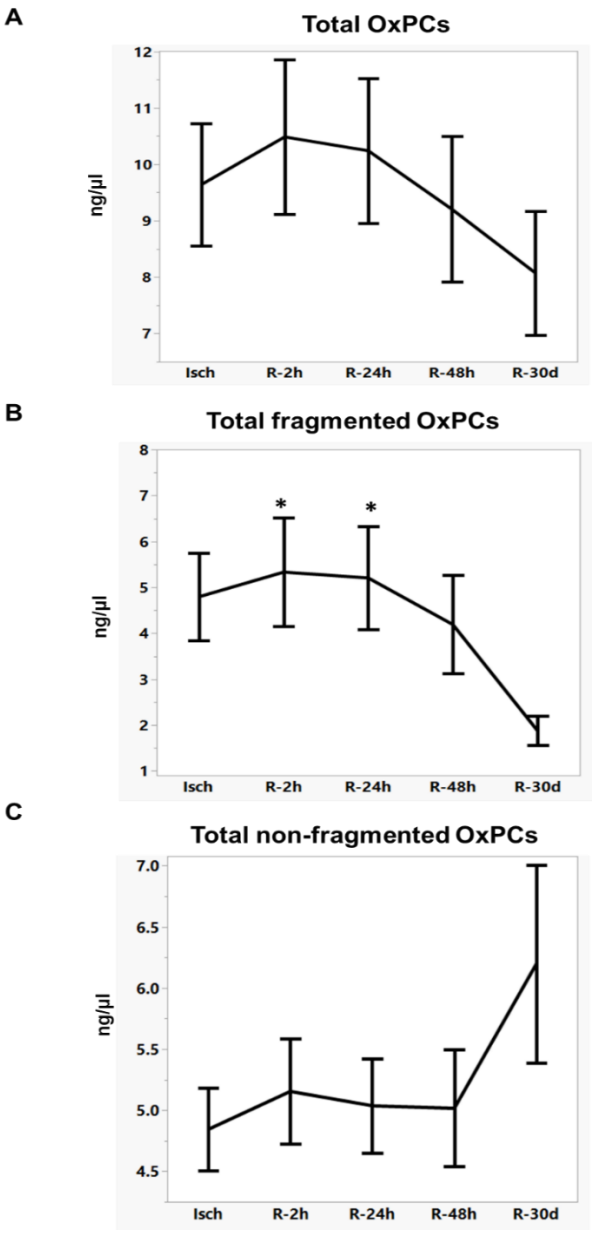

The chart represents means ± SEM. * Significant differences compared with the R-30d group, $p<0.05$..
Abbreviations: OxPC: Oxidized phosphatidylcholine.

Among fragmented OxPC species, levels of PONPC decreased significantly during 30 days after reperfusion, which was statistically significant compared with R-2h and R-24h groups (Isch: 1.87±0.39, R-2h: 2.3±0.55, R-24h: 2.36 ±0.55, R-48h: 1.98±0.57, and R-30d: 0.5±0.1 ng/µl of plasma, $p<0.05$) (Figure 19A). SONPC concentrations also decreased over 30 days and changes were statistically significant compared with R-2h, R-24h and R-48h groups (Isch: 0.57±0.13, R-2h: 0.69±0.13, R-24h: 0.68±0.17, R-48h:0.6±0.19, and R-30d: 0.12±0.03 ng/µl of plasma) (R-2h and R-30d: $p=0.01$, R-24h and R-30d: $p=0.01$, and R-48h and R-30d: $p=0.04$) (Figure 19B).

Non-fragmented OxPC species generally increased over 30 days post-PCI. At 30-day post-reperfusion, PAPC-OH levels were at the highest levels, which were statistically significant compared with all other groups (Isch: 1.12±0.14, R-2h: 1.16±0.15, R-24h: 1.54±0.19, R-48h: 1.88± 0.2 and R-30d: 2.66±0.39 ng/µl of plasma, $p<0.05$) (Figure 19C). Levels of SAPC-OH also rose post-reperfusion. Its levels at 24hr and 48hr post-reperfusion were significantly higher compared with the ischemic levels (Isch: 0.33±0.03 and R-24h: 0.60±0.09 ng/µl of plasma, $p=0.01$) (Isch: 0.33±0.03 and R-48h: 0.62±0.1 ng/µl of plasma, $p=0.01$). SAPC-OH levels continued to increase and its concentrations were significantly elevated at 30-day post-MI in comparison with Isch and R-2h groups (Isch: 0.33±0.03, R-2h: 0.40±0.04, R-30d: 0.69±0.14, $p<0.05$) (Figure 19D). Levels of isoPGF2alpha-SPC were significantly elevated at 30 days post-MI compared with other STEMI groups (Isch:0.2±0.02, R-2h: 0.2±0.02, R-24h: 0.19±0.02, R-48h: 0.19±0.02, and R-30d: 0.3±0.03 ng/µl of plasma, $p< 0.05$) (Figure 19E). Changes in the plasma levels of all identified OxPCs in STEMI patients and controls are presented in Table 12.

Figure 19: OxPC species that were significantly different during I/R

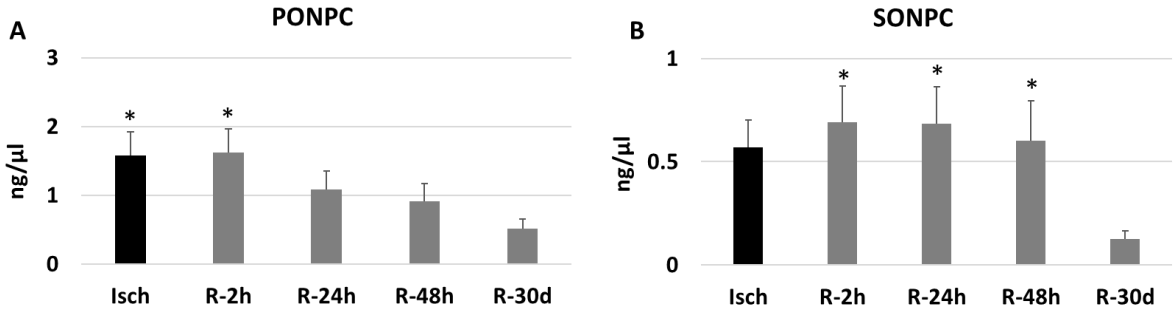

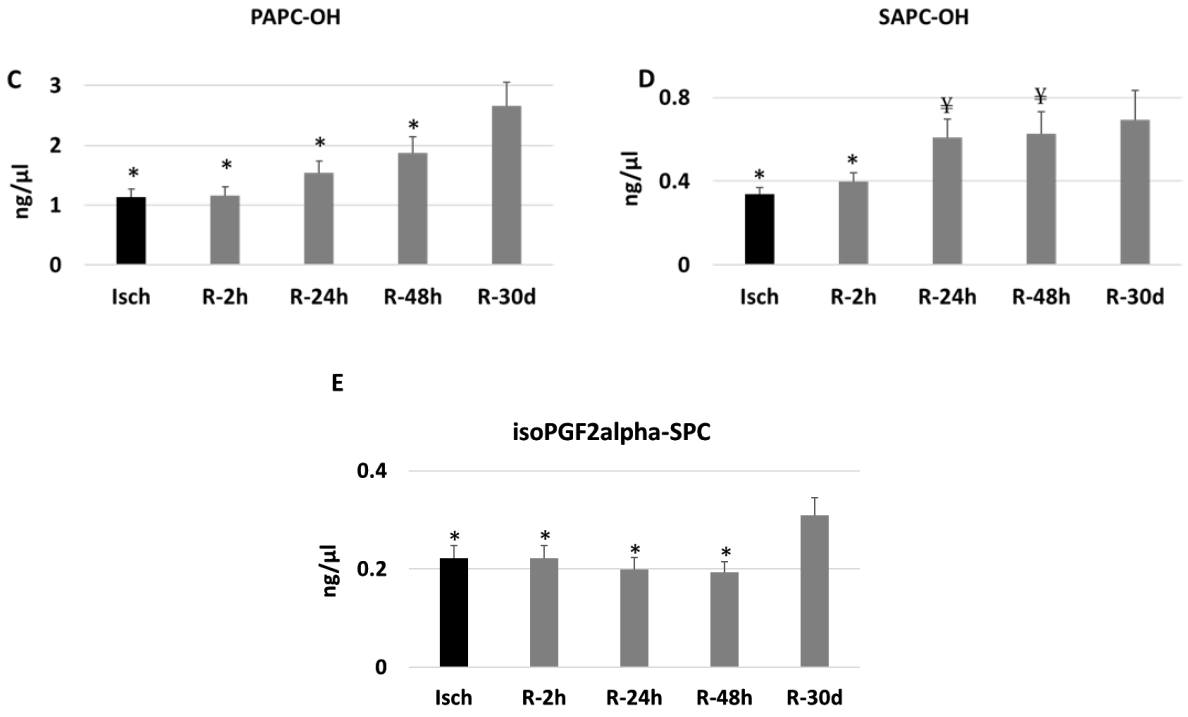

Values are means ± SEM. * Significant differences compared with the R-30d group, $p<0.05$. ¥ Significant differences compared with Isch group. **Abbreviations:** isoPG: isoprostanes, PAPC: 1-palmitoyl-2-arachidonoyl-snglycero-3-phosphocholine, PONPC: 1-palmitoyl-2-(9'-oxo-nonanoyl)-sn-glycero-3-phosphocholine, SAPC: 1-stearoyl-2-arachidonoyl-sn-glycero-3-phosphocholine, SONPC: 1-stearoyl -2-(9-oxo-nonanoyl)-snglycero-3-phosphocholine.

Inflammatory cytokines in post-PPCI STEMI patients

We measured the levels of 10 cytokines and chemokines in the plasma of STEMI patients. Among them, only levels of IFN-γ and IL-1β were significantly correlated with OxPC species in STEMI patients. In our study, levels of INF-γ were elevated during ischemia and early after refusion. at 24h post PCI, its levels decreased significantly in the plasma of STEMI patients. Following that, its levels increased slightly until 30 days (Isch: 20.26±2.15, R-2h: 17.99±2.05, R-24h: 10.17±2.11, R-48h:13.82±2.15, and R-30:15.32±2.15 pg/ml of plasma, $p<0.05$). IL-1β also experienced dramatic changes during I/R. There was a significant drop in the levels of IL-1β after 24h of post-PPCI until 30 days which were statistically significant in comparison with Isch and R-2h groups (Isch: 0.50±0.04, R-2h: 0.46±0.04, R-24h: 0.25±0.04, R-48h: 0.26±0.04, and R-30: 0.22±0.05 pg/ml of plasma, $p<0.05$) (Figure 20).

Figure 20: Alteration in the levels of INF-γ and IL-1β in STEMI patients during I/R

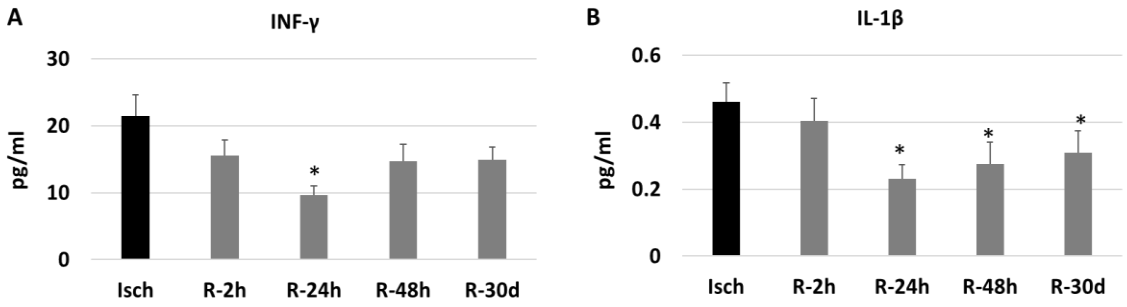

Values are means ± SEM. ***** Significantly different compared with Isch group, $p<0.05$. Ł Significantly different compared with R-2h, $p<0.05$. **Abbreviations:** IFN-γ: Interferon-gamma, IL-1β: Interleukin-1 beta.

Total levels of fragmented OxPCs were significantly correlated with INF-γ and IL-1β levels during I/R (total fragmented OxPCs and INF- γ correlation: r=0.30, p=0.001) (total fragmented OxPCs and IL-1β correlations: r=0.28, p=0.001). There were also weak but significant correlations between POVPC and cytokines levels during I/R (POVPC and INF-γ correlations: r=0.20, p=0.01, POVPC and IL-1β: r=0.16, p=0.045). Concentrations of PONPC were also weakly but significantly correlated with the inflammatory cytokines during I/R (PONPC and INF-γ correlation: r=0.41, p=0.001) (PONPC and IL-1β correlations: r=0.25, p=0.001).

OxPCs levels and markers of myocardial injury

We categorized STEMI patients based on plasma peak CK and TnT levels, which are the gold standards of myocardial injury (21). Patients with levels ≤ than median peak levels of CK were grouped as "low CK" group and patients with levels of > median peak CK levels considered as "high CK" group. As shown in Figure 21A, the levels of POVPC and PONPC in STEMI patients during ischemia were significantly higher in the "high CK" group compared with the "low CK" group ($p<0.05$). Categorizing POVPC and PONPC based on peak TnT levels also resulted in similar findings meaning that patients with higher TnT levels had higher POVPC and PONPC before PCI. However, differences between TnT groups were not statistically significant (Figure 21B).

Figure 21: Mean comparison of POVPC and PONPC levels based on CK (A) and TnT levels (B)

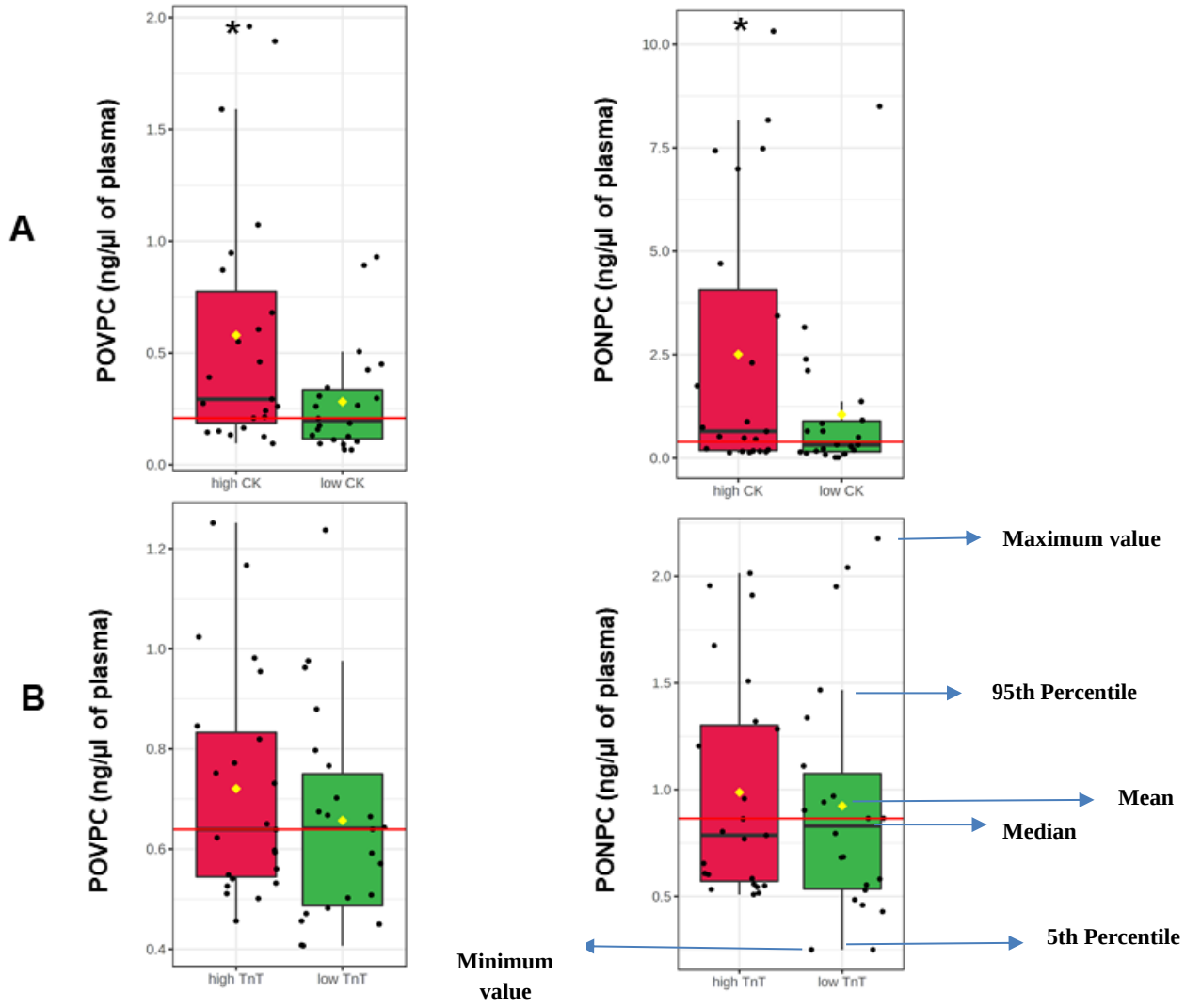

Values are means ± SEM. * Statistically significant difference, $p<0.05$. The box is determined by the 25th and 75th percentiles. The whiskers are determined by the 5th and 95th percentiles**. Abbreviations:** CK: creatine kinase, PONPC: 1-palmitoyl-2-(9'-oxo-nonanoyl)-sn-glycero-3-phosphocholine, POVPC: 1-palmitoyl-2-(5'-oxo-valeroyl)-sn-glycero-3-phosphocholine, TnT: Troponin T.

Analysis of OxPCs in thrombus

In order to see the potential contribution of ruptured plaque material to the plasma, OxPC levels were determined in recovered thrombectomy samples from 15 STEMI patients. Fragmented (aldo/acid) OxPCs and non-fragmented OxPCs containing terminal furans, isoprostanes and long-chain groups were identified in thrombectomy samples. All quantified OxPC species in thrombus are presented in Table 14.

Table 14: Quantified OxPCs in thrombus of STEMI patients

Component Name	Average ± SEM (pg/µg of protein)	Percentage of total OxPC
PONPC	1.26±0.18	19.81
POVPC	1.00±0.33	18.48
Isofuran-PC	0.67±0.15	9.90
SOVPC	0.60±0.19	8.78
PAzPC	0.45±0.07	6.65
4-oxo-butyryl-PC	0.38±0.13	5.54
PLPC-epoxy	0.36±0.00	5.31
PGPC	0.30±0.17	3.64
PLPC-OOH	0.25±0.04	3.29
SGPC	0.22±0.07	3.28
SONPC	0.22±0.07	1.66
PLPC-OOH	0.11±0.02	1.57
Succinoyl-PC	0.10±0.03	1.53
Acetal-POVPC	0.10±0.01	1.24
PLPC-OH	0.08±0.025	1.14
SLPC-OOH	0.07±0.03	1.03
SAzPC	0.07±0.02	1.01
KDiA-SPC	0.06±0.01	0.87
PLPC-keto	0.05±0.04	0.71
Furylbutanoyl-PC	0.04±0.01	0.71
PAPC-OH	0.04±0.03	0.56
Furyloctanoyl-PC	0.03±0.01	0.46
KDdiA-PC	0.03±0.01	0.45
HDiA-PC	0.03±0.02	0.45
KOHA-PC	0.03±0.02	0.31

KODA-PPC	0.02±0.02	0.30
SLPC-keto	0.02±0.01	0.27
HODA-PPC	0.01±0.01	0.23
HDdiA-PPC	0.01±0.01	0.21
10-OH-5,8,11-tridecatrienoyl-PC	0.01±0.01	0.18
HODA-SPC	0.01±0.00	0.12
isoPG(A2,J2)-SPC	0.00±0.01	0.10
KOdiA-PC	0.01±0.01	0.03
Acetal-PONPC	0.01±0.01	0.01
Acetal-SONPC	0.01±0.00	0.01

Values are means ± SEM. **Abbreviations:** HDdiA-PC: 1-palmitoyl-2-(9-hydroxy-11-carboxyundec-6-enoyl)-sn-glycero3-phosphocholine, HODA-PC: 9-hydroxy-12-oxododec-10-enoic acid ester of 2-lysophosphatidylcholine, isoPG: isoprostanes, KOdiA-PC: 1-palmitoyl-2-(5'-keto-6'-octenedioyl)-sn-glycero-3-phosphocholine, KOHA-PC: 1-palmityl-2-(4-oxo-7-oxohept-5-enoyl)-sn-glycero-3-phosphoserine, KOOA-PC: 1- stearoyl-(5-keto-8-oxo-6-octenoyl)-sn-glycero-3-phosphocholine, KOOA-SPC: 1-palmitoyl-(5-keto-8-oxo-6-octenoyl)-sn-glycero-3-phosphocholine, OH: hydroxyl, OOH: hydroperoxy. PAPC: 1-palmitoyl-2-arachidonoyl-snglycero-3-phosphocholine, PAzPC: 1-palmityl-2-azelayl-sn-glycero-3-phosphocholine, PEIPC: 1-palmitoyl-2-(5,6-epoxyisoprostane E2)-sn-glycero-3-phosphocholine, PGPC: 1-palmitoyl-2-glutaryl-sn-glycero-3-phosphocholine, PLPC: 1-palmitoyl-2-linoleoyl-sn-glycero-3-phosphocholine, PONPC: 1-palmitoyl-2-(9'-oxo-nonanoyl)-sn-glycero-3-phosphocholine, POVPC: 1-palmitoyl-2-(5'-oxo-valeroyl)-sn-glycero-3-phosphocholine , SAPC: 1-stearoyl-2-arachidonoyl-sn-glycero-3-phosphocholine, SAzPC: 1-stearoyl-2-azelaoyl-sn-glycero-3-phosphocholine, SEIPC: 1- stearoyl -2-(5,6-epoxyisoprostane E2)-sn-glycero-3-phosphocholine, SGPC : 1-stearoyl-2-glutaroyl-sn-glycero-3-phosphocholine, SLPC: 1-stearoyl-2-linoleoyl-sn-glycero-3-phosphocholine, SONPC: 1-stearoyl -2-(9-oxo-nonanoyl)-snglycero-3-phosphocholine, SOVPC: sn-1-stearoyl-2-oxovaleroyl-PC.

Fragmented OxPCs were dominant in thrombus, which constituted 77% of total OxPCs. Fifty-four per cent and 23% of all quantified OxPCs were aldo-OxPC and acid-OxPCs, respectively. Non-fragmented OxPCs constituted only 23% of total OxPC levels in thrombus (Figure 22).

Figure 22: Percentage of fragmented and non-fragmented OxPCs to total OxPCs in thrombus, plasma of STEMI patients (during ischemia, reperfusion) and controls

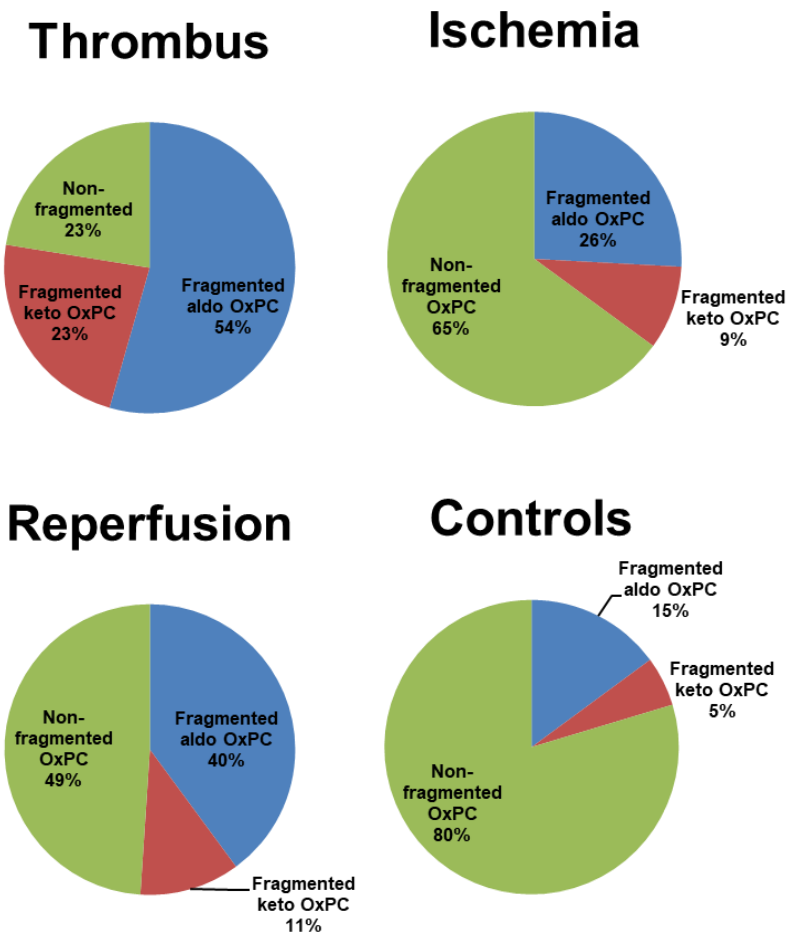

PONPC and POVPC were the two most abundant OxPC in STEMI thrombus, which made 19.8% and 18.4% of total identified OxPC. The percentages of the ten most abundant OxPCs to total OxPCs content of thrombus are compared with plasma levels in Figure 23.

Figure 23: Ten most abundant OxPCs in thrombus and plasma of STEMI patients during ischemia

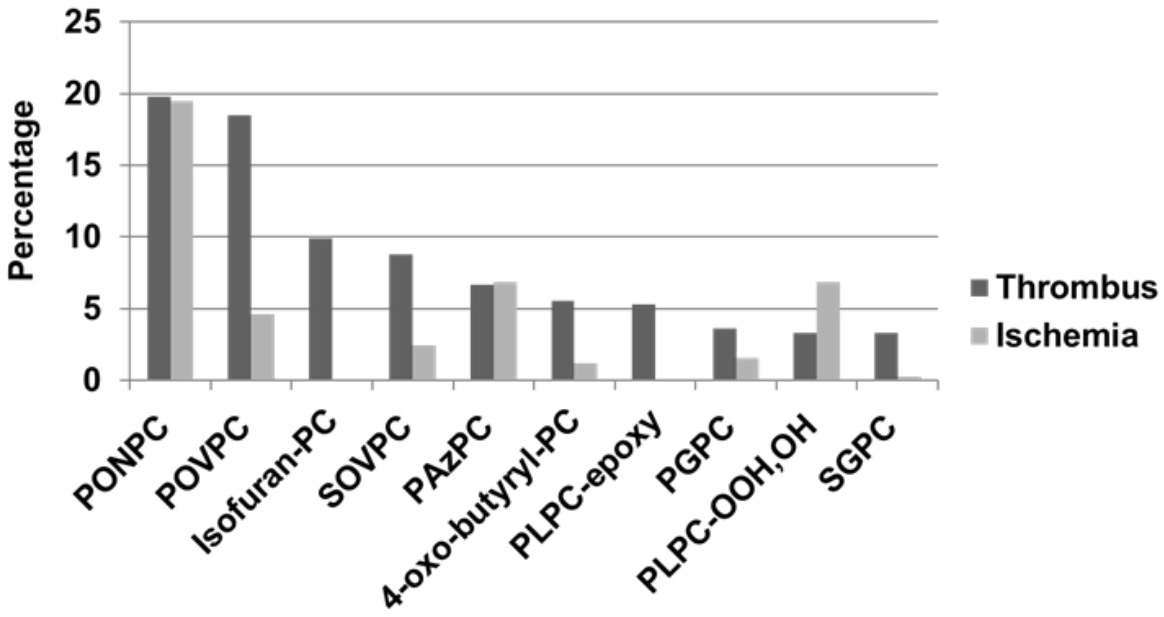

Abbreviations: PGPC: 1-palmitoyl-2-glutaryl-sn-glycero-3-phosphocholine, PLPC: 1-palmitoyl-2-linoleoyl-sn-glycero-3-phosphocholine, POVPC: 1-palmitoyl-2-(5'-oxo-valeroyl)-sn-glycero-3-phosphocholine, SGPC: 1- stearoyl -2-glutaryl-sn-glycero-3-phosphocholine, SOVPC: sn-1-stearoyl-2-oxovaleroyl-PC.

Discussion

There has been increasing evidence that OxPC molecules represent a novel class of bioactive lipids implicated in human pathophysiology (22). In the current study, we conducted a comprehensive analysis of OxPCs in patients presenting with STEMI and followed their OxPC levels in the acute phase and after 30 days post PCI. We were able to identify 22 OxPC species, including fragmented OxPC and non-fragmented hydroxyl/hydroperoxyl/ isoprostane OxPCs in our population. We have shown for the first time that there were increases in plasma levels of fragmented OxPC species during the ischemic episode in STEMI patients compared with controls which decreased during 30 days post-MI. Moreover, the plasma levels of POVPC and PONPC during ischemia were significantly higher in MI patients with higher peak CK levels. They were also significantly correlated with inflammatory cytokines (INF-γ and IL-1β) during I/R.

This study is the most comprehensive assessment of OxPC levels in human plasma. Previously, Stübiger et al., (2012) (23) conducted a targeted lipidomic analysis in plasma of 13 young patients with familial hypercholesterolemia and 7 normolipidemic individuals using LC-ESI-SRM and MALDI-QIT-TOF-MS/MS. Eight fragmented OxPC compounds containing stearyl or palmityl in their sn-1 position were identified and quantified in their population. SOVPC was the dominant OxPC in their study population. Recently, Ademowo (2020) et al,. (24) applied a targeted approach to analyze OxPCs species in plasma of healthy subjects (n=20), patients with chronic kidney disease (CKD) (n=13), patients with periodontitis (n=17) and patients with both CKD and periodontitis (n=20). Using HPLC-MS/MS, they were able to identify 12 fragmented OxPC species derived from PAPC/PLPC or SAPC/SLPC in their population. Moreover, Godzien et al., (2019) (25) used a non-targeted metabolomics approach for OxPC identification in serum of individuals with normal glucose hemostasis (n=57), patients with insulin resistance (n=52), prediabetics (n=49) and diabetic patients (n=40). They were able to identify 21 OxPC species, including 16 non-fragmented and 5 fragmented OxPC. However, only non-fragmented OxPC were quantified, as the levels of fragmented OxPC were below the limit of detection.

To find any potential roles of OxPC in I/R injury, we first compared the levels of OxPC compounds in the plasma of STEMI patients during ischemia with controls. We found that total levels of fragmented OxPCs increased significantly during the ischemic period compared with controls. In a study by Frey et al., (2000) (26), levels of an unknown fragmented OxPC, which was measured

in 5 patients undergoing coronary artery bypass grafting using liquid chromatography (after precolumn derivatization) showed a significant increase after 3h reperfusion compared with baseline values. However, as they did not use a mass spectrometry approach and they were not able to identify the exact structure of the compound in question. Non-fragmented OxPCs, on the other hand, were significantly lower in STEMI patients during ischemia compared with controls but increased gradually during 30-day post-PPCI, although not significantly (Table 13).

The significant elevation of fragmented OxPCs during early I/R (24h after PCI) compared with their levels at 30 days post-PCI can be attributed to enhanced ROS production and an inflammatory response. Acute restoration of blood following reperfusion leads to the formation of ROS as a result of an imbalance between the formation of free radicals and cellular protections against them (27). Both enzymatic (xanthin oxidase and NADPH oxidase) and non-enzymatic oxidations (mitochondrial dysfunction) have been identified during myocardial I/R (28). Enhanced oxidative stress can lead to cardiomyocyte cell death by disturbing cell membrane integrity as a result of pyroptosis, necroptosis and activating mitochondria-mediated apoptosis (29). Moreover, changes in fragmented OxPC concentrations were significantly correlated with the levels of inflammatory cytokines. Higher levels of IFN-γ and IL-1β before and right after PPCI suggested an increase in immune response required for the removal of cardiac dead cells in the acute phase after myocardial infarction (30, 31). Increased IFN-γ during the pre-PPCI can trigger IL-1β to recall innate immune response. At the later time-points 2h until 30 days of Post-PPCI, the reduction in the cytokine concentrations suggested an acquired response to MI following reperfusion (32, 33).

Few studies have assessed the levels of OxPC adducts on apo (B) and plasminogen following I/R in MI patients. In a study by Tsimikas et al,. (2003) (13), serial plasma samples were collected from 8 MI patients at the time of presentation to the hospital and subsequently at 4, 30, 120 and 210 days following MI. In this study, a 54% increase was seen in levels of OxPC on apo(B) measured by E06 antibody following MI, which reached statistical significance at 30 and 210 days following discharge. However, no such differences were observed in patients with stable angina, patients with normal coronary angiograms, and healthy controls during 7-month follow up (13). In our analysis, we measured free forms of OxPC species in plasma, but not the OxPC adducts. OxPC species, particularly fragmented forms, are bioactive and can rapidly interact with plasma proteins (11). Philippova et al., (2019) (34) also suggested that in OxPC analysis, results of HPLC-

MS/MS and immunoassay are related but not duplicates, as they observed weak correlations between free levels of 8 OxPC species measured by HPLC-MS/MS and E06 antibody in plasma of patients that underwent coronary angiography. They suggested that E06 recognizes both free form and covalent adducts of OxPCs which are bound to lipoproteins, cell membranes and other plasma proteins. However, these adducts are not recognizable by the HPLC-MS/MS method. Besides, the E06 antibody binds not only to fragmented OxPC but also to a fraction of non-fragmented OxPCs (15, 35).

We previously showed that fragmented aldo-OxPC, namely POVPC and PONPC enhanced significantly in both *in vitro* and *in vivo* models of I/R (15). Interestingly, in the current study, POVPC, SOVPC, PONPC, and SONPC were significantly elevated during ischemia compared with control. However, their levels reduced following reperfusion in which changes for PONPC and SONPC were statistically significant. It should be mentioned that SOVPC and SONPC have similar chemical structures to POVPC and PONPC; differing only in the stearyl group at the sn-1 position instead of a palmityl group. It's been demonstrated that the active group at the sn-2 position of PL determines the bioactivity of a particular PL (36). Therefore, the active aldehyde group on SOVPC and SONPC can rapidly interact with biomolecules causing tissue injury. We have shown that introducing POVPC and PONPC to cardiomyocytes cell culture activated cell death in a dose-response manner. PONPC was the most potent OxPC, as adding 1, 2, 5, and 10 mM of PONPC resulted in significant cardiomyocyte cell death, but only high concentrations of POVPC (10 mM) induced cell death (15). PONPC and POVPC cause mitochondrial permeability through activation of Bcl-2interacting protein 3 (Bnip3), which has a critical role in cell death during cardiomyocytes I/R injury. Moreover, recent data from our laboratory demonstrated that treatment of cardiomyocytes with 10 μM of POVPC and PONPC for 1h of ischemia and 1h of reperfusion caused cell death (37). In this study, both POVPC and PONPC suppressed glutathione peroxidase-4 (GPX4), an enzyme implicating in ferroptosis. Finally, treatment of cardiomyocyte cells with ferrostatin-1, which is an inhibitor of ferroptosis suppressed cell death induced by OxPCs (37). Previous studies have also shown the beneficial effects of blocking of ferroptosis in myocardial I/R injury (38-41).

In the current study, POVPC and PONPC levels during the ischemic period were significantly associated with higher peak CK levels (Figure 22). Previous studies confirmed that elevated CK

levels are associated with more extensive infarct size (22) and the rate of mortality (42). Furthermore, there were significant correlations between the levels of PONPC and POVPC with INF-γ and IL-1β concentrations during I/R. Both IFN-γ and IL-1β have been shown to mediate inflammation (31, 43). Inhibition of IL-β receptor in STEMI patients improved left ventricular (LV) function with reduced inflammatory markers (44, 45). Also, using IL-1β receptor inhibitors shown that are associated with a reduced rate of recurrent heart failure (HF) episodes (46). Moreover, the E06 antibody can inhibit cell death during I/R through the deactivation of aldo-OxPCs. Introducing E06 at 10 ug/ml concentration in culture prevented POVPC and PONPC-related cardiomyocytes cell death by 74%. Identical results were obtained in an *in vivo* study using transgenic mice that overexpressed single-chain variable fragment of the E06 antibody (E06-scFv-Tg). Infarct size after 60 mins of LAD and 7 days of reperfusion was significantly smaller in E06-mice compared with controls, which was attributed to the interaction of E06 and aldo-OxPCs (15).

Based on the finding of our study, we believe that aldo-OxPCs are mediators of I/R injury. Not only these compounds rise and fall with ischemia and reperfusion, but they are associated with increased CK levels, a marker of total infarct size. However, we did not see any linear correlations between CK and any OxPC species. One possible reason could be due to the activity of lipid-degrading enzymes such as lipoprotein-associated phospholipase A2 (Lp-PLA2), which increases at the early phase of ACS. PLA2 releases oxidized fatty acids in sn-2 positions of OxPCs and convert them to lyso-PC (47). The other reason would be the accumulation of OxPCs at the tissue level, as our previous study showed that OxPCs accumulated in renal tissue during I/R (18). The third reason may be attributed to the high reactivity of aldo-OxPC that can be bound to plasma protein such as apo (B100), lipoprotein (a) and plasminogen, as previous studies confirm the increased levels of these proteins following MI (13, 48).

The second part of the study was carried out to determine the OxPC content of coronary thrombectomy material. This will allow us to see any potential contribution of ruptured plaque material to plasma OxPC levels. In the current study, fragmented OxPCs were dominant in ruptured plaque material as 77% of total OxPCs were fragmented metabolites. Aldo-OxPCs were 2-time higher than acid-OxPCs, and PONPC and POVPC constituted 38.5% of the total identified OxPCs on thrombus. It has been shown that PONPC and POVPC are implicated in foam cell formation through interactions with the cluster determinant 36 (CD36) receptor on macrophages

and increasing OxLDL uptake (49). Our lab has previously shown (50) that iatrogenic plaque disruption can cause the release of oxidized lipids from arterial plaques from carotid, saphenous vein grafts, and renal artery during PCI. The presence of OxPC compounds was assessed by using both immunoassay and HPLC-MS/MS. PONPC and POVPC were the most common compound in iatrogenic plaque, which made up 50% of the identified OxPCs (50). However, only 6 fragmented OxPC species derived from PAPC and PLPC were measured in this study.

An immunohistochemistry study of the stages of plaque from initial fatty streaks to plaque rupture by van Dijk et al., (2012) (51) showed that as the plaque progresses, the composition of oxidized lipid epitopes will change. Coronary artery sections, carotid endarterectomy specimens were obtained from CVD patients who had died suddenly. E06 antibody was used to identify OxPL in atherosclerotic lesions. POVPC, which is bound to E06 antibody, was measured in carotid and saphenous vein graft distal protection devices using HPLC-MS/MS. They found OxPL levels differ significantly as lesions progress from early lesion to plaque rupture. OxPCs, specifically, adducts of POVPC were found in increasing abundance as plaques progressed and were at their highest levels in thin cap fibroatheroma and plaque rupture. The location of POVPC was primarily within the extracellular matrix and infiltrating macrophage components of the fibrotic capsule. Ruptured plaques had an increased level of infiltrating macrophages in comparison to thin cap fibroatheromas.

As it is shown in Figure 22, the OxPC profile of thrombus is different from plasma during I/R. While 77% of total OxPCs is fragmented species in the thrombus, it is only 35% of the total OxPC of plasma during ischemia. The composition of OxPCs in the plasma at the time of STEMI presentation was different from the composition of the coronary thrombus. The thrombus had a higher proportion of POVPC and SOVPC than plasma, although they both have high levels of PONPC (Figure 23). This indicates that plasma OxPCs are not explained by OxPCs eluting out of the thrombus, rather, the thrombus and plasma have different OxPC profiles that cannot be explained by a single common pathway.

The current study has several potential limitations: First, our sample size was relatively small considering the high prevalence of comorbidities and medication use in the STEMI population. However, serial blood sampling helped to lessen inter-individual variability and clinical

confounders. Moreover, due to the small sample size, we were not able to compare the effects of sex, age, ethnicity, etc in our population. Hence, it is important to validate the finding of this study in a relatively larger cohort study. Second, considering there are no available commercial standards for all individual OxPC species, the reported concentrations are relative rather than absolute.

In summary, this study showed that fragmented OxPCs are produced at significantly higher levels during ischemia, which decreased during 30 days after MI. Patients with higher levels of POVPC and PONPC during ischemia had elevated levels of CK, which is a marker of tissue injury following MI. The composition of thrombus and plasma OxPCs are distinct. Therefore, the origin of OxPCs in circulation at the onset of a STEMI is not strictly from the thrombus itself. Therefore, this study supports the hypothesis that OxPCs are produced during I/R and have roles in I/R injury.

Sources of funding: This work was supported by the National Institutes of Health (NIH) and Research Manitoba.

Disclosures: The authors declare no conflict of interest

References

1. Ladapo JA, Goldfeld KS, Douglas PS. Projected morbidity and mortality from missed diagnoses of coronary artery disease in the United States. International journal of cardiology. 2015;195:250-2.
2. Moens A, Claeys M, Timmermans J, Vrints C. Myocardial ischemia/reperfusion-injury, a clinical view on a complex pathophysiological process. International journal of cardiology. 2005;100(2):179-90.
3. Fröhlich GM, Meier P, White SK, Yellon DM, Hausenloy DJ. Myocardial reperfusion injury: looking beyond primary PCI. European heart journal. 2013;34(23):1714-22.
4. Lambert L, Brown K, Segal E, Brophy J, Rodes-Cabau J, Bogaty P. Association between timeliness of reperfusion therapy and clinical outcomes in ST-elevation myocardial infarction. Jama. 2010;303(21):2148-55.
5. Moens AL, Claeys MJ, Timmermans JP, Vrints CJ. Myocardial ischemia/reperfusion-injury, a clinical view on a complex pathophysiological process. International Journal of Cardiology. 2005;100(2):179-90.
6. Yellon DM, Hausenloy DJ. Myocardial reperfusion injury. New England Journal of Medicine. 2007;357(11):1121-35.
7. Solati Z, Ravandi A. Lipidomics of bioactive lipids in acute coronary syndromes. International journal of molecular sciences. 2019;20(5):1051.
8. Gargalovic PS, Imura M, Zhang B, Gharavi NM, Clark MJ, Pagnon J, et al. Identification of inflammatory gene modules based on variations of human endothelial cell responses to oxidized lipids. Proceedings of the National Academy of Sciences. 2006;103(34):12741-6.
9. Taleb A, Witztum JL, Tsimikas S. Oxidized phospholipids on apoB-100-containing lipoproteins: a biomarker predicting cardiovascular disease and cardiovascular events. Biomarkers in medicine. 2011;5(5):673-94.
10. Miller YI, Tsimikas S. Oxidation-specific epitopes as targets for biotheranostic applications in humans: biomarkers, molecular imaging and therapeutics. Current opinion in lipidology. 2013;24(5):426.
11. Binder CJ, Papac-Milicevic N, Witztum JL. Innate sensing of oxidation-specific epitopes in health and disease. Nature Reviews Immunology. 2016;16(8):485.
12. Bochkov V, Gesslbauer B, Mauerhofer C, Philippova M, Erne P, Oskolkova OV. Pleiotropic effects of oxidized phospholipids. Free Radical Biology and Medicine. 2017;111:6-24.
13. Tsimikas S, Bergmark C, Beyer RW, Patel R, Pattison J, Miller E, et al. Temporal increases in plasma markers of oxidized low-density lipoprotein strongly reflect the presence of acute coronary syndromes. Journal of the American College of Cardiology. 2003;41(3):360-70.
14. Tsimikas S, Lau HK, Han K-R, Shortal B, Miller ER, Segev A, et al. Percutaneous coronary intervention results in acute increases in oxidized phospholipids and lipoprotein (a) short-term and long-term immunologic responses to oxidized low-density lipoprotein. Circulation. 2004;109(25):3164-70.
15. Yeang C, Hasanally D, Que X, Hung MY, Stamenkovic A, Chan D, et al. Reduction of myocardial ischaemia-reperfusion injury by inactivating oxidized phospholipids. Cardiovasc Res. 2019;115(1):179-89.
16. Floch J. A simple method for the isolation and purification of total lipids from animal tissues. J biol Chem. 1957;226:497-509.
17. Ulmer CZ, Jones CM, Yost RA, Garrett TJ, Bowden JA. Optimization of Folch, Bligh-Dyer, and Matyash sample-to-extraction solvent ratios for human plasma-based lipidomics studies. Analytica chimica acta. 2018;1037:351-7.
18. Solati Z, Edel AL, Shang Y, O K, Ravandi A. Oxidized phosphatidylcholines are produced in renal ischemia reperfusion injury. PloS one. 2018;13(4):e0195172.
19. Gruber F, Bicker W, Oskolkova OV, Tschachler E, Bochkov VN. A simplified procedure for semi-targeted lipidomic analysis of oxidized phosphatidylcholines induced by UVA irradiation. Journal of lipid research. 2012;53(6):1232-42.

20. Marchese RD, Puchalski D, Miller P, Antonello J, Hammond O, Green T, et al. Optimization and validation of a multiplex, electrochemiluminescence-based detection assay for the quantitation of immunoglobulin G serotype-specific antipneumococcal antibodies in human serum. Clinical and Vaccine Immunology. 2009;16(3):387-96.
21. Blomberg DJ, Kimber WD, Burke MD. Creatine kinase isoenzymes: Predictive value in the early diagnosis of acute myocardial infarction. The American journal of medicine. 1975;59(4):464-9.
22. Stamenkovic A, Pierce GN, Ravandi A. Oxidized lipids: not just another brick in the wall. Canadian journal of physiology and pharmacology. 2019;97(6):473-85.
23. Stübiger G, Aldover-Macasaet E, Bicker W, Sobal G, Willfort-Ehringer A, Pock K, et al. Targeted profiling of atherogenic phospholipids in human plasma and lipoproteins of hyperlipidemic patients using MALDI-QIT-TOF-MS/MS. Atherosclerosis. 2012;224(1):177-86.
24. Ademowo OS, Sharma P, Cockwell P, Reis A, Chapple IL, Griffiths HR, et al. Distribution of plasma oxidised phosphatidylcholines in chronic kidney disease and periodontitis as a co-morbidity. Free Radical Biology and Medicine. 2020;146:130-8.
25. Godzien J, Kalaska B, Adamska-Patruno E, Siroka J, Ciborowski M, Kretowski A, et al. Oxidized glycerophosphatidylcholines in diabetes through non-targeted metabolomics: Their annotation and biological meaning. Journal of Chromatography B. 2019;1120:62-70.
26. Frey B, Haupt R, Alms S, Holzmann G, König T, Kern H, et al. Increase in fragmented phosphatidylcholine in blood plasma by oxidative stress. Journal of lipid research. 2000;41(7):1145-53.
27. Sinning C, Westermann D, Clemmensen P. Oxidative stress in ischemia and reperfusion: current concepts, novel ideas and future perspectives. Biomarkers in medicine. 2017;11(11):11031-1040.
28. Granger DN, Kvietys PR. Reperfusion injury and reactive oxygen species: The evolution of a concept. Redox Biology. 2015;6:524-51.
29. Mishra PK, Adameova A, Hill JA, Baines CP, Kang PM, Downey JM, et al. Guidelines for evaluating myocardial cell death. American Journal of Physiology-Heart and Circulatory Physiology. 2019;317(5):H891-H922.
30. Zimmer A, Bagchi AK, Vinayak K, Bello-Klein A, Singal PK. Innate immune response in the pathogenesis of heart failure in survivors of myocardial infarction. American Journal of Physiology-Heart and Circulatory Physiology. 2019;316(3):H435-H45.
31. Finger S, Knorr M, Molitor M, Schüler R, Garlapati V, Waisman A, et al. A sequential interferon gamma directed chemotactic cellular immune response determines survival and cardiac function post-myocardial infarction. Cardiovascular Research. 2019;115(13):1907-17.
32. Sardella G, De Luca L, Francavilla V, Accapezzato D, Di Roma A, Gianoglio O, et al. Effect of Coronary Percutaneous Revascularization on Interferon-γ and Interleukin-10 Producing CD4+ T Cells during Acute Myocardial Infarction. International Journal of Immunopathology and Pharmacology. 2007;20(4):791-9.
33. Hoyer FF, Nahrendorf M. Interferon-γ regulates cardiac myeloid cells in myocardial infarction. Oxford University Press; 2019.
34. Philippova M, Oskolkova OV, Bochkov VN. OxPLs-Masking/Degradation Immune Assay: An "All-Included" Analysis of Mechanisms Detoxifying Oxidized Phospholipids. European Journal of Lipid Science and Technology. 2019:1800511.
35. Friedman P, Hörkkö S, Steinberg D, Witztum JL, Dennis EA. Correlation of Antiphospholipid Antibody Recognition with the Structure of Synthetic Oxidized Phospholipids: Importance of Schiff Base Formation and Aldol Condensation. Journal of Biological Chemistry. 2002;277(9):7010-20.
36. Subbanagounder G, Leitinger N, Schwenke DC, Wong JW, Lee H, Rizza C, et al. Determinants of bioactivity of oxidized phospholipids: specific oxidized fatty acyl groups at the sn-2 position. Arteriosclerosis, thrombosis, and vascular biology. 2000;20(10):2248-54.
37. Stamenkovic A, O'Hara KA, Nelson DC, et al. Oxidized phosphatidylcholines trigger ferroptosis in cardiomyocytes during ischemia-reperfusion injury. American Journal of Physiology-Heart and Circulatory Physiology. 2021;320(3):H1170-H1184.

38. Gao M, Monian P, Quadri N, Ramasamy R, Jiang X. Glutaminolysis and transferrin regulate ferroptosis. Molecular cell. 2015;59(2):298-308.
39. Aoyagi T, Kusakari Y, Xiao CY, et al. Cardiac mTOR protects the heart against ischemia-reperfusion injury. Am J Physiol Heart Circ Physiol. Jul 2012;303(1):H75-85. doi:10.1152/ajpheart.00241.2012
40. Baba Y, Higa JK, Shimada BK, et al. Protective effects of the mechanistic target of rapamycin against excess iron and ferroptosis in cardiomyocytes. American Journal of Physiology-Heart and Circulatory Physiology. 2018;314(3):H659-H668.
41. Fang X, Wang H, Han D, et al. Ferroptosis as a target for protection against cardiomyopathy. Proc Natl Acad Sci U S A. Feb 12 2019;116(7):2672-2680. doi:10.1073/pnas.1821022116
42. Jeremias A, Baim DS, Ho KK, et al. Differential mortality risk of postprocedural creatine kinase-MB elevation following successful versus unsuccessful stent procedures. Journal of the American College of Cardiology. 2004;44(6):1210-1214.
43. Hoyer FF, Nahrendorf M. Interferon-γ regulates cardiac myeloid cells in myocardial infarction. Cardiovasc Res. 2019;115(13):1815-1816. doi:10.1093/cvr/cvz143
44. Silvain J, Kerneis M, Zeitouni M, et al. Interleukin-1β and risk of premature death in patients with myocardial infarction. Journal of the American College of Cardiology. 2020;76(15):1763-1773.
45. Abbate A, Van Tassell BW, Biondi-Zoccai G, et al. Effects of interleukin-1 blockade with anakinra on adverse cardiac remodeling and heart failure after acute myocardial infarction [from the Virginia Commonwealth University-Anakinra Remodeling Trial (2)(VCU-ART2) pilot study]. The American journal of cardiology. 2013;111(10):1394-1400.
46. Harouki N, Nicol L, Remy-Jouet I, et al. The IL-1β antibody gevokizumab limits cardiac remodeling and coronary dysfunction in rats with heart failure. JACC: Basic to Translational Science. 2017;2(4):418-430.
47. Li J, Wang H, Tian J, Chen B, Du F. Change in lipoprotein-associated phospholipase A2 and its association with cardiovascular outcomes in patients with acute coronary syndrome. Medicine (Baltimore). 2018;97(28):e11517-e11517. doi:10.1097/MD.0000000000011517
48. Leibundgut G, Arai K, Orsoni A, et al. Oxidized phospholipids are present on plasminogen, affect fibrinolysis, and increase following acute myocardial infarction. Journal of the American College of Cardiology. 2012;59(16):1426-1437.
49. Podrez EA, Byzova TV, Febbraio M, et al. Platelet CD36 links hyperlipidemia, oxidant stress and a prothrombotic phenotype. Nature medicine. 2007;13(9):1086-1095.
50. Ravandi A, Leibundgut G, Hung M-Y, et al. Release and capture of bioactive oxidized phospholipids and oxidized cholesteryl esters during percutaneous coronary and peripheral arterial interventions in humans. Journal of the American College of Cardiology. 2014;63(19):1961-1971.
51. Van Dijk RA, Kolodgie F, Ravandi A, et al. Differential expression of oxidation-specific epitopes and apolipoprotein (a) in progressing and ruptured human coronary and carotid atherosclerotic lesions. Journal of lipid research. 2012;53(12):2773-2790.

iii: Role of oxylipins in a clinical setting myocardial of I/R

Previous studies have shown that membrane enzymes, such as PLA2, can be activated during I/R. Subsequently, FAs liberated from membrane PLs can enter the enzymatic oxidative pathways and generate oxidized metabolites called oxylipins. Oxylipins, particularly n-6 derived compounds, can initiate inflammation, change ion channel functions, alter transcriptional programming, and cause ventricular remodeling, which can all contribute to I/R injury. However, if oxylipins are involved in myocardial I/R injury is unknown. Therefore, the current objectives of the following study include:

To examine how myocardial I/R affects the plasma oxylipin profile in STEMI patients.

To investigate which groups of oxylipins are mostly affected by myocardial I/R.

To observe if changes in plasma oxylipins concentrations correlate with markers of I/R injury.

We hypothesized that oxylipin metabolites increase during I/R and n-6 derived metabolites are correlated with markers of myocardial injury.

Oxylipin profile alterations in acute ST-segment Elevation Myocardial Infarction (STEMI): role of oxylipins in I/R injury

Zahra Solati[1,2], Arun Surendran[1,2], Ashim K Bagchi[2], Pawan K Singal[2], Harold M Aukema[3], and Amir Ravandi[1,2]

[1]Cardiovascular Lipidomics Laboratory, St. Boniface Hospital, Albrechtsen Research Centre,

[2]Department of Physiology and Pathophysiology, Rady Faculty of Health Sciences, University of Manitoba,

[3]Department of Food and Human Nutritional Sciences, University of Manitoba

Abstract

Objective: The goal of this study was to assess alterations in the plasma oxylipin profile of patients presenting with ST-segment Elevation Myocardial Infarction (STEMI) during ischemia/reperfusion (I/R) to identify clinically relevant oxylipins that play roles in I/R injury.

Method: Blood samples were collected from STEMI patients prior to primary PCI (PPCI) (Isch group) and at 4-time points following reperfusion, including 2h (R-2h), 24h (R-24h), 48h (R-48h) and 30-day (R-30d). As controls, blood samples were collected from age and sex-matched patients with non-obstructive coronary artery disease after diagnostic coronary angiography. High-performance lipid chromatography-mass spectrometry (HPLC-MS/MS) was used to identify and quantify oxylipins.

Results: On average, 57 oxylipin metabolites were quantified in the plasma of STEMI patients during 5-time points of I/R. Linoleic acid (LA)-derived oxylipins were the dominant metabolites which constituted 47%, 39% and 53% of all quantified oxylipins in STEMI patient during ischemia, reperfusion and controls, respectively. 20-carboxy-arachidonic acid (20-COOH-AA), 9- and 13- hydroxyoctadecadienoic acid (HODE) were the three most abundant oxylipins in the plasma of our participants. During ischemia, total plasma levels of oxylipins did not significantly differ between Isch and control groups (Isch: 200.87±16.00, Control:163.19±8.9 nM). However, docosahexaenoic acid (DHA)-derived oxylipins were significantly elevated in the Isch group compared with controls (Isch: 14.23±1.4, Control: 6.79±0.9 nM, $p<0.001$). Moreover, their ischemic levels were significantly correlated with the peak of creatine kinase (CK) and troponin T(TnT) (CK: $r=0.33$, $p<0.05$, TnT: $r=0.50$, $p<0.001$). Oxylipins were then categorized based on the generation pathway. Total concentrations of metabolites generated through 5-LOX and 15-LOX pathways were significantly elevated in the Isch group compared with controls (5-LOX: Isch=8.48±1.35, Control: 2.37±0.40 nM, $p<0.05$) (15-LOX: Isch: 13.28±1.66, Control: 6.92±0.72, $p<0.05$). However, total concentrations of the oxylipins produced through the 12-LOX pathway did not significantly differ between Isch and control groups (12-LOX: Isch: 2.66±0.52, Control: 1.89±0.45 nM). Total plasma levels of oxylipins produced through the CYP ω-hydroxylase (CYP450-h) pathway were also significantly elevated in the Isch group compared with controls (Isch: 63.06±7.69, Control: 39.50±27.04 nM, $p<0.05$). The ratio of epoxides (generated by

CYP450 epoxygenases (CYP450-e)) to diols (generated by soluble epoxide hydrolase (sEH)) were significantly lower in the Isch group compared with controls (Isch: 0.2±0.02, Control: 0.4±0.02, $p<0.001$). Following reperfusion, total oxylipin levels decreased significantly in STEMI patients (Isch: 118.72±12.19, R-2h: 98.40±9.2, R-24h: 62.84±6.48, R-48h: 61.33±6.18, and R-30d: 55.10±4.55 nM, $p<0.05$). Levels of the inflammatory markers, namely, tumour necrosis factor-α (TNF-α) and macrophage inflammatory protein-1α (MIP-1α) also experienced significant reductions post-PCI (TNF-α: Isch: 8.98±0.86, R-2h: 9.02±0.79, R-24h: 5.70±0.42, R-48h: 6.28±0.48, and R-30d: 7.66±0.72 pg/ml, $p<0.05$) (MIP-1α: Isch: 36.41±5.44, R-2h: 31.21±4.57, R-24h: 19.17±3.01, R-48h: 24.49±4.40, and R-30d: 24.25±4.64 pg/ml, $p<0.05$). Similar reduction trends were observed for total levels of 5-LOX and 12-LOX pathways post-PCI ($p<0.05$). However, total concentrations of 15-LOX and CYP450-h pathways did not differ significantly after PCI. Looking at individual compounds revealed that 17-Keto DHA, 17 Keto-docosapentaenoic acid (DPA) and 20-COOH-AA were the metabolites produced through these pathways that remained elevated for 30 days following-MI. This may reflect the increased activity of the dehydrogenase enzymes following MI. The ratio of epoxides to diols generated through n-6 fatty acids (FA) decreased significantly during 30 days post-reperfusion (Isch: 0.36±0.03, R-2h: 0.42±0.02, R-24h: 0.29±0.03, R-48h: 0.32±0.03, and R-30d: 0.21±0.04, $p<0.001$). Univariate receiver operating characteristic (ROC) curve analysis, which identifies potential biomarkers based on the area under the curve (AUC) showed that elevated ratio of epoxides to diols during the ischemia could be considered as a potential marker of having a smaller infarct size with AUC= 0.77 ($p=0.03$) based on CK and AUC=0.76 ($p=0.054$) based on TnT levels.

Conclusion: This study revealed significant alterations in the oxylipin profile of STEMI patients during I/R. Increasing levels of DHA-derived oxylipins and modulation of sEH enzyme activity during I/R could be proposed as potential treatment targets to decrease cardiac I/R injury.

Introduction

Myocardial infarction (MI) remains the leading cause of death worldwide (1). It is defined as myocardial cell death that occurs as a result of an acute ischemic event due to plaque rupture and thrombosis (2). According to the American Heart Association (AHA), every 40 seconds one American has an MI (3).

Timely reperfusion, using percutaneous coronary intervention (PCI), is considered as the main treatment option to survive myocardial cell after an ischemic event in patients with ST-Elevation Myocardial Infarction (STEMI) (1). However, reversible and irreversible damage can occur during both ischemia and reperfusion periods, which is referred to as ischemia/reperfusion (I/R) injury. I/R injury is thought to be responsible for 50% of the final infarct size (1). Several mechanisms have been proposed for I/R injury. Lack of oxygen during ischemia results in nutrient deprivation, metabolic acidosis, hyperkalemia, and calcium overload (4). Abrupt oxygen introduction following reperfusion leads to the formation of reactive oxygen species (ROS), as a consequence of antioxidant defence impairment. This results in endothelial dysfunction, DNA damage, activation of inflammatory responses and eventually cell death (5).

Membrane enzymes, such as phospholipase A2 (PLA2), are activated during I/R. PLA2 releases polyunsaturated fatty acids (PUFAs) from the sn-2 positions of membrane phospholipids (PL) (6). Released fatty acids (FA) can be further oxidized through three main enzymatic pathways including cyclooxygenase (COX), lipoxygenase (LOX), and cytochrome P450 (CYP450). Various forms of oxidized lipids are produced through these oxidative pathways. Peroxides are generated through the COX pathway, whereas hydroperoxides are produced through the LOX pathway. CYP450 epoxygenases (CYP-e) produce epoxides, which can be further metabolized to diols by the soluble epoxide hydrolase (sEH) enzyme. CYP450 ω-hydroxylases (CYP-h) catalyze the addition of a hydroxyl residue to a FA substrate (7).

The biological effects of oxylipins depend not only on the oxidative pathway that they were made through but also on the FA precursors. Oxylipins derived from n-6 PUFA, such as arachidonic acids (AA) and linoleic acids (LA) can initiate inflammation, change ion channels functions, alter transcriptional programming, and cause ventricular remodelling, which can all contribute to I/R injury (8). However, evidence from experimental and clinical studies showed that oxylipins

derived from n-3 PUFA have anti-inflammatory, anti-arrhythmic and cardio-protective properties (9). Previous studies have examined the roles of oxylipins in I/R injury (10, 11). However, a comprehensive analysis of the oxylipin profile in STEMI patients has not been well studied yet.

Previous studies have shown the role of inflammatory markers, such as tumour necrosis factor-α (TNF-α) and macrophage inflammatory protein-1α (MIP-1α) in myocardial dysfunction and remodelling after MI (12). On the other hand, anti-inflammatory markers, namely, interleukin-10 (IL-10) have significant impacts on modulating I/R injury through mitigating deleterious effects of inflammatory cytokines (13) and stimulating endogenous tissue repair pathways (14). However, how changes in cytokine levels can affect oxylipin profiles following MI has yet to be known.

Hence, this study aimed to investigate alterations in oxylipin profiles of STEMI patients during ischemia and various time points of reperfusion and how these changes are associated with cytokine inflammatory response.

Materials and Methods

Study participants: Blood samples were collected by venipuncture from STEMI patients at various time points of I/R: at presentation to St. Boniface cardiac catheterization labs before primary PCI (Isch) (n=45), which is considered the ischemic period. Samples were taken at 2 hrs following successful reperfusion by PCI (R-2h) (n=42), at 24h (R-24h) (n=44), at 48h (R-48h) (n=43) and then 30 days post PCI (R-30d) (n=29). All samples were collected in EDTA venipuncture tubes, centrifuged at 3000 rpm for 10 minutes, and were kept at -80℃ freezer until analysis. All patients aged above 18 years and had STEMI on 12 lead ECG, presented with chest pain, and had occluded coronary artery at baseline diagnosed by coronary angiography. Age and sex-matched controls were recruited from patients who were referred for coronary angiography but did not have any evidence of coronary disease. We collected blood samples from control patients following angiography (n=44). The study was approved by the University of Manitoba and the St. Boniface Hospital Research ethics boards.

Oxylipin Analysis

As mentioned before, the blood sample was centrifuged at 4°C to isolate the plasma and stored at -80°C. A hundred and fifty µl of plasma sample was used for oxylipin extraction. An established

solid-phase extraction technique was employed to extract plasma oxylipins. Extracted samples were analyzed by HPLC-MS/MS (AB SCIEX 4000 QTRAP) and multiple-reaction monitoring (MRM) as previously described (15, 16). Details of the deuterated internal standards, collision-induced dissociation mass transitions, retention times, detector response factors, the lower/upper limit of detection for analytes can be found in Table 15. The quantification limit was set at 5 levels above the background. Quantification of oxylipins was determined using the stable isotope dilution method (17) and expressed as nanomolar (nM).

Table 15: List of oxylipin compounds that were quantified in plasma of study participants by reversed-phase HPLC-MS/MS

Analyte	Pathway	Fatty Acid	Q1 Mass (Da)	Q3 Mass (da)	Internal standard name	Retention time (min)	Response factor	LLOD in 100ul (ng/ul)	ULOD in 100ul (ng/ul)
PGD2	COX	AA	351	271	(d4) PGD2.IS	7.91	2.28045	0.003	22.22
PGE2	COX	AA	351	271	(d4) PGE2.IS	7.59	8.68273	0.003	22.22
5-HETE	LOX	AA	319	115	(d8) 5-HETE.IS	17.13	0.90038	0.0002	22.22
5-oxoETE	LOX	AA	317	203	(d7) 5-oxoETE.IS	17.5	1.04473	0.0002	22.22
8-HETE	LOX	AA	319	155	(d8) 5-HETE.IS	16.66	1.24638	0.0009	22.22
9-HETE	LOX	AA	319	123	(d8) 5-HETE.IS	16.8	0.29958	0.003	22.22
11-HETE	LOX	AA	319	167	(d8) 12-HETE.IS	16.39	7.67408	0.0009	22.22
12-HETE	LOX	AA	319	135	(d8) 12-HETE.IS	16.56	0.15621	0.003	22.22
12-oxoETE	LOX	AA	317	153	(d7) 5-oxoETE.IS	16.54	0.12689	0.04	22.22
tetranor-12-HETE	LOX	AA	265	109	(d8) 12-HETE.IS	13.29	2.40204	0.0002	22.22
15-HETE	LOX	AA	319	175	(d8) 15-HETE.IS	16.05	0.85626	0.003	22.22
15-oxoETE	LOX	AA	317	113	(d7) 5-oxoETE.IS	16.11	3.26434	0.0002	22.22
9-HOTrE	LOX	ALA	293	171	(d4) 9-HODE.IS	14.46	1.50163	0.003	22.22
9-oxoOTrE	LOX	ALA	291	185	(d7) 5-oxoETE.IS	14.96	2.2951	0.0002	22.22
13-HOTrE	LOX	ALA	293	195	(d4) 13-HODE.IS	14.6	1.15092	0.003	22.22
5-HEPE	LOX	EPA	317	115	(d8) 5-HETE.IS	15.79	0.68513	0.003	22.22
12-HEPE	LOX	EPA	317	179	(d8) 12-HETE.IS	15.32	1.73582	0.003	22.22
15-HEPE	LOX	EPA	317	219	(d8) 15-HETE.IS	14.98	1.56695	0.148	22.22
4-HDoHE	LOX	DHA	343	101	(d8) 5-HETE.IS	17.32	0.39766	0.003	22.22
7-HDoHE	LOX	DHA	343	141	(d8) 5-HETE.IS	16.66	0.51513	0.0009	22.22
8-HDoHE	LOX	DHA	343	109	(d8) 5-HETE.IS	16.73	0.25003	0.003	22.22
10-HDoHE	LOX	DHA	343	153	(d8) 12-HETE.IS	16.35	1.68431	0.0002	22.22
14-HDoHE	LOX	DHA	343	205	(d8) 15-HETE.IS	16.29	0.78401	0.003	22.22
16-HDoHE	LOX	DHA	343	233	(d8) 15-HETE.IS	15.97	3.11823	0.0009	22.22

17-HDoHE	LOX	DHA	343	245	(d8) 15-HETE.IS	16.03	0.2437	0.042	22.22
17keto-DHA	LOX	DHA	341	297	(d7) 5-oxoETE.IS	16.28	0.11372	0.042	22.22
11-HDoHE	LOX/non-enz	DHA	343	149	(d8) 12-HETE.IS	16.48	0.88676	0.003	22.22
13-HDoHE	LOX/non-enz	DHA	343	221	(d8) 12-HETE.IS	16.17	0.50603	0.003	22.22
17-Keto DPA	LOX	DPA	343	247	(d7) 5-oxoETE.IS	16.86	0.1154	0.012	22.22
9-HODE	LOX	LA	295	171	(d4) 9-HODE.IS	15.93	1.33961	0.0002	22.22
9-oxoODE	LOX	LA	293	185	(d7) 5-oxoETE.IS	16.26	0.95769	0.012	22.22
13-HODE	LOX	LA	295	195	(d4) 13-HODE.IS	15.78	3.34877	0.0002	22.22
13-oxoODE	LOX	LA	293	167	(d7) 5-oxoETE.IS	15.95	0.65942	0.012	22.22
9,10,13-triHOME	LOX/CYP-e	LA	329	171	(d4) 9,10 diHOME.IS	7.44	39.48725	0.0002	22.22
9,12,13-triHOME	LOX/CYP-e	LA	329	211	(d4) 12,13 diHOME.IS	7.38	61.41712	0.0002	22.22
13-HOTrE-γ	LOX	GLA	293	193	(d4) 13-HODE.IS	14.88	3.26494	0.0034	22.22
8-HETrE	LOX	DGLA	321	157	(d8) 5-HETE.IS	17.07	1.87458	0.0009	22.22
15-HETrE	LOX	DGLA	321	221	(d8) 15-HETE.IS	16.7	3.79631	0.0009	22.22
5,6-DiHETrE	CYP-e	AA	337	145	(d11) 8,9 DiHETrE.IS	15.55	1.78532	0.0034	22.22
8,9-DiHETrE	CYP-e	AA	337	127	(d11) 8,9 DiHETrE.IS	14.85	1.77545	0.0034	22.22
11,12-DiHETrE	CYP-e	AA	337	167	(d11) 11,12 DiHETrE.IS	14.27	9.12136	0.0034	22.22
14,15-DiHETrE	CYP-e	AA	337	207	(d11) 14,15 DiHETrE.IS	13.56	8.93326	0.00028	22.22
12,13-EpODE	CYP-e	ALA	293	183	(d4) 12,13 diHOME.IS	16.17	21.70636	0.0009	22.22
12,13-diHODE	CYP-e	ALA	311	183	(d4) 12,13 diHOME.IS	11.24	34.86462	0.00028	22.22
16,17-DiHoDPE	CYP-e	DHA	361	233	(d11) 14,15 DiHETrE.IS	13.93	6.23301	0.00098	22.22
19,20-EpDoPE	CYP-e	DHA	343	241	(d11) 14,15 DiHETrE.IS	16.87	1.10022	0.012	22.22
19,20-DiHDoPE	CYP-e	DHA	361	229	(d11) 14,15 DiHETrE.IS	13.35	0.91613	0.012	22.22
9,10-EpOME	CYP-e	LA	295	171	(d4) 9,10 diHOME.IS	17.35	37.33091	0.0009	22.22
9,10-diHOME	CYP-e	LA	313	201	(d4) 9,10 diHOME.IS	13.24	79.72576	0.0009	22.22
12,13-EpOME	CYP-e	LA	295	195	(d4) 12,13 diHOME.IS	17.17	22.85861	0.0034	22.22
12,13-diHOME	CYP-e	LA	313	183	(d4) 12,13 diHOME.IS	12.71	34.6768	0.00028	22.22
16-HETE	CYP-h	AA	319	189	(d8) 15-HETE.IS	15.5	0.72228	0.0009	22.22
17-HETE	CYP-h	AA	319	247	(d8) 15-HETE.IS	15.4	2.73902	0.0034	22.22
18-HETE	CYP-h	AA	319	261	(d6) 20-HETE.IS	15.26	2.58404	0.0034	22.22
19-HETE	CYP-h	AA	319	231	(d6) 20-HETE.IS	14.88	0.17759	0.148	22.22
20-HETE	CYP-h	AA	319	245	(d6) 20-HETE.IS	15.01	0.32666	0.0034	22.22
20-COOH-AA	CYP-h	AA	333	271	(d5) EPA.IS	14.41	0.64699	0.012	22.22
18-HEPE	CYP-h	EPA	317	215	(d8) 15-HETE.IS	14.49	1.1901	0.003	22.22
20-HDoHE	CYP-h	DHA	343	241	(d6) 20-HETE.IS	15.7	0.8816	0.012	22.22

Abbreviations: AA: Arachidonic acid, ALA: Alpha linoleic acid, COX: Cyclooxygenase, CYP-e: Cytochrome P450 epoxygenase, CYP-h: Cytochrome P450 hydroxylase, DGLA: Dihemo gamma-linoleic acid, DHA: Docosahexaenoic acid, DiHDPE: Dihydroxydocosapentaenoic acid, DiHETE: Dihydroxyeicosatetraenoic acid, DiHETrE: Dihydroxy-eicosatrienoic acid, DPA: Docosapentaenoic acid, EPA: Eicosapentaenoic acid, EpDPE: Epoxydocosapentaenoic acid, EpODE: Epoxy-octadecadienoic acid, EpOME: Epoxy-octadecenoic acid, GLA: Gamma linolenic acid, HDoHE: Hydroxy-docosahexaenoic acid, HEPE: Hydroxyeicosapentaenoic acid, HETE: Hydroxyeicosatetraenoic acid, HETrE: Hydroxyeicosatrienoic acid, HODE: Hydroxyoctadecadienoic acid, HOTrE: Hydroxy-octadecatrienoic acid, LA: Linoleic acid, LLOD: Lower limit of detection, LOX: Lipoxygenase, MPO: Myeloperoxidase, non-enz: Non-enzymatic oxidation, Oxo-ETE: Oxo-eicosatetraenoic acid, OxoODE: Oxo-octadecadienoic acid, OxoOTrE: Oxo-octadecatrienoic acid, PG: Prostaglandin, TriHOME: Trihydroxy-octadecenoic acid,ULOD: Upper limit of detection.

Cytokine Analysis

Levels of 10 cytokines/chemokines were measured in STEMI patients during I/R using Mesoscale Discovery (MSD) ELISA protocol and read on MSD sector imager (18). Any sample below the detection limit of < 0.01 pg/ml for a given cytokine was excluded from the study.

Statistical Analysis

Data were analyzed using Origin (version 17, USA). One way analysis of variance (ANOVA) with a post-hoc Tukey test for multiple comparisons was used to determine statistical significance between study groups. Associations between specific oxidized metabolites and cytokine/chemokine levels were assessed by applying Pearson Correlations. Receiver operating characteristic (ROC) analysis was used to evaluate the diagnostic capability of oxylipins that can be considered as potential biomarkers. All data are presented as mean ± SEM. *P*-value <0.05 was considered a statistically significant level.

Results

Characteristics of controls and STEMI patients along with laboratory data, and cardiac injury markers, including creatine kinase (CK) and high sensitivity troponin (TnT), are presented in Table 11. In this study, 66.6% of the STEMI population and 56.3% of the controls were male (p=0.08). The mean age was 65.2±2.08 in the STEMI population and 60.2±1.49 in controls (p=0.06). The average body mass index (BMI) was significantly different between STEMI and controls populations (25.8±1.14 and 30.2±1.05, respectively) (p=0.008). Based on the laboratory data, the STEMI patients had normal triglycerides (TG), cholesterol (TC), low and high-density lipoprotein (LDL and HDL). There were no significant differences regarding angiotensin-converting enzyme

inhibitors/angiotensin-receptor blockers (ACEI/ARB), beta-blockers and statins use between STEMI and control groups (Table 11). The median ischemic period (from the onset of chest pain to reperfusion) was 150 min. Fifty% of participants had a right coronary artery (RCA) infarct, whereas 41.6% and 8% had left anterior descending coronary artery (LAD) and circumflex coronary artery occlusions, respectively. The prevalence of type 2 diabetes (20.8%), hypertension (41.6%), and dyslipidemia (41.6%) at presentation to the hospital were not significantly different in STEMI patients compared with controls (Table 11).

Plasma oxylipin levels in STEMI patient and controls

Sixty oxylipins were present at quantifiable levels in the plasma of controls: 53% and 31% of these were derived from LA and AA, respectively. On average, 57 oxylipin metabolites were quantified in the plasma of STEMI patients during I/R. LA-derived oxylipins constituted 47% and 39% of total quantifiable oxylipins during ischemia and reperfusion (average of reperfusion time-points), respectively. AA-derived oxylipins accounted for 36% and 45% of total quantifiable oxylipins during the ischemic episode and reperfusion, respectively. The percentage of oxylipins derived from other FA precursors are presented in Figure 24.

Figure 24: Percentages of oxylipins derived from different fatty acids in STEMI patients and controls

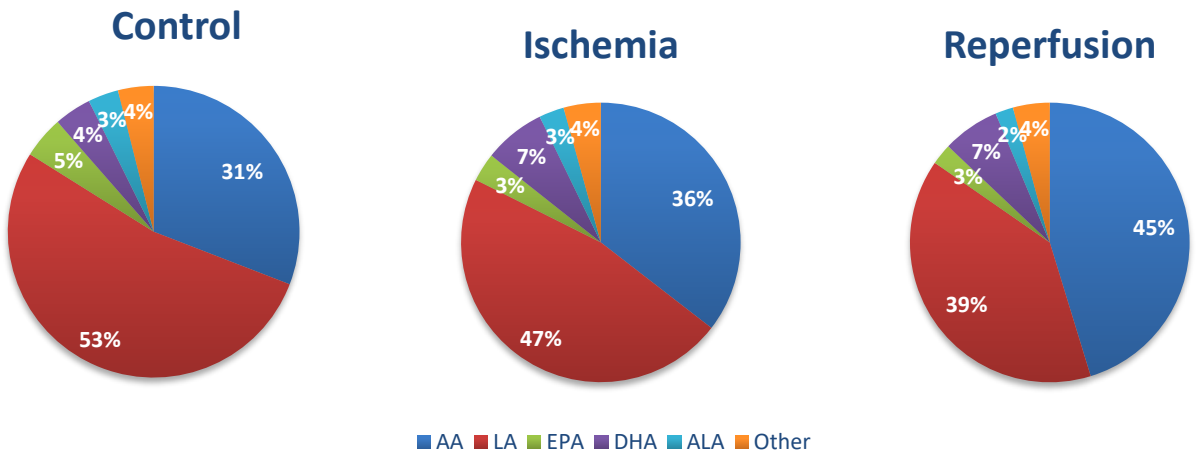

Abbreviations: AA: Arachidonic acid, ALA: Alpha linoleic acid, DHA: Docosahexaenoic acid, EPA: Eicosapentaenoic acid, LA: Linoleic acid.

The 20-carboxy-arachidonic acid (20-COOH-AA), an AA-derived oxylipin, along with 9 and 13-hydroxyoctadecadienoic acid (HODE) (LA-derived metabolites) were the most abundant oxylipins in the plasma of our participants. 20-COOH-AA constituted 30% and 41% of quantifiable oxylipins during ischemia and reperfusion in STEMI patients, respectively, and 23% of total oxylipins in controls (20-COOH-AA: Isch: 60.69±7.60, an average of reperfusion groups: 59.17±7.60, Control: 37.23±4.11 nM). The three most abundant oxylipins in the study groups were presented in Figure 25.

Figure 25: Percentages of the most abundant oxylipins in plasma of STEMI patients (during I/R) and controls

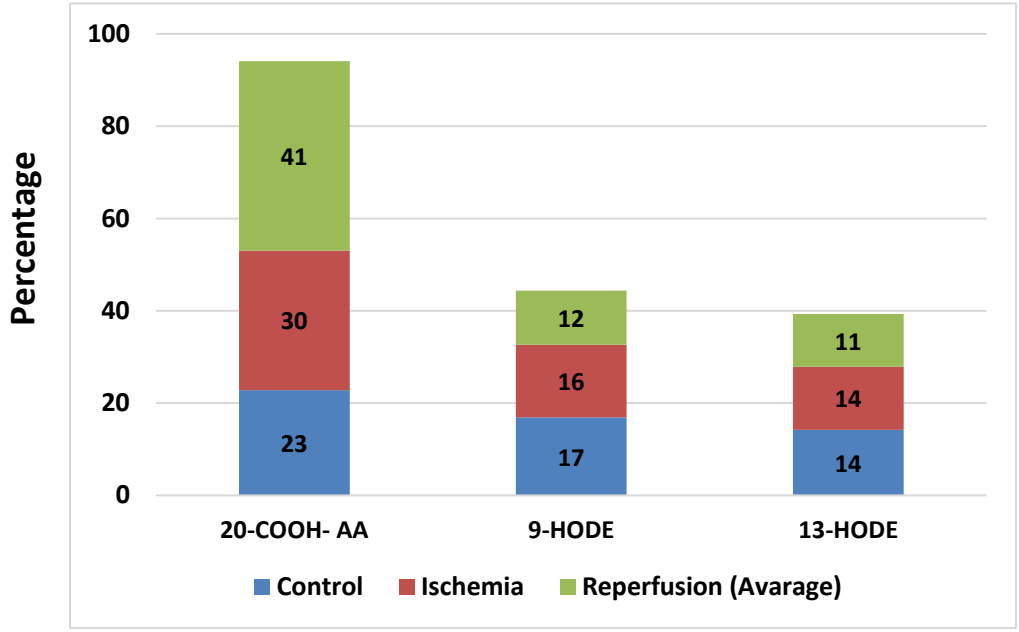

Abbreviations: AA: Arachidonic acid, HODE: Hydroxyoctadecadienoic acid.

Alterations in the plasma oxylipin profile of STEMI patients during the ischemic episode

There were no significant differences in total levels of oxylipins between Isch and control groups (Isch: 200.87±16.00, Control:163.19±8.9 nM) (Figure 26). Categorizing oxylipins based on their FA precursors showed that among all oxylipin groups, only total levels of DHA-derived oxylipins

were significantly elevated during ischemia compared with the control group (Isch: 14.23±1.46, Control: 6.79±0.96 nM, $p<0.05$) (Figure 26).

Figure 26: Changes in levels of oxylipin groups (based on FA precursors) in Isch and control groups

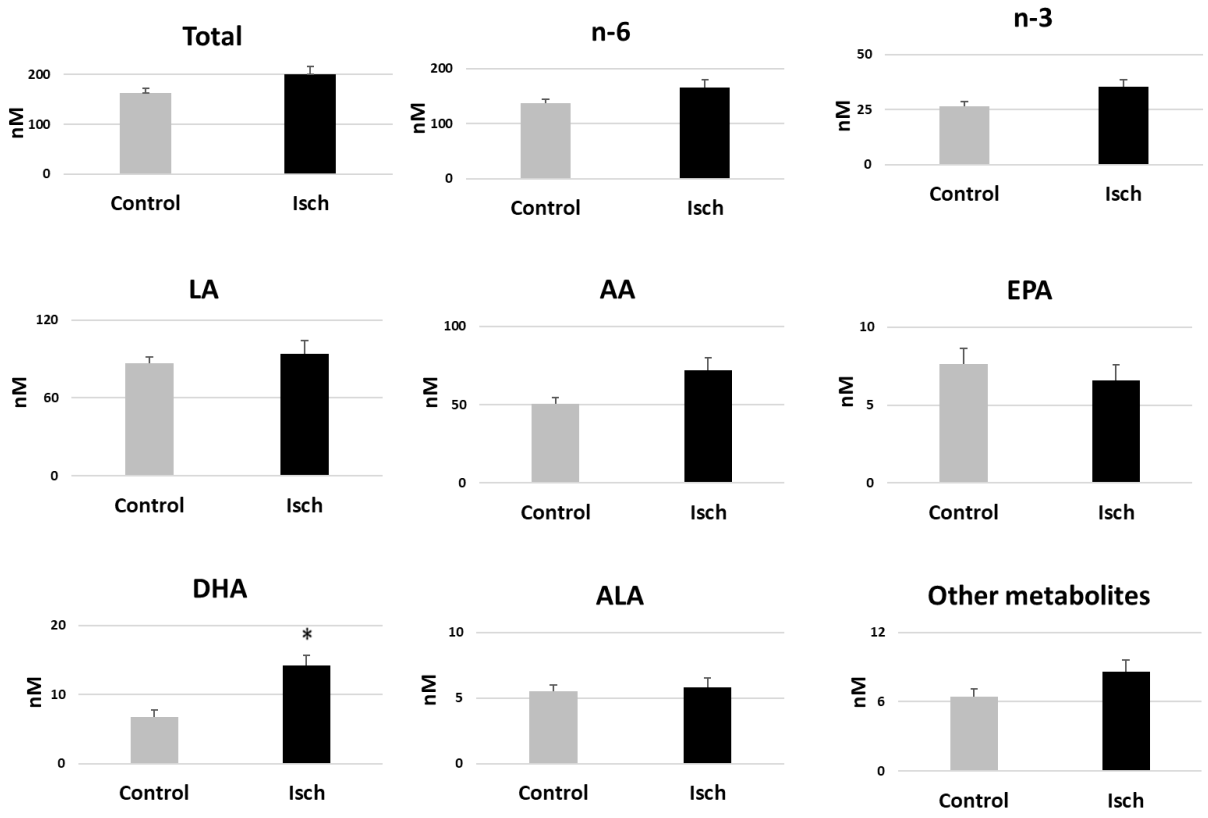

Values are means ± SEM. * Statistically significant difference compared with the control group ($p<0.05$).
Abbreviations: AA: Arachidonic acid, ALA: Alpha linoleic acid, DHA: Docosahexaenoic acid, EPA: Eicosapentaenoic acid, LA: Linoleic acid.

Moreover, total concentrations of this group of oxylipins (DHA-derived oxylipins) during ischemia were significantly correlated with peak levels of CK and TnT in STEMI patients (CK: $r=0.33$, $p=0.046$, TnT: $r=0.50$, $p=0.002$) (Table 16). Individual DHA-derived metabolites were also significantly correlated with levels of CK and TnT, which are presented in Table 16.

Table 16: Metabolites that were significantly correlated with markers of cardiac injury during ischemia in STEMI patients

Metabolite	FA Precursor	Pathway	CK (Pearson correlation)	TnT (Pearson correlation)
DHA-derived metabolites (total)	NA	NA	0.33*	0.50**
11-HDoHE	DHA	LOX/non-enz	0.56**	0.46**
13-HDoHE	DHA	LOX/non-enz	0.45**	-
17-keto DHA	DHA	LOX	-	0.56**
10-HDoHE	DHA	LOX	0.40*	0.34*
16-HDoHE	DHA	LOX	0.42*	-
17-HDoHE	DHA	LOX	0.37*	-
8-HDoHE	DHA	LOX	0.33*	-
16,17 EpDPE	DHA	CYP-e	0.34*	0.68**
19,20 DiHDoPE	DHA	CYP-e	-	0.52**
20-HDoHE	DHA	CYP-h	0.37*	-
17-Keto DPA	DPA	LOX	-	0.84**
5-HETE	AA	LOX	0.40*	-
11-HETE	AA	LOX	0.43**	-
12-HETE	AA	LOX	0.41*	-

Correlation is significant at the 0.01 level, *Correlation is significant at the 0.05 level. **Abbreviation: AA: Arachidonic acid, CK: Creatine kinase, CYP-e: Cytochrome P450 epoxygenase, CYP-h: Cytochrome P450 hydroxylase, DHA: Docosahexaenoic acid, DiHDoPE: Dihydroxydocosapentaenoic acid DPA: Docosapentaenoic acid, EpDPE: Epoxydocosapentaenoic acid, HDoHE: Hydroxy-docosahexaenoic acid, HETE: Hydroxyeicosatetraenoic acid, LOX: lipoxygenase, NA: not applicable. non-enz: Non-enzymatic oxidation, TnT: Troponin T.

We also compared total levels of oxylipins based on their generation pathways. As both STEMI patients and controls were on ASA therapy, no COX-derived oxylipins were quantified in STEMI patients in any I/R groups. However, prostaglandin D2 (PGD2) and PGE2 were the only COX metabolites that were quantified in the control groups (Table 17).

Table 17: All quantified oxylipins in Isch and control groups

Compounds	FA	PW	Control	Isch
PGD2	AA	COX	0.36±0.09	0.00±0.00*
PGE2	AA	COX	0.09±0.02	0.00±0.00*
11,12 DiHETrE	AA	CYP-e	0.35±0.02	0.32±0.04
14,15 DiHETrE	AA	CYP-e	0.35±0.02	0.39±0.05
5,6 DiHETrE	AA	CYP-e	0.15±0.01	0.20±0.03
8,9 DiHETrE	AA	CYP-e	0.20±0.01	0.19±0.03
16-HETE	AA	CYP-h	0.47±0.03	0.29±0.03*
18-HETE	AA	CYP-h	0.07±0.01	0.11±0.02
20-COOH- AA	AA	CYP-h	37.23±4.11	60.69±7.59*
20-HETE	AA	CYP-h	0.81±0.09	0.87±0.14
17-HETE	AA	CYP-h	0.04±0.01	00.0±00*
12-HETE	AA	LOX	2.72±0.43	0.75±0.30*
5-HETE	AA	LOX	1.80±0.12	3.95±0.92*
5-oxoETE	AA	LOX	0.21±0.02	0.10±0.01*
8-HETE	AA	LOX	0.72±0.06	1.00±0.15
tetranor 12-HETE	AA	LOX	0.99±0.10	0.47±0.07*
12-oxoETE	AA	LOX	0.81±0.19	0.00±0.00*
15-oxoETE	AA	LOX	0.18±0.02	0.06±0.00*
15-HETE	AA	LOX/COX	1.73±0.18	1.61±0.32
11-HETE	AA	LOX/COX/non-enz	0.47±0.05	0.44±0.12
9-HETE	AA	LOX/non-enz	0.40±0.07	0.30±0.20
12,13 diHODE	ALA	CYP-e	0.22±0.04	0.16±0.05
12,13 EpODE	ALA	CYP-e	0.20±0.01	0.07±0.00*
9-oxoOTrE	ALA	LOX	0.70±0.08	0.28±0.03*
9-HOTrE	ALA	LOX	4.38±0.39	5.29±0.71
15-HETrE	DGLA	LOX	0.39±0.02	0.31±0.06
8-HETrE	DGLA	LOX	0.17±0.01	0.26±0.06
19,20 EpDPE	DHA	CYP-e	0.00±0.00	0.02±0.00*
19,20 DiHDPE	DHA	CYP-e	1.17±0.09	1.59±0.17
16,17 DiHDPE	DHA	CYP-e	0.07±0.00	0.04±0.00
20-HDoHE	DHA	CYP-h	0.44±0.07	0.52±0.11
10-HDoHE	DHA	LOX	0.25±0.03	0.18±0.04
14-HDoHE	DHA	LOX	0.98±0.22	0.63±0.12
16-HDoHE	DHA	LOX	0.34±0.04	0.27±0.06
17-HDoHE	DHA	LOX	1.02±0.19	1.17±0.23
4-HDoHE	DHA	LOX	1.61±0.28	2.67±0.45
7-HDoHE	DHA	LOX	0.26±0.06	0.57±0.07*
8-HDoHE	DHA	LOX	0.38±0.07	0.86±0.16*
17-Keto DHA	DHA	LOX	0.00±0.00	5.3±0.92*
11-HDoHE	DHA	LOX/non-enz	0.22±0.05	0.06±0.04*
13-HDoHE	DHA	LOX/non-enz	0.00±0.00	0.24±0.10
17-keto DPA	DPA	LOX	5.21±0.64	4.55±0.82
14,15 diHETE	EPA	CYP-e	1.02±0.10	1.12±0.12
17,18 diHETE	EPA	CYP-e	4.44±0.94	2.67±0.26
18-HEPE	EPA	CYP-h	0.48±0.06	0.56±0.08
12-HEPE	EPA	LOX	0.90±0.23	0.80±0.23
5-HEPE	EPA	LOX	0.49±0.09	1.18±0.17*
15-HEPE	EPA	LOX/COX	0.29±0.04	0.25±0.04
13-HOTrE	GLA	LOX	3.59±0.40	3.02±0.39
13-HOTrE-y	GLA	LOX	0.65±0.06	0.47±0.06
12,13 diHOME	LA	CYP-e	2.85±0.16	5.99±2.38
12,13 EpOME	LA	CYP-e	3.21±0.22	1.84±0.16*
9,10 diHOME	LA	CYP-e	1.89±0.12	3.59±0.84
9,10 EpOME	LA	CYP-e	1.22±0.11	0.78±0.10*
13-HODE	LA	LOX	23.16±1.46	27.48±3.60

13-oxoODE	LA	LOX	5.88±0.45	3.58±0.27*
9-HODE	LA	LOX	27.53±1.77	31.68±3.61
9-oxoODE	LA	LOX	7.75±0.65	4.05±0.32*
9,12,13 triHOME	LA	LOX/ CYP-e	3.42±0.25	3.58±0.37
9,10,13 triHOME	LA	LOX/CYP-e	9.44±0.70	11.83±0.98

Values are means ± SEM. * Statistically significant difference compared with the control group (p<0.05).

Abbreviations: AA: Arachidonic acid, ALA: Alpha linoleic acid, COX: Cyclooxygenase, CYP-e: Cytochrome P450 epoxygenase, CYP-h: Cytochrome P450 hydroxylase, DGLA: Dihemo gamma-linoleic acid, DHA: Docosahexaenoic acid, DiHDPE: Dihydroxydocosapentaenoic acid, DiHETE: Dihydroxyeicosatetraenoic acid, DiHETrE: Dihydroxy-eicosatrienoic acid, DPA: Docosapentaenoic acid, EPA: Eicosapentaenoic acid, EpDPE: Epoxydocosapentaenoic acid, EpODE: Epoxy-octadecadienoic acid, EpOME: Epoxy-octadecenoic acid, GLA: Gamma linolenic acid, HDoHE: Hydroxy-docosahexaenoic acid, HEPE: Hydroxyeicosapentaenoic acid, HETE: Hydroxyeicosatetraenoic acid, HETrE: Hydroxyeicosatrienoic acid, HODE: Hydroxyoctadecadienoic acid, HOTrE: Hydroxy-octadecatrienoic acid, LA: Linoleic acid, LOX: Lipoxygenase, non-enz: Non-enzymatic oxidation, Oxo-ETE: Oxo-eicosatetraenoic acid, OxoODE: Oxo-octadecadienoic acid, OxoOTrE: Oxo-octadecatrienoic acid, PG: Prostaglandin, TriHOME: Trihydroxy-octadecenoic acid.

Total levels of the metabolites generated through the LOX pathway did not significantly differ between Isch and control groups (Isch: 118.72±12.19, Control:98.26±6.45nM) (Figure 27-A).

Figure 27: Total levels of oxylipins generated through LOX pathways in Isch and control groups

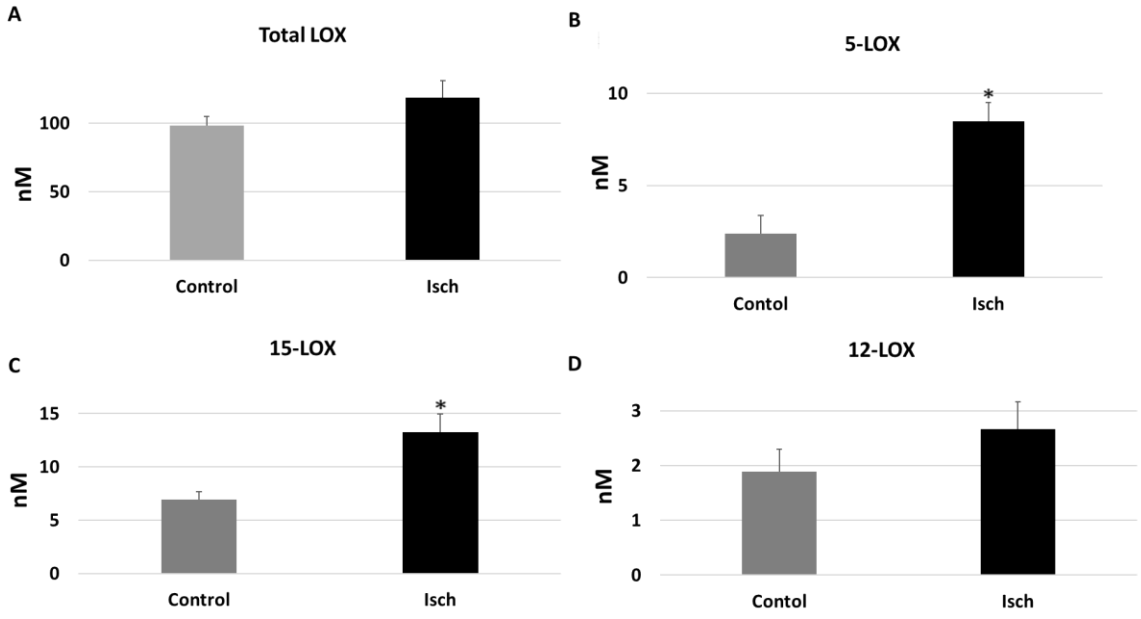

Values are means ± SEM. * Statistically significant difference compared with the control group (p<0.05).
Abbreviations: LOX: Lipoxygenase.

Sub-categorizing oxylipins based on 5/12/15 LOX pathways revealed that total levels of the compounds generated through the 5-LOX pathway (including 4-HDoHE, 5-HEPE, 5-HETE, 5-oxoETE, and 7-HDoHE) were significantly higher in the Isch group compared with controls (Isch=8.48±1.35, Control: 2.37±0.40 nM, $p<0.05$) (Figure 27B). Total levels of 5-LOX metabolites were also significantly correlated with TNF-α levels during ischemia in STEMI patients (r=0.36, $p<0.05$). Total levels of metabolites that were produced through the 15-LOX pathway (including 15-HEPE, 15-HETE, 15-HETrE, 15-oxoETE, 17-HDoHE, 17-Keto DHA, and 17-Keto DPA) were also significantly elevated in the Isch group in comparison with controls (Isch: 13.28±1.66, Control: 6.92±0.72, $p<0.05$) (Figure 27C). Looking at individual metabolites of this group revealed that only 17-Keto DHA increased significantly in this group (Table 17). Total levels of the compounds generated through the 12-LOX pathway (including tetranor-12-HETE, 12-HEPE, 12-HETE, and 14-HDoHE) were not significantly different between the Isch group and controls (Isch:2.66±0.52, Control: 1.89±0.45 nM) (Figure 27D). Interestingly their levels were significantly correlated with both TNF-α and MIP-1α levels during ischemia (TNF-α: r=0.46, $p<0.001$, MIP-1α: r=0.63, $p<0.001$).

Next step, levels of oxylipins that were generated from the CYP450 pathway were compared in Isch and control groups. As shown in Figure 28A, total levels of oxylipins generated through the CYP-h pathway were significantly elevated in Isch compared with the control group (Isch:63.06±7.69, Control: 39.50±4.1 nM, $p<0.05$).

Figure 28: Total levels of oxylipins generated through CYP450 pathways in Isch and control groups

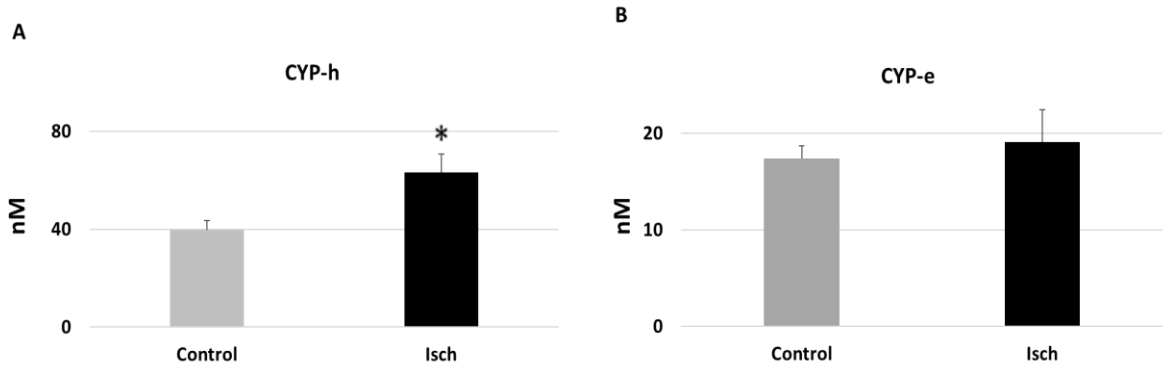

Values are means ± SEM. * Statistically significant difference compared with the control group (p<0.05).
Abbreviations: CYP-h: Cytochrome P450-hydroxylase, CYP-e: Cytochrome P450-epoxygenase.

Looking at changing patterns of individual compounds in this group showed that 20-COOH-AA was responsible for the observed elevation (Isch: 60.69±7.59, Control: 37.23±4.11 nM, p<0.05) (Table 17).

No significant differences were observed in total levels of oxylipins generated through the CYP-e pathway between Isch and control groups (CYP-e: Isch:19.08±3.35, Control: 17.40±1.29 nM) (Figure 28B). When the ratio of epoxides (EpETEs, EpOMEs, EpDPEs and EpODEs) to diol metabolites (DiHETrE, diHOME, DiHDPE, diHETE, and diHODE) were compared, there was a significant reduction in the total epoxide/diols during ischemia compared with controls, reflecting the elevated activity of sEH enzyme during ischemia (Isch: 0.2±0.02, Control:0.4±0.02, p<0.001) (Figure 29A).

Figure 29: Changes in ratios of epoxides/diols in STEMI patients in Isch and control groups

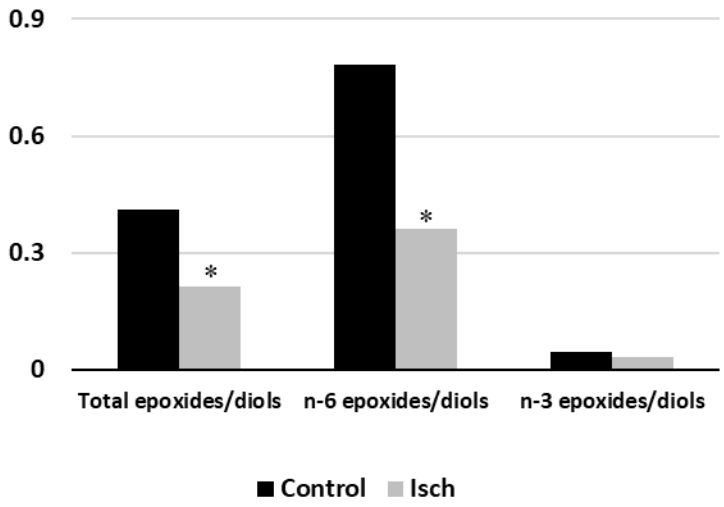

Total ratio of epoxides/diols, the ratio of epoxides/diols generated from n-6 fatty acids and the ratio of epoxides/diols generated from n-3 fatty acids in Isch and control groups. *Significantly different compared with the control group (p<0.05).

Interestingly, comparing the ratio of n-6 derived epoxides (EpETEs and EpOMEs) to their respective diols (DiHETrEs and diHOMEs) revealed a significant reduction in n-6 epoxides/diols during the ischemic episode in comparison with the control group (Isch:0.3±0.02, Control: 0.7±0.04, p<0.001) (Figure 29B). However, the ratio of n-3 derived epoxides (EpDPEs and

EpODEs) to diols (diHETE, DiHDPE, and diHODE) was not significantly different between Isch and control groups (Ischemia: 0.03±0.004, Control: 0.04±0.005) (Figure 29C). All oxylipin metabolites that were quantified in Isch and control groups are presented in Table 17.

Plasma oxylipin alterations in STEMI patients post-reperfusion

Next step, we compared the levels of oxylipins in STEMI patients during ischemia and multiple time-points of reperfusion. Total levels of oxylipins were significantly elevated during the ischemic period (Isch) and early after reperfusion (R-2h). Subsequently, their concentrations decreased significantly at 24h after reperfusion and then remained unchanged until 30 days post-MI (Isch: 200.87±16.00. R-2h: 190.87±17.00, R-24h: 123.34±10.87, R-48h: 127.01±11.28, and R-30d:135.95±13.88 nM, $p<0.05$) (Figure 30A).

Figure 30: Changes in levels of total oxylipins and markers of inflammation in STEMI patients during I/R

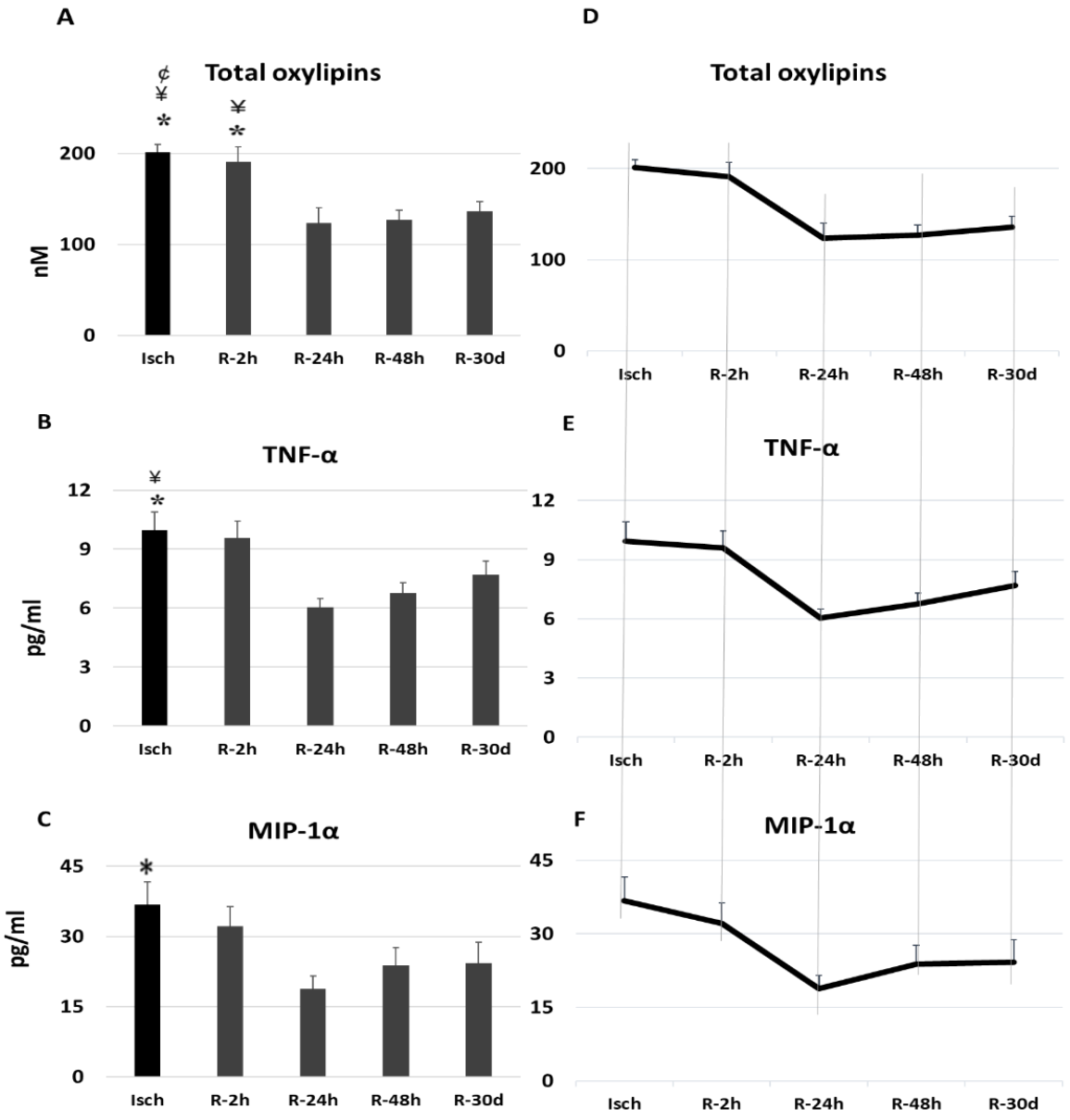

Values are means ± SEM. *Significant difference from R-24h, ¥ Significant difference from R-48h, ¢ Significant difference from R-30d (p<0.05). TNF-α: Tumour necrosis factor-α, MIP-1α: Macrophage inflammatory protein1-α.

Similarly, plasma concentrations of inflammatory markers, namely TNF-α and MIP-1α reduced significantly following reperfusion in STEMI patients (TNF-α: Isch: 8.98±0.86, R-2h: 9.02±0.79, R-24h: 5.70±0.42, R-48h: 6.28±0.48, and R-30d: 7.66±0.72 pg/ml, p<0.05) (MIP-1α: Isch:

36.41±5.44, R-2h: 31.21±4.57, R-24h: 19.17±3.01, R-48h: 24.49±4.40, and R-30d: 24.25±4.64 pg/ml, $p<0.05$) (Figure 30B and C). As it is presented in Figure 30D, E, and F, changing patterns of total oxylipins and inflammatory markers, namely, TNF-α and MIP-1α, were identical during 30 days post-MI. It should be mentioned that only changes in levels of these two markers of inflammation (not all) are presented here as their concentrations were significantly correlated with individual oxylipins during I/R (data not shown).

Oxylipins were then categorized based on their FA precursors (Figure 31). As it is presented in Figure 31, both n-6 and n-3 oxidized metabolites reduced significantly during 30 days of reperfusion (total n-6 metabolites: Isch: 165.59±13.81, R-2h: 162.12±15.51, R-24h: 101.34±9.19, R-48h: 106.49±10.03, and R-30d:118.55±13.03 nM, $p<0.05$) (total n-3 metabolites: Isch: 35.28±3.20, R-2h: 28.74±2.53, R-24h: 22.00±2.69, R-48h:20.58±2.18, and R-30d:17.39±1.60 nM, $p<0.05$). Changes in levels of other groups of oxylipins (based on the FA precursors) were presented in Figure 31.

Figure 31: Alteration in levels of total oxylipins and oxylipin groups (based on FA precursors) in STEMI patients during 30 days post-MI

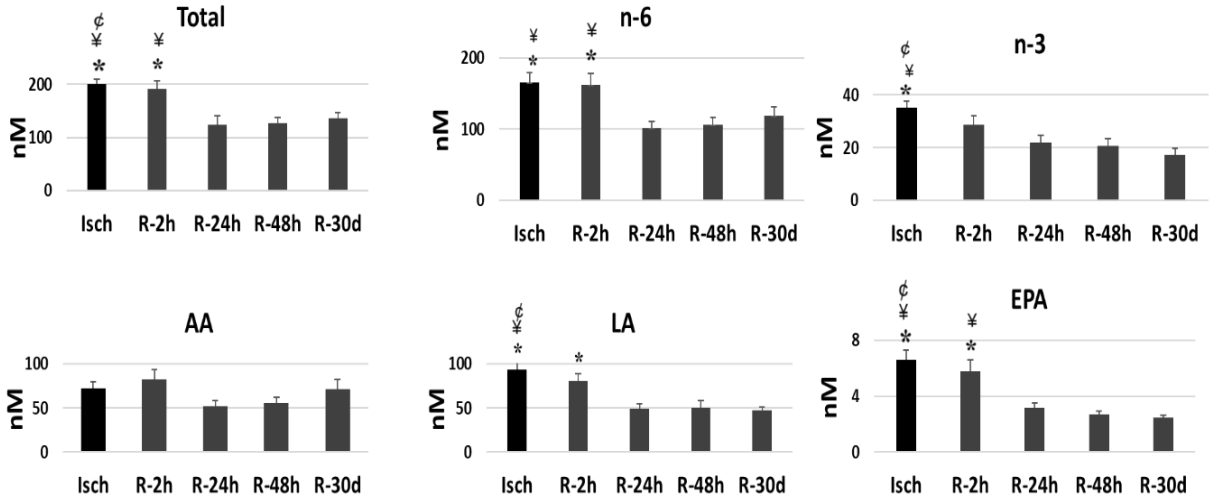

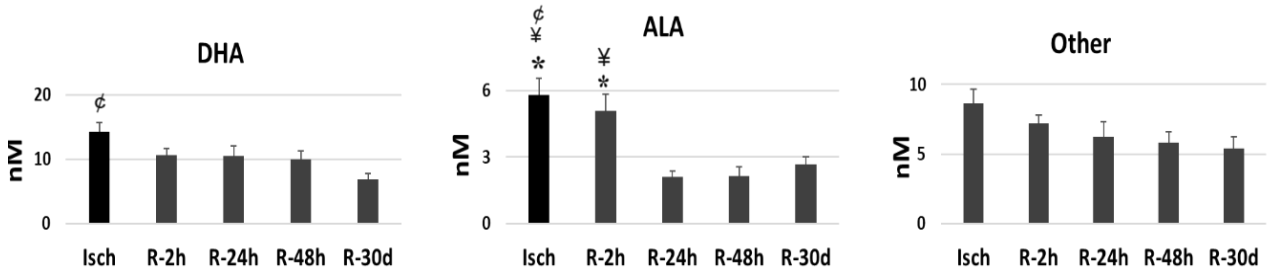

Values are means ± SEM. *Significant difference from R-24h, ¥ Significant difference from R-48h, ¢ Significant difference from R-30day (p<0.05). **Abbreviations:** AA: Arachidonic acid, ALA: Alpha linoleic acid, DHA: Docosahexaenoic acid, EPA: Eicosapentaenoic acid, LA: Linoleic acid.

Oxylipin metabolites were then classified based on their generation pathways. We found that total levels of the metabolites produced through the LOX pathway decreased significantly post-reperfusion (Isch: 118.72±12.19, R-2h: 98.40±9.2, R-24h: 62.84±6.48, R-48h: 61.33±6.18, and R-30d: 55.10±4.55 nM, p<0.05) (Figure 32A).

Figure 32: Total levels of oxylipins that were generated through LOX pathways in STEMI patients during I/R

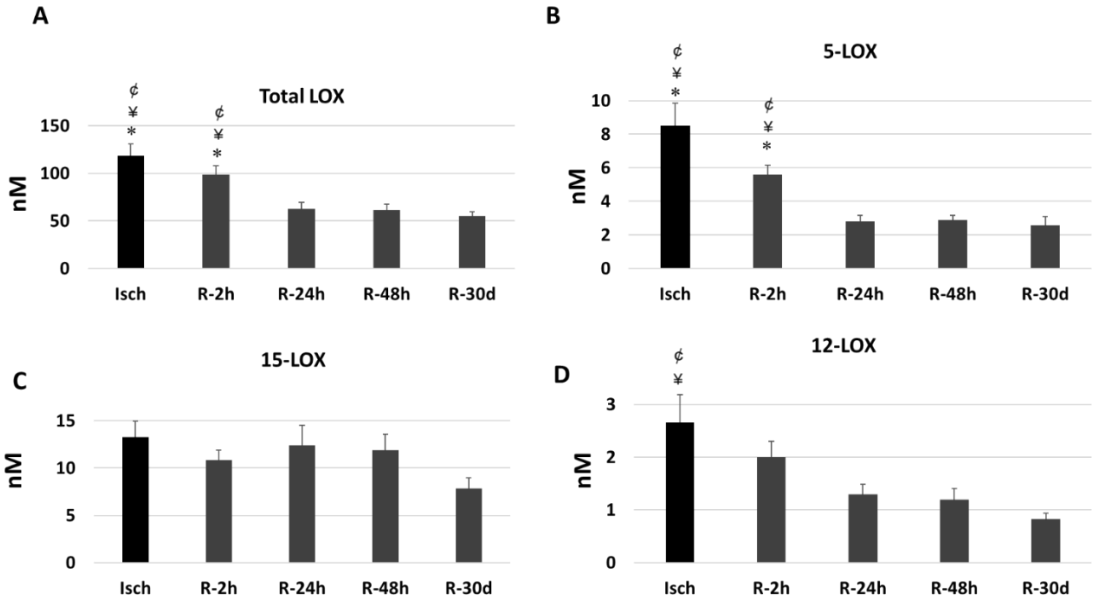

Values are means ± SEM. *Significant difference from R-24h, ¥ Significant difference from R-48h, ¢ Significant difference from R-30day, p<0.05. **Abbreviations:** LOX: Lipoxygenase.

Sub-categorizing LOX pathway revealed that total levels of metabolites that were generated through the 5-LOX pathway decreased significantly post-reperfusion (Isch: 8.49±1.35, R-2h: 5.58±0.54, R-24h: 2.83±0.33, R-48h: 2.89±0.27, and R-30d: 2.56±0.53 nM, $p<0.05$) (Figure 32B). Moreover, their levels were also significantly correlated with TNF-α and MIP-1α concentrations during I/R (TNF: r=0.27, $p<0.001$, MIP-1α: 0.20, $p<0.05$). Total levels of compounds that were produced through the 15-LOX pathway did not significantly differ between I/R groups (Isch: 13.28±1.66, R-2h:10.81±1.13, R-24h: 12.42±2.09, R-48h: 11.89±1.66, and R-30d: 7.84±1.13 nM) (Figure 32C). Looking at individual compounds in this group revealed that 17-Keto DHA and 17-Keto DPA were two compounds that their concentrations did not change during I/R (Table 18). Total levels of metabolites that were generated through the 12-LOX pathway also experienced significant reductions following reperfusion (Isch: 2.66±0.52, R-2h: 2:00±0.29, R-24h: 1.29±0.19, R-48h:1.19±0.21, and R-30d: 0.8±0.10 nM, $p<0.05$) (Figure 32D). Their levels were also significantly correlated with TNF-α and MIP-1α concentrations during I/R (TNF-α: r=0.24, $p<0.001$, MIP-1α: 0.26, $p<0.001$).

Table 18: All quantified oxylipins in STEMI groups during I/R

Compounds	FA	Pathway	Isch	R-2h	R-24h	R-48h	R-30d
11,12 DiHETrE	AA	CYP-e	0.32±0.04	0.35±0.05	0.23±0.03	0.25±0.03	0.33±0.02
14,15 DiHETrE	AA	CYP-e	0.39±0.05	0.40±0.05	0.24±0.03	0.23±0.02	0.33±0.02*
5,6 DiHETrE	AA	CYP-e	0.20±0.03	0.19±0.03	0.08±0.01	0.08±0.01	0.11±0.01*
8,9 DiHETrE	AA	CYP-e	0.19±0.03	0.20±0.04	0.10±0.01	0.09±0.01	0.13±0.01*
16-HETE	AA	CYP-h	0.29±0.03	0.27±0.03	0.20±0.02	0.20±0.02	0.33±0.03*
18-HETE	AA	CYP-h	0.11±0.02	0.15±0.03	0.04±0.01	0.03±0.01	0.05±0.01*
20-COOH-AA	AA	CYP-h	60.69±7.59	73.59±11.27	46.92±6.28	50.57±5.86	65.58±11.03
20-HETE	AA	CYP-h	0.87±0.14	0.69±0.09	0.39±0.05	0.38±0.05	0.54±0.13*
12-HETE	AA	LOX	0.75±0.3	0.52±0.16	0.46±0.14	0.53±0.16	0.12±0.07
5-HETE	AA	LOX	3.95±0.92	2.51±0.25	1.33±0.19	1.44±0.18	1.21±0.21*
5-oxoETE	AA	LOX	0.10±0.01	0.07±0.01	0.03±0.007	0.03±0.01	0.05±0.01*
8-HETE	AA	LOX	1.00±0.15	0.70±0.07	0.57±0.06	0.54±0.06	0.62±0.14*
tetranor 12-HETE	AA	LOX	0.47±0.07	0.65±0.10	0.38±0.05	0.29±0.04	0.38±0.04*
15-HETE	AA	LOX/COX	1.61±0.32	1.15±0.14	0.8±0.11	0.8±0.09	0.58±0.07*
11-HETE	AA	LOX/COX/non-enzyme	0.44±0.12	0.25±0.05	0.16±0.04	0.15±0.04	0.13±0.02*
9-HETE	AA	LOX/non-enz	0.30±0.2	0.10±0.06	0.10±0.05	0.12±0.06	0.27±0.13

15-oxoETE	AA	LOX	0.06±0.01	0.05±0.01	0.02±0.00	0.03±0.00	0.02±0.01*
12,13 diHODE	ALA	CYP-e	0.16±0.05	0.1±0.01	0.09±0.01	0.13±0.03	0.17±0.02
12,13 EpODE	ALA	CYP-e	0.07±0.01	0.09±0.01	0.06±0.01	0.08±0.03	0.07±0.01
9 oxoOTrE	ALA	LOX	0.28±0.03	0.28±0.04	0.1±0.02	0.1±0.03	0.09±0.02*
9-HOTrE	ALA	LOX	5.29±0.71	4.59±0.71	1.84±0.22	1.84±0.29	2.32±0.34*
15-HETrE	DGLA	LOX	0.31±0.06	0.21±0.03	0.09±0.01	0.12±0.02	0.10±0.01*
8-HETrE	DGLA	LOX	0.26±0.06	0.17±0.02	0.07±0.01	0.08±0.01	0.09±0.01*
16,17 DiHDPE	DHA	CYP-e	0.04±0.01	0.04±0.01	0.03±0.00	0.03±0.00	0.04±0.01
16,17 EpDPE	DHA	CYP-e	0.03±0.02	0.03±0.02	0.008±0.01	0.01±0.01	0.06±0.06
19,20 DiHDPE	DHA	CYP-e	1.59±0.17	1.72±0.26	0.93±0.12	0.89±0.11	0.83±0.07*
19,20 EpDPE	DHA	CYP-e	0.02±0.01	0.01±0.01	0.001±0.00	0.00±0.00	0.01±0.01*
20-HDoHE	DHA	CYP-h	0.52±0.11	0.35±0.06	0.21±0.05	0.17±0.05	0.14±0.05*
10-HDoHE	DHA	LOX	0.18±0.04	0.08±0.01	0.08±0.03	0.05±0.01	0.08±0.02*
14-HDoHE	DHA	LOX	0.63±0.12	0.35±0.05	0.28±0.05	0.26±0.05	0.22±0.04*
16-HDoHE	DHA	LOX	0.27±0.06	0.16±0.03	0.12±0.03	0.09±0.02	0.09±0.02*
17-HDoHE	DHA	LOX	1.17±0.23	0.84±0.14	0.58±0.10	0.53±0.09	0.27±0.15*
17-keto DHA	DHA	LOX	5.3±0.92	4.27±0.63	6.74±1.25	6.36±1.09	3.87±0.70
4-HDoHE	DHA	LOX	2.67±0.45	1.68±0.23	0.82±0.09	0.96±0.09	0.80±0.16*
7-HDoHE	DHA	LOX	0.57±0.07	0.37±0.06	0.25±0.04	0.26±0.05	0.20±0.08*
8-HDoHE	DHA	LOX	0.86±0.16	0.69±0.11	0.3±0.09	0.28±0.07	0.26±0.11*
11-HDoHE	DHA	LOX/non-enz	0.06±0.04	0.00±0.00	0.03±0.03	0.00±0.00	0.00±0.00
13-HDoHE	DHA	LOX/non-enz	0.24±0.1	0.06±0.03	0.08±0.04	0.02±0.02	0.00±0.00
17-keto DPA	DPA	LOX	4.55±0.82	4.08±0.49	4.08±0.99	3.97±0.77	2.89±0.85
14,15 diHETE	EPA	CYP-e	1.12±0.12	1.12±0.21	0.77±0.09	0.63±0.05	0.65±0.04*
17,18 diHETE	EPA	CYP-e	2.67±0.26	2.63±0.39	1.6±0.19	1.57±0.18	1.18±0.10*
18-HEPE	EPA	CYP-h	0.56±0.08	0.41±0.06	0.15±0.03	0.09±0.01	0.14±0.02*
12-HEPE	EPA	LOX	0.8±0.23	0.47±0.07	0.15±0.03	0.10±0.03	0.08±0.02*
5-HEPE	EPA	LOX	1.18±0.17	0.94±0.14	0.38±0.07	0.18±0.05	0.29±0.08*
15-HEPE	EPA	LOX/COX	0.25±0.04	0.19±0.04	0.07±0.01	0.07±0.01	0.08±0.01*
13-HOTrE	GLA	LOX	3.02±0.39	2.35±0.28	1.84±0.32	1.50±0.18	2.07±0.24*
13-HOTrE-y	GLA	LOX	0.47±0.06	0.34±0.05	0.11±0.02	0.10±0.01	0.19±0.03*
9,10 diHOME	LA	CYP-e	3.59±0.84	3.05±0.49	2.86±0.91	3.93±1.86	3.21±0.40
12,13 EpOME	LA	CYP-e	1.84±0.16	2.16±0.20	1.32±0.16	1.38±0.25	1.12±0.13*
12,13 diHOME	LA	CYP-e	5.99±2.38	3.96±0.42	3.78±0.55	4.25±1.24	4.97±0.60
9,10 EpOME	LA	CYP-e	0.78±0.10	0.83±0.10	0.39±0.07	0.51±0.16	0.34±0.08*
13-HODE	LA	LOX	27.48±3.60	23.23±2.84	14.82±2.03	14.19±1.98	13.63±1.19*
13-oxoODE	LA	LOX	3.58±0.27	3.09±0.27	2.06±0.18	2.15±0.25	1.77±0.16*
9-HODE	LA	LOX	31.68±3.61	28.23±3.75	13.18±1.62	13.41±1.97	12.59±1.40*
9-oxoODE	LA	LOX	4.05±0.32	4.12±0.42	1.87±0.24	2.05±0.27	1.50±0.20*

9,10,13 triHOME	LA	LOX/CYP-e	11.83±0.98	9.01±0.85	6.83±0.67	7±0.61	5.87±0.70*
9,12,13 triHOME	LA	LOX/CYP-e	3.58±0.37	2.74±0.24	2.43±0.27	2.31±0.22	2.59±0.31*

Values are means ± SEM. * Statistically significant difference between study groups (p<0.05). **Abbreviations:** AA: Arachidonic acid, ALA: Alpha linoleic acid, COX: Cyclooxygenase, CYP-e: Cytochrome P450 epoxygenase, CYP-h: Cytochrome P450 hydroxylase, DGLA: Dihemo gamma-linoleic acid, DHA: Docosahexaenoic acid, DiHDPE: Dihydroxydocosapentaenoic acid, DiHETE: Dihydroxyeicosatetraenoic acid, DiHETrE: Dihydroxy-eicosatrienoic acid, DPA: Docosapentaenoic acid, EPA: Eicosapentaenoic acid, EpDPE: Epoxydocosapentaenoic acid, EpODE: Epoxy-octadecadienoic acid, EpOME: Epoxy-octadecenoic acid, GLA: Gamma linolenic acid, HDoHE: Hydroxy-docosahexaenoic acid, HEPE: Hydroxyeicosapentaenoic acid, HETE: Hydroxyeicosatetraenoic acid, HETrE: Hydroxyeicosatrienoic acid, HODE: Hydroxyoctadecadienoic acid, HOTrE: Hydroxy-octadecatrienoic acid, LA: Linoleic acid, LOX: Lipoxygenase, non-enz: Non-enzymatic oxidation, Oxo-ETE: Oxo-eicosatetraenoic acid, OxoODE: Oxo-octadecadienoic acid, OxoOTrE: Oxo-octadecatrienoic acid, PG: Prostaglandin, TriHOME: Trihydroxy-octadecenoic acid.

Total levels of metabolites that were generated through the 12-LOX pathway also experienced significant reductions following reperfusion (Isch: 2.66±0.52, R-2h: 2:00±0.29, R-24h: 1.29±0.19, R-48h:1.19±0.21, and R-30d: 0.8±0.10 nM, p<0.05) (Figure 32D). Their levels were also significantly correlated with TNF-α and MIP-1α concentrations during I/R (TNF-α: r=0.24, p<0.001, MIP-1α: 0.26, p<0.001).

Regarding CYP450 pathway metabolites, it is found that changes in total levels of oxylipins produced through the CYP-h were not statistically significant (Isch: 63.37±7.86, R-2h: 75.50±11.37, R-24h: 47.93±6.30, R-48h: 51.48±5.87, and R-30d: 66.81±11.03 nM, p=0.1) (Figure 33A). Looking at individual compounds, such as 16-HETE, 18-HETE, 20-HETE, 20-HDoHE, and 18-HEPE, showed that all CYP-h derived metabolites, except for 20-COOH-AA, decreased significantly following reperfusion (Table 18).

Figure 33: Total levels of oxylipins that were generated through the CYP450 pathway in STEMI patients during I/R

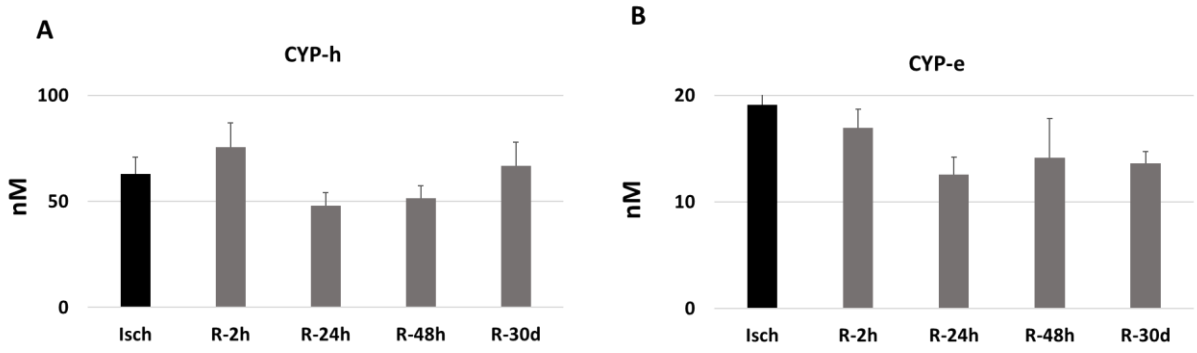

Values are means ± SEM. **Abbreviations:** CYP-e: Cytochrome P450 epoxygenase, CYP-h: Cytochrome P450 hydroxylase.

Total levels of the metabolite generated through the CYP-e pathway did not differ significantly during I/R (Isch: 19.08±3.35, R-2h: 16.96±1.7, R-24h: 12.56±1.65, R-48h: 14.12±3.67, and R-30d: 13.62±1.08 nM, p=0.3) (Figure 33B). Similar to the ischemic time, the ratio of n-6 (but not n-3) derived epoxides/diols reduced significantly during I/R (n-6 ratio of epoxides/diols: Isch: 0.36±0.03, R-2h: 0.42±0.02, R-24h: 0.29±0.03, R-48h: 0.32±0.03, and R-30d: 0.21±0.04, p<0.001) (n-3 ratio of epoxides/diols: Isch: 0.032±0.004, R-2h: 0.038±0.006, R-24h: 0.036±0.01, R-48h: 0.037±0.01, and R-30d: 0.07±0.04, p=0.5) (Figure 34). Alterations in concentrations of all individual metabolites during I/R are presented in Table 18.

Figure 34: Changes in ratios of epoxides/diols in STEMI patients during I/R

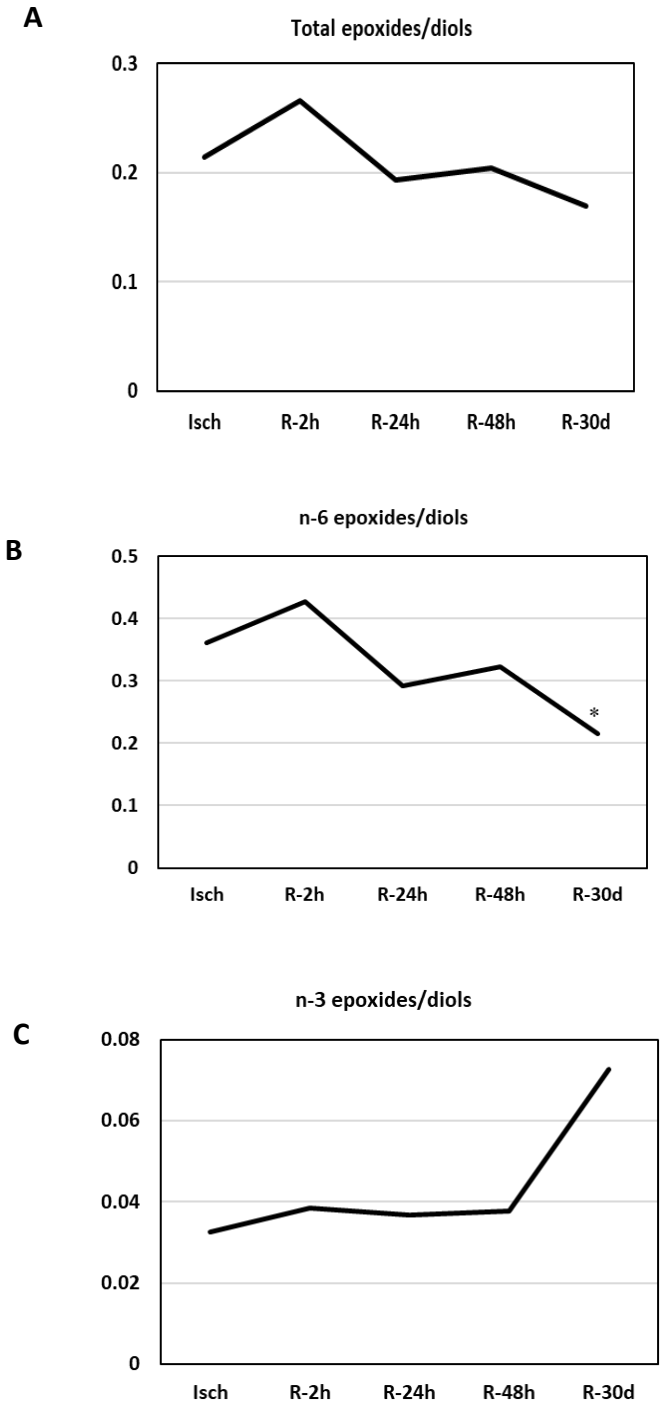

Total ratio of epoxides/diols (A), the ratio of epoxides/diols generated from n-6 fatty acids (B) and the ratio of epoxides/diols generated from n-3 fatty acids (C) during I/R. *Significantly different compared with the control group (p<0.05).

Oxylipins and clinical biomarkers of cardiac cell death

We used the biomarker analysis to find the potential oxylipin biomarkers that can distinguish STEMI patients with larger infarct size, based on gold standard biomarkers of cardiac cell death, namely, CK and TnT (19, 20). STEMI patients were classified as “high” and” low” based on the median of peak CK and TnT levels. Patients with above-median levels of peak CK and TnT considered as “high CK” or “high TnT” groups and patients with below-median levels of peak CK and TnT named as “low CK” and “low TnT” groups (median of peak CK: 1111.5 ng/L, the median of peak TnT: 2189 ng/L). Univariate receiver operating characteristic (ROC) curve analysis was used to identify potential biomarkers based on the area under the curve (AUC). We found that epoxides to diols ratio could be a potential biomarker of infarct size with AUC= 0.77 (p=0.03) based on CK levels and AUC=0.76 (p=0.054) based on TnT levels (Figure 34). Interestingly other oxylipins that could be logically suggested as biomarkers (such as high abundent metabolites (20-COOH AA, 9- and 13-HODE), 5-LOX derived metabolites and 17-Keto DHA that increased significantly during ischemia) were not statistically relevant, based on ROC curve analysis.

Figure 35: Epoxides/diols ratio during ischemia can be used as a biomarker of cardiac injury in STEMI patients

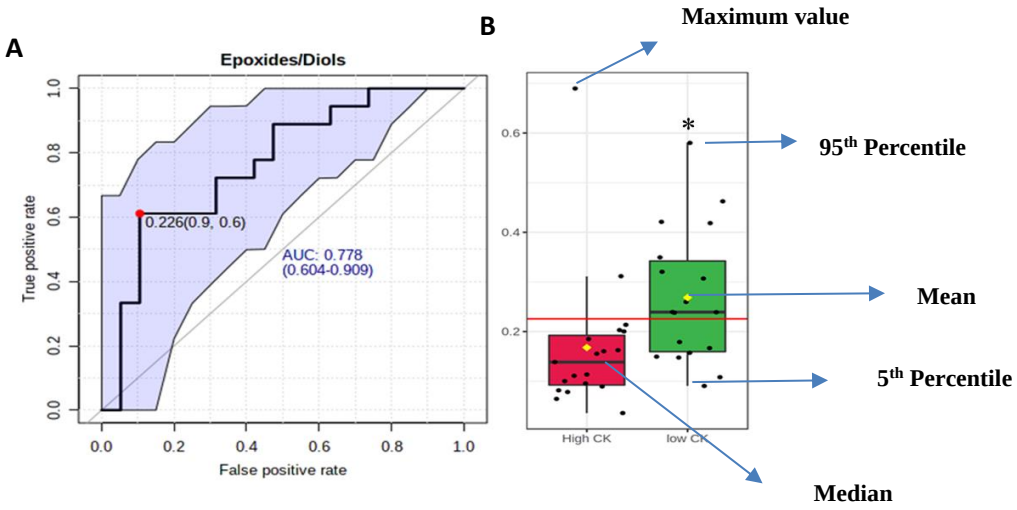

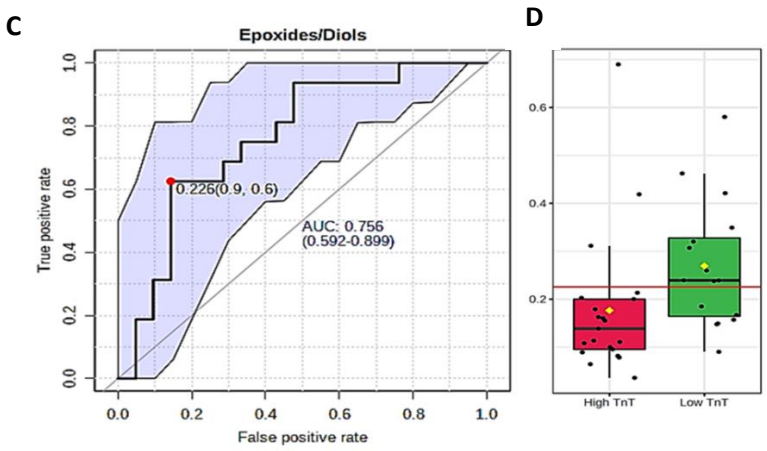

A: ROC based on creatine kinase (CK) levels, **B:** levels of epoxides/diols in patients with "low CK" and "high CK" levels. **C:** ROC based on Troponin T (TnT) levels, **D:** levels of epoxides/diols in patients with "low TnT" and "high TnT" levels. The box is determined by the 25th and 75th percentiles. The whiskers are determined by the 5th and 95th percentiles**.**

Discussion

The results of this study demonstrated significant changes in the oxylipin profile of STEMI patients during I/R. We also found that a certain group of oxylipins can be used as a potential biomarker of myocardial injury after MI.

LA-derived oxylipins were the dominant metabolites in the plasma of our participants, both STEMI patients and controls at baseline. This observation is consistent with previous studies (21-23), in which authors suggested that elevated plasma levels of oxidized metabolites of LA can be attributed to the higher consumption of vegetable oils containing LA in the western diet (24, 25). 20-COOH-AA, 9-HODE, and 13-HODE were the three most abundant compounds in the plasma of our participants. These findings are in line with the findings of previous research. For instance, Quehenberger et al., (2010) (26) conducted a detailed lipidomics analysis of standard reference material plasma (SRM1950) using HPLC-MS/MS. 13-HODE and 9-HODE were the most abundant oxylipins measured in SRM 1950 plasma. However, 20-COOH-AA was not measured in these samples. In a study by Loomba et al., (2015) (27) 13-HODE, 20-COOH-AA, and 9-HODE were the dominant oxylipins in the plasma of healthy controls. In two other studies also 13-HODE and 9-HODE were the dominant oxylipins in the plasma of healthy individuals, However, the reported concentrations in these studies were hugely different compared with previous studies (28, 29). Therefore, it can be suggested that 13-HODE 9-HODE and 20-COOH-AA are among the most abundant oxylipins in human plasma, but there is a large variation in the reported concentrations between studies.

To understand how ischemia affects plasma oxylipins levels, we compared oxylipin profiles of STEMI patients during the ischemic episode with controls. Our data demonstrated that among all oxylipin groups, DHA-derived metabolites may have significant impacts during ischemia. Firstly, DHA-derived oxylipins were the only group of oxylipins (based on FA precursor) that elevated significantly during ischemia compared with controls. Secondly, 10 out of 14 metabolites that were significantly correlated with the markers of cardiac injury (such as CK and TnT) were DHA-derived oxylipins (Table 16). Thirdly, 17-keto DHA had the largest fold change among all oxylipin metabolites during ischemia (115-Fold change) and its levels were significantly correlated with IL-10 levels during ischemia (r=0.51, p<0.05) (data not shown). 17-keto DHA is a metabolite of the 17-HDHA (also abbreviated as 17-HDoHE), which is generated through 15-LOX and COX-2

pathways. Interestingly, aspirin can also increase the production of 17-HDHA from COX-2 (28). Subsequently, 17-HDHA can be converted to 17-keto DHA by the action of a dehydrogenase enzyme (28, 29). It is reported that 17-keto DHA is an agonist of peroxisome proliferator-activated receptors (PPAR) alpha (α) and gamma (γ) (30). PPARs are transcription factors that regulate the expression of genes involved in lipid metabolism, energy production, oxidative stress and inflammation (31). Previous data suggested that elevated activities of both PPAR-α and γ during I/R were accompanied by cardioprotective effects (32, 33). Increased concentrations of DHA-derived compounds following MI was also seen in a prospective observational study, in which specialized pro-resolving mediators were quantified in patients with STEMI (n=15), stable coronary artery disease (CAD) (n=10), and healthy controls (n=10) (10). It is found that levels of DHA-derived oxylipins that were generated through the LOX pathway, namely, protectins, increased significantly after the onset of STEMI compared with both CAD and control groups. They suggested that elevated levels of DHA-derived oxylipins after vascular injury would be parts of the defensive mechanism to limit further tissue damage, through modulating inflammation (10). It should be mentioned that we did not detect plasma levels of protectins in our study, but our results also demonstrated the significant changes of DHA-derived oxylipins during myocardial I/R.

To find out which oxidative pathway activated mostly during ischemia, we categorized oxylipins based on their generation pathways. Total levels of the oxylipins produced through the LOX pathway did not differ significantly between Isch and control groups. However, we found that 5-LOX derived oxylipin were significantly elevated during ischemia and their levels were also significantly correlated with TNF-α levels at this time-point. Total levels of metabolites generated through the 15-LOX were also significantly elevated during the ischemic episode. However, the only metabolite that increased significantly in this group was 17-keto DHA, which could be related to aspirin-enhanced COX-2 oxidation (28). Although total levels of 12-LOX derived metabolites did not change during ischemia, their levels were significantly correlated with the levels of inflammatory markers. These data may propose that 5-LOX pathway, rather than 12 and 15-LOX, is more activated during ischemia. Previous studies also reported elevated levels of the LOX derived compounds in myocardial ischemia. As mentioned before, it has been shown that DHA-derived metabolites generated through the LOX pathway were significantly elevated in STEMI patients compared with CVD patients and healthy controls (10). Hultén et al., (2012) (34) also

reported the upregulated mRNA expression of arachidonate (A)LOX-15, increased levels of ALOX-15 enzyme (but not ALOX-12) and its product, 15-HETE in the biopsies from the ischemic heart of patients who underwent coronary bypass surgery compared with non-ischemic heart tissue (35). However, serum levels of 15-HETE were not significantly different in patients with ischemic heart compared with controls (35). Previous experimental studies showed that pharmacological inhibition of LOX enzymes can attenuate cardiac I/R injury. For instance, administration of 1-keto-β-boswellic acid (11-keto BA), which is a selective 5-LOX inhibitor, demonstrated dose-dependent cardioprotective effects in an *in vivo* model of cardiac I/R, through the elevation of the antioxidant capacity and prevention of the inflammatory response (36). In another study, administration of baicalein, which is a 12/15-LOX enzymes inhibitor, led to the suppression of apoptosis and caspase 3 activity in the *in vitro* model of I/R (37). Moreover, baicalein treatment decreased infarct size and attenuated myocardial apoptosis, oxidative stress and inflammatory responses in an *in vivo* model of cardiac tissue (37). Taken together these data suggest that the LOX pathways, particulary 5-LOX enzymes, are activated during myocardial I/R and inhibition of these oxidative pathways can decrease cardiac injury through the suppression of apoptosis and modulation of oxidative and inflammatory responses (38).

Total levels of oxylipins derived through the CYP-h pathway were significantly elevated in the Isch group compared with controls. Looking at changing patterns of individual compounds in this group showed that 20-COOH-AA was responsible for the observed elevation (Table 17). 20-COOH-AA is a major metabolite of 20-HETE, which is formed by the action of alcohol dehydrogenase (ADH). Increased levels of 20-HETE during I/R has been reported in previous studies, which can induce vasoconstriction and inflammation in the vasculature (39). Although the biological properties of 200-COOH-AA are not well studied, previous studies reported its vasodilatory effects in the porcine coronary artery (40) and being a dual activator of PPAR-α and PPAR-γ receptors in COS-7 cells (41). Therefore, it can be suggested that conversion of 20-HETE to 20-COOH-AA by ADH could be a defensive mechanism against ischemia to increase vasodilation and modulate inflammation. However, further studies are needed to confirm it.

Total levels of oxylipins that were generated through the CYP-e pathway did not significantly differ between Isch and control groups. However, the total epoxides/diols ratio reduced significantly during ischemia, which reflects the elevated activity of the sEH enzyme during the

ischemic episode. The reduction in epoxides/diols was seen in n-6 but not n-3 derived metabolites, suggesting that the sEH enzyme has more affinity to n-6 than n-3 FAs substrates. Previously, it was reported that the administration of both EpOME and DiHOME (LA metabolites) reduced post-ischemic functional recovery and contractility of the heart. However, the administration of sEH inhibitors blocked only the destructive effects of EpOME, but not DiHOME. They suggested that increased activity of sEH and therefore higher levels of DiHOME, can result in cardiotoxic effects through increasing ROS production, left ventricular (LV) depression, mitochondrial damage, changing action potential properties in ventricular myocytes, and tachycardia (42).

Taken together, plasma oxylipin profile alters significantly during the ischemic episode. Changes in the oxylipin profile were significantly associated with the markers of cardiac injury and cytokine concentrations. Among all oxylipin groups, levels of DHA-derived oxylipins increased significantly during ischemia. Their levels were also significantly correlated with IL-10 levels, suggesting their roles in modulating inflammation and thus protecting the myocardium against ischemia (10). Increased levels of 20-COOH-AA during ischemia, which can be attributed to higher ADH enzyme activity, can be another mechanism to protect the myocardium, most probably through its vasodilatory and anti-inflammatory effects (40,41). On the other hand, the sEH enzyme activated during the ischemic episode, which can have cardiotoxic effects through increasing ROS productions and/or inflammation by producing diols (43).

The second goal of this study was to investigate the effects of reperfusion on the oxylipin profile. As it is shown in Figure 30, levels of oxylipins were the highest during ischemia and 2h after reperfusion, with no significant differences between these two groups. Subsequently, oxylipin levels experienced significant reductions at 24h following reperfusion. The levels of oxylipins remained unchanged between 24h until 30-day post-PCI. Levels of inflammatory markers, namely TNF-α and MIP-1α also reduced significantly after PCI (Figure 30). Interestingly, changing patterns of these inflammatory markers and total oxylipin levels during 30 days post-PCI were identical.

Categorizing oxylipins based on the FA precursors showed that the levels of oxylipin groups decreased significantly early after PCI. Elevated levels of oxylipins during ischemia and early after

reperfusion can be attributed to higher inflammatory and oxidative responses at this period, which diminished gradually after reperfusion.

After categorizing the oxylipins based on the generation pathway, it is revealed that total levels of LOX derived oxylipins decreased significantly after reperfusion. Sub-categorizing showed that total levels of the metabolites generated through the 5/12 LOX pathways reduced significantly after reperfusion. Their concentrations were also significantly correlated with the levels of inflammatory markers, namely TNF-α and MIP-1α. This may suggest that the 5/12 LOX pathways activities reduced by diminishing inflammatory responses after reperfusion. However, total levels of metabolites generated through the 15-LOX did not differ significantly during I/R. Looking at individual compounds in this group revealed that 17-Keto DHA and 17-Keto DPA are two compounds in this group that remained elevated during I/R. As mentioned before, 17-Keto DHA is produced from 17-HDHA (a DHA metabolite) by a dehydrogenase enzyme, namely 15-hydroxyprostaglandin dehydrogenase (15-PGDH). The 17-Keto DPA is also generated through the same generation pathways but from DPA (28). Therefore, the elevated levels of 17-Keto DHA and 17-Keto DPA can reflect the elevated activities of the dehydrogenase enzymes for 30 days post-PCI. Previously, it is reported that both 17-Keto DHA and 17-Keto DPA are PPAR-γ agonists (44). Activation of PPAR-γ leads to the cascade of events, such as activating Nrf2-dependent antioxidant responses and anti-inflammatory effects by modulating cytokine levels (28). 20-COOH-AA (a metabolite of the CYP-h pathway) was another compound that remained elevated during I/R. 20-COOH-AA is also a dual activator of PPAR-α and γ (41) and its vasodilatory effects have been shown in the porcine coronary artery (40). Similar to 17-Keto DHA and DPA, 20-COOH-AA is also produced by a hydrogenase enzyme. Therefore, it can be concluded that the activity of dehydrogenase enzymes remained elevated for 30 days post-MI, most probably to modulate oxidative and inflammatory responses. However, more investigations are needed to confirm these findings.

Total levels of the metabolites produced through the CYP-e pathway also did not differ significantly during I/R (Figure 33). However, there were significant reductions in the ratio of n-6 epoxides/diols following reperfusion (Figure 34), demonstrating that the sEH enzyme activity remained elevated during the 30 days of reperfusion. Interestingly, n-3 metabolites of sEH did not change significantly during I/R. Previous experimental studies showed that increased ratios of

EpOME/DiHOME (LA metabolites) and EpETrEs/ DiHETrEs (AA metabolites) were associated with better coronary reactive hyperemic response (45) and therefore vasodilation in coronary and aortas (46). Also, DiHOMEs were reported to have deleterious effects, including cytotoxic, cardio-depressive, and vascular contraction (47, 48). Furthermore, it is reported that polymorphism in the sEH gene (which led to higher sEH activity) were associated with cardiovascular diseases (49, 50). On the contrary, n-3 derived epoxides have been reported to modulate I/R injury. Samokhvalov et al., (2019) (51) demonstrated that the administration of 19,20 EpDPE to HL-1 cardiac cells (cardiac muscle cell line) resulted in cell viability, elevated mitochondria activity, and better contractility during hypoxia /reoxygenation. Moreover, they also showed that perfusion of 19,20 EpDPE 20 min before ischemia decreased I/R injury by preserving mitochondrial function and inhibiting nucleotide like receptor protein 3 (NLRP3) inflammasome activation (52). Therefore, we can postulate that elevated n-6 derived diols compared with n-3 metabolites could lead to I/R injury following MI.

Taken together, reperfusion caused significant reductions in plasma oxylipins levels in STEMI patients. These reductions were also significantly associated with cytokine changing patterns. 17-keto DHA, 17-Keto DPA, and 20-COOH-AA were three metabolites that remained elevated post-reperfusion. These compounds are produced by dehydrogenase enzymes from a particular oxylipin metabolite (28,30). Therefore, it can be suggested that these dehydrogenases remained activated for 30 days post-MI. Since all these three metabolites are PPARs agonists (41,44), they can modulate inflammatory and oxidative responses during I/R. However, further investigations are required to confirm these results. Moreover, sEH activity remained elevated during the first month after reperfusion, which led to increased levels of n-6 derived diols (DiHOME and DiHETrEs). Considering the cardiotoxic properties of this group of oxylipins, they have a role in I/R injury in STEMI patients.

The last goal of this study was to find a biomarker to predict the severity of the myocardial injury. We found that the ratio of epoxides to diols during ischemia could be a potential marker of having a smaller infarct size. This suggests that patients with lower ratios of epoxides to diols at baseline have a larger infarct size with AUC= 0.77 (p=0.03) based on CK levels and AUC=0.76 (p=0.054) based on TnT levels (Figure 35). Therefore, inhibiting the sEH enzyme before PCI would be considered a potential therapeutic option.

In conclusion, this study demonstrated a significant alteration in oxylipin profiles of STEMI patients. Increased levels of DHA-derived metabolite and inhibition of sEH enzyme activity could be considered as potential therapeutic options for I/R injury.

References

1. Prabhu SD, Frangogiannis NG. The biological basis for cardiac repair after myocardial infarction: from inflammation to fibrosis. Circulation research. 2016;119(1):91-112.
2. Thygesen K, Alpert JS, Jaffe AS, Chaitman BR, Bax JJ, Morrow DA, et al. Fourth universal definition of myocardial infarction (2018). Journal of the American College of Cardiology. 2018;72(18):2231-64.
3. Virani SS, Alonso A, Benjamin EJ, Bittencourt MS, Callaway CW, Carson AP, et al. Heart Disease and Stroke Statistics-2020 Update: A Report From the American Heart Association. Circulation. 2020:Cir0000000000000757.
4. Ravindran S, Kurian GA. The role of secretory phospholipases as therapeutic targets for the treatment of myocardial ischemia reperfusion injury. Biomedicine & Pharmacotherapy. 2017;92:7-16.
5. Wu M-y, Yiang G-t, Liao W-T, Tsai AP-Y, Cheng Y-L, Cheng P-W, et al. Current mechanistic concepts in ischemia and reperfusion injury. Cellular Physiology and Biochemistry. 2018;46(4):1650-67.
6. Nicholls SJ, Kastelein JJP, Schwartz GG, Bash D, Rosenson RS, Cavender MA, et al. Varespladib and Cardiovascular Events in Patients With an Acute Coronary Syndrome: The VISTA-16 Randomized Clinical Trial. JAMA. 2014;311(3):252-62.
7. Gabbs M, Leng S, Devassy JG, Monirujjaman M, Aukema HM. Advances in Our Understanding of Oxylipins Derived from Dietary PUFAs. Advances in Nutrition. 2015;6(5):513-40.
8. Jenkins CM, Cedars A, Gross RW. Eicosanoid signalling pathways in the heart. Cardiovascular research. 2009;82(2):240-9.
9. Mason RP, Libby P, Bhatt DL. Emerging Mechanisms of Cardiovascular Protection for the Omega-3 Fatty Acid Eicosapentaenoic Acid. Arteriosclerosis, thrombosis, and vascular biology. 2020;40(5):1135-47.
10. Fosshaug LE, Colas RA, Anstensrud AK, Gregersen I, Nymo S, Sagen EL, et al. Early increase of specialized pro-resolving lipid mediators in patients with ST-elevation myocardial infarction. EBioMedicine. 2019;46:264-73.
11. Horii Y, Nakaya M, Ohara H, Nishihara H, Watari K, Nagasaka A, et al. Leukotriene B4 receptor 1 exacerbates inflammation following myocardial infarction. The FASEB Journal. 2020.
12. Bhavsar I, Miller CS, Al-Sabbagh M. Macrophage inflammatory protein-1 Alpha (MIP-1 alpha)/CCL3: as a biomarker. General Methods in Biomarker Research and their Applications. 2015:223.
13. Bagchi AK, Surendran A, Malik A, Jassal DS, Ravandi A, Singal PK. IL-10 attenuates OxPCs-mediated lipid metabolic responses in ischemia reperfusion injury. Scientific reports. 2020;10(1):1-16.
14. Steen EH, Wang X, Balaji S, Butte MJ, Bollyky PL, Keswani SG. The role of the anti-inflammatory cytokine interleukin-10 in tissue fibrosis. Advances in wound care. 2020 Apr 1;9(4):184-98.
15. Monirujjaman M, Devassy JG, Yamaguchi T, Sidhu N, Kugita M, Gabbs M, Nagao S, Zhou J, Ravandi A, Aukema HM. Distinct oxylipin alterations in diverse models of cystic kidney diseases. Biochim Biophys Acta Mol Cell Biol Lipids. 2017 Dec;1862(12):1562-1574.
16. Leng S, Winter T, Aukema HM. Dietary LA and sex effects on oxylipin profiles in rat kidney, liver, and serum differ from their effects on PUFAs. J Lipid Res. 2017 Aug;58(8):1702-1712.
17. Deems R, Buczynski MW, Bowers-Gentry R, Harkewicz R, Dennis EA. Detection and quantitation of eicosanoids via high performance liquid chromatography-electrospray ionization-mass spectrometry. Methods in enzymology. 2007;432:59-82
18. Babuin L, Jaffe AS. Troponin: the biomarker of choice for the detection of cardiac injury. Cmaj. 2005;173(10):1191-202.
19. Caligiuri SP, Aukema HM, Ravandi A, Pierce GN. Elevated levels of pro-inflammatory oxylipins in older subjects are normalized by flaxseed consumption. Experimental gerontology. 2014;59:51-7.
20. Gouveia-Figueira S, Späth J, Zivkovic AM, Nording ML. Profiling the oxylipin and endocannabinoid metabolome by UPLC-ESI-MS/MS in human plasma to monitor postprandial inflammation. PLoS One. 2015;10(7).

21. Schuchardt JP, Schmidt S, Kressel G, Dong H, Willenberg I, Hammock BD, et al. Comparison of free serum oxylipin concentrations in hyper-vs. normolipidemic men. Prostaglandins, Leukotrienes and Essential Fatty Acids. 2013;89(1):19-29.
22. Whelan J, Fritsche K. Linoleic Acid. Advances in Nutrition. 2013;4(3):311-2.
23. Blasbalg TL, Hibbeln JR, Ramsden CE, Majchrzak SF, Rawlings RR. Changes in consumption of omega-3 and omega-6 fatty acids in the United States during the 20th century. The American Journal of Clinical Nutrition. 2011;93(5):950-62.
24. Quehenberger O, Armando AM, Brown AH, Milne SB, Myers DS, Merrill AH, et al. Lipidomics reveals a remarkable diversity of lipids in human plasma. J Lipid Res. 2010;51(11):3299-305.
25. Loomba R, Quehenberger O, Armando A, Dennis EA. Polyunsaturated fatty acid metabolites as novel lipidomic biomarkers for noninvasive diagnosis of nonalcoholic steatohepatitis. J Lipid Res. 2015;56(1):185-92.
26. Shearer GC, Harris WS, Pedersen TL, Newman JW. Detection of omega-3 oxylipins in human plasma and response to treatment with omega-3 acid ethyl esters. J Lipid Res. 2010;51(8):2074-81.
27. Chen G-y, Zhang Q. Comprehensive analysis of oxylipins in human plasma using reversed-phase liquid chromatography-triple quadrupole mass spectrometry with heatmap-assisted selection of transitions. Analytical and bioanalytical chemistry. 2019;411(2):367-85.
28. Groeger AL, Cipollina C, Cole MP, Woodcock SR, Bonacci G, Rudolph TK, et al. Cyclooxygenase-2 generates anti-inflammatory mediators from omega-3 fatty acids. Nature chemical biology. 2010;6(6):433.
29. Valdes AM, Ravipati S, Menni C, Abhishek A, Metrustry S, Harris J, et al. Association of the resolvin precursor 17-HDHA, but not D-or E-series resolvins, with heat pain sensitivity and osteoarthritis pain in humans. Scientific reports. 2017;7(1):1-8.
30. Egawa D, Itoh T, Akiyama Y, Saito T, Yamamoto K. 17-OxoDHA is a PPARα/γ dual covalent modifier and agonist. ACS Chemical Biology. 2016;11(9):2447-55.
31. Ravingerova T, Adameova A, Carnicka S, Nemcekova M, Kelly T, Matejikova J, et al. The role of PPAR in myocardial response to ischemia in normal and diseased heart. General physiology and biophysics. 2011;30(4):329-41.
32. Yue T-l, Bao W, Jucker BM, Gu J-l, Romanic AM, Brown PJ, et al. Activation of peroxisome proliferator–activated receptor-α protects the heart from ischemia/reperfusion injury. Circulation. 2003;108(19):2393-9.
33. Zhong C-B, Chen X, Zhou X-Y, Wang X-B. The role of peroxisome proliferator-activated receptor γ in mediating cardioprotection against ischemia/reperfusion injury. Journal of cardiovascular pharmacology and therapeutics. 2018;23(1):46-56.
34. Magnusson LU, Lundqvist A, Asp J, Synnergren J, Johansson CT, Palmqvist L, et al. High expression of arachidonate 15-lipoxygenase and proinflammatory markers in human ischemic heart tissue. Biochemical and Biophysical Research Communications. 2012;424(2):327-30.
35. Lundqvist A, Sandstedt M, Sandstedt J, Wickelgren R, Hansson GI, Jeppsson A, et al. The Arachidonate 15-Lipoxygenase Enzyme Product 15-HETE Is Present in Heart Tissue from Patients with Ischemic Heart Disease and Enhances Clot Formation. PLoS One. 2016;11(8):e0161629-e.
36. Elshazly SM, Abd El Motteleb DM, Nassar NN. The selective 5-LOX inhibitor 11-keto-β-boswellic acid protects against myocardial ischemia reperfusion injury in rats: involvement of redox and inflammatory cascades. Naunyn Schmiedebergs Arch Pharmacol. 2013;386(9):823-33.
37. Song L, Yang H, Wang H-X, Tian C, Liu Y, Zeng X-J, et al. Inhibition of 12/15 lipoxygenase by baicalein reduces myocardial ischemia/reperfusion injury via modulation of multiple signaling pathways. Apoptosis. 2014;19(4):567-80.
38. Xin L, Gao J, Lin H, Qu Y, Shang C, Wang Y, et al. Regulatory Mechanisms of Baicalin in Cardiovascular Diseases: A Review. Frontiers in Pharmacology. 2020;11:1601.
39. Rocic P, Schwartzman ML. 20-HETE in the regulation of vascular and cardiac function. Pharmacology & therapeutics. 2018;192:74-87.

40. Kaduce TL, Fang X, Harmon SD, Oltman CL, Dellsperger KC, Teesch LM, et al. 20-hydroxyeicosatetraenoic acid (20-HETE) metabolism in coronary endothelial cells. Journal of Biological Chemistry. 2004;279(4):2648-56.
41. Fang X, Dillon JS, Hu S, Harmon SD, Yao J, Anjaiah S, et al. 20-Carboxy-arachidonic acid is a dual activator of peroxisome proliferator-activated receptors α and γ. Prostaglandins & other lipid mediators. 2007;82(1-4):175-84.
42. Bannehr M, Löhr L, Gelep J, Haverkamp W, Schunck W-H, Gollasch M, et al. Linoleic acid metabolite DiHOME decreases post-ischemic cardiac recovery in murine hearts. Cardiovascular toxicology. 2019;19(4):365-71.
43. Deng Y, Theken KN, Lee CR. Cytochrome P450 epoxygenases, soluble epoxide hydrolase, and the regulation of cardiovascular inflammation. Journal of molecular and cellular cardiology. 2010;48(2):331-41.
44. Cipollina C. Endogenous generation and signaling actions of omega-3 fatty acid electrophilic derivatives. BioMed research international. 2015;2015.
45. Hanif A, Edin ML, Zeldin DC, Morisseau C, Nayeem MA. Effect of soluble epoxide hydrolase on the modulation of coronary reactive hyperemia: role of oxylipins and PPARγ. PLoS One. 2016;11(9).
46. Nayeem MA. Role of oxylipins in cardiovascular diseases. Acta Pharmacol Sin. 2018;39(7):1142-54.
47. Edin ML, Wang Z, Bradbury JA, Graves JP, Lih FB, DeGraff LM, et al. Endothelial expression of human cytochrome P450 epoxygenase CYP2C8 increases susceptibility to ischemia-reperfusion injury in isolated mouse heart. The FASEB Journal. 2011;25(10):3436-47.
48. Moghaddam MF, Grant DF, Cheek JM, Greene JF, Williamson KC, Hammock BD. Bioactivation of leukotoxins to their toxic diols by epoxide hydrolase. Nature medicine. 1997;3(5):562-6.
49. Koerner IP, Jacks R, DeBarber AE, Koop D, Mao P, Grant DF, et al. Polymorphisms in the human soluble epoxide hydrolase gene EPHX2 linked to neuronal survival after ischemic injury. Journal of Neuroscience. 2007;27(17):4642-9.
50. Lee CR, North KE, Bray MS, Fornage M, Seubert JM, Newman JW, et al. Genetic variation in soluble epoxide hydrolase (EPHX2) and risk of coronary heart disease: The Atherosclerosis Risk in Communities (ARIC) study. Human molecular genetics. 2006;15(10):1640-9.
51. Samokhvalov V, Jamieson KL, Darwesh AM, Keshavarz-Bahaghighat H, Lee TY, Edin M, et al. Deficiency of Soluble Epoxide Hydrolase Protects Cardiac Function Impaired by LPS-Induced Acute Inflammation. Frontiers in pharmacology. 2019;9:1572.
52. Darwesh AM, Jamieson KL, Wang C, Samokhvalov V, Seubert JM. Cardioprotective effects of CYP-derived epoxy metabolites of docosahexaenoic acid involve limiting NLRP3 inflammasome activation. Canadian Journal of Physiology and Pharmacology. 2018;97(6):544-56.

CHAPTER III-GENERAL DISCUSSION

In this work for the first time, we have defined the oxolipidomics changes in oxidized lipid species including both non-enzymatically generated OxPCs and enzymatically generated oxylipins during I/R injury. As mentioned before, both OxPC and oxylipin metabolites are bioactive and it is suggested that they have implications for the pathology of I/R injury.

It has been reported that OxPC species are potent inducers of cell death in smooth muscle cells, macrophages, and endothelial cells (1-3). Previous data from our laboratory have revealed that fragmented OxPCs, namely, PONPC, POVPC, PGPC, and KOdiAPC were produced following I/R in rat myocardium (4) and exogenous administration of OxPCs to cardiac cells triggers cell death (particularly POVPC and PONPC) in a dose-dependent manner (4). Therefore, the aim of the first study of this thesis was firstly to define the OxPC profile during I/R and then determine the temporal changes in their tissue levels following reperfusion. Secondly, our goal was to understand if tissue levels of OxPCs are correlated with the marker of tissue injury. Utilizing a rat model of renal I/R and a targeted oxolipidomic approach, we have shown for the first time that OxPC species were produced following renal I/R. Fifty-five distinct OxPC species were identified in rat kidney following I/R, including a variety of fragmented (aldehyde and carboxylic acid-containing species) and non-fragmented products. SOVPC, PONPC, and PAzPC were the three most abundant compounds generated after I/R in kidney tissue. Fragmented aldehyde containing OxPC (aldo-OxPC), particularly PONPC and SONPC increased significantly as early as 6h of reperfusion. Significant increments for fragmented acid-containing OxPCs (carboxy-OxPCs), such as PGPC and PAzPC, occurred after 24h of reperfusion. Furthermore, levels of aldo-OxPCs were more strongly (compared with other OxPCs groups) associated with the severity of I/R injury ($r=0.9$, $p<0.001$).

These findings were in accordance with the results obtained from our rat myocardial I/R model, in which exposure of rat myocardium to 1h of ischemia followed by 24h of reperfusion led to an increase in tissue levels of POVPC, PONPC, PGPC, and PAzPC concentrations (4). However, only 5 OxPC species were measured in this study. Interestingly, POVPC and PONPC, which are aldo-OxPC species, but not other identified OxPCs were elevated in the mitochondrial fraction of cardiomyocytes and mitochondria membrane. These two species also triggered the opening of the

mitochondria permeability pore in a concentration-dependent manner (4). Therefore, these data support our findings that OxPCs are generated and accumulated at tissue levels as a result of I/R and reflect the involvement of OxPC species in I/R injury. Moreover, based on these results, fragmented aldo-OxPCs were more potent at cell injury compared with other species.

Several mechanisms have been proposed for the toxicity of fragmented OxPCs. Incubation of rat vascular smooth muscle cells (rVSMCs) with 50 μM of POVPC and PGPC led to apoptotic events including DNA fragmentation, phosphatidylserine (PS) exposure on the cell surface, and reduction of the nuclear volume. In this study, POVPC was found more apoptogenic compared with PGPC (5). Ramprecht et al. showed that POVPC and PGPC induced apoptosis in human melanoma cells isolated from different stages of tumour progression. Human melanocytes (FOM), and melanoma cell lines including primary melanoma cells (SBcl2, WM35) or metastatic melanoma cells (WM9, WM164) were incubated with 25 μM and 50 μM of POVPC and PGPC for 6h. Lower concentrations of POVPC (25 μM) induced apoptosis in only SBcl2 and WM164 cells but with a higher concentration (50 μM), it stimulated apoptosis pathway in all cell groups. PGPC with either concentration of 25 or 50 μM induced apoptosis in only SBcl2 and WM9 cells, showing that POVPC is more apoptogenic than PGPC in these cell lines (6). The proposed mechanism of cell toxicity of POVPC and PGPC was through the "sphingomyelinase- mitogen-activated protein kinases (MAPK)" pathway. These fragmented OxPCs can activate sphingomyelinase, leading to the generation of ceramide from sphingomyelin (SM) (6). Ceramide then activates c-Jun N-terminal kinase (JNK) and p38 MAPK, which leads to caspase activation, PS exposure, and apoptosis (7).

It has been also reported that OxPC species induce apoptosis through mitochondrial damage and activating the intrinsic pathway. Exogenous administration of 5 μM of 1-O-hexadecyl- 2-azelaoyl-sn-glycero-3-phosphocholine (HAzPC), which is a synthetic fragmented OxPC and homolog of PAzPC, to promyelocytic HL60 cells and human umbilical vein endothelial cell (HUVEC) led to the activation of the apoptotic pathway. They showed that HAzPC migrates to mitochondria and activates the intrinsic caspase cascade. HAzPC, by interacting with Bcl-2 family proteins releases mitochondrial cytochrome c (cyt c) and apoptosis-inducing factor (AIF) and activates caspase 9 in these cells. This suggests that HAzPC targets intracellular mitochondria signaling and activates the intrinsic apoptotic cascade (8).

Recent data from our laboratory demonstrated that fragmented OxPCs activate the ferroptosis pathway (9). Ferroptosis is an iron-mediated type of regulated cell death that occurs due to exhaustion of glutathione, inhibition of glutathione peroxidase 4 (GPX4), and thus the accumulation of lipid hydroperoxide (10). GPX4 enzyme converts the toxic lipid peroxide to lipid alcohol by concurrent oxidizing of reduced glutathione (GSH) to oxidized glutathione (GSSG) (11, 12). In this study, treatment of cardiomyocytes with 10 μM of POVPC and PONPC caused cell death. However, caspase 3 activation, TUNEL staining, and nuclear HMGB1 activity were unaffected in cells treated with either POVPC or PONPC, demonstrating that apoptosis and necrosis pathways were not involved in cell death. In this study, both POVPC and PONPC suppressed GPX4, an enzyme implicated in ferroptosis. Finally, treatment of cardiomyocytes with ferrostatin-1, which is an inhibitor of ferroptosis suppressed cell death induced by OxPCs. Previous studies have also shown the beneficial effects of blocking of ferroptosis in myocardial I/R injury (13-16). Activation of ferroptosis has been reported in renal I/R as well (17). Oxolipidomic analysis of mouse kidneys lacking GPX4 (Gpx4−/− mouse) revealed that accumulation of phospholipid hydroperoxides such as PC, PE, and cardiolipin peroxide in the kidney leads to ferroptosis (18). A ferroptosis inhibitor has been shown to lessen renal I/R injury in an *in vitro* model (19).

In the next study of this thesis, we wanted to identify the OxPCs changes in the clinical setting of coronary reperfusion injury. We aimed to determine if: 1) OxPC species increase in the plasma following myocardial I/R; 2) Can any OxPCs predict the magnitude of I/R injury? To address these questions, blood samples were collected from STEMI patients at presentation before primary percutaneous coronary intervention PCI (PPCI) (ischemia) and at 4-time points post-PPCI representing as reperfusion groups. As controls, blood samples were collected from patients with non-obstructive coronary artery disease after diagnostic coronary angiography. Aspiration thrombectomy was also done in selected STEMI patients.

Twenty-two OxPC species were identified and quantified in the plasma of our participants using our HPLC-MS/MS system. PONPC, SONPC, and POVPC were the most abundant fragmented OxPC compounds in the plasma of our participants. Our study is of significance since few studies utilized HPLC-MS/MS for the determination of plasma OxPC levels. In plasma of STEMI patients, fragmented OxPCs were significantly elevated immediately after ischemia when

compared with control levels. Their concentrations remained elevated for 48h after reperfusion but rebounded to control levels at 30 days of I/R. The trend for non-fragmented OxPCs was opposite, in which they decreased during ischemia, and then increased gradually during 30 days of reperfusion. Interestingly, among fragmented OxPCs, levels of total aldo-OxPCs, but not acid-OxPCs, differed significantly during I/R. SOVPC, PONPC, and SONPC were three compounds responsible for the significant mean differences in the aldo-OxPCs concentrations. Moreover, the composition of OxPCs in the plasma at the time of STEMI presentation was different from the composition of coronary thrombus. Thrombus had a higher proportion of POVPC and SOVPC than plasma, although they both had high levels of PONPC. This indicates that plasma OxPC profile is not explained by OxPCs eluting out of the thrombus, rather, thrombus and plasma have different OxPC profiles that cannot be explained by a single common pathway.

Previous investigations in determining OxPC levels post PCI in plasma of STEMI patients have utilized the E06 antibody to determine OxPL/apoB concentrations. In these studies, OxPL/apoB concentrations peaked at 4-days post PCI (54% increase) compared with baseline levels. Subsequently, it decreased over 30 days but was still significantly higher (36%) compared with baseline levels. As mentioned before, in our study, total levels of fragmented OxPCs decreased significantly but non-fragmented OxPCs concentrations did not change over 30 days post-PCI. Therefore, our findings are not a duplicate of the E06 results. There are some possible explanations: 1) E06 antibody recognizes both free form and covalent adducts of aldo-OxPCs on apo (B100). Due to the high activity of fragmented OxPCs, particularly aldo-OxPCs, they can be attached to plasma proteins such as apo (B100), lipoprotein (a), albumin, and plasminogen, as previous studies confirmed the increased levels of these proteins following MI (20, 21). However, we measured only free forms of OxPCs species in the plasma of our participants. 2) OxPCs are readily detoxified by lipid-degrading enzymes such as lipoprotein-associated phospholipase A2 (Lp-PLA2), which elevates acutely after MI (22). Therefore, increased activation of Lp-PLA2 can affect plasma OxPC levels, although we did not measure Lp-PLA2 activity in this study. 3) OxPCs accumulate at the tissue levels, as we showed increased levels of OxPCs in renal tissue during I/R (23). Therefore, plasma levels may not be representative of tissue concentrations.

In the current study, we also found that plasma concentrations of POVPC and PONPC during the ischemic episode (before PCI) were significantly associated with peak creatine kinase (CK) levels,

which is a marker of myocardial injury. Patients who had elevated CK levels after MI (higher than the median CK levels), also had elevated POVPC and PONPC concentrations at baseline (ischemia) (2 times higher than patients with lower CK levels). These data are in accordance with the results of renal I/R in that OxPC species were correlated with the markers of tissue injury. Furthermore, there were weak but significant correlations between the levels of PONPC and POVPC with interferon-gamma (INF-γ) and interleukin-1β (IL-1β) concentrations during I/R. Following acute myocardial ischemia, pro-inflammatory responses are initiated to eliminate necrotic cell debris from the ischemic area. Reperfusion, however, exacerbates proinflammatory responses which leads to cell death and I/R injury (24). IFN-γ is one of the cytokines secreted by T-cells that stimulates the neutrophils and monocytes chemotaxis to the site of injury. It has been shown that deletion of IFN-γ from CD4+ T cells led to the reduction of infarct size and accumulation of T-cell and neutrophil in myocardium at 24 h post-infarction (25). IL-1β is another inflammatory cytokine produced following I/R. It has been reported that pro-inflammatory response following MI can cause cardiomyocyte apoptosis, contractile dysfunction, matrix deposition which lead to adverse left ventricular (LV) remodeling following MI (24). Inhibition of IL-1β receptor with anakinra in STEMI patients improved left ventricular (LV) function with reduced inflammatory markers (26, 27). Also, the administration of IL-1β antibody led to a reduced rate of recurrent heart failure (HF) (28).

Taken together, the correlation between OxPC species, namely, PONPC and POVPC with CK levels and inflammatory cytokines can suggest their roles in I/R injury and LV remodeling following I/R.

This study has several potential limitations: First, our sample size was relatively small considering the high prevalence of comorbidities and medication use in the STEMI population. Due to the small sample size, we were not able to rule out the effects of confounding factors such as sex, age, ethnicity, etc. However, serial blood sampling helped to reduce inter-individual variability and clinical confounders. Hence, it is important to validate the findings of this study in a relatively larger cohort study. Second, considering there are no available commercial standards for individual OxPC species, the reported concentrations are relative rather than absolute.

As a summary, we showed for the first time that OxPC species, particularly fragmented species, were produced and accumulated at tissue levels (kidney tissue) following I/R and their levels were significantly associated with the marker of tissue injury. Furthermore, we also demonstrated for the first time that levels of OxPCs also altered in a clinical setting of myocardial I/R as fragmented OxPCs concentrations decreased significantly over 30 days post-reperfusion while non-fragmented OxPCs experienced non-significant increases during this time in patients with STEMI. Plasma and thrombus have different OxPC profiles. Furthermore, levels of fragmented OxPCs, namely POVPC and PONPC, were significantly correlated with markers of cardiac injury and inflammation in this population.

Future directions (OxPC part):

The results of both studies presented here (AKI and MI) revealed that OxPCs, particularly, aldehyde containing species increase during I/R and were significantly correlated with the markers of tissue injury, such as plasma creatinine and peak plasma CK levels. Considering that OxPC compounds are immunogenic, antibody treatment may serve as a therapeutic option for I/R injury. One of the potential candidates for the neutralization of OxPCs is the E06 antibody. Recent data from our laboratory showed that introducing E06 at 10 ug/ml concentration prevented POVPC and PONPC-related cardiomyocyte cell death by 74% (4). Similar findings were obtained in an *in vivo* model using transgenic mice overexpressing single-chain variable fragment of the E06 antibody (E06-scFv-Tg) (4). In this experiment, infarct size was significantly smaller (66%) in E06-mice compared with controls, which was attributed to the interaction of E06 and aldo-OxPCs (4). Based on the promising results of these studies, we are currently conducting a pilot study in a swine model of MI. After an ischemic episode induced by balloon occlusion, the E06 antibody (0.5 mg) was distributed by an intracoronary catheter at the time of reperfusion. The preliminary results are demonstrating a decrease in the infarct size in animals received E06 compared to the ones that received saline infusion. This will be the final goal of our future studies to prevent I/R injury. However, further studies are needed to find the right dose (probably for different diseases associated with I/R), the pharmacokinetics of E06 administration in humans, and the chronic systemic effects of the E06 infusion before clinical studies can be initiated.

In this thesis, we also investigated the role of enzymatically produced oxidized lipids (oxylipins), as another group of bioactive lipid molecules that implicate in I/R injury. Previous studies showed

the activation of membrane enzymes, such as PLA2 during I/R. This acute response leads to the breakdown of membrane phospholipids, release of polyunsaturated fatty acids (PUFAs), and generation of oxylipins (29). Oxylipins exert various biological effects in I/R injury. For instance, oxylipins derived from n-6 PUFA, such as arachidonic acids (AA) and linoleic acids (LA) are involved in inflammation, changing ion channels functions, and ventricular remodeling (30) whereas oxylipins derived from n-3 PUFA have anti-inflammatory, anti-arrhythmic and cardio-protective properties (31).

The questions we sought to investigate here were as follows: how does myocardial I/R affect the oxylipin profile in STEMI patients? Are oxylipin changes correlated with markers of myocardial injury? Can any oxylipin metabolite or group predict the magnitude of I/R injury? To respond to these questions, we analyzed the plasma oxylipin profile of our STEMI samples using HPLC-MS/MS.

The oxylipin profile underwent dramatic changes during I/R. We believe docosahexaenoic acid (DHA) oxidized metabolites have significant roles during ischemia due to the following reasons. Firstly, categorizing oxylipins based on their FA precursors showed that among all oxylipin groups, only total levels of DHA-derived oxylipins were significantly elevated during ischemia compared with the control group, particularly metabolites that were generated through the lipoxygenase (LOX) pathway. Secondly, their concentrations were correlated with the markers of cardiac injury (CK) and troponin (TnT) during the ischemic episode. Ten out of 14 metabolites that were significantly correlated with CK and TnT levels were DHA-derived metabolites. DHA-derived metabolites were also significantly correlated with interleukin-10 (IL-10), which is an anti-inflammatory cytokine. These data suggest that elevated levels of DHA-derived oxylipins during ischemia could be parts of the defensive mechanism to limit further tissue damage by modulating inflammation (32) and promoting the cardiac healing process (33).

Preclinical studies have shown that both acute and chronic administration of n-3 FA can decrease myocardial I/R injury through activation of anti-apoptotic pathways (34), microvascular protection (35), modulating inflammation (36), and decreasing infarct size (37). However, changes in oxylipin profiles were not assessed in these studies.

Zirpoli et al. examined the effects of the acute administration of n-3 rich triglyceride (n-3 TG) emulsions on myocardial I/R injury in both *in vivo* and *ex vivo* models. In the *in vivo* model, myocardial ischemia was induced by ligation of the left anterior descending coronary artery (LAD) in C57BL/6 mice (12-14 weeks old). N-3 TG emulsion (1.5g/kg body weight) was administrated immediately after inducing ischemia and before reperfusion. Mice were sacrificed after 48h of reperfusion. They found that infarct size was significantly smaller in the n-3 TG emulsion group compared with saline-treated mice ($p<0.05$). Moreover, plasma lactate dehydrogenase (LDH), which is a key marker of myocardial injury, was significantly lower in n-3 TG treated mice compared with controls ($p<0.05$). In the *ex vivo* model, hearts were perfused (using the Langendorff technique) and treated with n-3 TG emulsion (300 mgTG/100ml) during reperfusion. Myocardial I/R injury was determined by assessing the left ventricular developed pressure (LVDP) recovery in hearts. Heart perfusates were also collected after 1h reperfusion to detect total LDH levels. In this model, LVDP recovery was improved in the n-3 TG emulsion group that was treated with n-3 TG emulsion compared with the control ($p<0.05$). LDH release was also significantly lower in the n-3 TG emulsion group compared with the control ($p<0.05$). In this study, the cardioprotective effects of n-3 emulsion were mediated through the activation of anti-apoptotic pathways namely PI3K/AKT signalling pathways (34).

The positive effects of n-3 PUFA, including fish oil and triacylglycerol (TAG) form of DHA and eicosapentaenoic acid (EPA), were shown on microvascular permeability following myocardial I/R by Souza et al (35). They examined the effects of 14 days pre-treatment of male Syrian hamsters (7–10 weeks old) with fish oil (0.5 ml/day), and various dosages of EPA and DHA in TAG forms (0.004, 0.02, 0.1 ml/day) on vascular permeability following I/R. Hamsters were exposed to 30 min of myocardial ischemia followed by 15, 30, or 45 min of reperfusion. They found that the TAG form of both EPA and DHA decreased vascular macromolecular permeability and leukocyte adhesion to endothelium. Nevertheless, only DHA supplementation reduced leukocyte rolling following I/R. Farias et al., (36) investigated if a diet containing n-3 PUFA (0.6 g/kg/day; DHA:EPA = 3:1) can decrease I/R injury in a rat myocardial I/R. Following 8 weeks of supplementation of ten-week-old male Wistar rats, hearts were subjected to 30 min of ischemia and 120 min of reperfusion. Rats in the supplemented group developed significantly smaller infarct size (2-times smaller) and higher LVDP compared with the non-supplemented group. Tissue levels of oxidative stress markers (such as thiobarbituric acid reactive substances (TBARS) and total

carbonyls) were significantly reduced whereas markers of antioxidant activity (namely, catalase, superoxide dismutase (SOD), glutathione peroxidase activity, and GSH/GSSG ratio) were significantly elevated in the supplemented group compared with control. Moreover, NF-κB activity and nuclear factor erythroid 2-related factor 2 (Nrf2) levels in cardiac tissue were significantly reduced in the supplemented group compared to the control.

Clinical studies have also confirmed the positive effects of n-3 PUFA supplementation on I/R injury following MI. In a double-blind, placebo-controlled trial the effects of 4 g/d ω-3 supplementations were assessed on LV remodeling after acute MI. Patients (n=358) were randomly assigned to either take 4 g/d ω-3 along with conventional therapy or conventional therapy alone. After 6 months of acute MI, ω-3 supplementation resulted in significant reductions of left ventricular end-systolic volume indexed (LVESVI) to body surface area (-5.4%) and non-infarct myocardial fibrosis (-2.1%) compared with control. Although infarct size reduced after 6 months in both groups, changes were not statistically significant (-8.8±39.9% in the ω-3 group versus -1.9±57.7% in the controls). Moreover, ω-3 supplementation was also correlated with significant decreases in myeloperoxidase and lipoprotein-associated PLA2 levels and also concentrations of suppression of tumorigenicity 2 (ST2), which is a marker of myocardial fibrosis. Therefore, it was concluded that ω-3 supplementation provides an improvement in LV remodeling and non-infarct myocardial fibrosis through the suppression of inflammation at both systemic and myocardial levels after acute MI (38). A recent randomized control trial assessed the effects of ω-3 PUFA adjunctive therapy in MI patients who underwent PCI. Sixty patients were randomized within 3-7 days after hospital admission to either receive ω-3 PUFA (2gr/d) and guideline-adjusted therapy (10 mg/d rosuvastatin) or just guideline-adjusted therapy. Lipid profile and endothelial function were assessed during the first 3 months after AMI. They found that supplementation with 2gr/d ω-3 significantly decreased serum levels of triglycerides (-6.3%), apolipoprotein B (-4.9%), and lipoprotein (a) (-37.0%) and significantly increased serum concentrations of nitric oxide (62.2. Besides, the changes in the levels of these variables were positively correlated with changes in the levels of 16,17- EpDPE (a DHA metabolite), and epoxyeicosatetraenoic acids (EpETE) (a metabolite of EPA) (39).

Taken together, these data support the cardioprotective effects of n-3 FA on myocardial I/R injury. One of the drawbacks of these studies is that changes in oxylipin levels were not assessed in these

studies (only one study measured oxylipin metabolites after ω-3 supplementation (39)). Therefore, it is unknown which groups of oxylipins mediate the cardioprotective effects of ω-3 supplementation post-MI. Moreover, in clinical studies, the effects of chronic administrations of n-3 FA treatment were investigated in STEMI patients. Considering that in our study alterations in DHA-derived oxylipins occured acutely during the ischemic episode, the acute infusion of DHA (in a form of emulsion) before PCI, rather than chronic supplementation after MI, could be examined as a potential therapeutic option.

We also found the increased levels of 20-carboxy-arachidonic acid (20-COOH-AA), 17-Keto DHA, and 17-Keto docosapentaenoic acid (17-Keto DPA) during I/R. All these three compounds are produced by dehydrogenase enzymes from a particular oxylipin metabolite. The 20-COOH-AA is a major metabolite of 20- hydroxyeicosatetraenoic acid (20-HETE) and is formed by the alcohol dehydrogenase (ADH) from this oxylipin (40). The 17-Keto DHA is produced from 17-HDHA (a 15-LOX and COX-2 metabolite) by a dehydrogenase enzyme, namely 15-hydroxyprostaglandin dehydrogenase (15-PGDH). The 17-Keto DPA is also generated through the same pathway but from DPA rather than DHA (41). Therefore, it can be suggested that the elevated concentrations of these compounds during I/R can be attributed to the higher activity of dehydrogenase enzymes. However, more investigations are needed to confirm it. Previously, it has been reported that these three compounds are agonists of PPAR-α and/or γ (42,43). Activation of PPARs leads to the cascade of events, such as activating Nrf2-dependent antioxidant responses and anti-inflammatory effects by modulating cytokine levels (41). Several experimental studies showed that agonists of PPARs can reduce infarct size and improve cardiac and left ventricular functions after myocardial I/R (44).

The last important finding of our study was the increased levels of the metabolites produced by the soluble epoxide hydrolase (sEH) during I/R. We found a lower epoxides/diols ratio, particularly n-6 derived metabolites, in STEMI patients before and during 30 days after PCI. It has been reported that epoxides have cardioprotective and vasodilatory properties whereases diols exert cardiotoxic and vasoconstrictive effects. The ratio of epoxides to diols during ischemia was also correlated with increased levels of cardiac injury biomarker in our population.

Previous experimental studies showed that elevated ratios of EpOME/DiHOME (LA-metabolites) and EpETrEs/DiHETrEs (AA-metabolites) were correlated with the improved coronary reactive hyperemic response (45) and thus vasodilation in coronary arteries and aortas (46). Also, DiHOMEs exert cardiotoxic effects, such as cytotoxicity, cardio-depressive properties and cause vascular contraction (47, 48). Furthermore, polymorphism in the sEH gene (which was correlated with elevated sEH activity) has been associated with having cardiovascular diseases (49, 50).

Several preclinical studies demonstrated that the genetic deletion or pharmacological inhibition of sEH are associated with smaller infarct size and better post-ischemic recovery in an *in vivo* model of myocardial I/R. Motoki et al., (51) showed that infarct size was significantly smaller in sEH knockout mice and mice that were injected 12-(3-adamantan-1-yl-ureido)-dodecanoic acid butyl ester (AUDA-BE) compared with controls. AUDA-BE is an sEH inhibitor, which was injected 30 min before left coronary artery (LCA) occlusion or during ischemia 10 min before reperfusion (52). Furthermore, in a study by Chaudhary et al., (53) young and aged sEH null mice were exposed to 30 min of ischemia and 40 min of reperfusion. They showed that young and aged sEH null mouse hearts demonstrated significantly improved post-ischemic LVDP recovery (38.5% and 31.1%, respectively) and better contraction and relaxation rates compared to age-matched wild type. Similar effects were observed in young mice overexpressing CYP2J2 (CYP2J2 Tr), but not in aged mice. Mice overexpressing CYP2J2 have higher levels of 5,6-, 8,9-, 11,12-, and 14,15-EpETrEs. Therefore, they administered sEH inhibitor in aged CYP2J2 Tr to increase EpETrEs concentrations and assessed the cardiac recovery following I/R. CYP2J2 Tr mouse hearts were perfused with *t*-AUCB (100 nM), which resulted in improvement of post-ischemic functional recovery in aged CYP2J2 Tr hearts compared to controls (33.9% vs. 15.4%, respectively). This improvement was inhibited by MS-PPOH (CYP epoxygenase inhibitor) (15.9%). These data confirmed that *t*-AUCB induced cardioprotection in aged CYP2J2 Tr mice is due to inhibition of oxylipin metabolism. Moreover, sEH inhibition and thereby EpETrEs can protect the aged mouse hearts against I/R injury.

The proposed mechanism is that sEH deficiency or inhibition can limit innate immune responses through revoking the NLRP3 inflammasome cascade activation. During I/R, ROS, which are produced by dysfunctional mitochondria, can be sensed by NLRP3 protein which results in NLRP3 inflammasome aggregation (54). The NLRP3 inflammasome then facilitates the activation of

caspase-1 which converts pro-IL-1β to mature IL-1β. Subsequently, IL-1β initiates the cytokine and chemokine secretions which lead to the recruitment of neutrophils and monocytes and therefore, severe inflammatory responses and thus cell injury (55). Moreover, activated NLRP3 inflammasome transmits and translocates thioredoxin-interacting protein (Txnip) to the mitochondria which causes inhibition of antioxidant thioredoxin 2 (Trx-2) and leads to cardiomyocyte cell death during I/R (56, 57). In a study by Darwesh et al., (58), it was shown that sEH deficiency or inhibition prevents NLRP3 inflammasome activation by preserving mitochondria through preventing Txnip translocation, ameliorating ROS production and therefore, improved post-ischemic functional recovery. Taken together these data support the idea that sEH activity increases during I/R and the oxylipin products of this enzyme implicate in I/R injury. Hence, inhibiting the sEH enzyme before PCI could be considered as a potential therapeutic option.

As mentioned before, the main limitation of our study was a relatively small sample size. Therefore, the findings of this study should be confirmed in a larger cohort study.

Future directions (Oxylipin part):

Based on the findings of our study, increasing DHA-derived oxylipins levels, elevating 20-COOH-AA, 17-Keto DHA and 17-Keto DPA concentrations and inhibiting sEH enzyme during the ischemia or early after reperfusion can be considered as potential treatment options. Acute administration of n-3 FA, in a form of lipid emulsions, is a novel approach that has been studied in both experimental and clinical studies. In contrast to oral supplementation, IV administration results in acute integration of these FAs onto plasma lipids and membrane cells within 30 to 60 min (59-61). These abrupt changes in membrane FAs are beneficial in the settings of acute organ injury. As mentioned before, Zirpoli et al showed that acute administration of n-3 TG emulsion decreased infarct size in both *in vivo* and *ex vivo* models of myocardial I/R (34). Kollareth et al., (62) recently investigated the effects of acute administration of the DHA triglyceride emulsions in an *in vivo* model of cerebral I/R. Therefore, a clinical trial that assesses the effects of acute administration of DHA emulsion in STEMI patients could investigate their impact. In previous clinical studies, the effects of IV infusion of n-3 FAs have been tested in patients in intensive care (63), before cardiac surgery (64) and in healthy participants (65). For example, three IV infusion of triglyceride emulsion rich in both EPA and DHA (0.2 g/kg fish oil emulsion) before cardiac

surgery decreased the levels of IL-6 significantly after cardiac surgery compared with the control groups. It also led to rapid and significant increases in n-3 FAs levels in platelets and atrial tissue membranes (64). Therefore, administration of 0.2 g/kg fish oil emulsion before PCI can be examined in STEMI patients in a double-blind randomized control trial. The primary outcomes of this study will be plasma oxylipin profile, infarct size, and LV function at 30 days post-MI. Secondary outcomes will be markers of endothelial injury (such as e-selectin, p-selectin, vascular cell adhesion marker (VCAM-1), and intercellular adhesion molecule (ICAM-1)), and inflammation (such as TNF-α, INF- γ, IL-1β, IL-6, IL-8, etc).

We also found in our study that increased levels of 20-COOH, 17-Keto DHA and 17-Keto DPA during I/R. We postulated that their elevated levels are due to higher activity of dehydrogenase enzymes following MI. To test this hypothesis, a series of *in vitro* and *in vivo* studies can be designed. To examine how I/R affects the activity of these enzymes and their oxylipin metabolites an *in vitro* study can be conducted. Cardiomyocytes can be exposed to 1h of ischemia and reperfusion. Cell death, dehydrogenase enzymes activity (namely, ADH and 15 PGDH), along with the levels of their oxylipin products (including 20-COOH, 17-Keto DHA and 17-Keto DPA) can be measured during I/R. Next step, the effects of dehydrogenase enzyme inhibitors on cell death, and the levels of 20-COOH, 17-Keto DHA and 17-Keto DPA can be tested. 4-methylpyrazole (4-MP) (66) and SW033291(67) can be used as ADH and 15-PGDH inhibitors, respectively. Next, 20-COOH-AA, 17-Keto DHA and 17-Keto DPA can be exogenously administered to cardiomyocytes to see if the effects of dehydrogenases are due to higher concentrations of these metabolites. To investigate the mechanisms of action, apoptosis/necrosis pathways, PPARs activities, NF-κB, and Nrf2 can be also assessed in these experiments.

If the results of the studies are promising, an *in viv*o experiment can be conducted. Dehydrogenase enzymes inhibitors, 20-COOH-AA, 17-Keto DHA and 17-Keto DPA can be infused during ischemia and post-reperfusion in different study groups in a rat model of myocardial I/R. Infarct size, LV function, necrotic and apoptotic cell death assays, proinflammatory cytokine levels can be measure and compared between study groups.

The third finding of our study was the elevated levels of diols, which was attributed to the higher sEH enzyme activity. The beneficial effects of sEH enzyme inhibition have been shown in the

experimental model of myocardial I/R (52, 53, 58). Currently, a clinical trial is assessing the effects of sEH inhibitor drug (GSK2256294 (10 mg/day)) on cerebral ischemia (NCT03318783). Pharmacokinetics, pharmacodynamics and adverse effects of GSK2256294 evaluated in a clinical study in healthy and obese smokers (2–20 mg). GSK2256294 was well-tolerated with no serious adverse events attributable to this drug (68). Hence, the administration of this medication before PCI in MI patients can be tested in a double-blind randomized control trial (pilot study). STEMI patients will receive either sEH inhibitor (GSK2256294: 15 mg) along with the conventional therapy or conventional therapy and placebo after PCI in a single dose once daily for 30 days. Same as the DHA trial, primary outcomes will be plasma oxylipin profile, infarct size and LV function. As mentioned before, the secondary outcome will be markers of endothelial injury and inflammation.

Conclusion

Data of the current thesis demonstrated that oxidized lipids, namely OxPCs and oxylipins are produced during I/R. Using a targeted oxolipidomics approach, we were able to show that fragmented OxPC species are the predominant group of OxPCs in the plasma of patients with STEMI. Their levels increased during the ischemic episode but decreased during 30 days post-reperfusion. Also, PONPC and POVPC levels, which are categorized as a fragmented aldo-OxPC group, were correlated with levels of cardiac injury biomarker and inflammatory cytokines in these patients. Oxylipins also underwent major changes during 30 days post-MI. DHA-derived compounds were the only group of oxylipins that increased during the ischemic episode and their levels were significantly correlated with the markers of cardiac injury. On the contrary, ratios of epoxides/diols, particularly n-6 derived compounds, decreased during ischemia and 30 days post-reperfusion. The ratio of epoxides to diols during the ischemia was correlated with the levels of cardiac injury biomarker. Therefore, decreasing levels of the aldo-OxPCs by using antibody E06, increasing DHA-derived oxylipins levels and inhibiting the sEH enzyme can be proposed as potential therapeutic options for myocardial I/R in STEMI patients.

Chapter III References

1. Stemmer U, Dunai ZA, Koller D, Pürstinger G, Zenzmaier E, Deigner HP, et al. Toxicity of oxidized phospholipids in cultured macrophages. Lipids in health and disease. 2012;11(1):110.
2. Loidl A, Sevcsik E, Riesenhuber G, Deigner H-P, Hermetter A. Oxidized phospholipids in minimally modified low density lipoprotein induce apoptotic signaling via activation of acid sphingomyelinase in arterial smooth muscle cells. Journal of Biological Chemistry. 2003;278(35):32921-8.
3. Gargalovic PS, Imura M, Zhang B, Gharavi NM, Clark MJ, Pagnon J, et al. Identification of inflammatory gene modules based on variations of human endothelial cell responses to oxidized lipids. Proceedings of the National Academy of Sciences. 2006;103(34):12741-6.
4. Yeang C, Hasanally D, Que X, Hung M-Y, Stamenkovic A, Chan D, et al. Reduction of myocardial ischaemia-reperfusion injury by inactivating oxidized phospholipids. Cardiovasc Res. 2019;115(1):179-89.
5. Fruhwirth GO, Moumtzi A, Loidl A, Ingolic E, Hermetter A. The oxidized phospholipids POVPC and PGPC inhibit growth and induce apoptosis in vascular smooth muscle cells. Biochimica et Biophysica Acta (BBA)-Molecular and Cell Biology of Lipids. 2006;1761(9):1060-9.
6. Ramprecht C, Jaritz H, Streith I, Zenzmaier E, Köfeler H, Hofmann-Wellenhof R, et al. Toxicity of oxidized phosphatidylcholines in cultured human melanoma cells. Chemistry and physics of lipids. 2015;189:39-47.
7. Fruhwirth GO, Hermetter A. Mediation of apoptosis by oxidized phospholipids. Lipids in Health and Disease: Springer; 2008. p. 351-67.
8. Chen R, Yang L, McIntyre TM. Cytotoxic phospholipid oxidation products cell death from mitochondrial damage and the intrinsic caspase cascade. Journal of Biological Chemistry. 2007;282(34):24842-50.
9. Stamenkovic A, O'Hara KA, Nelson DC, Maddaford TG, Edel AL, Maddaford G, et al. Oxidized phosphatidylcholines trigger ferroptosis in cardiomyocytes during ischemia/reperfusion injury. Am J Physiol Heart Circ Physiol. 2021.
10. Lei P, Bai T, Sun Y. Mechanisms of ferroptosis and relations with regulated cell death: a review. Frontiers in physiology. 2019;10:139.
11. Brigelius-Flohé R, Maiorino M. Glutathione peroxidases. Biochimica et Biophysica Acta (BBA)-General Subjects. 2013;1830(5):3289-303.
12. Yang WS, SriRamaratnam R, Welsch ME, Shimada K, Skouta R, Viswanathan VS, et al. Regulation of ferroptotic cancer cell death by GPX4. Cell. 2014;156(1-2):317-31.
13. Gao M, Monian P, Quadri N, Ramasamy R, Jiang X. Glutaminolysis and transferrin regulate ferroptosis. Molecular cell. 2015;59(2):298-308.
14. Aoyagi T, Kusakari Y, Xiao CY, Inouye BT, Takahashi M, Scherrer-Crosbie M, et al. Cardiac mTOR protects the heart against ischemia-reperfusion injury. Am J Physiol Heart Circ Physiol. 2012;303(1):H75-85.
15. Baba Y, Higa JK, Shimada BK, Horiuchi KM, Suhara T, Kobayashi M, et al. Protective effects of the mechanistic target of rapamycin against excess iron and ferroptosis in cardiomyocytes. American Journal of Physiology-Heart and Circulatory Physiology. 2018;314(3):H659-H68.

16. Fang X, Wang H, Han D, Xie E, Yang X, Wei J, et al. Ferroptosis as a target for protection against cardiomyopathy. Proc Natl Acad Sci U S A. 2019;116(7):2672-80.
17. Su L, Jiang X, Yang C, Zhang J, Chen B, Li Y, et al. Pannexin 1 mediates ferroptosis that contributes to renal ischemia/reperfusion injury. J Biol Chem. 2019;294(50):19395-404.
18. Friedmann Angeli JP, Schneider M, Proneth B, Tyurina YY, Tyurin VA, Hammond VJ, et al. Inactivation of the ferroptosis regulator Gpx4 triggers acute renal failure in mice. Nat Cell Biol. 2014;16(12):1180-91.
19. Friedmann Angeli JP, Schneider M, Proneth B, Tyurina YY, Tyurin VA, Hammond VJ, et al. Inactivation of the ferroptosis regulator Gpx4 triggers acute renal failure in mice. Nat Cell Biol. 2014;16(12):1180-91.
20. Tsimikas S, Bergmark C, Beyer RW, Patel R, Pattison J, Miller E, et al. Temporal increases in plasma markers of oxidized low-density lipoprotein strongly reflect the presence of acute coronary syndromes. Journal of the American College of Cardiology. 2003;41(3):360-70.
21. Leibundgut G, Arai K, Orsoni A, Yin H, Scipione C, Miller ER, et al. Oxidized phospholipids are present on plasminogen, affect fibrinolysis, and increase following acute myocardial infarction. Journal of the American College of Cardiology. 2012;59(16):1426-37.
22. Li J, Wang H, Tian J, Chen B, Du F. Change in lipoprotein-associated phospholipase A2 and its association with cardiovascular outcomes in patients with acute coronary syndrome. Medicine (Baltimore). 2018;97(28):e11517-e.
23. Solati Z, Edel AL, Shang Y, O K, Ravandi A. Oxidized phosphatidylcholines are produced in renal ischemia reperfusion injury. PloS one. 2018;13(4):e0195172.
24. Ong S-B, Hernández-Reséndiz S, Crespo-Avilan GE, Mukhametshina RT, Kwek X-Y, Cabrera-Fuentes HA, et al. Inflammation following acute myocardial infarction: multiple players, dynamic roles, and novel therapeutic opportunities. Pharmacology & therapeutics. 2018;186:73-87.
25. Yang Z, Day Y-J, Toufektsian M-C, Xu Y, Ramos SI, Marshall MA, et al. Myocardial infarct-sparing effect of adenosine A2A receptor activation is due to its action on CD4+ T lymphocytes. Circulation. 2006;114(19):2056-64.
26. Silvain J, Kerneis M, Zeitouni M, Lattuca B, Galier S, Brugier D, et al. Interleukin-1β and risk of premature death in patients with myocardial infarction. Journal of the American College of Cardiology. 2020;76(15):1763-73.
27. Abbate A, Van Tassell BW, Biondi-Zoccai G, Kontos MC, Grizzard JD, Spillman DW, et al. Effects of interleukin-1 blockade with anakinra on adverse cardiac remodeling and heart failure after acute myocardial infarction [from the Virginia Commonwealth University-Anakinra Remodeling Trial (2)(VCU-ART2) pilot study]. The American journal of cardiology. 2013;111(10):1394-400.
28. Harouki N, Nicol L, Remy-Jouet I, Henry J-P, Dumesnil A, Lejeune A, et al. The IL-1β antibody gevokizumab limits cardiac remodeling and coronary dysfunction in rats with heart failure. JACC: Basic to Translational Science. 2017;2(4):418-30.
29. Nicholls SJ, Kastelein JJP, Schwartz GG, Bash D, Rosenson RS, Cavender MA, et al. Varespladib and Cardiovascular Events in Patients With an Acute Coronary Syndrome: The VISTA-16 Randomized Clinical Trial. JAMA. 2014;311(3):252-62.
30. Jenkins CM, Cedars A, Gross RW. Eicosanoid signalling pathways in the heart. Cardiovascular research. 2009;82(2):240-9.

31. Mason RP, Libby P, Bhatt DL. Emerging Mechanisms of Cardiovascular Protection for the Omega-3 Fatty Acid Eicosapentaenoic Acid. Arteriosclerosis, thrombosis, and vascular biology. 2020;40(5):1135-47.
32. Fosshaug LE, Colas RA, Anstensrud AK, Gregersen I, Nymo S, Sagen EL, et al. Early increase of specialized pro-resolving lipid mediators in patients with ST-elevation myocardial infarction. EBioMedicine. 2019;46:264-73.
33. Jung M, Ma Y, Iyer RP, DeLeon-Pennell KY, Yabluchanskiy A, Garrett MR, Lindsey ML. IL-10 improves cardiac remodeling after myocardial infarction by stimulating M2 macrophage polarization and fibroblast activation. Basic research in cardiology. 2017 May 1;112(3):33.
34. Zirpoli H, Abdillahi M, Quadri N, Ananthakrishnan R, Wang L, Rosario R, et al. Acute administration of n-3 rich triglyceride emulsions provides cardioprotection in murine models after ischemia-reperfusion. PLoS One. 2015;10(1):e0116274.
35. Souza MdGCd, Conde CMS, Laflôr CM, Sicuro FL, Bouskela E. n-3 PUFA Induce Microvascular Protective Changes During Ischemia/Reperfusion. Lipids. 2015;50(1):23-37.
36. Farías JG, Carrasco-Pozo C, Carrasco Loza R, Sepúlveda N, Álvarez P, Quezada M, et al. Polyunsaturated fatty acid induces cardioprotection against ischemia-reperfusion through the inhibition of NF-kappaB and induction of Nrf2. Exp Biol Med (Maywood). 2017;242(10):1104-14.
37. Liu R, Li Z, Wang Q. Resolvin D1 Attenuates Myocardial Infarction in a Rodent Model with the Participation of the HMGB1 Pathway. Cardiovascular Drugs and Therapy. 2019;33(4):399-406.
38. Heydari B, Abdullah S, Pottala JV, Shah R, Abbasi S, Mandry D, et al. Effect of Omega-3 Acid Ethyl Esters on Left Ventricular Remodeling After Acute Myocardial Infarction. Circulation. 2016;134(5):378-91.
39. Yuan M, Zhang Y, Hua T, Liu X-L, Liu T, Yuan R-Y, et al. Omega-3 polyunsaturated fatty acid supplementation improves lipid metabolism and endothelial function by providing a beneficial eicosanoid-pattern in patients with acute myocardial infarction: A randomized, controlled trial. Clinical Nutrition. 2021;40(2):445-59.
40. Kaduce TL, Fang X, Harmon SD, Oltman CL, Dellsperger KC, Teesch LM, et al. 20-hydroxyeicosatetraenoic acid (20-HETE) metabolism in coronary endothelial cells. J Biol Chem. 2004;279(4):2648-56.
41. Wendell SG, Golin-Bisello F, Wenzel S, Sobol RW, Holguin F, Freeman BA. 15-Hydroxyprostaglandin dehydrogenase generation of electrophilic lipid signaling mediators from hydroxy ω-3 fatty acids. Journal of Biological Chemistry. 2015 Feb 27;290(9):5868-80.
42. Fang X, Dillon JS, Hu S, Harmon SD, Yao J, Anjaiah S, et al. 20-Carboxy-arachidonic acid is a dual activator of peroxisome proliferator-activated receptors α and γ. Prostaglandins & other lipid mediators. 2007;82(1-4):175-84.
43. Cipollina C. Endogenous generation and signaling actions of omega-3 fatty acid electrophilic derivatives. BioMed research international. 2015;2015.
44. Wagner K-D, Wagner N. PPARs and Myocardial Infarction. International Journal of Molecular Sciences. 2020;21(24):9436.
45. Hanif A, Edin ML, Zeldin DC, Morisseau C, Nayeem MA. Effect of soluble epoxide hydrolase on the modulation of coronary reactive hyperemia: role of oxylipins and PPARγ. PLoS One. 2016;11(9).

46. Nayeem MA. Role of oxylipins in cardiovascular diseases. Acta Pharmacol Sin. 2018;39(7):1142-54.
47. Edin ML, Wang Z, Bradbury JA, Graves JP, Lih FB, DeGraff LM, et al. Endothelial expression of human cytochrome P450 epoxygenase CYP2C8 increases susceptibility to ischemia-reperfusion injury in isolated mouse heart. The FASEB Journal. 2011;25(10):3436-47.
48. Moghaddam MF, Grant DF, Cheek JM, Greene JF, Williamson KC, Hammock BD. Bioactivation of leukotoxins to their toxic diols by epoxide hydrolase. Nature medicine. 1997;3(5):562-6.
49. Koerner IP, Jacks R, DeBarber AE, Koop D, Mao P, Grant DF, et al. Polymorphisms in the human soluble epoxide hydrolase gene EPHX2 linked to neuronal survival after ischemic injury. Journal of Neuroscience. 2007;27(17):4642-9.
50. Lee CR, North KE, Bray MS, Fornage M, Seubert JM, Newman JW, et al. Genetic variation in soluble epoxide hydrolase (EPHX2) and risk of coronary heart disease: The Atherosclerosis Risk in Communities (ARIC) study. Human molecular genetics. 2006;15(10):1640-9.
51. Motoki A, Merkel MJ, Packwood WH, Cao Z, Liu L, Iliff J, et al. Soluble epoxide hydrolase inhibition and gene deletion are protective against myocardial ischemia-reperfusion injury in vivo. Am J Physiol Heart Circ Physiol. 2008;295(5):H2128-34.
52. Motoki A, Merkel MJ, Packwood WH, Cao Z, Liu L, Iliff J, et al. Soluble epoxide hydrolase inhibition and gene deletion are protective against myocardial ischemia-reperfusion injury in vivo. American journal of physiology Heart and circulatory physiology. 2008;295(5):H2128-H34.
53. Chaudhary KR, Zordoky BNM, Edin ML, Alsaleh N, El-Kadi AOS, Zeldin DC, et al. Differential effects of soluble epoxide hydrolase inhibition and CYP2J2 overexpression on postischemic cardiac function in aged mice. Prostaglandins Other Lipid Mediat. 2013;104-105:8-17.
54. Zhou R, Yazdi AS, Menu P, Tschopp J. A role for mitochondria in NLRP3 inflammasome activation. Nature. 2011;469(7329):221-5.
55. Mastrocola R, Penna C, Tullio F, Femminò S, Nigro D, Chiazza F, et al. Pharmacological inhibition of NLRP3 inflammasome attenuates myocardial ischemia/reperfusion injury by activation of RISK and mitochondrial pathways. Oxidative medicine and cellular longevity. 2016;2016.
56. Zhou R, Tardivel A, Thorens B, Choi I, Tschopp J. Thioredoxin-interacting protein links oxidative stress to inflammasome activation. Nature immunology. 2010;11(2):136-40.
57. Saxena G, Chen J, Shalev A. Intracellular shuttling and mitochondrial function of thioredoxin-interacting protein. Journal of Biological Chemistry. 2010;285(6):3997-4005.
58. Darwesh AM, Keshavarz-Bahaghighat H, Jamieson KL, Seubert JM. Genetic deletion or pharmacological inhibition of soluble epoxide hydrolase ameliorates cardiac ischemia/reperfusion injury by attenuating NLRP3 inflammasome activation. International Journal of Molecular Sciences. 2019;20(14):3502.
59. Carpentier YA, Peltier S, Portois L, Sener A, Malaisse WJ. Rapid lipid enrichment in ω3 fatty acids: Liver data. International journal of molecular medicine. 2008;21(3):367-73.
60. Pittet YK, Berger MM, Pluess T-T, Voirol P, Revelly J-P, Tappy L, et al. Blunting the response to endotoxin in healthy subjects: effects of various doses of intravenous fish oil. Intensive care medicine. 2010;36(2):289-95.

61. Simoens CM, Deckelbaum RJ, Massaut JJ, Carpentier YA. Inclusion of 10% fish oil in mixed medium-chain triacylglycerol–long-chain triacylglycerol emulsions increases plasma triacylglycerol clearance and induces rapid eicosapentaenoic acid (20: 5n− 3) incorporation into blood cell phospholipids. The American journal of clinical nutrition. 2008;88(2):282-8.
62. Manual Kollareth DJ, Deckelbaum RJ, Liu Z, Ramakrishnan R, Jouvene C, Serhan CN, et al. Acute injection of a DHA triglyceride emulsion after hypoxic-ischemic brain injury in mice increases both DHA and EPA levels in blood and brain(☆). Prostaglandins Leukot Essent Fatty Acids. 2020;162:102176.
63. Calder PC, Deckelbaum RJ. Intravenous fish oil in hospitalized adult patients: reviewing the reviews. Current Opinion in Clinical Nutrition & Metabolic Care. 2013;16(2):119-23.
64. Berger MM, Delodder F, Liaudet L, Tozzi P, Schlaepfer J, Chiolero RL, et al. Three short perioperative infusions of n-3 PUFAs reduce systemic inflammation induced by cardiopulmonary bypass surgery: a randomized controlled trial. Am J Clin Nutr. 2013;97(2):246-54.
65. Carpentier YA, Hacquebard M, Portois L, Dupont IE, Deckelbaum RJ, Malaisse WJ. Rapid cellular enrichment of eicosapentaenoate after a single intravenous injection of a novel medium-chain triacylglycerol: fish-oil emulsion in humans. The American journal of clinical nutrition. 2010;91(4):875-82.
66. Dudka J, Burda F, Madej B, Szumilo J, Tokarska E, Korobowicz A, Klepacz R, Korobowicz E. Effect of selected alcohol dehydrogenase inhibitors on the human heart lactate dehydrogenase activity-an in vitro study. Acta Physiologica Hungarica. 2004 Nov 1;91(3-4):235-41.
67. Kim HJ, Kim SH, Kim M, Baik H, Park SJ, Kang MS, Kim DH, Kim BW, Markowitz SD, Bae KB. Inhibition of 15-PGDH prevents ischemic renal injury by the PGE2/EP4 signaling pathway mediating vasodilation, increased renal blood flow, and increased adenosine/A2A receptors. American Journal of Physiology-Renal Physiology. 2020 Dec 1;319(6):F1054-66.
68. Lazaar AL, Yang L, Boardley RL, Goyal NS, Robertson J, Baldwin SJ, et al. Pharmacokinetics, pharmacodynamics and adverse event profile of GSK2256294, a novel soluble epoxide hydrolase inhibitor. Br J Clin Pharmacol. 2016;81(5):971-9.

CHAPTER IV: APPENDICES

Appendix 1: Research Ethics Board Approval

UNIVERSITY OF MANITOBA | Research Ethics and Compliance

RECEIVED 14 Jun 2018

Research Ethics - Bannatyne
P126-770 Bannatyne Avenue
Winnipeg, MB
Canada R3E 0W3
Phone +204-789-3255
Fax +204-789-3414

BIOMEDICAL RESEARCH ETHICS BOARD (BREB)
CERTIFICATE OF ANNUAL APPROVAL

PRINCIPAL INVESTIGATOR: Dr. Amir Ravandi	**INSTITUTION/DEPARTMENT:** U of M and SBGH/Internal Medicine	**ETHICS #:** HS18132 (B2013:100)
BREB MEETING DATE (If applicable):	**APPROVAL DATE:** June 11, 2018	**EXPIRY DATE:** **June 24, 2019**
STUDENT PRINCIPAL INVESTIGATOR SUPERVISOR (If applicable):		

PROTOCOL NUMBER: NA	**PROJECT OR PROTOCOL TITLE:** Oxidized Phosphatidylcholines as Markers of Reperfusion Injury in Patients with ST Elevation Myocardial Infarction (STEMI)
SPONSORING AGENCIES AND/OR COORDINATING GROUPS: U of M Internal Funds	

Submission Date of Investigator Documents: May 7, 2018	**BREB Receipt Date of Documents:** May 28, 2018

REVIEW CATEGORY OF ANNUAL REVIEW: **Full Board Review** ☐ **Delegated Review** ☒

THE FOLLOWING AMENDMENT(S) and DOCUMENTS ARE APPROVED FOR USE:

Document Name(if applicable)	Version(if applicable)	Date

Annual approval

*Annual approval implies that the most recent **BREB approved** versions of the protocol, Investigator Brochures, advertisements, letters of initial contact or questionnaires, and recruitment methods, etc. are approved.*

Consent and Assent Form(s):

Research Participant Information and Consent Form	V. 3	May 28, 2016

CERTIFICATION

The University of Manitoba (UM) Biomedical Research Board (BREB) has reviewed the annual study status report for the research study/project named on this ***Certificate of Annual Approval*** as per the category of review listed above and was found to be acceptable on ethical grounds for research involving human participants. Annual approval was granted by the Chair or Acting Chair, UM BREB, per the response to the conditions of approval outlined during the initial review (full board or delegated) of the annual study status report.

BREB ATTESTATION

The University of Manitoba (UM) Biomedical Research Board (BREB) is organized and operates according to Health Canada/ICH Good Clinical Practices, Tri-Council Policy Statement 2, and the applicable laws and regulations of Manitoba. In respect to clinical trials, the BREB complies with the membership requirements for Research Ethics Boards defined in Division 5 of the Food and Drug Regulations of Canada and carries out its functions in a manner consistent with Good Clinical Practices.

QUALITY ASSURANCE
The University of Manitoba Research Quality Management Office may request to review research documentation from this research study/project to demonstrate compliance with this approved protocol and the University of Manitoba Policy on the Ethics of Research Involving Humans.

CONDITIONS OF APPROVAL:

1. The study is acceptable on scientific and ethical grounds for the ethics of human use only. ***For logistics of performing the study, approval must be sought from the relevant institution(s).***
2. This research study/project is to be conducted by the local principal investigator listed on this certificate of approval.
3. The principal investigator has the responsibility for any other administrative or regulatory approvals that may pertain to the research study/project, and for ensuring that the authorized research is carried out according to governing law.
4. **This approval is valid until the expiry date noted on this certificate of annual approval. A Bannatyne Campus Annual Study Status Report** must be submitted to the REB within 15-30 days of this expiry date.
5. Any changes of the protocol (including recruitment procedures, etc.), informed consent form(s) or documents must be reported to the BREB for consideration in advance of implementation of such changes on the **Bannatyne Campus Research Amendment Form.**
6. Adverse events and unanticipated problems must be reported to the REB as per Bannatyne Campus Research Boards Standard Operating procedures.
7. The UM BREB must be notified regarding discontinuation or study/project closure on the **Bannatyne Campus Final Study Status Report**.

Appendix 2: Research Participant Information and Consent Form

Novel Lipid Biomarkers of Myocardial Reperfusion Injury - STEMI

Principal Investigator: Dr. Amir Ravandi MD PhD FRCPC

Institute of Cardiovascular Sciences

351 Tache Ave., Winnipeg, Mb. R2H 2A6

Tel: 235-3671 (Office); 204-235-3325 (Lab)

You are being asked to participate in this research study because you have experienced a heart attack. During your cardiac catheterization procedure, bloodwork is routinely sent to help with treatment and prognostic decisions. At the same time, a blood sample was acquired and set aside for use within a research study, should you consent. Also, if applicable, material retrieved from the blocked artery was collected at the time of the procedure. This information is to give you more details regarding the study and your involvement in it, should you decide to participate. **This Study is voluntary. If you decide now not to participate in the study, or at any time withdraw from the study, your normal medical care will not be affected in any way.** If you decide to participate now, and change your mind later, you should contact the study coordinator by mail or telephone. The samples collected will then be discarded.

Please read the attached Research Participant Information and Consent Form that outlines the research and your role in it. Should you have any questions you may contact the study staff regarding the study and your decision to participate. You may also discuss it with your regular doctor, friends and family. Please contact the study doctor or study staff to explain any words or information that you do not clearly understand. The full scientific version of the study is available upon request. A total of 192 participants will be enrolled in this study.

Participant Initials: _____

WHAT IS THE RESEARCH ABOUT?

The aim of the research project is to discover new blood markers that cause injury once blood supply is re-established to the heart. To do this research, we need volunteers who are experiencing a heart attack to donate small amounts of blood and the material that resulted in the blocked artery recovered at the time of the procedure. As well, we also need volunteers who do not have any 'obstructive' (>60% blockage) coronary artery disease to make a comparison. During your angiogram procedure, hospital staff took 2 blood samples of two teaspoons (10 mL) each (4 teaspoons or 20 mL total) for this research. There were two reasons this was not discussed before the sample was collected; first, if you were in the catheterization laboratory with a heart attack, any delay to angiogram would result in further heart muscle damage, second, to avoid having to do an additional needle poke to collect a blood sample.

As well, if a clot was identified during your angiogram, it was removed and also sent to be stored and would be processed for analysis if you agree to participate in the study.

Your blood specimen was kept aside and the sample was assigned an alpha-numerical code and labeled with that code at the laboratory. No other identifying information was attached to the samples. If you decide not to participate in the study, the sample will be not be used for research and will be destroyed. Otherwise, we will keep a secure record linking your identity to the samples you provided.

If you agree to participate, we will collect medical information from you and your medical record to determine the amount and type of molecules that predict heart damage. Delegated study staff will review the hospital records relevant to the diagnosis and determine if and why you present to hospital over the next 30 days. These records will include such things as the electrocardiogram, the results of certain blood tests, and any other tests carried out to diagnose your condition. As well, when you were admitted with a ST elevation myocardial infarction (a specific type of heart attack), 2 blood samples of 2 teaspoons (10 mL) each were collected with your standard bloodwork during your catheterization procedure (as previously mentioned).

Participant Initials: _____

And then additional blood samples of 2 teaspoons (10 mL) each are to be collected at 1 day and at 2 days after your angiogram. Also, if available, material retrieved from the blocked artery was

collected at the time of the procedure. These samples will be tested for levels of oxidized phospholipids and other biomarkers. During a follow up visit with the cardiologist 4-6 weeks after the heart attack we will collect one last 2 teaspoon (10 mL) blood sample to compare the changes to the samples collected during the heart attack.

Samples will be stored in a freezer at the St. Boniface General Hospital Research Centre in the lab of the principal investigator for up to 5 years. Upon completion of the study any leftover sample will be destroyed. At no time will genetic testing be done on your sample.

This Study is voluntary. If you decide now not to participate in the study, or at any time withdraw from the study, your normal medical care will not be affected in any way.

WHAT WILL I HAVE TO DO?

If you decide to remain enrolled in the study, you will need to be a patient at St. Boniface Hospital for the first 2 days and then when you come back to St. Boniface Hospital Cardiac Clinics to see the cardiologist there will be one additional study blood sample taken (2 teaspoons or 10 mL).

IS THE STUDY CONFIDENTIAL?

Information gathered in this research may be published or presented in public forums; however your name will not be used or revealed. Medical records that contain your identity will be treated as confidential in accordance with the Personal Health Information Act of Manitoba. All data obtained during the study will be stored with an alpha-numerical code instead of your name, and only Dr. Amir Ravandi and delegated study staff will know the code that links the sample to your medical records. Despite efforts to keep your personal information confidential, absolute confidentiality cannot be guaranteed. Organizations that may inspect and/or copy your research results for quality assurance and data analysis include groups such as the Research Ethics Board at the University of Manitoba and St. Boniface General Hospital.
Participant Initials: _____

WHAT ARE THE POSSIBLE HARMS OR BENEFITS?

This is a research study, so you will not personally benefit by participating in this study. Eventually, the results of this study may benefit future patients with a heart attack. You will receive no payment or reimbursement for any expenses related to taking part in this study. The measurements to be carried out for this study will not immediately reveal any diagnostic information, so there is no possibility that the researchers will accidentally/incidentally discover anything relevant to your present health status.

WHAT ELSE SHOULD I KNOW?

You have the right to withdraw from the study at any time. The Investigators reserve the right to end your participation for any reason.

You are entitled to know the scientific and technical results at the end of the research project, and may request that a copy of any reports be sent to you upon completion of the study.

WHO CAN I CONTACT FOR MORE INFORMATION?

Dr. Amir Ravandi, Principal Investigator,

SBGH Research Centre Institute of Cardiac Sciences, 204-235-3325.

For questions about your rights as a research subject, you may contact:

University of Manitoba Biomedical Research Ethics Board, 789-3255.

CONSENT FORM

I have received a copy of and I have read the Research Participant Information and Consent Form for the study titled “Novel lipid biomarkers of myocardial reperfusion injury”. I understand the nature of the study, including the potential risks and benefits. I understand that my decision whether to participate or not should not be rushed, and that if I am hesitant I should not participate. I have had adequate time to consider the information.

Participant Initials: _____

I have talked to delegated study staff and all my questions about the study have been answered. If I have any more questions, I may contact or the Biomedical Research Ethics Board at the University of Manitoba, at 789-3255. I understand that I will be given a copy of this consent form, after signing it.

I understand that my blood specimen will be assigned an alpha-numeric code and stored in a freezer at the SBGH Research Center Institute of Cardiac Sciences, and will be thawed to take samples for the spectroscopy measurements. The remainder will be kept frozen, to be available in the event that it is necessary to redo a spectrum. Upon completion of the study, any remaining sample will be destroyed**.** I understand that all data obtained during the study will be stored with an alpha-numerical code instead of my name, and that the investigators will have information which relates my name to the code.

I understand that information regarding my personal identity will be kept confidential, but that confidentiality is not guaranteed. I agree to the inspection of my research records by the Health Research Ethics Board at the University of Manitoba and St. Boniface General Hospital.
I understand that clinical and laboratory data collected on me will be used in analyzing the results of this study. I give permission for a researcher to access my medical records relevant to this study and review my clinical and treatment history and results from laboratory tests relevant to this study. I realize that by signing this document I am not waiving any legal rights.

I hereby agree to participate in the research study, "Novel lipid biomarkers of myocardial reperfusion injury'' and I understand that I can end my participation at any time and for any reason. My consent has been given freely.

_____

Name of research subject (Print)

_____ _____

Signature of research subject Date (d/m/y) and time of day

_____ _____

Name of person obtaining consent Role in Study

_____ _____

Signature of person obtaining consent Date (d/m/y) and time of day